Investigating the role of Microphthalmia-Associated Transcription Factor M in melanoma development and drug resistance

Tine Norman Alver

Department of Tumor Biology
Institute for Cancer Research
Oslo University Hospital

Faculty of Medicine
University of Oslo

Oslo 2020

UiO : Faculty of Medicine
University of Oslo

Oslo University Hospital

HELSE SØR-ØST

Series of dissertations submitted to the
Faculty of Medicine, University of Oslo

ISBN 978-82-8377-651-5

Cover: Hanne Baadsgaard Utigard.
Print production: Reprosentralen, University of Oslo.

Acknowledgments

The work presented in this thesis was performed at the Department of Tumor Biology, Oslo University Hospital, The Norwegian Radium Hospital, between November 2014 and January 2020. This work was kindly supported by Helse Sør-Øst (project number 2014044). I would also like to thank Radiumhospitalets Legater for funding me during the writing of this thesis.

First of all, I would like to express my gratitude towards my main supervisor Sigurd Læines Bøe. I sincerely appreciate your guidance, and I thank you for always being available.

I am also very grateful to my co-supervisor and group leader Professor Eivind Hovig. Thank you for allowing me to be a part of your research group, for the encouragement, inspiration, and support throughout these years.

I would also like to thank the head of the department, Gunhild Mælandsmo for support and encouragement and for allowing us to practice yoga during work hours.

To my “støttekontakt”, Karen-Marie Heintz; You are a truly special human, and I thank you for all your help and support. Per Olaf Ekstrøm, you are the department resident McGyver, and you have gone beyond to assist me in numerous tasks. Further, I want to thank all my colleagues at the department of Tumor Biology for providing an excellent working environment both professionally and socially.

Lastly, I want to express how much I appreciate and love my friends and family, especially my children Herman and Lotte, for putting up with me during these years.

Table of contents

Abbreviations

α-MSH	Alpha-Melanocyte-Stimulating Hormone
AKT	Protein Kinase B
ALX3	Aristaless-like homeobox 3
AP-1	Activator Protein-1
APEX1	Apurinic/Apyrimidinic Endodeoxyribonuclease
ARID1A	AT-rich Interaction Domain 1A
ARID2	AT-rich interaction domain 2
ATF4	Activating Transcription Factor 4
AXL	Tyrosine-Protein Kinase UFO
BCL2	B-cell Lymphoma 2
BIRC7	Baculoviral IAP Repeat-Containing Protein 7
BRAF	V-Raf Murine Sarcoma Viral Oncogene
BRAFi	V-Raf Murine Sarcoma Viral Oncogene Inhibitor
BRN2	POU Domain Transcription Factor
c-KIT	Proto-Oncogene c-KIT
c-MET/HGFR	Hepatocyte Growth Factor Receptor
cAMP	Cyclic Adenosine Monophosphate
CBP	CREB-Binding Protein
CCND1	Cyclin D1
CDK2	Cyclin-Dependent Kinase 2
CDK4	Cyclin-Dependent Kinase 4
CDK6	Cyclin-Dependent Kinase 6
CDKN1A	Cyclin-Dependent Kinase Inhibitor 1A
CDKN2A	Cyclin-Dependent Kinase Inhibitor 2A
ChIP seq	Chromatin Immunoprecipitation Sequencing
COT/MAP3K8	Mitogen-Activated Protein Kinase Kinase
CREB	cAMP Response Element-Binding Protein

CTLA-4	CTL Antigen 4
DCT	Dopachrome Teutomerase
DEC1	Deleted in Esophageal Cancer 1
DIAPH1 (p27)	Diaphanous Related Formin 1
DNA	Deoxyribonucleic Acid
E-BOX	Enhancer Box
EGF	Epidermal Growth Factor
EGFR	Epidermal Growth Factor Receptor
EMT	Epithelial to Mesenchymal Transition
ERBB	V-erb-b2 Avian Erythroblastic Leukemia Viral Oncogene
ERBB2/HER2	V-erb-b2 Avian Erythroblastic Leukemia Viral Oncogene Homolog 2
ERBB3/HER3	V-erb-b2 Avian Erythroblastic Leukemia Viral Oncogene Homolog 3
ERBB4/HER4	V-erb-b2 Avian Erythroblastic Leukemia Viral Oncogene Homolog 4
ERK	Extracellular Signal-Regulated Kinase
FDA	Food and Drug Administration
FOXD3	Forhead Box D3
GAS6	Growth Arrest Spesific 6
GLI2	Zinc Finger Protein GLI2
GNA11	G Protein Subunit Alpha 11
GNAQ	G Protein Subunit Alpha q
GPR143	G Protein Coupled Receptor 143
GSK3	Glycogen Synthase Kinase-3
HGF	Hepatocyte Growth Factor
HIF1α	Hypoxia-Inducible Factor 1α
HPS4	Hermansky-Pudlak Syndrome 4
HRAS	V-Ha-Ras Harvey Rat Sarcoma Viral Oncogene Homolog

IDH1	Isocitrate Dehydrogenase (NADP(+)) 1
IGF-1R	Insulin Like Growth Factor 1 receptor
IL-2	Interleukin 2
KIT	V-kit Hardy-Zuckerman 4 Feline Sarcoma Viral Oncogene
KRAS	V-Ki-Ras2 Kirsten Rat Sarcoma 2 Viral Oncogene Homolog
LEF1	Lymphoid Enhancer Binding Factor 1
LYST	Lysosomal Trafficking Regulator
M-BOX	E-box
MAPK	Mitogen-Activated Protein Kinase
MAX	MYC Associated Factor X
MC1R	Melanocortin 1 Receptor
MDM2	MDM2 Proto-Oncogene
MEK	Mitogen Activated Protein Kinase Kinase
MEKi	Mitogen Activated Protein Kinase Kinase inhibitor
MERTK	MER Proto-Oncogene
MITF	Microphthalmia-Associated Transcription Factor
MLANA	Melanoma Antigen Recognized By T-Cells 1
mRNA	Messenger Ribonucleic Acid
mTOR	Mammalian target of rapamysin
MYC	Myc Proto-Oncogene
NC	Neural Crest
NF1	Neurofibromin 1
NRAS	Neuroblastoma RAS Viral (V-Ras) Oncogene Homolog
NRG1-beta	Neuregulin 1-beta
OC-2	One Cut Homebox 2
p300	Histone Acetyl Transferase p300
PAX3	Paired Box 3
PD-1	Programmed Cell Death Receptor 1

PD-L1	Programmed Death Ligand 1
PDGFRa	Platelet Derived Growth Factor Receptor Alpha
PDGFRb	Platelet Derived Growth Factor Receptor Beta
PI3K	Phosphoinositide 3-Kinase
PIAS3	Protein Inhibitor Of Activated STAT3
PIK3CA	Phosphatidylinositol-4,5-Biphophate 3-Kinase Catalytic Subunit
PKA	Protein kinase A
POMC	Proopiomelanocortin
PPP6C	Protein Phosphatase 6 Catalytic Subunit
PTEN	Phosphatase And Tensin Homolog
Rab27a	Ras-Related Protein Rab-27A
RB1	RB Transcriptional Corepressor 1
RNA	Ribonucleic Acid
RNA-seq	Ribonucleic Acid sequencing
RPLP0	60S Acidic Ribosomal Protein P0
RSK	Ribosomal Protein S6 Kinase
RT-PCR	Real Time Polymerase Chain Reaction
RTK	Receptor Tyrosine Kinase
SAE1	SUMO1 Activating Enzyme Subunit 1
SAE2	Ubiquitin Like Modifier Activating Enzyme 2
SH2	Src Homology-2
SILV	SILVER Locus Protein Homolog
siRNA	Small Interfering RNA
SLC24A5	Solute Carrier Family 24 Member 5
SLC45A2	Solute Carrier Family 45 Member 2
SNAI2	Snail Family Transcriptional Repressor 2
SOX10	SRY-Box Transcription Factor 10
SRC	SRC Proto-Oncogene

T-cell	T-Lymphocyte
TAD	Transactivation Domain
TBP	TATA-Box Binding Protein
TBX2	T-Box Transcription Factor 2
TEAD	Transcriptional Enhancer Factor TEF-1
TERT	Telomerase Reverse Transcriptase
TFE3	Transcription Factor Binding To IGHM Enhancer 3
TFEB	Transcription Factor EB
TFEC	Transcription Factor EC
TKD	Tyrosine Kinase Domain
TME	Tumor Microenvironment
TP53	Tumor Protein P53
TYR	Tyrosinase
TYRO3	TYRO3 Protein Tyrosine Kinase
TYRP1	Tyrosine-Related Protein 1
UBC9	Ubiquitin Conjugating Enzyme E2
USF	Upstream Stimulatory Factor
USP13	Ubiquitin Specific Peptidase 13
UVA	Ultraviolet A
UVB	Ultraviolet B
UVR	Ultraviolet Radiation
VEGFR2	Vascular Endothelial Growth Factor 2
WNT	Wingless-Related Integration Site

List of papers

I. MITF depletion elevates expression levels of ERBB3 receptor and its cognate ligand NRG1-beta in melanoma

Alver TN, Lavelle TJ, Longva AS, Øy GF, Hovig E, Bøe SL

Oncotarget. 2016 Aug 23;7(34):55128-55140

II. Dysregulation of MITF in the context of defective MC1R and RB1/p16/CDK4 leads to melanocyte transformation

Alver TN*, Lavelle TJ*, Heintz KM, Wernhoff P, Nygaard V, Nakken S, Øy GF, Bøe SL, Urbanucci A, Hovig E

*Shared first authorship
Submitted manuscript

III. Co-operative induction of RTK`s contributes to adaptive MAPK drug resistance in melanoma through the PI3K pathway.

Alver TN, Heintz KM, Hovig E, Bøe SL

Submitted manuscript

1. Introduction

1.1 Cancer

Cancer is the second leading cause of death globally and was responsible for approximately 9.6 million deaths last year (Bray et al., 2018), and in 2018, over 34000 new cases were registered in Norway alone (Cancer in Norway, 2018). Defining features of cancer cells are that they are able to escape the strict external control of growth and proliferation and acquire the ability to invade adjacent tissue normally habited by other cell types. Invasiveness is an essential characteristic of cancer cells and allows them to spread to other organs and disrupt their normal function (Egeblad et al., 2010; Nowell, 1976).

Their tissue of origin most frequently classifies cancers, and to date, over 100 types have been identified (Hanahan & Weinberg, 2000). A common denominator for most cancer types is that the evolution of cancer cells are commonly thought to be a multistep process of independent events. In 2000, Hanahan and Weinberg first proposed that these events can be organized into several biological capabilities, termed the hallmarks of cancer, following an extended review according to recent findings in the field in 2011 (Hanahan & Weinberg, 2011). These proposed hallmarks consist of the following capabilities: Sustained proliferative signaling, evading growth suppressors, avoiding immune destruction, replicative immortality, activation of invasion and metastasis, induction of angiogenesis, resistance to cell death, genetic instability, Inflammation and deregulation of cellular energetics. In addition, the authors proposed that tumor-promoting inflammation and genome instability and mutations as enabling characteristics (Hanahan & Weinberg, 2011).

These reviews have been widely cited and accepted as a comprehensive work in cancer biology; however, they have not remained unchallenged. Arguments questioning what defines a hallmark has been raised (Lazebnik, 2010). First, some of the proposed hallmarks may also apply to benign tumors such as induction of angiogenesis, sustained proliferative signaling, evading growth suppressors, resistance to cell death, and replicative immortality in contrast to invasion and

metastasis which is a trait exclusively found in malignant tumors (Lazebnik, 2010). Secondly, eight years have passed since Hanahan, and Weinberg published their updated review, and additional "hallmarks" have been proposed since, including involvement of tumor stroma and phenotype switching.

1.2 Melanoma

Melanoma is a form of skin cancer that arises from malignant transformation of melanocytes, the pigment-producing cells of the skin, iris, meninges, and inner ear (Cichorek et al., 2013; Tachibana, 1999). Although melanoma accounts for only 1% of skin cancers, it accounts for around 75% of skin cancer-related deaths (Siegel et al., 2018). Melanoma is one of the most aggressive and treatment-resistant cancers. Also, the incidence is now increasing at a higher rate than any other human cancer (Bray et al., 2018; Guy et al., 2015). Norway is among the European countries with the highest incidence rate of malignant melanoma, and the rate has increased tenfold over the last 60 years (Cancer Registry of Norway (2018)).

1.2.1 Normal melanocyte development and function

Melanocytes are neural crest-derived precursor cells originating from the embryonic ectoderm. A group of these cells undergo an epithelial-mesenchymal transition (EMT) and migrate out of the neuroepithelium. EMT refers to a phenotypic switch where cells lose their cell contacts and epithelial polarity, and undergo a de-differentiation into a more stem cell mesenchymal-like state (Thiery, 2003). These cells are transient multipotent cells before becoming lineage-restricted during further differentiation into melanoblasts (Ernfors, 2010; Goldstein & Tucker, 2001). Melanocytes are cells in our skin that can absorb ultraviolet radiation (UVR) and survive a considerable amount of stress (Brenner & Hearing, 2008). Since the skin is our primary barrier to the external environment, the melanocytes contribute to both thermoregulation and photoprotection through the production of melanin (Lin & Fisher, 2007). Melanocytes are located and securely attached to the basal layer of the epidermis, where each of them is surrounded by 30-40 keratinocytes through long dendritic extensions, together forming the epidermal melanin unit (Fitzpatrick & Breathnach, 1963). Melanosomes are the pigment-producing/containing organelles produced in melanocytes. Melanosomes are passed on to keratinocytes, where they

affect basal pigmentation as well as photoprotection (Ando et al., 2012). Melanocytes communicate with surrounding keratinocytes through paracrine hormones and cell adhesion molecules (Haass et al., 2005). This interaction allows for adaptation to external stimuli through cross-talk between melanocytes, keratinocytes, and the skin microenvironment (J. X. Wang et al., 2016).

Melanocytes have been shown to produce two main types of pigment: dark brown/black eumelanin, representing dark hair phenotype, and red/yellow sulfated pheomelanin displaying a fair skin, red hair, and freckles (RHC) phenotype (Potterf et al., 1999). Photoprotective pigment synthesis is stimulated by the binding of α-melanocyte-stimulating hormone (α-MSH) to melanocortin 1 receptor (MC1R) on melanocytes following UVR exposure. MC1R is a transmembrane, G-protein-coupled receptor. MC1R activates cyclic adenosine monophosphate (cAMP) production and cAMP response element-binding protein (CREB)-mediated transcriptional activation of the melanocyte master regulator microphthalmia-associated transcription factor (MITF). In turn, MITF activates the transcription of pigment synthesis genes and melanin-production enzymes (Levy et al., 2006). Melanosomes contain enzymes that catalyze pigment syntheses such as tyrosinase (TYR), the rate-limiting enzyme, dopachrome tautomerase (DCT), and tyrosinase-related protein (TYRP1) (Cichorek et al., 2013). The activity of these three enzymes correlates directly with melanin content (Abdel-Malek et al., 1993). Both eumelanin and pheomelanin are derived from the precursor tyrosine. Melanogenesis produces a mixture of eumelanin and pheomelanin in different ratios, which is determined by TYR activity and substrate availability (Simon et al., 2009). The difference in skin phenotype among individuals is mainly dictated by eumelanin levels, which has a direct correlation with the extent of pigmentation (Wakamatsu et al., 2006).

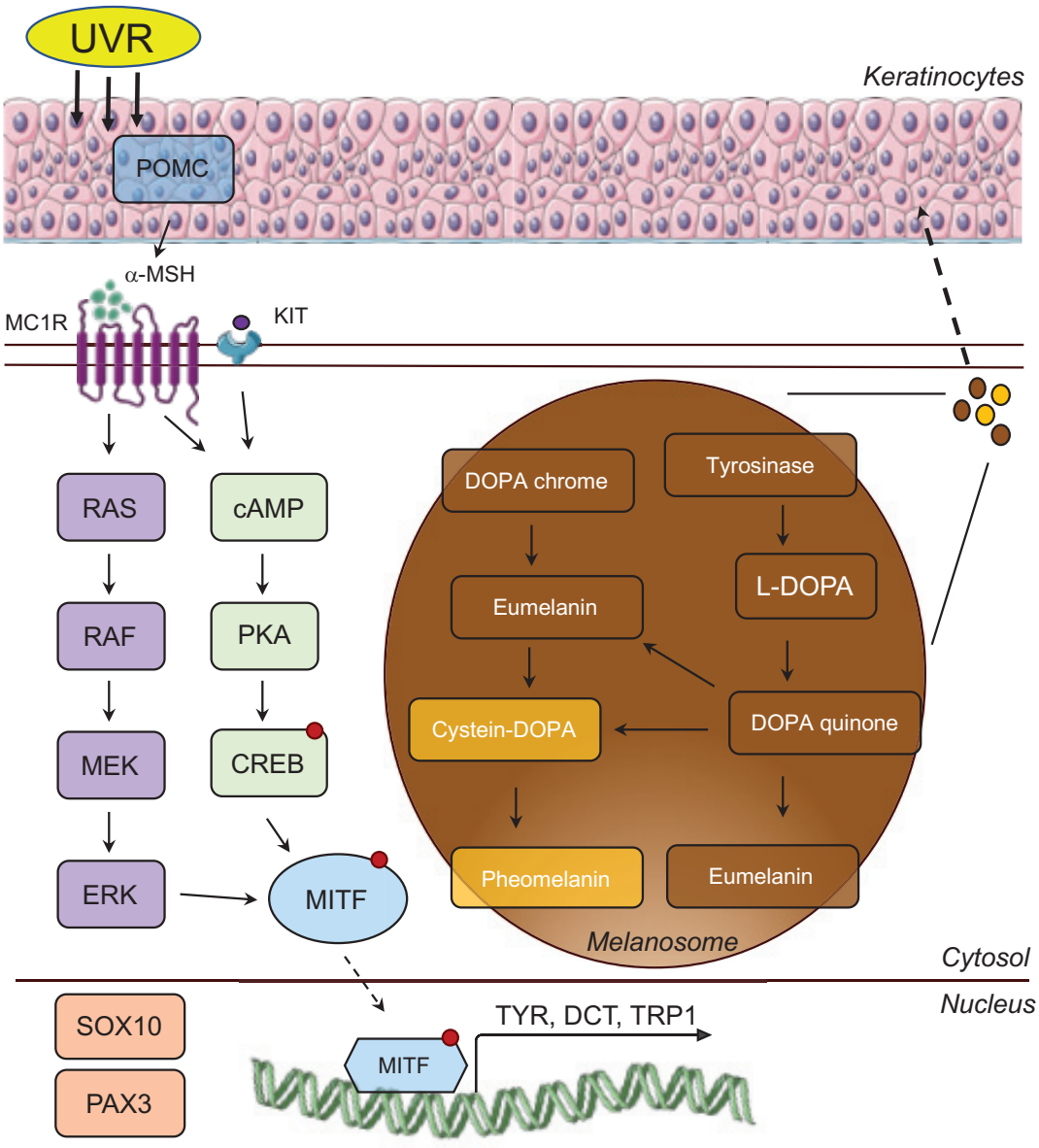

Figure 1. Pigmentation synthesis. Adapted from (D'Mello et al., 2016). Simplified overview of eumelanin and pheomelanin synthesis within the melanosomes. UVR (UVA/UVB) irradiation of keratinocytes in the skin leads to secretion of ligands such as α-MSH, which in turn activates downstream signaling activating MITF in melanocytes. MITF activates transcription of enzymes which catalyzes eumelanin and pheomelanin synthesis.

1.2.2 Melanoma risk and predisposition

The transformation of melanocytes into melanoma is considered a multi-step process, as it involves environmental, genetic, and phenotypic risk factors. The main environmental risk factor for melanoma is chronic and intermittent exposure to UVA/UVB radiation. UVA/UVB may cause DNA damage through the formation of pyrimidine dimers that may result in inflammatory responses, immunosuppression, and gene mutations (Vink & Roza, 2001). Although proper use of sunscreen may prevent part of the damage from UVA/UVB exposure, there are intrinsic risk factors that predispose to melanoma. Phenotypic characteristics such as fair skin, red hair, freckles, and multiple melanocytic nevi are associated with increased melanoma risk (Sturm, 2002; Sturm et al., 2003). Lastly, a family history of melanoma has been shown to be a risk factor. Interestingly, Shekar and colleagues estimated that approximately 55% of the variation in melanoma burden was due to genetic effects when studying twins (Shekar et al., 2009). Among the heritable factors are:

CDKN2A

Cyclin-dependent kinase inhibitor 2A (CDKN2A) was the first gene associated with melanoma susceptibility (Hussussian et al., 1994; Kamb et al., 1994) and is considered to be a melanoma high-risk gene (Potrony et al., 2015). The CDKN2A locus is the most frequently deleted region in melanoma. This deletion occurs with high penetrance in familial melanoma (20-40%) (Mangas et al., 2016). CDKN2A encodes the two tumor suppressors $p16^{ink4a}$ and $p14^{ARF}$, which both function in cell cycle regulation (Desnoo & Hayward, 2005). $p16^{ink4a}$ is an inhibitor of the cyclin-dependent kinases CDK4 and CDK6 and prevents cell cycle progression in healthy cells, while $p14^{ARF}$ is a positive regulator of p53, an important tumor suppressor. Inactivation of CDKN2A through deletion, silencing, or mutation leads to uncontrolled cell proliferation (J. Liu et al., 2014).

CDK4

Following the discovery of CDKN2A, a gene screening approach was taken to identify other possible hereditary melanoma genes. Screening for p16 binding partners rapidly led to the identification of CDK4 mutations. This mutation inhibits p16 from inactivating the kinase, leading to increased phosphorylation of Retinoblastoma

protein (RB) and, in the end, uncontrolled G1 to S phase transition in the cell cycle (L. Zuo et al., 1996).

MC1R

Another essential gene implicated, and one of the most studied in melanoma susceptibility, is the MC1R gene. The MC1R gene is highly polymorphic, with more than 200 coding variants reported, showing a prevalence of any of these variants in healthy controls of about 60% (Tagliabue et al., 2018). Some of these variants are shown to reduce or completely cease the function of the receptor, leading to a shift in pigmentation synthesis from eumelanin (dark color phenotype) to pheomelanin (RHC phenotype). This causes the cells to be more sensitive to UVB, and therefore more prone to DNA damage and melanoma risk.

MITF

The MITF germline missense mutation p.E318K is associated with both familial and sporadic melanoma susceptibility. In 2010, Maubec et al. showed that coexisting melanoma and renal cell carcinoma in theme patients support a genetic predisposition underlying the association between these two cancer types that, in part was independent of CDKN2A (Maubec et al., 2010). Following this study, Bertolotto and colleagues then discovered that a MITF germline missense mutation (p.E318K) occurred at a significantly higher frequency in genetically enriched patients affected with melanoma, renal cell carcinoma, or both (Bertolotto et al., 2011). MITF p.E318K increases MITF transcriptional activity through abrogating a sumoylation motif. This mutant protein-enhanced melanocytic and renal cell clonogenicity, invasion, and migration, which is consistent with a gain-of-function role in tumorigenesis (Bertolotto et al., 2011).

TERT

The most recent findings in melanoma susceptibility involve genes that are involved in telomere maintenance. A novel germline mutation in the promoter region of the telomerase reverse transcriptase gene (TERT), was the first melanoma high-risk gene mutation to be described since CDKN2A was identified (Aoude et al., 2015;

Horn et al., 2013; Potrony et al., 2016). The TERT gene encodes the catalytic subunit of telomerase, which is the enzyme that maintains telomere length. Telomerase is usually silenced in healthy tissue, causing telomeres to shorten with each cell division. When the critical telomere length is reached, cells undergo senescence and then apoptosis (Shampay & Blackburn, 1988). The expression of telomerase is considered a hallmark of tumorigenesis, as over 90% of human cancers express the enzyme (Bell et al., 2016; Low & Tergaonkar, 2013). In 2013, Horn *et al*. and Huang *et al*. found two hotspot mutations in the TERT promoter, in around 71% of melanomas, including both somatic and germline mutations (Horn et al., 2013; F. W. Huang et al., 2013). This suggested that TERT is involved in both familial and sporadic melanoma (Horn et al., 2013).

1.2.3 Genetics of melanoma initiation and progression

Years of investigating melanocyte transformation into invasive melanoma have revealed a remarkable genetic complexity, comprising of thousands of mutations, amplifications, deletions, translocations and alterations in DNA methylation within a single tumor (Hodis et al., 2012). There are many ways of classifying melanoma, and despite the complexity and abundance of genetic lesions, several key driver mutations have been identified (Cancer Genome Atlas Network, 2015). However, in order for melanoma to progress, a sequence of molecular alterations and mutation events has to occur, regardless of genetic background. In what order these alterations occur is incompletely understood, but a model for the minimal biological changes required for melanoma progression has been suggested (Bennett, 2003; Soo et al., 2011). This model illustrates a proposed sequence of events and lesions, where each step illustrates events that may occur during progression towards metastatic melanoma (Figure 2).

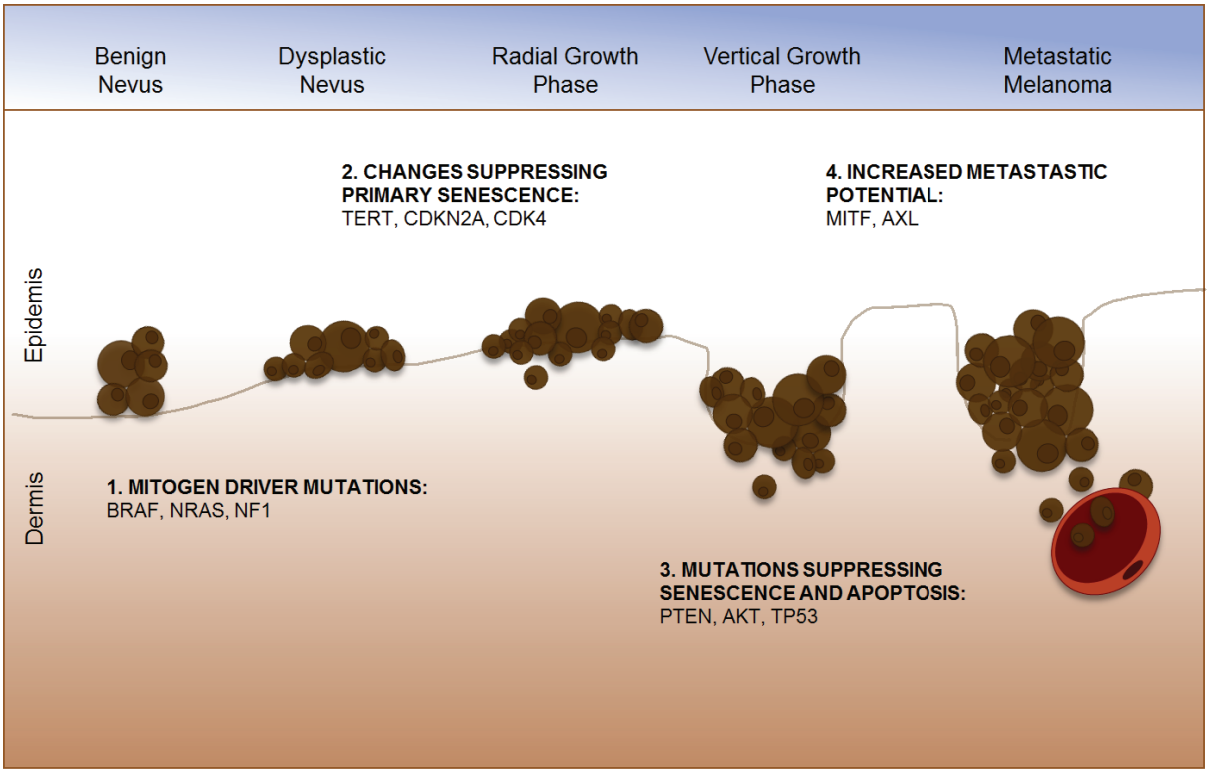

Figure 2. **Model for melanoma progression**. Figure adapted from (Arrangoiz et al., 2016). These steps are meant as a suggestion to represent the most common alterations that have to occur in order for melanoma to progress. 1. MAPK pathway mutations in benign nevus, 2. Alterations suppressing primary senescence in dysplastic nevus, 3. Further alteration affecting senescence and apoptosis in vertical growth phase (VGF) where the cells are becoming invasive, 4. Metastatic melanoma.

Somatic mutations

Aberrations in the MAPK pathway is a central step and considered an early event in melanoma development. Genomic subtypes suggested by the cancer genome atlas network in 2015: BRAF, NRAS, and NF1 are central proteins in this pathway (Table 1.) (Cancer Genome Atlas Network, 2015).

Mutation Subtypes	BRAF	RAS	NF1	Triple Wild-Type
MAPK pathway	BRAF V600, K601	(N/H/K) RAS G12, G13, Q61	NF1 LoF mut; (BRAF non hot spot mut)	KIT COSMIC mut/amp, PDGFRa amp, KDR (VEGFR2) amp; rare COSMIC GNA11 mut, GNAQ mut
PI3K/Akt pathway	PTEN mut/del (~20%); (rare AKT1/3 and PIK3CA COSMIC mut	AKT3 overexpression (~40%); (rare AKT1/3 and PIK3CA COSMIC mut)	AKT3 overexpression (~30%)	AKT3 overexpression (~20%)
Cell-cycle pathway	CDKN2A mut/del/h-meth (~60%); (CDK4 COSMIC mut)	CDKN2A mut/del/h-meth (~70%); CCND1 amp (~10%), (CDK4 COSMIC mut)	CDKN2A mut/del/h-meth (~70%); RB1 mut (~10%)	CDKN2A mut/del/h-meth (~40%); CCND1 amp (~10%), CDK4 amp (15%)
DNA damage response and cell death pathways	TP53 mut (~10%); (note: TP53 wild-type in ~90% of BRAF subtype)	TP53 mut (20%)	TP53 mut (~30%)	MDM2 amp (~15%) BCL2 upregulation
Epigenetics	IDH1 mut (rare EZH2 COSMIC mut); ARID2 mut (~15%)	IDH1 mut (rare EZH2 COSMIC mut); ARID2 mut (~15%)	IDH1 mut (EZH2 mut); ARID2 mut (~30%)	IDH1 mut (rare EZH2 COSMIC mut)
Telomerase pathway	Promotor mut (~75%)	Promotor mut (~70%)	Promotor mut (~85%)	Promotor mut (<10%) TERT amp (~15%)
Other pathways	PD-L1 amp, MITF amp, PPP6C mut (~10%)	PPP6C mut (~15%)		

Table 1. Melanoma genomic subtypes. Genomic subtypes as suggested by the Cancer Genome Atlas. Pathway alteration in BRAF, RAS, NF1 and Triple Wild-Type (WT)

In 2002 Davies and colleagues identified a single mutation in the v-Raf murine sarcoma viral oncogene (BRAF) after a genome-wide screening of a number of tumor samples focusing on the MAPK pathway (H. Davies et al., 2002; Mehnert & Kluger, 2012). This discovery was of great importance, as approximately 40-60% of all melanomas harbor an activating mutation in the BRAF gene. 90% of the mutations in BRAF is a valine to glutamine substitution at amino acid 600 (V600E). This mutation results in constitutive phosphorylation of extracellular signal-regulated kinase ERK leading to an increase in proliferation and survival (Dhillon et al., 2007).

The second most common cause of abnormal MAPK pathway signaling is found in the RAS family proteins. The RAS family (HRAS, KRAS, and NRAS) are a group of

GTPases that regulate proliferation and malignant transformation by activation of both MAPK and the PI3K pathway. Although all three isoforms are found to be mutated in melanoma, NRAS mutations are most frequent (15-30%) and were among the first mutations to be described in melanoma (Kodaz et al., 2017; Padua et al., 1984). Importantly, these mutations are often found to be mutually exclusive with BRAF mutations; however, co-mutations have been reported (Fedorenko et al., 2013).

The tumor suppressor neurofibromin 1 (NF1) has just recently been classified as one of the key drivers of melanoma (Cancer Genome Atlas Network, 2015). Since the NF1 protein is a negative regulator of RAS, a loss-of-function mutation in NF1 leads to sustained MAPK and PI3K pathway signaling. NF1 mutations are found in 10-13% of all melanomas (Cirenajwis et al., 2017; Sondka et al., 2018). Although BRAF and RAS mutations are believed to be mutually exclusive, NF1 mutations commonly co-occur with other alterations in the MAPK pathway. This implies that a mutation in NF1 alone is not equally as effective as BRAF and RAS mutations with respect to MAPK pathway activation and the accumulation of additional mutations are needed for progression (Krauthammer et al., 2015).

Even though the MAPK pathway is linked to aggressive melanoma biology, both BRAF and NRAS mutations are frequently found in benign nevi (Poynter et al., 2006). Overexpression of BRAF alone is not sufficient to transform melanocytes (Patton et al., 2005), as sustained signaling will lead to oncogene-induced senescence. Figure 3 illustrates some of the most described pathway aberrations in melanoma.

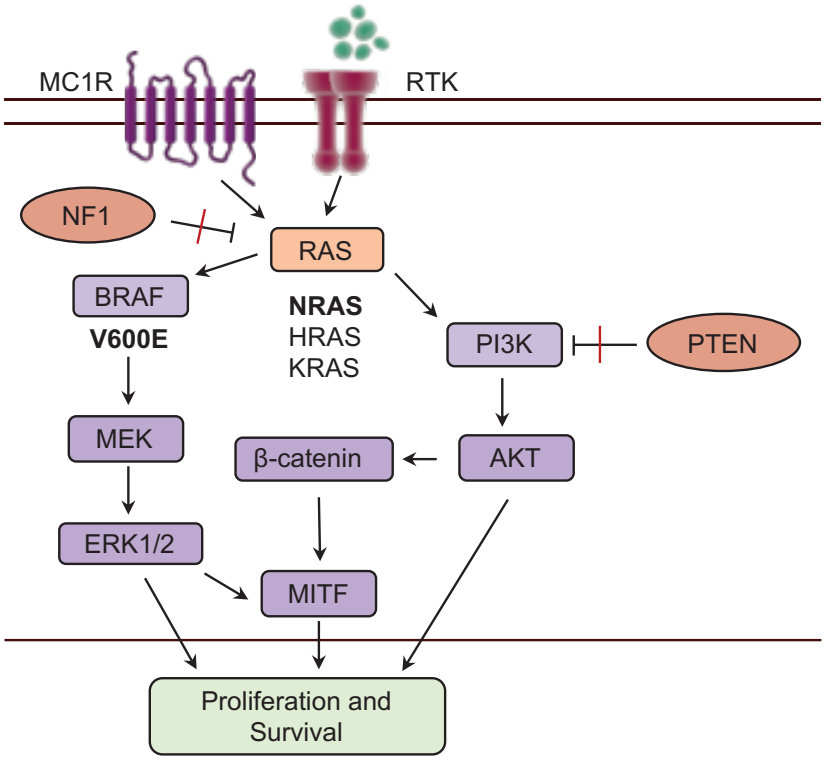

Figure 3. Pathway aberrations. Schematic diagram detailing the most described pathway genes thought to be aberrant in melanoma. Red line symbolizes loss of inhibitory effect.

Immortalization and progression

A mandatory step for the transformation of melanocytes into melanoma is to obtain cell immortality. Mutations in TERT will lead to increased telomerase activity, prolonged telomere maintenance, and cellular immortality. However, once the cells reach the state of early melanoma (stages 0-1), they can persist in this condition for several years before becoming invasive (Shain et al., 2015; Weinstock & Sober, 1987). This indicates a need for additional genetic alterations, perhaps involving the epidermis and the microenvironment, as well as an escape from immune surveillance for transformation to occur (Shain & Bastian, 2016).

Once the cells have escaped primary senescence and transformation has occurred, they become invasive melanoma cells. The invasive melanoma cells "inherit" the driver mutations activating the MAPK pathway, as well as the TERT mutations accumulated during the early stages of progression. Cultured human melanocytes seem to acquire two co-operative genetic changes for immortality: TERT expression and p16 pathway disruption (Shain et al., 2015). Invasive melanomas display a high

frequency of CDKN2A inactivation, which has not been detected in melanoma precursor lesions (Shain et al., 2015). Other aberrations in the p16 pathway, including CDK4 and RB family mutations, cyclin D1 (CCND1), and CDK4 amplifications, have also been reported (Bastian, 2014; Forbes et al., 2015; Hodis et al., 2012).

In addition to genetic alterations in the p16 pathway, mutations affecting chromatin remodeling complex members such as ARID2 and ARID1A appear during the transformation into invasive melanoma (Shain et al., 2015). Besides immortalization through TERT/CDKN2A dysregulation, alterations in p53 and phosphatase and tensin homolog (PTEN) are often found at later stages of melanoma development (Birck et al., 2000; Lassam et al., 1993; Reifenberger et al., 2000; Stretch et al., 1991). PTEN is regarded as the most important negative regulator of the PI3K pathway, as it antagonizes PI3K-AKT signaling by its lipid phosphatase activity (J. Li et al., 1998). PTEN has been implicated not only in suppressing cancer growth but also in regulating embryonic development, cell adhesion and migration, apoptosis, stem cell growth and differentiation (Blind, 2014; Ciuffreda et al., 2014; Engelman et al., 2006; Laurent et al., 2014; Maehama & Dixon, 1998; Myers et al., 1998; Sansal & Sellers, 2004; Song et al., 2012). Inactivation of PTEN by mutations and deletions plays a crucial role in the pathogenesis in many of both hereditary and sporadic melanomas (20-40%). During tumor development, loss of PTEN activity leads to increased PI3K-AKT signaling, followed by uncontrolled proliferation and reduced apoptosis. Genetic alterations in PTEN are generally mutually exclusive with NRAS mutations due to their redundancy in PI3K signaling (Goel et al., 2006).

Moreover, activating mutations and amplifications of RTKs such as c-KIT, although rare in cutaneous melanoma, have been frequently reported in uveal and mucosal melanoma (Woodman & Davies, 2010). Somatic mutations have also been reported in the ERBB4 receptor gene (～20%). Although these mutations have been reported to occur throughout the gene, functional studies suggest that many of these mutations result in increased PI3K-AKT activation (Prickett et al., 2009). Point mutations in the PIK3CA gene that encodes the catalytic subunit of PI3K occur, but are rare with a reported prevalence of 3-5% (Curtin et al., 2006). Other rare point

mutations have also been reported in AKT1 and AKT3 (1-2%), respectively (M. A. Davies et al., 2008).

MITF amplifications have been observed in about 10% of primary, and around 21% of late-stage melanoma. MITF is also suggested to be a dominant oncogene (Garraway et al., 2005). Melanomas harboring high levels of MITF protein display a high degree of proliferation, while having weak metastatic potential (Verfaillie et al., 2015). However, melanomas that have progressed to a metastatic state display weak proliferation and low MITF levels. This may indicate that an epigenetic phenotype switch plays a role in the development of melanoma metastasis (Hoek et al., 2006).

1.2.4 Phenotype switching in melanoma

A high degree of phenotypic plasticity is a hallmark of malignant melanoma. Phenotype switching is a phenomenon in which melanoma cells interconvert between proliferative and invasive cell states in an epithelial-to-mesenchymal transition (EMT) like manner. In 2006, Hoek and colleagues identified two main groups of cells (by gene expression profiling of 86 melanoma cell lines), which were distinctive in their transcriptional signatures. They observed one group with distinct invasive properties and a low ability to proliferate (invasive phenotype), while the other group displayed opposite features, namely high proliferative properties and weak invasiveness (proliferative phenotype) (Hoek et al., 2006). Sensi and colleagues were the first to demonstrate the existence of populations in melanoma tumor samples. They identified MITF expression as a marker for the proliferative phenotype, while AXL expression was linked to an invasive phenotype in patient tumor samples, which is in agreement with observations from Hoek and colleagues (Sensi et al., 2011). Evidence of heterogeneity has also been shown at the RNA level in patient tumor samples (Tirosh et al., 2016). Moreover, a recent study has identified the transcription factors MITF and SOX10 as master regulators of the proliferative state, while activator protein-1 (AP-1) and transcriptional enhancer factor TEF-1 (TEAD) as regulators of the invasive cell state (Verfaillie et al., 2015). Depending on the balance between expression and activity of these proposed transcriptional regulators, cells are capable of adaptive phenotype plasticity. Since these transcriptional changes are often mediated by activation of signaling pathways

through extracellular factors, the tumor microenvironment (TME) plays a crucial role in this regard (I. S. Kim et al., 2017). Metabolic conditions and other factors in the microenvironment may also contribute to modify the phenotype of the cells back and forth between proliferative and invasive states (Cheli et al., 2012; Ferguson et al., 2017; I. S. Kim et al., 2017). These microenvironmental effects on plasticity may contribute to the inter- and intratumor phenotype heterogeneity often observed in melanoma (Tirosh et al., 2016). For a simplified illustration of phenotype switch mechanisms, see figure 4.

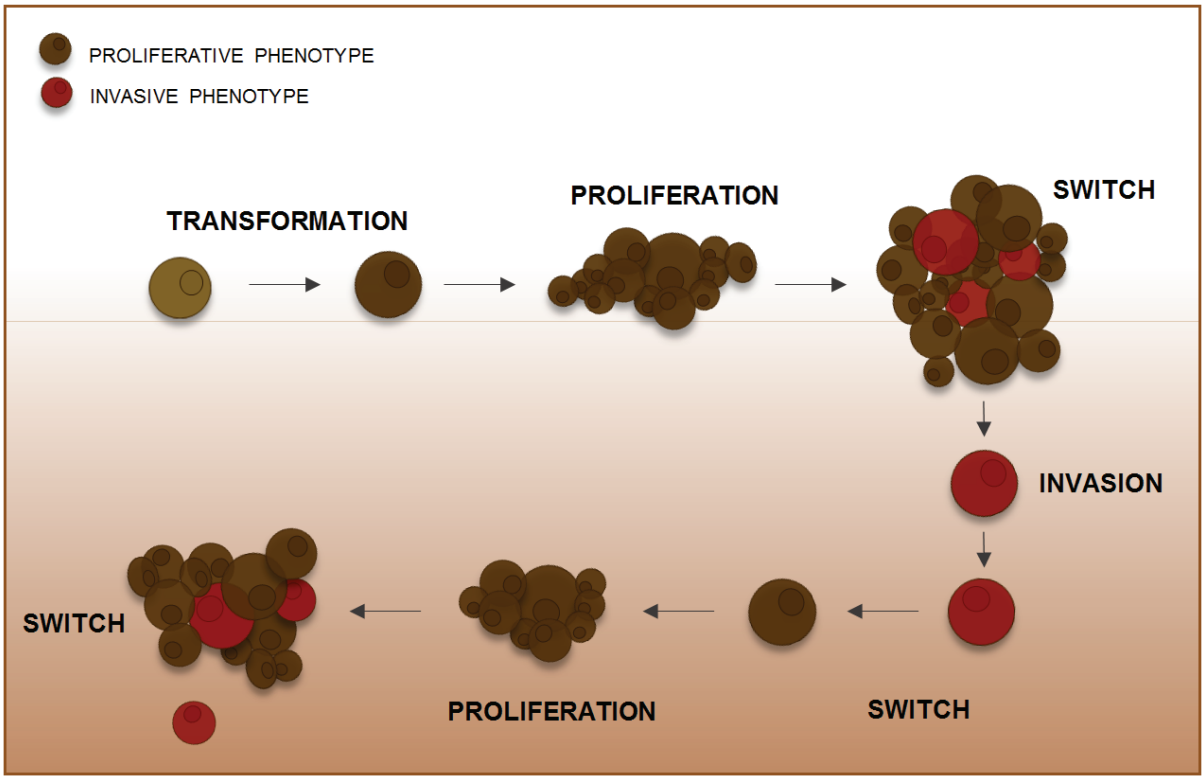

Figure 4. Phenotype switch. Adapted from (Hoek, Schlegel, Eichhoff, et al., 2008). Following transformation melanoma cells are believed to be of proliferative phenotype promoting tumor growth. Changing conditions in the tumor microenvironment may cause some of the cells to switch to an invasive phenotype promoting metastasis formation.

1.3 MITF

MITF is called the master regulator of melanocyte development, function, and survival and represents a melanocytic lineage-specific transcriptional regulator of the pigment pathway in melanocytes. MITF is expressed in a tissue-specific manner in melanocytes, osteoclasts, mast cells, retina, and the inner ear, and is an important regulator of multiple biological processes such as differentiation, proliferation, migration, and senescence. MITF has also been shown to play a substantial part in melanoma predisposition, progression, and treatment resistance.

1.3.1 MITF-structure and expression

The *MITF* locus is mapped to chromosome 3 in humans. It spans over 229 kbp. MITF is a member of the helix-loop-helix leucine zipper (bHLH-Zip) transcription factors and belongs to the Myc superfamily of transcription factors (Ledent et al., 2002). MITF binds to DNA in homo- or heterodimerization together with the related MiT (microphthalmia) family members TFEB, TFEC, and TFE3 (Hemesath et al., 1994). The MiT family members all share a common b-HLH-zip dimerization motif. The b-HLH-zip motif contains a positively charged fragment involved in DNA binding as well as a transactivation domain (TAD) (Hemesath et al., 1994). As a result of the differential usage of alternative promoters, a single *MITF* gene produces several isoforms. Nine different isoforms of MITF are known to exist, including MITF-A, MITF-B, MITF-C, MITF-D, MITF-E, MITF-H, MITF-J, MITF-Mc, and MITF-M (Kawakami & Fisher, 2017). These isoforms differ in the N-terminus of the protein, due to alternative first exons and show tissue-specific expression. The expression of the shortest isoform MITF-M (hereby termed MITF) (a 419-residue protein) is limited to melanocytes and melanoma cells.

Functionally, MITF binds to so-called E-box sequences, usually containing a 6-base pair CACATG motif. The specificity depends on the flanking sequences, the central bases, and the amino acid sequence of the basic region of the motif (Goding & Arnheiter, 2019). Studies have shown that MITF bind a specific E-box variant termed the M-box (Lowings et al., 1992). The M-box consists of a core CATGTG E-box motif (Aksan & Goding, 1998). Later studies have also revealed that MITF also recognizes the palindromic sequence CACGTG. Although other transcription factors such as

myelocytomatosis oncogene cellular homolog (MYC), myc-associated factor X (MAX) and upstream stimulatory factor (USF) also commonly bind this palindromic sequence, MITF does not form heterodimers with other b-HLH-Zip transcription factors than MiT family members.

1.3.2 MITF target genes

Over the last two decades, more than 40 MITF target genes have been identified (Hoek, Schlegel, & Eichhoff, 2008). Moreover, ChIP-seq analyses of genomewide MITF binding has indicated that MITF binds between 12000 and 100000 genomic sites (Hoek, Schlegel, & Eichhoff, 2008; Webster et al., 2014). However, the binding of a transcription factor to DNA might not necessarily translate to the regulation of a nearby gene. In fact, Strub and colleagues showed that only 465 genes could be confirmed as directly regulated by MITF (Strub et al., 2011). MITF is shown to promote differentiation-related functions, including melanosome biogenesis, transport, and equilibrium. MITF is also essential for pigment production in melanocytes through direct transcriptional control over key pigmentation genes, such as TYR, TYRP1, and DCT, MLANA, SILV, and SLC24A5 (Fang et al., 2002; Yasumoto et al., 1995). Table 2 lists MITF target genes involved in differentiation.

MITF target genes	Biological role	References
DIFFERENTIANTION		
Tyrosinase	Melanin synthesis enzyme	Fang, Tsuji, & Setaluri, 2002
TYRP1	Melanin synthesis enzyme	Yasumoto, Yokoyama, Shibata, Tomita, & Shibahara, 1995
DCT	Melanin synthesis enzyme	Yasumoto, Yokoyama, Shibata, Tomita, & Shibahara, 1995
MC1R	Receptor pigmentation pathway	Busca and Ballotti, 2000
KIT	Receptor pigmentation pathway	Phung et al., 2011
GPR143	Melanosome biogenisis	Cortese et al., 2005
MLANA	Melanosome biogenisis	J.Du et al., 2003
HPS4	Melanosome biogenisis	Hoek et al., 2008
LYST	Melanosome biogenisis	Hoek et al., 2008
SILVER	Melanosome biogenisis	J.Du et al., 2003
Rab27a	Melanosome transport	Bahadoran et al., 2001
SLC45A2	Ionic equilibrium	Du and Fisher, 2002
SLC24A5	Ionic equilibrium	Du and Fisher, 2002

Table 2. MITF target genes involved in melanocyte differentiation.

In addition to being involved in melanocyte differentiation and pigmentation, MITF is involved in other processes, such as cellular senescence, apoptosis, proliferation, migration/invasion and regulation of transcription (Table 3).

MITF target genes	Biological role	References
PROLIFERATION AND SURVIVAL		
DIAPH1 (p27)	Cell cycle inhibition	Carreira et al., 2006
CDKN1A	Cell cycle inhibition	Vidal et al., 1995
CDKN2A	Cell cycle inhibition	Loercher et al., 2005
CDK2	Cell cycle progression	Du et al., 2004
TBX2	Cell cycle progression	Yajima et al., 2011
c-MET	Metastatic potential	McGill et al., 2006
BCL2	Inhibition of apoptosis/survival	McGill et al., 2002
BIRC7	Inhibition of apoptosis/survival	Vucic et al., 2000
SNAI2	Metastatic potential	Sanchez-Martin et al., 2005
HIF1α	Inhibition of apoptosis/survival	Busca et al., 2005
APEX1	Inhibition of apoptosis/survival	Liu et al., 2009

Table 3. MITF target genes involved in melanocyte proliferation and survival.

1.3.3 Transcriptional regulation of MITF

MITFs role as the master regulator of melanocyte differentiation, growth, and survival is reflected by its complex regulation as illustrated below in figure 5.

The cAMP-mediated cAMP response binding protein (CREB) transcription factor is shown to activate MITF in response to increased cAMP levels downstream of the MC1-receptor (Huber et al., 2003). CREBs ability to activate MITF has been reported to depend on Sry-related HMG-box (SOX10) (Huber et al., 2003). SOX10 is a member of the high-mobility group-domain SOX family of transcription factors and is demonstrated to play an important role in vertebrate neural crest development, including the establishment and maintenance of the melanocyte lineage. Bondurand and colleagues found that SOX10 binds directly to the MITF promoter, and they also revealed that SOX10 acts synergistically with paired box 3 (PAX3) on the MITF

promoter (Bondurand et al., 2000). Previous work had already described the transcription factor PAX3 as an essential regulator of MITF (Watanabe et al., 1998), and therefore crucial for melanocyte lineage survival during early development (Lang et al., 2005)

Further, the POU domain transcription factor (BRN2) is a neuronal-specific transcription factor that binds to the proximal region of the MITF promoter. BRN2 is an ERK target gene and is widely expressed in melanoma cells (Goodall et al., 2004; Wellbrock et al., 2008). BRN2 ablation has been shown to reduce MITF levels (J. A. Thomson et al., 1995; Thurber et al., 2011), and Wellbrock et al. showed that BRN2 increases transcription at the MITF promoter in BRAF mutant melanoma (Wellbrock et al., 2008). However, MITF expression has also been shown to remain unaltered or to increase after BRN2 depletion (Goodall et al., 2008; Thurber et al., 2011). WNT/ß-catenin activates MITF expression through a LEF1/TCF site in the MITF promoter, and in zebrafish, it induces MITF-driven differentiation during early development (Dorsky et al., 2000; Takeda et al., 2000). In addition, constitutive activation of ß-catenin alters endogenous MITF levels, and might, therefore, be involved in the phenotypic effects of ß-catenin-lymphoid enhancer-binding factor 1 (LEF1)/TCF on melanoma growth and survival (Widlund et al., 2002).

Thomas and Erickson identified forkhead box D3 (FOXD3) as a suppressor of MITF in zebrafish and quail. FOXD3 has been reported to suppress MITF by preventing PAX3 binding to the MITF promoter (Thomas & Erickson, 2009). FOXD3 is also widely expressed in melanoma cells and has been demonstrated to convey resistance to BRAF inhibitors through repression of MITF expression, as well as activation of the v-erb-b2 avian erythroblastic leukemia viral oncogene homolog 3 (ERBB3) receptor (Abel et al., 2013).

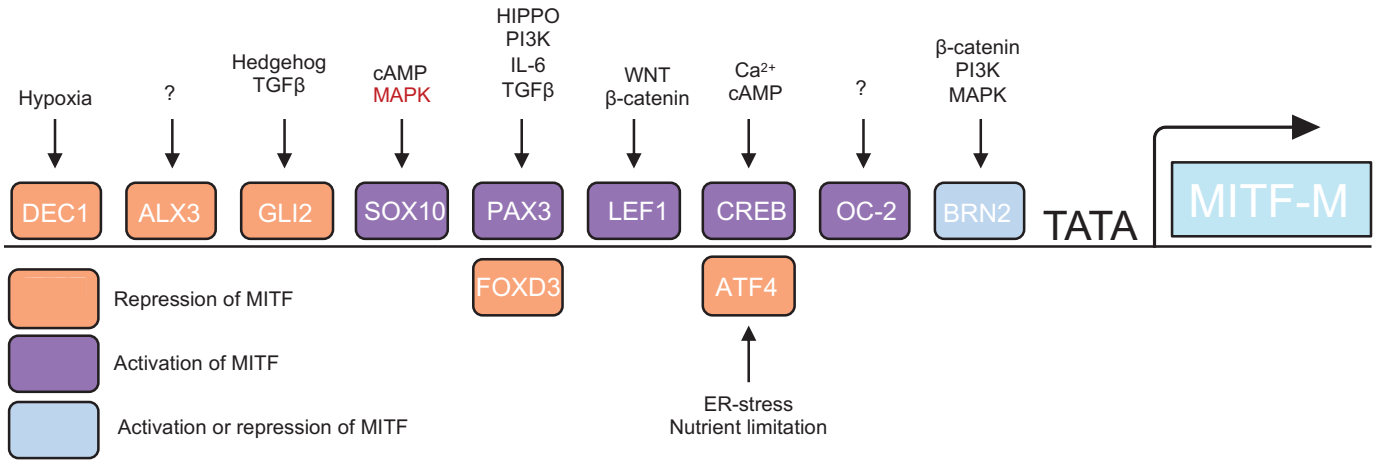

FIgure 5. Regulators of MITF. Adapted from Goding and Arnheiter 2019. Simplified figure showing transcription factors that positively or negatively regulate the MITF promoter, and their signaling pathway response.

1.3.4 Post-translational regulation of MITF

The activity of MITF depends on co-operating partner availability and its numerous post-translational modifications, including phosphorylation, sumoylation, ubiquitination, and acetylation. The understanding of MITF as a target of phosphorylation is relatively limited and somewhat ambiguous. The most studied phosphorylation of MITF was initially described by Hemesath and colleagues, showing phosphorylation by ERK at S73 (Hemesath et al. 1998). Since then, other studies have confirmed this finding, and that ERK2 binds directly to the N-terminus of MITF (Sato-Jin et al. 2008; Molina et al. 2005). Initially, it has been reported that S73 phosphorylation increased binding of MITF to p300 and CBP transcription cofactors (Price et al. 1998) (see figure 6), and at the same time, S73 phosphorylation also targets MITF for ubiquitin-dependent proteolysis (Price et al. 1998; Wu et al. 2000). Recently, phosphorylation of S73 by ERK was suggested to act as a priming event for S69 phosphorylation by the WNT-pathway related kinase GSK3. This dual phosphorylation event was shown to activate a nuclear export signal (Ngeow et al. 2018). GSK3 has been reported to phosphorylate MITF at multiple sites, and S298 has been of great interest, as a mutation at this site is linked to Wardenburg Syndrom II (Takeda 2000). Further, three more sites, S397, S401, and S405, have been reported as GSK3 phosphorylation sites and suggested to be involved in MITF

protein stability (Ploper et al. 2015). Also, RSK phosphorylation of S409 appears to affect protein stability via priming for GSK3 phosphorylation (Ploper et al. 2015). More recently, AKT is, like RSK, shown to phosphorylate MITF on S409. This study proposes that AKT promotes MITF degradation. They also report that AKT-mediated phosphorylation stimulates MITF to interact with p53 and CDKN1A expression (C. Wang et al. 2016).

MITF is also modified by the small ubiquitin-like modifier SUMO. SUMOylation is a multistep process involving continuous actions of E1 (SAE1/SAE2), E2 (UBC9), and E3 (PIAS3) enzymes (Gareau & Lima 2010). In vitro assays have shown that SUMOylation of MITF occurs on two lysine residues, K182 and K316 (Murakami & Arnheiter 2005; Miller et al. 2005). Interestingly, the germline MITF E318K mutation seems to prevent the SUMOylation of MITF on K316, leading to a predisposition for melanoma (Bertolotto et al. 2011). SUMOylation has been suggested to impact protein localization, stability, and/or activity (Andreou & Tavernarakis 2010). However, inhibition of MITF SUMOylation does not seem to affect the cellular stabilization or localization of MITF (Murakami & Arnheiter 2005), but rather the transcriptional activity (Bertolotto et al. 2011; Yokoyama et al. 2011). HypoSUMOylated MITFE318K cells have been shown to have a higher global transcriptional activity that may lead to gain-of-function properties (Bertolotto et al. 2011). Ubiquitination is another proposed modification of MITF and is likely to control protein stability. While the mechanisms behind this event are unclear, ubiquitin-specific protease 13 (USP13) has been identified as a MITF deubiquitination enzyme (Zhao et al. 2011). MITF has also been shown to be a substrate of caspases after D345 in the C-terminal domain. Interestingly, a non-cleavable MITF mutant (D345A) renders melanoma cells resistant to apoptotic stimuli (Larribere et al. 2005). Lastly, when cells express a constitutively active mutant form of the KIT receptor (KITD816V) formation of a complex between KIT, SRC and MITF lead to phosphorylation of Y22, Y35 and Y90 in the MITF N-terminal (Phung et al. 2017). Schematic illustration of modifications is shown in figure 6.

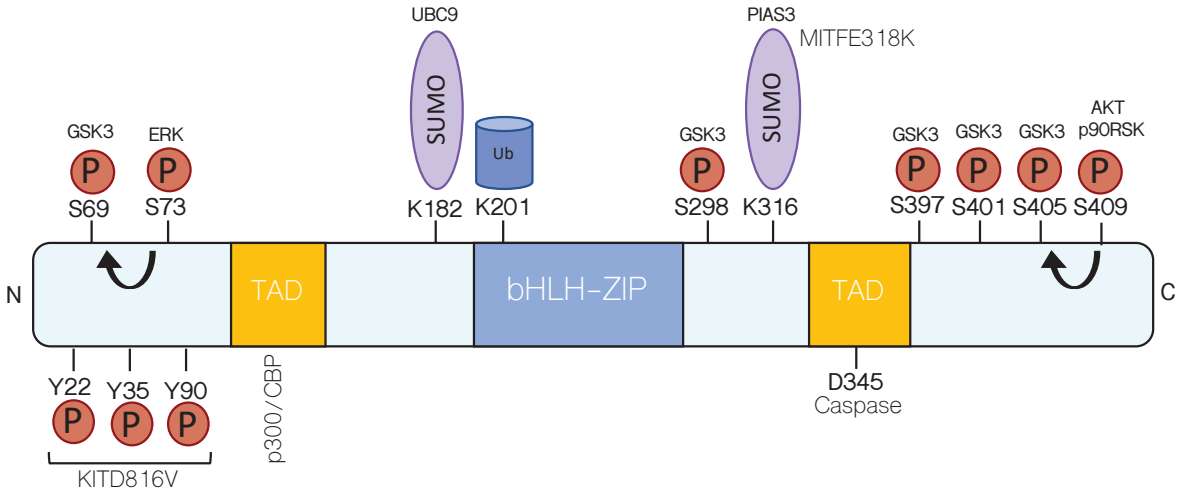

Figure 6. Post translational modifications of MITF. Schematic domain structure of MITF protein and key post-translational modifications. Phosphorylation can enhance MITF transcriptional activity, enhance interaction between p300/CBP, or promote proteasome-dependent degradation of MITF. Other modifications include SUMOylation, ubiquitination and caspase-mediated cleavage.

1.4 Melanoma treatment

Melanoma is exceptionally challenging to treat because of its genetic complexity and high mutation burden. As mentioned above, the Cancer Genome project/Sanger Institute identified oncogenic mutations in the MEK-upstream kinase BRAF in over 50% of all melanomas (H. Davies et al., 2002). This discovery leads to an explosion in novel melanoma studies with a focus on the MAPK signaling pathway. Prior to 2011, the only approved treatments for metastatic melanoma were high dose Interleukin 2 (HD IL-2) and the chemotherapy agent dacarbazine, but neither of these treatments increased overall survival of melanoma patients. However, recognition of key molecular mutations that drive tumorigenesis and advancement in our understanding of tumor immunology has led to breakthroughs over the last few years. Treatment is now mainly based on two pillars: targeted therapy and immunotherapy.

The first targeted therapy to demonstrate substantial efficacy against advanced melanoma was vemurafenib, an adenosine triphosphate-competitive BRAF inhibitor (Chapman et al., 2011), which was approved by the FDA in 2011. Compared to chemotherapy, vemurafenib improved clinical response, and a large number of

patients experienced rapid tumor regression, but unfortunately, the majority of patients become resistant and experienced relapse over time (Wagle et al., 2011). Of note, studies have also shown that BRAFV600E heterogeneous cells exhibit a paradoxical activation of BRAFWT after vemurafenib treatment (Halaban et al., 2010; Hall-Jackson et al., 1999). As targeting BRAF primarily has shown to eventually lead to resistance, targeting downstream effectors of BRAF has been investigated as a strategy (Sarkisian & Davar, 2018). Consequently, in 2013 Trametinib, a MEK1/2 inhibitor, was approved by the FDA as monotherapy in BRAF mutated melanoma based on prolonged overall survival in trials. Moreover, a combined treatment of trametinib and dabrafenib (BRAF-mutant inhibitor) was FDA-approved in 2014, and just last year, the FDA approved the combination of encorafenib (BRAFi) and binimetinib (MEKi). This combination has provided clinically beneficial results as shown by the improvement in both progression-free and overall survival compared to vemurafenib monotherapy in patients (Dummer et al., 2018).

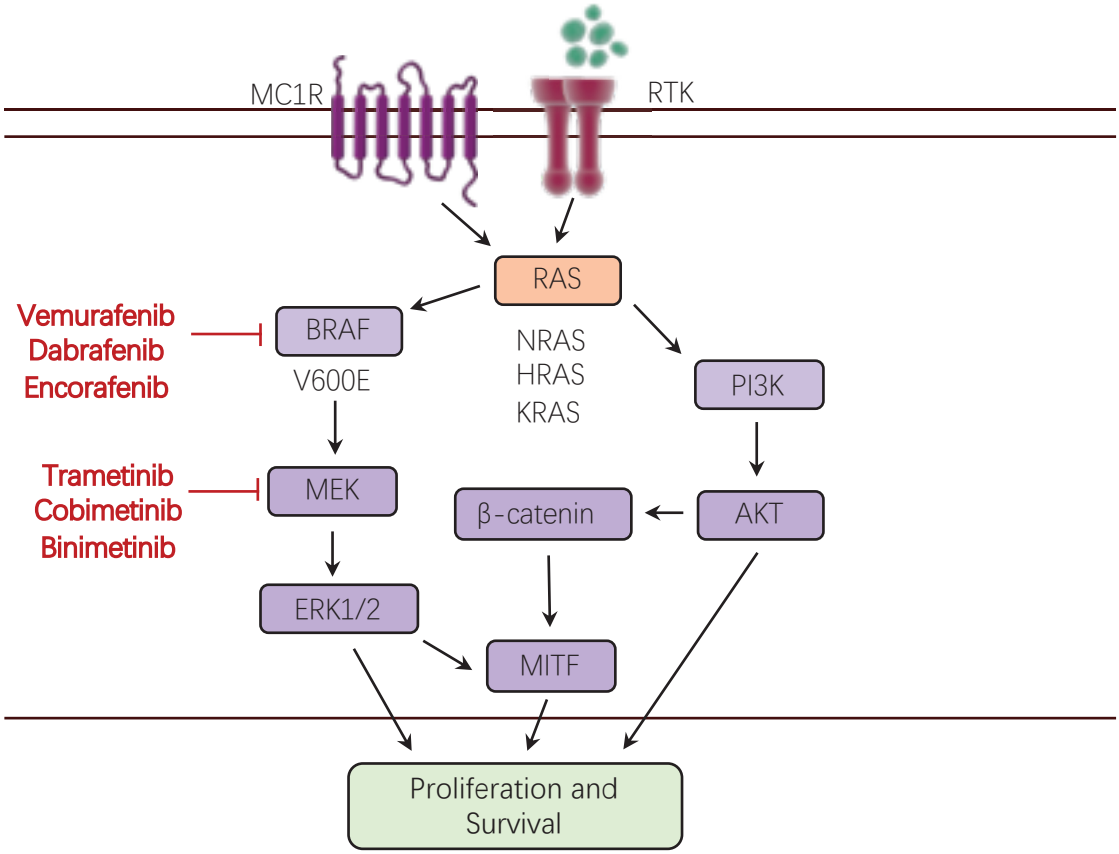

Figure 7. FDA approved small molecular inhibitors targeting the MAPK pathway. Vemurafenib, dabrafenib and encorafenib targeting BRAFV600E. Trametinib, cobimetinib and binimetinib targeting MEK.

Recently, immunotherapy has been introduced into the clinic and has shown promising results in several cancers, especially melanoma. Immunotherapy is now at the frontline of melanoma treatment. Ipilimumab, a human monoclonal antibody against cytotoxic T-lymphocyte-associated protein antigen 4 (CTLA-4), was approved by the FDA in 2011 (Lipson & Drake, 2011). CTLA-4 is an inhibitory checkpoint receptor that blocks T-cell activation, which induces an immune response in approximately 20% of the patients (Domingues et al., 2018). Although ipilimumab has led to prolonged overall survival, its role has decreased with the development of antibodies against programmed cell death receptor 1 (PD-1). Nivolumab and pembrolizumab, two anti-PD-1 antibodies, are currently showing higher efficacy and less toxicity compared to ipilimumab (Marconcini et al., 2018). Combined treatment with ipilimumab and nivolumab has been FDA approved for the treatment of advanced melanoma, regardless of mutation status (Wróbel et al., 2019). Just recently, the five-year outcome in patients receiving combined nivolumab and ipilimumab was reported (Larkin et al., 2019). This study shows that overall survival after five years was 52% in the nivolumab -ipilimumab combination group, 44% in the nivolumab group alone, compared with the ipilimumab group (26%) (Larkin et al., 2019). Overall, these new agents have improved patient survival significantly compared to previous treatment regimes.

Despite recent progress, both targeted- and immunotherapy has their limitations. Although recent evidence suggests that Immunotherapy can lead to durable responses for patients, the overall response rate is low (12-58%) as there are currently no biomarkers to predict which patients will respond to the treatment (Haslam & Prasad, 2019; Larkin et al., 2019). In contrast, BRAF and MEK inhibitors have shown to have a high overall response rate in BRAF-mutated melanoma, but unfortunately, the effect seems to be short-lived (Kakadia et al., 2018). Heterogeneity in treatment response is also a significant hurdle to overcome. Therefore, there is a need for more trials to be conducted, further investigating combination treatments, dosages, and new therapies. For timeline describing FDA approved treatment see figure 8.

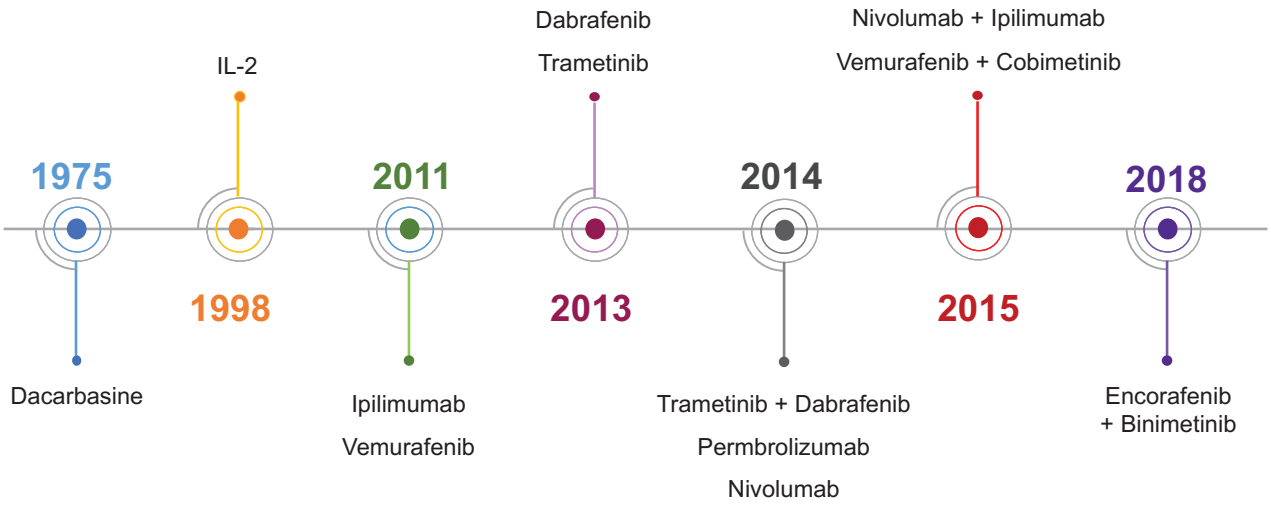

Figure 8. Timeline showing FDA approved drugs for the treatment of advanced melanoma.

1.4.1 New strategies for melanoma treatment

New treatment strategies are needed in order to overcome the numerous resistance mechanisms in melanoma. As mentioned in the previous section, combination therapy is one of the current strategies for overcoming resistance.

Combination of BRAF and MEK inhibitors

The combination of BRAF and MEK inhibitors extends survival compared to BRAF monotherapy by counteracting MEK mediated MAPK-reactivation in resistance (Atkinson et al., 2016). Unfortunately, acquired resistance has once again become a significant obstacle, and novel approaches and treatment combinations are needed (Kakadia et al., 2018).

Combination of PI3K pathway and MAPK inhibitors

Approaches aiming at inhibiting the MAPK and PI3K pathways simultaneously have been proposed as a treatment option (Smalley et al., 2006). Preclinical data have demonstrated that the combination of MAPK and PI3K pathway inhibitors provide good efficacy in BRAFV600E mutant cell lines (Gopal et al., 2010; Villanueva et al., 2010). Upon resistance, the addition of an AKT or mTOR inhibitor to persistent BRAF

inhibitor treatment, or switching to combining a MEK inhibitor with PI3K pathway inhibitor has also been proposed as a treatment option to overcome resistance (Atefi et al., 2011). Clinical studies have investigated the combination of MAPK and PI3K pathway inhibitors in melanoma as well as in other cancers (ClinicalTrials.gov; NCT01390818, NCT01449058). However, even though these combinations are well tolerated, the data presented show modest clinical activity, and modifications such as drug delivery timing may be needed.

Combination of MAPK inhibitors and immunotherapy

The potential role of combination regimens containing MAPK inhibitors and immunotherapies is currently of considerable interest. One of the challenges in treating patients with immunotherapy is so-called "cold tumors." These tumors have been shown to have low T-cell infiltrates, increased regulatory T-cells, limited immunogenicity, and unfavorable tumor microenvironment (TME) (Rodallec et al., 2018). Interestingly, BRAF and MEK inhibitor treatment have been shown to increase tumor-infiltrating lymphocytes in patient samples (Wilmott et al., 2012). Moreover, studies done in mice and melanoma cell lines have shown that BRAF inhibitor treatment increases T-cell infiltration, increase interferon-gamma and upregulates melanoma lineage antigens including MLANA, SILV, TYRP-1 and DCT (Boni et al., 2010; C. Liu et al., 2013; Sapkota et al., 2013). In vitro studies have shown that MEK inhibitors alone may impair T-cell function and proliferation (Boni et al., 2010; Vella et al., 2014). However, studies on BRAF, in combination with MEK inhibitors, show that T cell infiltration persists under such treatment (Frederick et al., 2013; Hu-Lieskovan et al., 2015). Initial trials combining BRAF inhibitor vemurafenib with CTLA-4 checkpoint blocking antibody ipilimumab led to severe toxicity and was discontinued (Ribas et al., 2013). However, currently, several ongoing trials are testing the safety of combinations and continuous treatment with BRAF, MEK, and PD-1 or PDL1 inhibitors (ClinicalTrials.gov; NCT02130466, NCT02967692, NCT02908672). Preliminary results from one of the studies (ClinicalTrials.gov; NCT02130466) combining dabrafenib (BRAFi), trametinib MEKi and pembrolizumab (PD-1) in 15 patients initially showed that 73% experienced adverse events (grade 3/4) treated with this combination (Ribas et al., 2019). Nevertheless, after careful adjustments in treatment regiment, a subset of patients show a long-duration response after two

years (Ribas et al., 2019). In addition, an ongoing study is exploring triple therapy, as well as applying an induction period where patients receive BRAF and MEK inhibitors and then applying PD-1 inhibitors at a later time point, which may improve toxicity issues during treatment (ClinicalTrials.gov; NCT02858921).

Combination of MAPK inhibitors and RTK inhibitors or antibodies

Upregulation of RTKs has been implicated in resistance mechanisms after BRAF inhibitor treatment, and several preclinical studies suggest the combination of RTK inhibitor and MAPK pathway inhibitors as a treatment strategy in melanoma. Members of the ERBB RTK family has been shown to be upregulated following BRAF inhibitor treatment, and several studies have shown that combining BRAF/MEK inhibitors with the pan ERBB inhibitor lapatinib or antibodies against ERBB3 provides a therapeutic benefit both *in vitro* and *in vivo* (Abel et al., 2013; Fattore et al., 2013). Finally, an ongoing study at Haukeland hospital is in the process of assessing the efficacy of the AXL inhibitor R428 (BGB324/bemcentinib) in combination with dabrafenib and trametinib or the PD-1 inhibitor pembrolizumab (ClinicalTrials.gov; NCT02872259).

Drug holiday

MAPK inhibitor-resistant tumor cells may develop drug dependency, and this has been reported to be relayed by an ERK2-dependent phenotype switch (Kong et al., 2017). Recent studies have shown that tumor cells die after drug withdrawal, so several studies have looked at intermittent dosing or drug holiday as a potential treatment strategy for resistant melanoma. An ongoing clinical trial is currently investigating the effect of intermittent dosing (EudraCT:2016-005228-27). The patients are randomized to receive dabrafenib and trametinib either continuously or intermittently (dabrafenib days 1-21 and trametinib days 1-14) on a 28-day cycle.

1.4.2 Resistance against MAPK inhibitors in melanoma

Small molecule inhibitors to MAPK inhibitors have been shown to benefit a majority of patients with tumors carrying the BRAFV600E mutation (Larkin & Fisher, 2012). However, resistance commonly occurs, and the resistance to targeted therapy may be innate or acquired. Innate resistance to BRAF inhibitors is rare and occurs in less than 15-20% of patients with BRAF-mutated melanoma (Bollag et al., 2010; Chapman et al., 2011). On the other hand, acquired resistance occurs in nearly 100% of patients treated with BRAF inhibitors within the first year of treatment (K. B. Kim et al., 2011).

Wagle et al. 2011 first described resistance to BRAF inhibition in a 38-year-old male patient with subcutaneous metastatic nodules who had received treatment with the BRAFi vemurafenib. Initially, the patient experienced complete regression of subcutaneous lesions, but unfortunately, after 16 weeks, the patient experienced a widespread relapse with rapid disease progression and died several weeks later (Wagle et al., 2011). Numerous mechanisms of resistance to targeted inhibitors have been suggested. Reactivation of the MAPK pathway in response to treatment is the most described. (Lito et al., 2013; Whittaker et al., 2013).

Reactivation of the MAPK pathway may be achieved through numerous mechanisms allowing the cells to bypass BRAF inhibition. Alterations such as CRAF overexpression, BRAF splice variation, or amplification have been described (Poulikakos et al., 2011; Shi et al., 2012). Upstream from BRAF, overexpression of NRAS and loss of NF1 can lead to BRAF independent MEK-ERK activation (Greger et al., 2012; Nazarian et al., 2010), and amplification of mitogen-activated protein kinase kinase kinase 8 (COT/MAO3K8) has also been reported to reactivate the MAPK pathway (Johannessen et al., 2010).

Aside from MAPK signaling, the PI3K pathway is often activated in drug-resistant melanomas. Increased PI3K signaling may be due to deletion or loss of function in PTEN (～10%) (Q. Zuo et al., 2018), or activating mutations in AKT (Shi et al., 2014). Finally, receptor tyrosine kinase (RTK) upregulation resulting in PI3K activation has

been reported to play a crucial role in overcoming BRAF inhibition (Nazarian et al., 2010; Villanueva et al., 2010).

Within the scope of this thesis, we have mainly focused on resistance driven by the RTK receptors ERBB3 and AXL; and a phenotype switch driven resistance mechanism orchestrated by MITF. Figure 9 below summarizes the most described resistance mechanisms following MAPK inhibition.

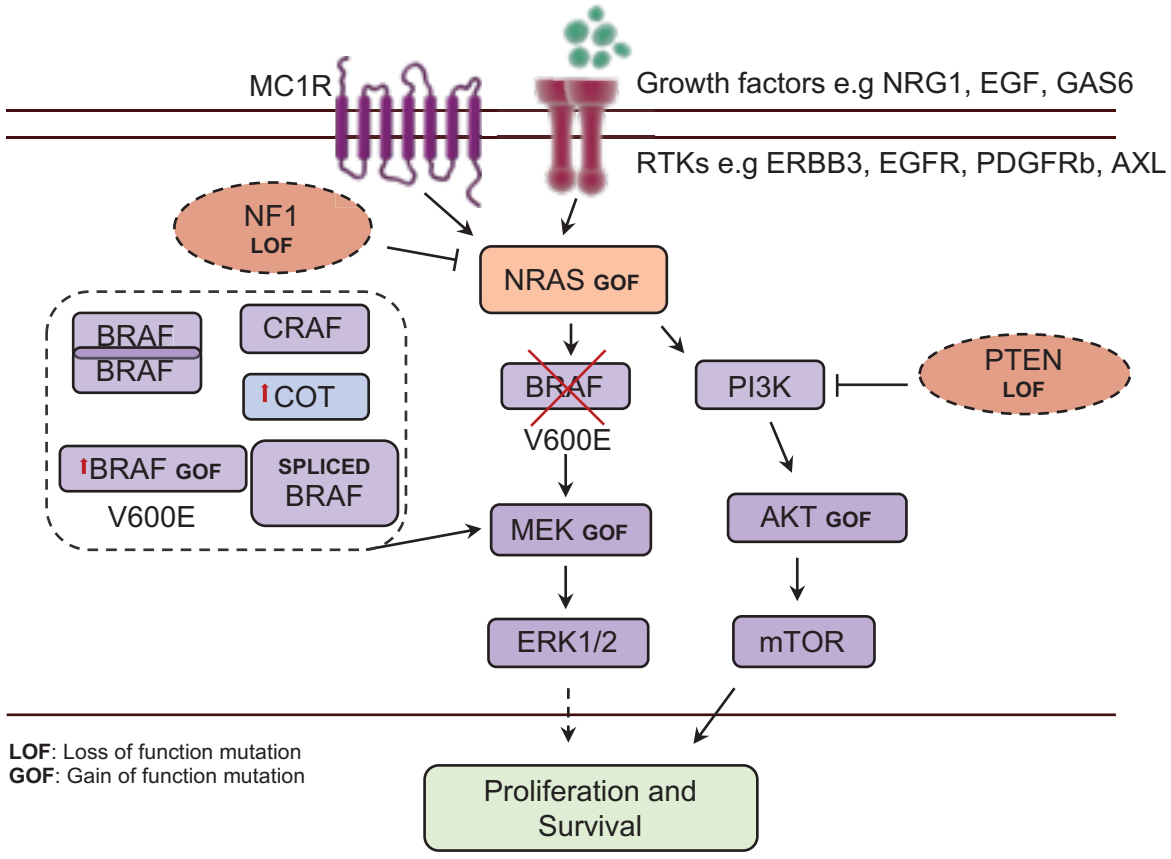

Figure 9. Common mechanisms of resistance to MAPK inhibitors. Reactivation of the MAPK pathway, as well as the PI3K pathway, most frequently via mechanisms such as gain-of-function mutations, loss of tumor suppressor genes, activation of other RAS isoforms such as CRAF.

Receptor tyrosine kinases (RTKs)

RTKs are high-affinity surface receptors for several growth factors, hormones, and cytokines, and the MAPK and PI3K pathways are primarily activated by RTKs. RTKs are a diverse family with approximately 58 receptors, which can be grouped into 20

categories (Robinson et al. 2000; Lemmon & Schlessinger 2010). The mechanism of action and the critical components of the RTKs intracellular signaling pathways are highly conserved in evolution (Robinson et al. 2000). RTKs share a similar protein structure comprised of an extracellular ligand-binding domain, a single transmembrane helix, and a cytoplasmic region containing the protein tyrosine kinase (TK) domain plus additional carboxy (C-) terminal and juxtamembrane regulatory regions (Lemmon & Schlessinger 2010). Under normal physiological conditions, RTKs are activated by their cognate protein-ligands. In the absence of a ligand, RTKs are tethered to the membrane in either mono -or dimeric form but remain inactive (Hubbard 2004). Ligand binding to extracellular regions stabilizes the dimeric structure (Lemmon & Schlessinger 2010; Du & Lovly 2018; Hubbard 2004). For most RTKs, conformational changes allow for trans-auto phosphorylation of each tyrosine kinase domain, and a release of the cis-autoinhibition. This conformational change allows the tyrosine kinase domain (TKD) to assume its active conformation. Further, autophosphorylation of RTKs also recruits and activates a wide variety of downstream signaling proteins such as Src homology-2 (SH2) or phosphotyrosine binding (PTB) domains. These domains bind to specific phosphotyrosine residues within the RTK and engage downstream mediators that generate crucial cellular signaling (Du & Lovly 2018; Pawson et al. 2001). Under normal conditions, RTKs are tightly regulated by tyrosine phosphatases, preventing uncontrolled signaling (Ostman & Böhmer 2001). For a schematic overview of basic RTK functions, see figure 10.

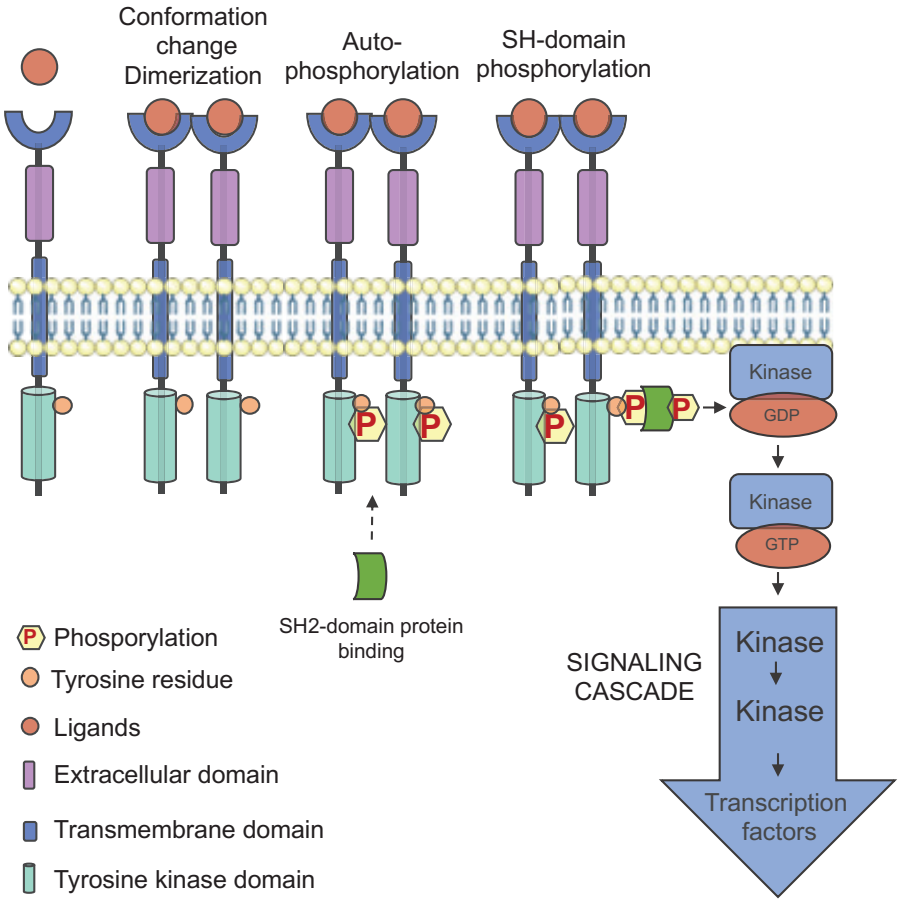

Figure 10. Basic RTK function.

Inspired by sciencedirect.com/topics/neuroscience/enzyme-linked-receptor. Overview of basic RTK function under normal conditions.

Genetic changes or abnormalities that alter normal RTK function and regulation play a role in or contribute to numerous diseases, including cancer (Hubbard & Miller, 2007; Lemmon & Schlessinger, 2010). Oncogenic RTK signaling include activation by gain-of-function mutations (Z. Wang et al., 2011), overexpression and genomic amplification (Lopez-Gines et al., 2010), chromosomal rearrangements (Stransky et al., 2014), constitutive activation by kinase domain duplication (K. Kemper et al., 2016), and autocrine activation (Ciardiello & Tortora, 2001) (Figure 11).

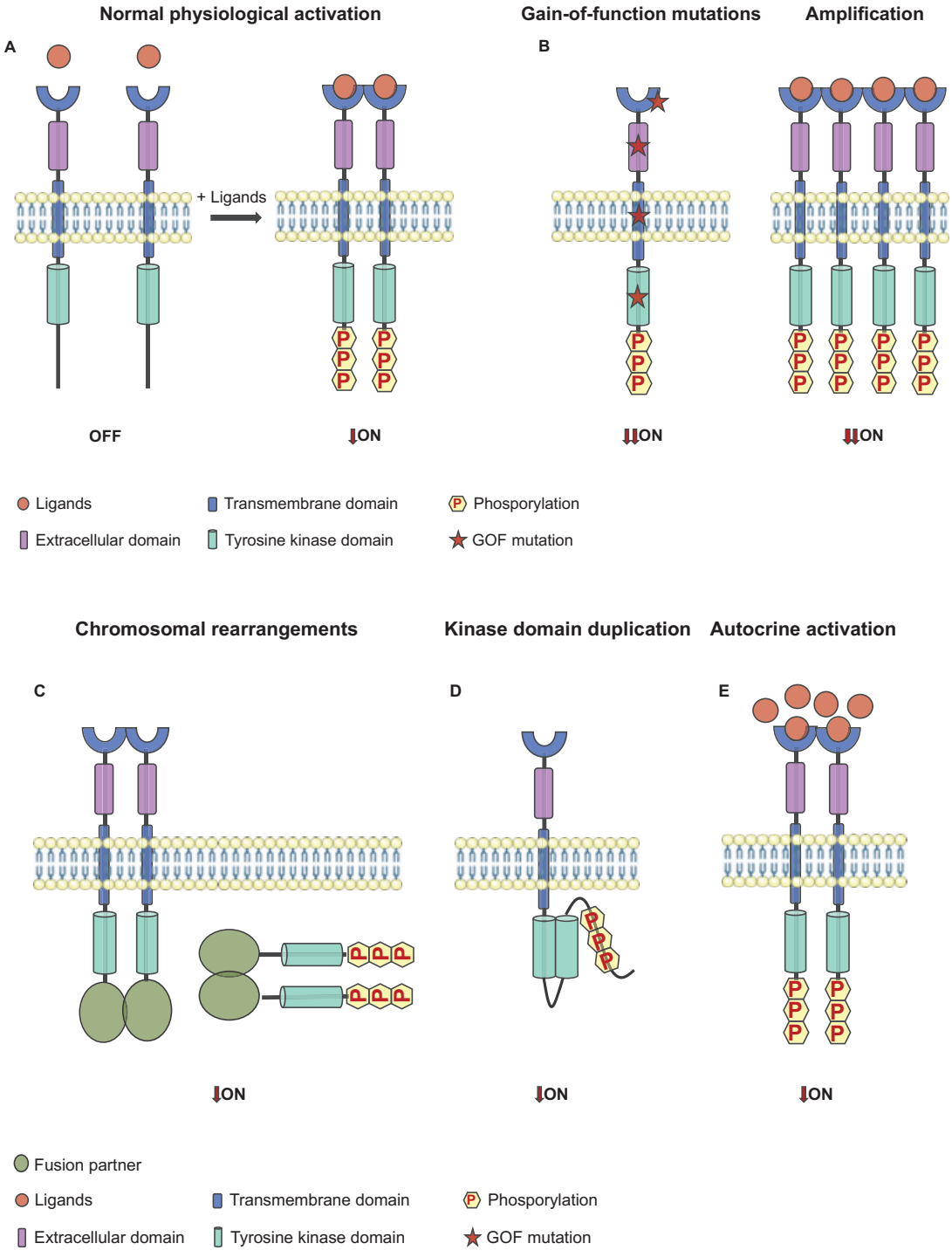

Figure 11. Mechanisms of normal physiological and oncogenic signaling. Adapted from Du and Lovly 2018. **A.** Normal ligand-mediated RTK activation. Ligand binding leads to activation of the kinase domain and subsequent phosphorylation of the C-terminal tail. **B.** Gain of function mutations in different parts of the RTK, or receptor amplification results in aberrant down-stream signaling. **C.** Chromosomal rearrangements may result in a hybrid fusion oncoprotein. **D**. Kinase domain duplication forming an intramolecular dimer in the absence of ligands. **E**. Autocrine activation from an increased concentration of ligand.

Importantly, the upregulation of RTKs is strongly implicated in the MAPK pathway inhibitor adaptive and acquired resistance. Attempts to inhibit kinases in the MAPK pathway have revealed extensive feedback looping and compensatory mechanisms involving redirection of RTKs, receptor redundancy and increased growth factor secretion (Abel et al., 2013; Capparelli et al., 2015; Girotti et al., 2013; Müller et al., 2014; Nazarian et al., 2010; Straussman et al., 2012; Villanueva et al., 2010). A list of the most well-studied mechanisms is outlined in table 4.

RTKs and Growth Factors	References
PDGFRβ	Nazarian et al. 2010
IGF-1R	Villanueva et al. 2010
HGF	Straussman et al. 2012
EGFR	Girotti et al 2013; Ji et al. 2015
ERBB3	Abel et al. 2013
AXL	Müller et al. 2014
NRG1	Capparelli et al. 2015

Table 4. The most studied RTK and growth factors involved in resistance. Overview of the most well-studied RTKs and growth factors implicated in MAPK pathway inhibitor resistance.

The RTKs which have been most frequently linked to MAPK inhibitor drug resistance in melanoma are the ERBB family receptor ERBB3, and the TAM family receptor AXL. The ERBB family of receptor RTKs are essential regulators of cell differentiation, survival, proliferation, and migration. Abnormal activation of ERBBs is considered to be a hallmark of many cancers (Bill et al., 2010; Bublil & Yarden, 2007). The ERBB comprises four members: epidermal growth factor (EGF) receptor (also termed ERBB1/HER1), ERBB2/Neu/HER2, ERBB3/HER3, and ERBB4/HER4 (Hynes & Lane, 2005; Olayioye et al., 2000). ERBB ligands are growth factor members of the epidermal growth factor (EGF) family (Roskoski, 2014). Under normal conditions, activation of the ERBB receptors is controlled by the temporal and spatial expression of their ligands (Fuller et al., 2008). Binding of ligands induces the formation of homo- and heterodimers, tyrosine kinase activation, and c-terminal tail phosphorylation of tyrosines (Mishra et al., 2018). Adapter proteins are recruited, leading to the activation of intracellular signaling pathways (Hynes & Lane, 2005).

The ERBB family member ERBB3 has been implicated in the development of resistance to BRAF inhibitors. The ERBB family member ERBB3 was first identified by Kraus and colleagues in 1989 and suggested to be involved in oncogenic signaling (Kraus et al., 1989). ERBB3 harbors weaker kinase activity than the other ERBB family members but initiates strong downstream PI3K/AKT signaling through heterodimerization with other ERBB RTKs such as ERBB2 (Riethmacher et al., 1997). The ERBB2 receptor harbors a kinase domain but lacks a known ligand (Burgess et al., 2003). ERBB3 upregulation has been associated with several malignancies, including ovarian, breast, gastric, bladder, prostate, lung, and colorectal cancer, as well as squamous cell carcinoma, and melanoma (Beji et al., 2012; Hayashi et al., 2008; Koumakpayi et al., 2006; Lipton et al., 2013; Nielsen et al., 2015; Qian et al., 2015; Reschke et al., 2008; Siegfried et al., 2015; Tanner et al., 2006). In BRAFV600E mutated melanoma, ERBB3 is phosphorylated in response to BRAF or MEK inhibition leading to sustained PI3K signaling (Abel et al., 2013; Fattore et al., 2013). Moreover, forkhead box D3 (FOXD3) has been shown to induce ERBB3 expression after BRAF inhibition (Abel et al., 2013). Additionally, the ERBB3 ligand NRG1 has also been found to contribute to increased PI3K signaling after vemurafenib treatment (Capparelli et al., 2015; Fattore et al., 2013)

The TAM receptor family comprises TYRO3, AXL, and MERTK and was first identified in 1991 (Lai & Lemke, 1991). Similar to the other RTKs, the TAM receptors regulate survival, growth, differentiation, adhesion, and motility. However, the TAM family is distinguished from other RTKs by a rare conserved amino acid sequence, KWIAIES, within its intracellular tyrosine kinase domain (Graham et al., 2014). In normal tissue, TAM receptors contribute to immune response regulation, including clearance of apoptotic cells, and inhibition of cytotoxic immune evasion in response to apoptosis. Due to these functions, deficiencies in TAM signaling are associated with chronic inflammatory and autoimmune diseases (Rothlin et al., 2015). TAM receptors are overexpressed or ectopically expressed in a wide variety of human cancers (Graham et al., 2014).

The TAM family member AXL was initially identified as a transforming gene in chronic myelogenous leukemia (Liu et al. 1988). Protein S and the vitamin-K dependent growth arrest-specific protein 6 (GAS6) are known TAM receptor ligands.

AXL has the highest affinity for GAS6 (Lemke, 2013). Further, heterodimerization with non-TAM RTKs such as EGFR, which causes rapid phosphorylation of AXL, has been reported (Vouri et al., 2016). Signaling pathways activated downstream of the AXL receptor include the MAPK and PI3K pathways (Y. Li et al., 2014). AXL is a supposed driver of a variety of cellular processes that are critical for development, growth, and tumor metastasis, such as proliferation, migration, EMT and immune modulation (Gay et al., 2017; Gjerdrum et al., 2010; Guo et al., 2017). The AXL receptor is ubiquitously expressed at low levels but might be upregulated upon an immune response or cellular damage (i.e., anti-cancer-therapy or hypoxia) (Gay et al., 2017). AXL has been implicated as a contributor to therapy resistance in numerous cancers, including non-small cell lung cancer, renal cell carcinoma, gastrointestinal stromal tumors, leukemia, squamous cell carcinoma and breast cancer (Brand et al., 2015; Dufies et al., 2011; Hsieh et al., 2016; L. Liu et al., 2009; Macleod et al., 2005; Z. Zhang et al., 2012; Zhou et al., 2016). High levels of the AXL receptor have also been described as a marker for BRAF inhibitor insensitivity (Konieczkowski et al., 2014), as well as being up-regulated in response to MAPK inhibition in melanoma (Miller et al., 2016; Müller et al., 2014).

MITFs role in resistance to MAPK inhibitors

MITF seems to play an ambivalent, but important, role in melanoma resistance and its role has been shown to be context-dependent. While MITF has been implicated in both innate (Cohen-Solal et al., 2018) and the acquired resistance (Manzano et al., 2016) to MAPK inhibitors, its specific contribution remains a matter of intense debate. (Carreira et al., 2006; Müller et al., 2014; Smith et al., 2016).

Melanoma cells are not only capable of rapidly adapting to therapies by acquiring novel aberrations, but also, as in melanoma development, have the ability to switch phenotype in an EMT- like manner in order to bypass drug treatment. A proposed model for phenotype switching is the MITF “rheostat" model (Carreira et al., 2006). In this model, melanoma cells are organized according to MITF activity and phenotype (Figure 12).

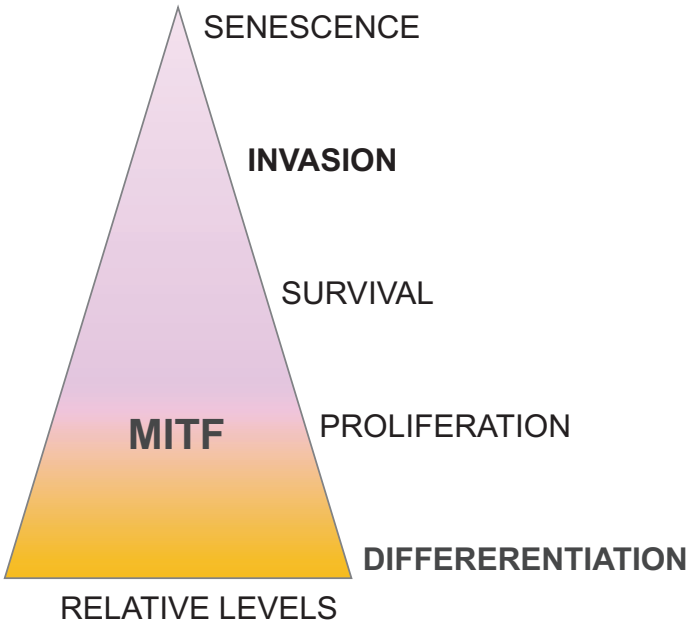

Figure 12. MITF rheostat model. According to this rheostat model, MITFs varied transcriptional activity contributes to various cellular programs spanning from proliferation at high levels of MITF to invasion and senescence at low transcriptional activity,

Müller and colleges reported that cells with low MITF expression display invasive properties and an EMT-like signature. The authors suggest that the cells that acquire resistance lose MITF and undergo dedifferentiation. Further, they found an inverse correlation between low MITF levels and increased expression of the AXL receptor. In contrast, others have reported MITF to be upregulated in response to BRAF inhibition in tumor samples (Smith et al., 2016). Recently it has been suggested that this inconsistency in MITF behavior may be due to an interaction between PAX3 and BRN2 (Smith et al., 2019) Here, the authors suggest that a PAX3/BRN2 rheostat model controls MITF expression downstream of BRAF. They found that low ERK activity leads to increased PAX3 levels and therefore high MITF expression, and in contrast high ERK activation BRN2 levels are high leading to decreased MITF expression. Further, they suggest that this rheostat is maintained during MAPK inhibitor treatment in tumors which further supports the complexity of MITFs role in MAPK inhibitor resistance.

Gene expression changes that result in a phenotypic switch during melanoma development, and in response to treatment, have been strongly linked to progression

and development of resistance. (Müller et al., 2014). Based on these findings, drug-induced phenotype switching from proliferative to invasive phenotype has been proposed as a possible resistance mechanism in melanoma (Kristel Kemper et al., 2014).

2. Aims of study

The understanding of melanoma pathogenesis is crucial for therapeutic discovery. MITF is not only the master regulator of melanocyte development, function, and survival, but has been heavily implicated in melanoma predisposition, initiation, progression, metastasis and drug resistance. In the studies included in this thesis, we aimed to further elucidate the mechanism behind some of these events.

Specific aims of this project were to:

I. Identify novel MITF targets involved in drug resistance.
II. Investigate the role of MITF in the context of MC1R status as inherited MC1R mutations contribute to an increased risk for developing malignant melanoma.
III. Investigate the role of the SOX10/MITF axis in the development of drug resistance in various mutational backgrounds in melanoma.

3. Summary of papers

Paper I

MITF depletion elevates expression levels of ERBB3 receptor and its cognate ligand NRG1-beta in melanoma.

Alver TN, Lavelle TJ, Longva AS, Øy GF, Hovig E, Bøe SL

Oncotarget. 2016 Aug 23;7(34):55128-55140

In this work, we aimed to investigate MITFs role in the regulation of the RTK ERBB3, as MITF has been shown to inversely correlate with other known RTKs, and to play a role in acquired resistance to vemurafenib in melanoma. Here we found that depletion of MITF increases ERBB3 receptor and its cognate ligand expression in melanoma cell lines. We also found that MITF regulates ERBB3 in a FOXD3 dependent as well as independent manner. To address MITF binding in the proximity to ERBB3, NRG1-beta, and FOXD3 we performed ChIP-seq analyses in the Hermes 4C cell line. We found MITF binding signals in the proximity of ERBB3, NRG1-beta, and FOXD3 promoters, suggesting a regulatory function of MITF. Further, we utilized The Human Genome Atlas (TCGA) to investigate the correlation between these genes in patient samples. Here we found a positive correlation between SOX10 and ERBB3. Further, a correlation was also found between FOXD3 and ERBB3, SOX10 and FOXD3, SOX10 and MITF. MITF and NRG1-beta showed the weakest correlation with ERBB3. Finally, we treated the BRAFV600E mutated cell lines SKMEL28 and WM983B with vemurafenib. After two weeks of treatment, we found an extensive down-regulation of MITF followed by an increase in both FOXD3 and ERBB3 protein levels. Together, these results show that depletion of MITF results in increased expression levels of both the ERBB3 receptor and its ligand NRG1-beta, which may have implications for acquired drug resistance in melanoma.

Paper II

Dysregulation of MITF in the context of defective MC1R and RB1/p16/CDK4 leads to melanocyte transformation.

Alver TN*, Lavelle TJ*, Heintz K-M, Wernhoff P, Nygaard V, Nakken S, Øy GF, Bøe SL Urbanucci A, Hovig E

The aim of this study was to investigate the role of MITF as a context-dependent oncogene. We utilized lentiviral transduction to introduce hemagglutinin (HA)-tagged MITF into the immortalized melanocyte cell lines Hermes 4C (MC1R mutated (R160W/D294N)) and in the wild type cell line Hermes 3C. Fluorescence microscopy, RT-PCR, and western blot confirmed successful transduction. Surprisingly, we found endogenous MITF to be undetectable in the transduced Hermes 4C hereby, termed 4C-HA-MITF, and a small reduction in the transduced Hermes 3C hereby, termed 3C-HA-MITF compared to non-transduced parental cell lines. We also found that the MITF regulator SOX10 was undetectable in 4C-HA-MITF at both RNA and protein levels. Further, we observed an altered morphology in the 4C-HA-MITF cells, pointing to a possible transformation event. Transformation was confirmed *in vivo,* where all the injected mice formed tumors (n=10). We then performed ChIP seq on the transduced cell lines and found enhanced MITF chromatin binding in 4C-HA-MITF compared to 3C-HA-MITF. Gene expression array analysis disclosed decreased transcription of key melanocyte specific genes involved in pigmentation and melanosome formation in the 4C-HA-MITF cell line, suggesting a possible de-differentiation. Moreover, we found an upregulation of known EMT related genes affiliated with an invasive melanoma phenotype. Specifically, we observed a marked upregulation of the suggested EMT marker receptor tyrosine kinase AXL, accompanied by a down regulation of the tumor suppressor PTEN. We found that these alterations increased activation of both the MAPK and the PI3K-pathway. We here present a model that may be utilized for further studies on the changes occurring during transformation of malignant melanoma.

Paper III

Co-operative induction of RTK`s contributes to adaptive MAPK drug resistance in melanoma through the PI3K pathway.

Alver TN, Heintz KM, Hovig E, Bøe SL

In this paper we wanted to investigate the MITF/SOX10 axis involvement in RTK mediated resistance to BRAF inhibitors. The study was initiated by investigating possible correlations in patient samples using The Cancer Genome Atlas (TCGA). Here we found an apparent inverse relationship between MITF/SOX10/ERBB3 and AXL. This was supported by both RT PCR and expression analyses in a melanoma cell line panel spanning various mutational backgrounds. Further, we showed that siRNA modulation of MITF and SOX10 affect both ERBB3 and AXL levels in the WM115 cell line. Moreover, siRNA modulation of both AXL and ERBB3 in five cell lines revealed a receptor redundancy as downregulation of AXL led to an upregulation of ERBB3 in all five cell lines. Also, we observed an apparent two-way redundancy in the WM983B and FEMXI cell lines respectively. In an attempt to elucidate the relevance of this observation we wanted to study the receptors during vemurafenib treatment in five melanoma cell lines. We found that during the first week of treatment ERBB3, MITF and SOX10 levels were elevated, before being reduced after resistance was aquired. We also observed a small elevation in the AXL ligand GAS6 levels after 72h treatment. Finally, at the time of resistance AXL and EGFR levels were elevated as well as the NRG1 ligand. Taken together, these results suggest that ERBB3, MITF and SOX10 are elevated in a pre-resistant cell state in our melanoma cell lines, while AXL and EGFR are up-regulated in a stable vemurafenib-resistant state in a subset of melanoma cells.

4. Methodological considerations

4.1 Cell systems and assays

Advances in genomics have, during the last decade, given new opportunities for translational research. However, there is still a need for reliable preclinical models to study basal cancer biology and test hypothesis. Human cancer-derived cell lines are integral models used to study the biology of cancer and to test the therapeutic effect of cancer agents (Sharma et al., 2010). Another benefit is that cell systems are relatively inexpensive to work with compared to animal models. They are also easy to cultivate and expand, which makes it possible to set up extensive studies and screens. Nevertheless, it is crucial to keep in mind the limitations of cell cultures. The cells are grown in an artificial environment that is simplified compared to human physiological conditions, and one major criticism is that after prolonged culturing and passaging, cells might accumulate new mutations and phenotypic drift as they adapt to their artificial environment (Wenger et al., 2004). Cross-contamination is also a risk when keeping cells in culture over a period of time, as well as infections, such as mycoplasma. However, it is customary to frequently test the cells for contamination as well as DNA fingerprinting to check for genetic drift. Another significant limitation of human cell lines is the limited image they provide of the tumor as a whole as cell lines can not reflect the heterogeneity found in tumors. Finally, the lack of stromal cells and a functional immune system has to be considered when utilizing cell lines in experiments, in particular as the focus on these compartments and their role in cancer progression and resistance has increased substantially over the last years.

4.1.1 Cell lines

The melanoma cell lines used in **Paper I and III** SKMEL28, MeWo, and A375 are commercial cell lines obtained from American Type Culture Collection (ATCC). WM35, WM115, WM1341B, WM1366, WM983B, WM45.1, WM239A, WM266.4, WM852, WM1382, WM9, WM793B from the Wistar Institute and finally, LOXIMVI was established in-house. The cell line panel used was chosen based on the diversity in genetic background, reflecting various aspects of mutational importance in melanoma. In **Paper III**, we chose cell lines based on expression levels of MITF,

SOX10, AXL, and ERBB3. In **Paper II**, we utilized the two immortalized melanocyte cell lines Hermes 3C and Hermes 4C to study the effect of MITF overexpression in the context of MC1R loss. Both cell lines were purchased from Wellcome Trust Functional Genomics Cell Bank (Gray-Schopfer et al., 2006). These cell lines are both immortalized by ectopic TERT expression and inactivation of the RB1/p16/CDK4 complex. Hermes 4C was chosen because of its MC1R mutation, while Hermes 3C was chosen as an MC1R wild type (WT) control cell line.

4.1.2 Lentiviral transduction

In **Paper I and II,** we utilized lentiviral modified cells in an attempt to overexpress MITF in the Hermes 3C and 4C cell lines. pLVX-IRES-mCherry is a vector-based on HIV-1, that allows for simultaneous expression of the protein of interest and a fluorescent marker (mCherry). The vector expresses the protein of interest and a fluorescent protein in a bicistronic mRNA transcript. This is an advantage, as it can be used as an indicator of transduction efficiency, as well as a marker for selection. The selection of transfected clones was performed by fluorescence-activated cell sorting (FACS), and bulk transduced cells expressing the mCherry marker were pooled. This selection method was applied rather than select for one clone. This method represents a more heterogeneous collection of cells. FACS sorting also allowed us to select for more physiologically correct expression of MITF.

Lentiviral transduction is a well-established and effective technique for gene delivery in mammalian cells. When appropriately modified, lentivirus systems can target a huge variety of cells, including hard-to-transduce or quiescent cells (Dropulić, 2011). Lentivirus systems are also versatile and can carry up to 9 kbp of heterologous DNA, potentially organized in several genes. Moreover, lentivirus tends to integrate the host genome away from cellular promoters, which reduces the risk of insertional mutagenesis and oncogenicity considerably (Cereseto & Giacca, 2004).

4.1.3 Cell sorting by Flow cytometry

In **Paper I and II**, cells were transduced with lentivirus containing the red fluorescent marker, mCherry. After transduction, it is common to sort the heterogeneous mixture

of cells to select for the successfully transduced cells. Fluorescent Activated Cell Sorting (FACS) utilizes flow cytometry for sorting a heterogeneous cell suspension (M. He et al., 2015). The advantage of this method is that this system is able to sort the cells according to the strength of the dye emission, allowing for a more physiological expression of transduced cells.

4.1.4 RNA interference experiments

In **Paper I, II, and III,** knockdown experiments with chemically synthesized double-stranded small interfering RNA (siRNA) were used in order to reduce endogenous expression of MITF, SOX10, ERBB3, and AXL respectively. siRNA transfection is used for transient downregulation of target genes using short dsRNA molecules (20-24bp) that bind to complementary mRNA, causing their degradation prior to translation (Elbashir et al., 2001). One of the challenges using this method is the lack of specificity, as an overlap of 11-15 nucleotides is sufficient for off-target binding. This means that the observed effects may be due to non-specific knockdown of genes with similar nucleotide sequence as a gene of interest (Jackson et al., 2003). Moreover, the introduction of siRNA into cells requires the use of a transfection reagent. We used the commercial agent Lipofectamin^{TM} RNAiMAX which is cationic liposome formulation. This formulation complexes with the negatively charged RNA molecule that allows for overcoming the repulsion of the electrostatic cell membrane (Dalby et al., 2004). This reagent is supposedly very gentle to the cells, but the anionic agent might elicit unknown effects during transfection. To minimize these off-target effects, the use of low dose siRNA may reduce off-target effects. In our experiments, we included negative controls that contained the same nucleotide composition, but not the same sequence as the experiment siRNA (scrambled siRNA). Limitations when using siRNA is that it might not be fully effective, leaving functioning protein. In our experiments, several different siRNAs were tested as well as looking at downstream effectors targets to ensure sufficient knockdown.

4.1.5 Small molecule inhibitor treatments

Small molecular inhibitors were used in all three papers. In **Paper I**, the BRAF inhibitor vemurafenib (PLX4032) was used to supplement the siRNA experiments,

and to investigate the clinical significance of our findings. In **Paper II**, the small molecular inhibitors R428 (AXL inhibitor), trametinib (MEK inhibitor), MK-2206 (AKT inhibitor) were used to terminate PI3K pathway signaling. In **Paper III**, vemurafenib was used to make resistant cell lines, while R428 was used to demonstrate reduced cell viability in cell lines harboring high levels of AXL and low MITF expression. Both siRNA and small molecule inhibitor treatment targets protein. However, while siRNA treatment downregulates the protein expression, inhibitors will simply abrogate the proteins function (Hojjat-Farsangi, 2015). These differences may contribute to a difference in phenotype after treatment (Weiss et al., 2007)). Small molecule inhibitor treatment may elicit off-target effects such as targeting proteins of similar conformation. To avoid off-target effects, concentrations over 10μM should not be employed (Weiss et al., 2007). When using new chemical compounds that have not been validated *in vivo*, alternative methods such as knockdown of the target of interest should be considered for verification. Lastly, for well-established inhibitors, a negative control such as the solvent DMSO should be included in the experiment.

4.1.6 Viability and proliferation assays

In **Paper II** 3-(4,5-dimethylthiasol-2-yl)-5-(3-carboxymethoxyphenyl)-2-(4-sulfo Phenyl)-2H-tetrazolium (MTS) was used to measure cell viability after drug treatment. MTS is a colorimetric method for the quantification of viable cells. The NAD(P)H-dependent dehydrogenase enzymes in metabolically active cells cause reduction of MTS reagent in the presence of phenazine ethosulfate, into a water-soluble formazan product (Cory et al., 1991). This reaction will yield a significant color change that has a linear correlation with the dehydrogenase activity in metabolically active cells, and can easily be quantified by measuring the absorbance at 490-500 nm. MTS is a and uncomplicated assay as it is possible to simply add the compound to the cell culture media and await the colorimetric response. MTS is widely used in cancer research for measuring viability, proliferation, and drug toxicity, and one of the advantages of this method is the ability to measure cell number without disturbing the integrity of the cells. However, there are limitations to this method. Drug treatment may affect cell metabolism, thus mask the actual effect on viability by impaired reduction of the MTS compound. There have also been reports that the type of medium, serum albumin, and fatty acids may create inaccuracies when applying the MTS assay (K. T. Huang

et al., 2004). Finally, as this assay only provides an estimate of live cells, it is essential to supplement this method with additional analyses. Therefore, to complement the MTS-measurements, we also measured cell proliferation using the IncuCyte® Live-Cell Analyses. This system provides live imaging of cell culture plates over time and estimates the cell density in each well. The IncuCyte® will also reveal any morphological changes that may appear during drug treatment.

4.1.7 *In vivo* experiments

In vivo, animal experiments were performed in **Paper II** to verify that our transformed cells could establish xenografts. NOD scid gamma (NSG) mice bred at the institutional facility were used in the experiment. NSG mice lack mature T cells, B cells, and natural killer (NK) cells. The deficient immune system in these mice increases the chance of tumor engraftment, while it limits the options to monitor immune aspects of molecular changes. The mice were injected subcutaneously, bilaterally in the flanks under anesthesia. We divided the mice into three different experimental groups: Hermes 4C control, Hermes 4C empty vector, and Hermes 4C-HA-MITF to ensure that only the transformed cell line would form tumors. Once tumors formed in animals injected with the 4C-HA-MITF cell line (passage 0), the tumors were excised, and a small piece of this primary tumor was subcutaneously inserted into two new mice (passage 1) and so on, until passage 3. This is done to ensure a stable line of xenografts.

In vivo models are frequently used in cancer research as they better reflect the complexity of the tumor, and to some degree, the microenvironment found in human patients. However, tumors established with human cancer cell lines or patient-derived material require a deficient immune system, which excludes the role of the immune system found in patients. This excludes the study of relevant interactions between different types of immune cells and cancer cells during initiation and maintenance. Further, after implantation of patient-derived material, a selection pressure will be imposed by the host animal, leading to a gradual loss of the human stroma and a gain of murine cells (Varna et al., 2014).

Regardless, as of now, animal models are the superior method compared to other model systems for gaining insight into cancer molecular biology and patient drug-response. See chapter 7.3 Ethical considerations for further perspectives.

4.2 Experimental tools for molecular characterization

4.2.1 Western immunoblotting

Western immunoblotting was applied as a method for protein detection in **Papers I**, **II**, and **III**. Western immunoblotting is a widely used protein detection method, which involves separating native or denatured proteins according to size by gel electrophoresis. The proteins are then transferred to a protein-binding membrane, following the detection by antibodies specific to the target protein. Among the advantages of this method is its sensitivity. The technique has the ability to detect as little as 1-3 µg of total protein in a sample (Murphy & Lamb, 2013). Another advantage is the specificity. Both the fact that the proteins are separated according to size and the use of specific antibodies with affinity to specific proteins will leave little room for misinterpretation. Despite both the sensitivity and specificity, western blots may still produce imprecise results. False negative results may occur if a large protein is not given enough time to transfer from the gel to the membrane, also false positives may occur if an antibody reacts with a non intended protein. Many researchers use western blotting as a quantitative method. However, it is essential that your bands are within the linear range of detection, as over-saturation will yield false results (Mollica et al., 2009). In our experiments, we have not quantified our western blots as we argue we are looking at considerable alterations in protein expression, and not small changes that need quantification for detection.

Antibodies

An important factor to consider when selecting an antibody is both specificity and sensitivity to the intended target. Polyclonal antibodies have high sensitivity as they can recognize and bind to many different epitopes of a single antigen. However, the risk of non-specific protein binding is high. In all three papers, we utilized only monoclonal antibodies. Though these are less sensitive, monoclonal antibodies are much more specific, as they have monovalent affinity and only recognize the same

epitope of an antigen. This also makes the interaction vulnerable to alterations affecting the specific epitope.

4.2.2 Real time PCR

Real-time reverse transcription-polymerase chain reaction (RT PCR) to measure steady-state mRNA levels was performed in **Paper I, II, and III.** This technique combines reverse transcription of RNA into complementary DNA (cDNA) using the retroviral enzyme, reverse transcriptase. Further, the cDNA is used as a template for exponential amplification using PCR.

Fluorescent DNA labeling techniques such as SYBR Green and TaqMan allows for real-time detection of PCR products. We utilized the fluorescent probe SYBR Green technology, in which SYBR Green binds to the double-stranded DNA of the PCR products, leading to light being emitted upon excitation as the PCR products accumulate, the intensity of the fluorescence increases. SYBR Green is an effortless probe to use as there is no need to pre-design, as it is non-specific. However, this is also a potential problem, as SYBR Green does not discriminate between double-stranded DNA and possible primer-dimers (Rajeevan et al., 2001; Schmittgen et al., 2000). This problem can be reduced by testing the efficiency and specificity of primers in several cell backgrounds before use, or utilizing a standard curve in each experiment. In our studies, extensive testing of primer efficiency and specificity was performed in several different cell lines prior to experiments.

Normalization of results is a challenge when analyzing RT PCR data. Incorporating reference genes to correct for variations among samples, and to ensure reproducibility and reliability of the data is a widely used strategy. It is of importance to select reference genes that are stable between samples for the validity of comparisons. It is common to utilize housekeeping genes as a reference as they are thought to be stably expressed across cell types (Nelson & Cox, 2004). However, studies have shown considerable variation between samples (Dheda et al., 2004). We incorporated TATA box binding protein (TBP) and 60S acidic ribosomal protein P0 (RPLP0) as they have shown to be two of the most stable housekeeping genes in several cell types (Eissa et al., 2017). We tested these as well as a panel of other

housekeeping genes in around ten melanoma cell lines. The result showed that TBP and RPLP0 were the most stable throughout all the cell lines.

4.2.3 Chromatin immunoprecipitation followed by high throughput sequencing (ChIPseq)

ChIP-seq was performed in **Paper I and II.** This method is commonly applied to detect protein-DNA interactions. The method is based on the enrichment of DNA fragments bound explicitly by a protein of interest (Schmidt et al., 2009). This method allows for the identification of binding sites of a given transcription factor, in our case, MITF.

ChiP requires chromatin cross-linking to create a stable covalent binding between protein-DNA complexes. This is achieved by brief exposure to formaldehyde or other-cross linking agents. Next, cells are lysed to discard most of the cytosolic proteins, leaving only nuclear content. The next step is to shear the chromatin by sonication or otherwise. This is a crucial step to get right because if the fragments are too big, the antibody will not be able to pull down the DNA fragments. However, if chromatin, for instance, is over-sonicated, the fragments will be too small, and there is a chance that the protein structure will be disturbed, as well as epitope availability. The best fragment size will typically be between 200-600 base pairs (Park, 2009). The next step involves mixing the shared fragments with an antibody of interest. In our case, we utilized human influenza hemagglutinin-tagged (HA-tagged) MITF-M as there are no MITF-M specific antibodies of sufficient quality. We, therefore, utilized an HA-antibody to pull down the protein-DNA complexes. Ha-tags are widely used for protein localization. However, to what extent the HA-tag may impose unspecific effects have been debated (Saiz-Baggetto et al., 2017).

4.3 Ethical considerations

Animal experiments

The increasing role of *in vivo* studies in cancer research over the last few decades has generated a considerable and warranted debate. The following concerns have been raised: 1. Animals have an intrinsic value and deserve respect; 2. Animals are sentient beings with the ability to feel pain; 3. Our treatment of animals, including in research, reflects on us as moral beings (Workman et al., 2010).

Regardless, animal models are frequently used and remain essential for reflecting the complexity of the tumor and the tumor microenvironment found in cancer patients (95% in mice) (Workman et al., 2010). The use of animal models is, however, restricted both due to expenses and ethical concerns. Further, guidelines for animal welfare should be employed in all experiments. The guidelines are strictly outlined in "Dyrevelferdsloven" (animal welfare act) [1]. The 3 R's are well-established principles used as a guideline when planning and are defined as: Replacement: alternatives to *in vivo* studies should always be carefully considered, and thorough *in vitro* testing should always be done before initiating an experiment; Reduction**:** in order to reduce the number of animals used in an experiment, careful selection of statistical methods and study design is essential; Refinement: ensuring best possible living conditions for the animals. Enriching the environment, reducing pain, discomfort, and distress as much as possible during the animals' participation in the experiment (Russell & Burch, 1959).

In **Paper II,** we undertook a number of *in vitro* experiments prior to initiating animal experiments. We verified that our melanocyte cell Hermes 4C was transformed by observing phenotypic alterations by microscopy followed by both anchorage and growth factor independence assays. Unfortunately, these experiments were not sufficient to conclude and publish that transformation had occurred. Therefore, animal experiments were deemed necessary to validate our findings pertaining to true transformation events. We chose NSG mice to reduce the number of animals as this breed has a better tumor-take as well as a more prolonged survival (Ishikawa et al., 2005; Shultz et al., 2005). The lowest possible number of animals was obtained.

[1] lovdata.no/dokument/NL/lov/2009-06-19-97

Nonetheless, sufficient animals for the experiment to be statistically significant were required. The animal facilities at the Norwegian Radium Hospital have strict guidelines to ensure animal welfare during the experiments. Environmental parameters such as temperature, humidity, and lighting as well as fresh water, food, and clean cages two times a week where the mice also receive chewing sticks, paper houses, and fresh nesting material.

In conclusion, animal ethics is an important issue, and hopefully, new approaches involving alternative model-systems are imminent so that we can minimize the use of animal experiments in the future.

Transparency and reproducibility

Distribution of knowledge drives scientific progress, and advances are primarily based on previous observations. Transparency and reproducibility are two central features of science (McNutt, 2014), but despite being embraced by most scientists as defining features of disciplinary norms, evidence shows that this is not always the case (Ioannidis et al., 2014; John et al., 2012; Nosek et al., 2015).

Academic success is dependent on publishing, and the norm emphasizes and favor novel, positive results. In the present culture, negative results are published less frequently, and if published, yield a low impact. This creates a situation where researchers will lack the incentive to be transparent in their research, and might even cherry-pick which results to publish.

Reproducibility is not only crucial between labs, but between individual experiments. Two distinctions that have been discussed is the difference between technical and biological replicates. A technical replicate would, for example, be testing the same sample multiple times. This may be used to test the robustness of the technique or protocol. Biological replicates are parallel measurements of independent samples of the same origin. This yields information about how robust the results are and help determine if the experiments are biologically relevant (Blainey et al., 2014). During our experiments, we have aimed to apply ethical thinking, transparency, and reproducibility to the best of our ability

5. Results and discussion

Malignant melanoma has a rising incidence. Generally, this is a cancer type with a high mutational burden. MITF is a master transcription factor that plays a dominant role in both melanocyte and melanoma biology, and MITF has been extensively studied over the last two decades (Goding & Arnheiter 2019; Hartman & Czyz 2015; Kawakami & Fisher 2017). MITF has been identified as being involved in a wide range of processes in melanoma, including predisposition, initiation, progression, invasion and drug resistance (Bianchi-Smiraglia et al., 2017; Cheli et al., 2011; Hartman & Czyz, 2015; Kozar et al., 2019; Yokoyama et al., 2011). However, the role of MITF in melanoma is complex, and therefore often leads to inconsistent findings. The purpose of this thesis was to further explore the functional roles of MITF in melanoma development and drug resistance. Here, I will begin by discussing **Paper II,** where we discovered that overexpression of HA-MITF in the context of compound mutated MC1R led to malignant transformation, as MITF involves central cellular processes in melanoma. In **Paper I,** we investigated if MITF plays a role in the regulation of ERBB3 receptor and it`s cognate ligand NRG1, with potential implications for treatment resistance. We followed up in **Paper III,** where we investigated the role of the MITF/SOX10 axis upon RTK`s and their cognate ligands during the development of vemurafenib resistance.

5.1 From melanocyte to melanoma

5.1.1 Development and progression

Melanomagenesis is a complex process involving multiple steps, including environmental factors such as UV-radiation. Melanoma risk also has a genetic component, not necessarily due to family history of melanoma, but due to the hereditary phenotype RHC (Red hair and fair skin) because of MC1R variant predisposition. The association between MC1R variants and melanoma frequency has mainly been linked to RHC variants, but recent studies show that also non-RHC variants have a higher incidence rate. In fact, individuals carrying any MC1R variant have been found to possess a 60% higher risk of developing melanoma compared to non-carriers independently of UV-radiation (Tagliabue et al., 2018; Wendt et al., 2016).

As briefly discussed in chapter 1.1.2, CDKN2A was the first melanoma susceptibility gene to be identified more than 20 years ago and is still considered the main high-risk gene in melanoma (Potrony et al., 2016). Germline CDKN2A mutations have been found in about 30-40% of melanoma-prone families worldwide, and in melanoma, loss of CDKN2A function is often found after deletions, DNA methylation, and histone modification. The penetrance of CDKN2A mutations in multiple-case melanoma families has been found to vary across continents, indicating that variations in the genetic backgrounds, host characteristics, and/or sun exposure contributes to the differences in penetrance (Bishop et al., 2002). Both MC1R and CDKN2A play important roles in preserving genomic stability in melanocytes. One product of the CDKN2A locus, p16, plays an essential role in the regulation of senescence in melanocytes (Haferkamp et al., 2009; Rayess et al., 2012; Sviderskaya et al., 2003). As previously mentioned in chapter 1.1.2, hTERT is another important gene implicated in melanoma initiation and progression. hTERT expression enables escape from oncogene-induced senescence and is detected in 90% of human cancers and over 60 % of melanomas (Bell et al., 2015; Cancer Genome Atlas Network, 2015).

The tipping point where cells escape senescence and become invasive melanoma is incompletely understood. Therefore, in **Paper II,** we investigated the consequence of MITF dysregulation in melanocytes expressing mutated MC1R, hTERT, and nonfunctional RB1/CDKN2A pathway signaling. Introducing hTERT expression and CDKN2A loss of function into these cells immortalizes them, but does not transform them. Here, we found that stable transduction of ectopic HA-MITF alone leads to the consistent transformation of the MC1R mutant Hermes 4C cell line, but not of the MC1R wild type cell line Hermes 3C.

The work in **Paper II** was inspired by Garraway and colleagues, where they suggested MITF to be a context-dependent oncogene. They found that overexpressing HA-MITF in immortalized melanocytes alone did not transform the cells. However, co-introducing BRAFV600E and HA-MITF successfully transformed the melanocytes (Garraway et al., 2005). In agreement with this study, we found that overexpressing HA-MITF in Hermes 3C melanocytes immortalized by expression of

hTERT and CDKN2A loss of function is not sufficient for transformation to occur. However, forced expression of HA-MITF in the MC1R mutated, hTERT expressing, CDKN2A loss of function Hermes 4C cell line consistently led to transformation. Other researchers have also suggested that overexpression of BRAFV600E alone is sufficient to transform melanocytes with an MC1R loss in an hTERT/p53DD/CDK4(R24C) background (Cao et al., 2013). This is in line with the literature stating that any MC1R variant is associated with vulnerability towards melanoma independently of phenotypic features (Tagliabue et al., 2018).

As discussed in chapter 4.2.3, we utilized HA-tagged MITF due to the lack of specific MITF-M antibodies in these experiments, as we aimed to address MITF binding sites in WT MC1R (3C) versus mutated MC1R (4C). A limitation with this protocol, which also has been used in previous studies (Wellbrock and Marais 2005; Garraway et al., 2005), is that we cannot verify whether the transformation would find place if using an untagged MITF construct. An approach to verify whether the transformation stems from untagged MITF or is due to the tagged variant would be to transduce the 4C cell line with an untagged MITF construct. This could have been attempted, even without specific antibodies. Secondly, our study would have benefitted from the inclusion of several MC1R-mutated melanocyte cell lines. Similarly, the inclusion of additional immortalized wild-type MC1R melanocyte cell lines would have further verified and strengthened our observations.

5.1.2 Phenotype plasticity in melanoma progression

EMT is a key process involved in the progression of metastasis in epithelial cancer. In melanoma, an EMT-like phenotype switch promoting progression and EMT-related genes have been implicated in metastasis progression (F. Z. Li et al., 2015). Phenotype switching has been suggested to involve transcriptional reprogramming in melanoma. Two distinct programs have been identified and defined as either having a proliferative or invasive phenotype (Falletta et al., 2017; I. S. Kim et al., 2017). The transcriptomes of these phenotypes are controlled by distinct transcriptional master regulators. These master regulators have the ability to direct cellular features, and they are under strict temporal and spatial control during development (Iwafuchi-Doi & Zaret, 2014). Differentiated cells will not typically switch identity under normal conditions. However, dysregulation of master transcription factors is a major threat to

any multicellular organism, as they are able to overwrite established cellular programs by forcing new cellular features (Baumann et al., 2019). Our ChIP-seq analyses revealed increased chromatin binding in the transformed 4C HA-MITF (MC1R-RHC) compared to 3C HA-MITF (MC1R WT). This observation could be interesting; however, this finding may be purely descriptive in the sense that we do not know the degree of MITF chromatin binding in the parental immortalized cell lines. The fact that we find increased binding between the transduced cell lines does not tell us if the difference is as a result of the transduction of endogenous HA-MITF, or if this is already the case in the immortalized parental cell lines. In fact, this would be interesting to investigate further as to our knowledge these cell lines are both derived from normal diploid melanocytes, albeit from two different individuals, carrying the same induced alterations, except for 4C carrying two variant MC1R alleles: R160W/DD294H (Gray-Schopfer et al., 2006). However, MITF binding reflected the abnormal chromatin structure previously reported in melanoma (Verfaillie et al., 2015). We also found that the distribution of MITF binding sites corresponds with the sequence motif of transcription factors, including SOX10, MITF, AP-1, and TEAD in the transformed 4C cell line.

As previously mentioned in chapter 1.2.4, the master transcription factors SOX10 and MITF are identified as regulators of the proliferative phenotype, and AP1 and TEAD as regulators of the invasive melanoma phenotype (Verfaillie et al., 2015). **In Paper II**, we found that our HA-MITF-induced transformed cells displayed a loss of endogenous MITF and SOX10 and upregulation of FOS/FOSL-1 (AP-1 proteins), indicating a shift in the transcriptional program likely caused by changes in chromatin structure, with a consequent gain of invasive properties. The loss of SOX10 and endogenous MITF was identified by RNA expression array and verified by RT PCR and western blot analyses. MITF consists of at least nine different isoforms, and since our MITF antibody is specific for the isoform of interest, MITF-M, we have utilized MITF-M specific siRNA in a range of melanoma cell lines as well as the 3C and 4C cell lines to identify the appropriate band in our blots (∼52 kDa). As the HA-tag is suggested to be ∼ 3 kDa, we were able to differentiate between endogenous and exogenous MITF protein expression.

Support for the transition from proliferative to invasive cell state was observed through the upregulation of EMT-related genes, including the RTK AXL. AXL has been reported to be associated with EMT in many cancers (Antony & Huang, 2017; Asiedu et al., 2014; Goyette et al., 2018; G. Zhang et al., 2018), and in **Paper II**, we found that AXL-PI3K signaling may be the primary driver for the HA-MITF induced transformed cells. This was supported by the reduction in proliferation after AXL inhibition compared to inhibition of MEK. In addition, we measured reduced PTEN expression, which is in line with an increase in AKT levels. PTEN is one of the most frequently inactivated tumor suppressors in cancer.

Moreover, it has been suggested that WT MC1R has a protective relationship with PTEN in preventing proteolysis after UV-radiation. In contrast, MC1R-RHC variants do not associate with PTEN, rendering this phenotype more sensitive to UV damage, thus leading to aberrant PI3K signaling (Cao et al., 2013). This implies that PTEN regulation is more ambiguous in the mutant MC1R 4C cell line. Following these findings, we would expect lower PTEN protein levels in 4C versus 3C. However, our data do not show a discrepancy in either 3C or 4C basal RNA nor protein levels with respect to PTEN expression. This implies that a reduction in PTEN is only observed between 4C and transformed 4C, which may indicate an alternative mechanism than the one suggested by Cao and colleagues. Furthermore, the role of PTEN in our transformation model should be further explored by modulation of PTEN, and by use of other cell lines.

5.2 Dysregulation of MITF

5.2.1 MITFs role in RTK expression

RTK receptor-mediated autocrine activation has been suggested to be largely responsible for PI3K and MAPK pathway activation in melanoma (Boregowda et al., 2016). Communication between cells will typically be mediated by growth factors/ligands and cytokines either released by secretory cells, or by target cells themselves secreting and self-activating (autocrine activation) (Singh & Harris, 2005). In cancer, sustained autocrine activation has been suggested to induce malignant transformation (Walsh et al., 1991). Moreover, loss of MITF has been suggested to enhance an autocrine resistance loop involving the RTK EGFR following MAPK

inhibitor treatment (Ji et al., 2015), and MITF low melanoma has been reported to be insensitive to a range of inhibitors due to high levels of AXL (Müller et al., 2014). In **Paper I**, we wanted to further explore MITF`s role in ERBB3 expression.

Initially, our mRNA expression array data led to the discovery of the ERBB3 receptor as a target of MITF. Data showed that the depletion of MITF by siRNA in SKMEL28 resulted in an upregulation of ERBB3 mRNA. ERBB3 has previously been shown to be upregulated by FOXD3 after MAPK treatment in BRAFV600E cell lines (Abel et al., 2013), and FOXD3 has been reported to inhibit MITF (Curran et al., 2009; Kos et al., 2001; Thomas & Erickson, 2009), and vice versa (S. He et al., 2011), In **Paper I,** we further explored the link between these transcription factors in connection to ERBB3. Our data suggest that MITF can regulate ERBB3 both through and independently of FOXD3. Of note, siFOXD3 alone did not affect ERBB3 levels in the NF1-mutated cell line MeWo, which is in concordance with Abel and colleagues, implying that FOXD3 only seems to regulate ERBB3 in BRAFV600E-mutated melanomas (Abel et al., 2013).

In **Paper III**, we wanted to further investigate the role of the SOX10/MITF axis in relation to RTK`s during vemurafenib treatment in a panel of melanoma cell lines. The initial TCGA analysis done in **Paper I** showed a positive correlation between MITF, SOX10 and ERBB3, and an inverse relationship between the latter genes and the NRG1 ligand. In **Paper III**, we found an inverse correlation between AXL and MITF, which has previously been suggested (Müller et al., 2014; Sensi et al., 2011). Interestingly, we also measured an inverse correlation between AXL and SOX10, as well as between AXL and ERBB3. Importantly, RT-PCR and expression array data of our melanoma cell line panel confirmed the correlations we found in the patient samples. Together, these data allowed us to stratify the melanoma cell lines into AXL high MITF/SOX10/ERBB3 low, AXL low MITF/SOX10/ERBB3 high, and a small group displaying the same levels of MITF/SOX10/ERBB3 and AXL, where these latter cell lines display a more heterogeneous phenotype. However, even though our expression and RT PCR data from cell lines are in agreement with TCGA patient data, a further investigation of protein expression levels would have strengthened the results, as mRNA levels do not necessarily reflect protein expression levels. This is

especially evident in MITF expression as it may undergo a plethora of both post-transcriptional and post-translational modifications.

5.2.2 MITFs role in therapy-induced phenotype plasticity

The knowledge that melanoma has the ability to adapt to MAPK inhibitors is now well established. Treatment-induced phenotypic plasticity will typically involve the rewiring of signaling pathways. It is also known that during the early phase of MAPK inhibitor treatment, up to 78% of patient samples display an increase in MITF High cells (Rambow et al., 2018). This is in agreement with our findings in **Paper III,** where we observed an increase in MITF levels at 72 h and after one week in our melanoma cell lines. In this MITF high state tumors are suggested to be somewhat MAPK inhibitor tolerant before becoming resistant (Smith et al., 2016). However, in **Paper I**, we measured loss of MITF expression after two weeks of vemurafenib treatment in melanoma cell lines SKMEL28 and WM983B, suggesting a switch in levels between one and two weeks after treatment in our cell lines. Studies have also shown that during early drug response phase, cell populations with different phenotype signatures, namely invasive and neural-crest stem cell-like, may co-emerge within the same tumor (Rambow et al., 2018).

RTK redundancy during MAPK inhibition

Upregulation of a range of RTKs, such as PDGFR, IGF1R, EGFR, AXL, in response to treatment has been reported (Girotti et al., 2013; Ji et al., 2015; Müller et al., 2014; Nazarian et al., 2010; Villanueva et al., 2010). The upregulation of RTK receptors is paralleled by a loss of MITF and its upstream regulators PAX3 and SOX10 (Smith et al., 2019; Verfaillie et al., 2015)**.** AXL-expressing MITF low cells are believed to signal independently of the MAPK pathway, thus rendering them resistant to MAPK inhibition (Müller et al., 2014). In **Paper III**, we propose that MITF and SOX10 levels prior to treatment may predict whether melanoma cells utilize RTK upregulation to achieve resistance or not. Cell lines harboring high levels of MITF prior to treatment showed an upregulation of the RTK AXL after becoming resistant, while cell lines harboring low levels of MITF did not. When measuring protein levels in the MITF low cell line A375, we observed a minor increase of ERBB3 and pAKT, as well as a minor reduction in AXL levels. Moreover, we detected a major upregulation of pERK. In contrast, in the MITF high cell line SKMEL28, we detected an increase in AXL and

pAKT levels, without any detectable change in pERK levels. This may imply that MITF low cell lines mainly utilize reactivation of the MAPK pathway as a standard mechanism of vemurafenib resistance, while MITF high cell lines often switch to a MITF low/AXL high phenotype that signals through the PI3K pathway. However, this should be further explored, e.g., in cell lines of different phenotypes for more robust conclusions. A proposed model for stratification of our melanoma cell lines is outlined in figure 13.

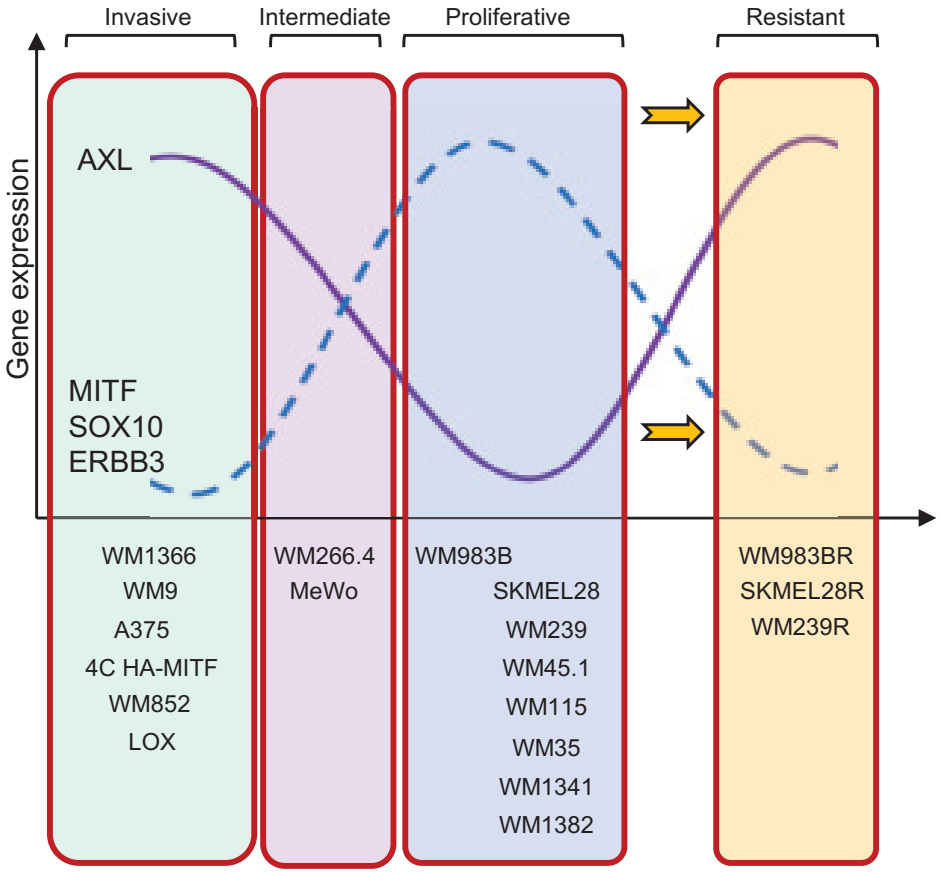

Figure 13. Illustration suggesting how melanoma cell lines may be stratified according to their transcriptional signature. WM1366 is classified as a primary melanoma. However, in **Paper III** we found that this cell line displays high AXL and low MITF, SOX10 and ERBB3 perhaps indicating that the cell line is on the verge of becoming invasive/metastatic. Further, WM9, A375, WM852, and LOX were stratified as being of the invasive phenotype. Included in this figure is 4C HA-MITF our transformed cell line from **Paper II.** WM266.4 and MeWo is classified as intermediate as they harbor medium/high levels of both signatures. WM983, SKMEL28, WM239, WM45.1, WM115, WM35, WM1341 and WM1382 classifies as having the proliferative signature. Lastly, the illustration depicts the gene signature in three of our treatment-resistant cell lines resembling the invasive phenotype.

The analyses of cell lines during treatment and resistance were mainly based on RT PCR observations. This method has its limitations as standard deviations may be high between experiments. This is particularly evident when measuring NRG1, GAS6, and EGF ligand mRNA levels. The reason for this may be that ligands are more dynamic, and has a higher turnover than the RTKs. Therefore, the exact cells stage when the cells are harvested may impact the results. We performed three biological and six technical replicates in all RT PCR experiments which should suffice to capture most variability. However, an increase in the number of biological replicates likely would have lowered the standard deviations and yielded more robust results. Further, our result would have been strengthened by employing further high throughput screenings. However, the availability of methods, time- and budget-constraints are frequent limitations in experimental design.

The AXL receptor is suggested to be the most prominent resistance marker, as around 70% of relapsed melanoma display increased expression of the receptor (Boshuizen et al., 2018). Indeed, several researchers suggest that inhibiting AXL in combination with MAPK inhibitors is a treatment option. However, as we and others have shown, other RTK receptors are also in play. Receptor redundancy through kinase switching has been described (S. Thomson et al., 2008). Interestingly, in **Paper III**, we find that knocking down AXL by siRNA increases the levels of ERBB3 in melanoma cell lines of various mutational backgrounds. This finding may not be directly equivalent to the effect of inhibitor treatment, as the AXL protein is still present compared to after siRNA treatments. However, the mechanism behind this relationship should be further explored, and further experiments treating with AXL inhibitor should be done to determine the boundaries of this effect. We also observed a two-way redundancy between ERBB3 and AXL in two of our cell lines (WM983B and MeWo), indicating a co-operative relationship between the receptors, at least in these two cell lines.

In addition, EGFR is also upregulated in the resistant cell lines. This is in agreement with observations of Ji and colleagues, suggesting that MITF loss after vemurafenib resistance is linked to EGFR expression. Further, they found that both the AXL and EGFR ligands GAS6 and HB-EGF (Heparin binding-EGF) were concomitantly upregulated in the resistant cell line SKMEL28. However, EGF was not (Ji et al.,

2015). We found GAS6 to be upregulated in SKMEL28, but not in our other cell lines. In agreement with Ji and colleagues, EGF was not upregulated in any of our resistant cell lines (Ji et al., 2015). The ERBB3 ligand NRG1 has previously been suggested to promote compensatory signaling through ERBB3 signaling in melanoma and colorectal cancer after BRAF inhibitor treatment (Capparelli et al., 2015; Prasetyanti et al., 2015). Accordingly, we found that NRG1 was upregulated in three out of four cell lines, suggesting sustained PI3K signaling through NRG1-ERBB3, in addition to GAS6-AXL and EGF-EGFR. This adaptive RTK receptor behavior during inhibitor treatment is illustrated in **Figure 14**. Initially, the results presented here would argue that treating MITF high cell lines with an AXL and BRAF inhibitor combination would be wise in order to avoid acquired resistance. However, the receptor redundancy between AXL and ERBB3 we observed in **Paper III** needs to be taken into consideration and further explored.

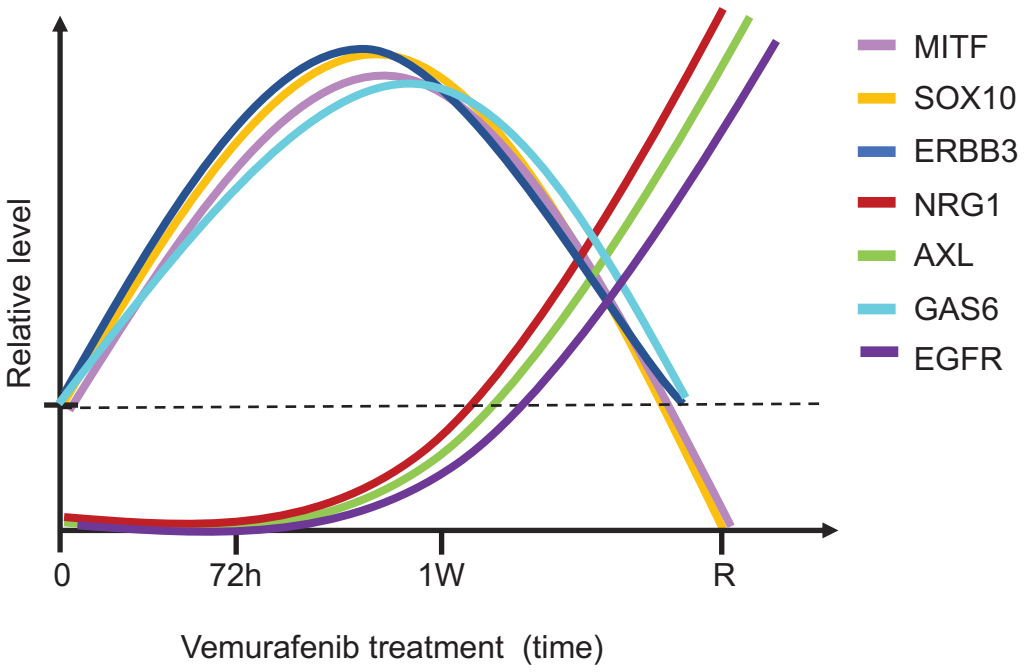

Figure 14. The graph illustrates the adaptive behavior of RTK receptors and their ligands during vemurafenib treatment in WM983B, SKMEL28, and WM239 cell lines.

Overcoming melanoma plasticity may be difficult to achieve due to the numerous factors working in conjunction to promote cancer cell growth. This has proven to be a major hinder during small molecule inhibitor treatments alone. Differential methods for drug delivery should perhaps be explored to somehow outsmart kinase

redundancy. Moreover, immunotherapy has emerged as a promising treatment option in melanoma. However, the response rate is low due to immunologically cold tumors. Interestingly, BRAF inhibition has been shown to increase T-cell recognition in melanoma (Boni et al., 2010). This discovery indicates that an induction period treating with BRAF inhibitor in an attempt to increase tumor immune cell infiltration, with a subsequent switching to immunotherapy, is an interesting approach and is currently being tested (ClinicalTrials.gov; NCT02858921). Further, a recent publication explored the dysregulation of MITF in both a murine and human cell line model. They found opposing effects on immune-cell attraction. Nevertheless, their results clearly suggest that MITF might be involved in immune cell migration, and should be further explored with respect to immunotherapy treatment in melanoma (Wiedemann et al., 2019).

6. Concluding remarks and future perspectives

Genetic alterations are of undeniable importance in melanoma development. However, detailed knowledge of the mechanisms behind molecular and epigenetic changes remains largely unknown. This may be due to the lack of sufficient models to study individual stages as well as the remarkable signaling complexity during melanomagenesis. In this thesis, we have attempted to elucidate more of the roles of MITF in melanoma initiation, progression and drug resistance.

In **Paper II**, we found that overexpression of HA-MITF in the context of mutated MC1R in an hTERT expressing melanocyte cell line containing CDKN2A loss of function led to malignant transformation. Within the scope of this paper, we characterized the transformed cells by exploring them at the RNA and protein levels. Further, animal testing was performed to confirm tumorigenicity. Lastly, we performed chromatin immunoprecipitation followed by sequencing to map MITF binding sites. MITF has been suggested to a context-dependent oncogene, and we here suggest that our construct/model could be further utilized to investigate the role of MITF as an oncogene in familial melanomas harboring p16/TERT/MC1R backgrounds.

To further explore our findings, additional experiments could pursue different open questions. It is currently not clear to what extent chromatin conformation changes contribute to driving the transformation, and if being the case, whether this event is reversible. Reintroducing SOX10 in the transformed cell line to explore whether this would activate endogenous MITF expression, could perhaps shed light on the potential to reverse the transformation. Further, stable knockdown of MC1R in the MC1R WT 3C HA-MITF in combination with overexpression of HA-MITF construct could perhaps verify the role and importance of mutant MC1R in the transformation process.

In **Paper II and III,** we explored MITF with respect to RTK regulation and treatment resistance. We found that the downregulation of MITF increased the expression of both ERBB3 and its cognate ligand NRG1. Further, we propose that identifying expression levels of MITF/SOX10/ERBB3 and AXL prior to treatment initiation may

help to predict the likelihood of the cells to utilize RTK upregulation as a mechanism to achieve resistance after vemurafenib treatment or not.

Exploring receptor redundancy after administering various AXL inhibitors in both resistant and untreated cell lines would perhaps uncover whether the apparent receptor redundancy we found between AXL and ERBB3 could be clinically relevant and not only an effect observed after siRNA treatment.

Single-cell analyses of the cell lines during treatment, and after resistance, could identify whether there are subpopulations of pre-resistant cells in our cell lines, and perhaps also uncover whether vemurafenib treatment-resistance is achieved by selection of pre-existing clones in the cell population. These pre-existing clones would then potentially harbor an invasive phenotype with high levels of AXL and low SOX10, MITF and ERBB3 levels.

7. Reference list

Abdel-Malek, Z., Swope, V., Collins, C., Boissy, R., Zhao, H., & Nordlund, J. (1993). Contribution of melanogenic proteins to the heterogeneous pigmentation of human melanocytes. *Journal of Cell Science*, *106 (Pt 4)*, 1323–1331.

Abel, E. V., Basile, K. J., Kugel, C. H., 3rd, Witkiewicz, A. K., Le, K., Amaravadi, R. K., Karakousis, G. C., Xu, X., Xu, W., Schuchter, L. M., Lee, J. B., Ertel, A., Fortina, P., & Aplin, A. E. (2013). Melanoma adapts to RAF/MEK inhibitors through FOXD3-mediated upregulation of ERBB3. *The Journal of Clinical Investigation*, *123*(5), 2155–2168.

Aksan, I., & Goding, C. R. (1998). Targeting the microphthalmia basic helix-loop-helix–leucine zipper transcription factor to a subset of E-box elements in vitro and in vivo. *Molecular and Cellular Biology*. https://mcb.asm.org/content/18/12/6930.short

Ando, H., Niki, Y., Ito, M., Akiyama, K., Matsui, M. S., Yarosh, D. B., & Ichihashi, M. (2012). Melanosomes are transferred from melanocytes to keratinocytes through the processes of packaging, release, uptake, and dispersion. *The Journal of Investigative Dermatology*, *132*(4), 1222–1229.

Antony, J., & Huang, R. Y.-J. (2017). AXL-Driven EMT State as a Targetable Conduit in Cancer. *Cancer Research*, *77*(14), 3725–3732.

Aoude, L. G., Wadt, K. A. W., Pritchard, A. L., & Hayward, N. K. (2015). Genetics of familial melanoma: 20 years after CDKN2A. *Pigment Cell & Melanoma Research*, *28*(2), 148–160.

Arrangoiz, R., Dorantes, J., Cordera, F., Juarez, M. M., Paquentin, E. M., & de León, E. L. (2016). Melanoma review: epidemiology, risk factors, diagnosis and staging. *Cancer Research and Treatment: Official Journal of Korean Cancer Association*, *4*(1), 1–15.

Asiedu, M. K., Beauchamp-Perez, F. D., Ingle, J. N., Behrens, M. D., Radisky, D. C., & Knutson, K. L. (2014). AXL induces epithelial-to-mesenchymal transition and regulates the function of breast cancer stem cells. *Oncogene*, *33*(10), 1316–1324.

Atefi, M., von Euw, E., Attar, N., Ng, C., Chu, C., Guo, D., Nazarian, R., Chmielowski, B., Glaspy, J. A., Comin-Anduix, B., Mischel, P. S., Lo, R. S., & Ribas, A. (2011). Reversing melanoma cross-resistance to BRAF and MEK inhibitors by co-targeting the AKT/mTOR pathway. *PloS One*, *6*(12), e28973.

Atkinson, V., Long, G. V., Menzies, A. M., McArthur, G., Carlino, M. S., Millward, M., Roberts-Thomson, R., Brady, B., Kefford, R., Haydon, A., & Cebon, J. (2016). Optimizing combination dabrafenib and trametinib therapy in BRAF mutation-positive advanced melanoma patients: Guidelines from Australian melanoma medical oncologists. *Asia-Pacific Journal of Clinical Oncology*, *12 Suppl 7*, 5–12.

Bahadoran, P., Aberdam, E., Mantoux, F., Buscà, R., Bille, K., Yalman, N., de Saint-Basile, G., Casaroli-Marano, R., Ortonne, J. P., & Ballotti, R. (2001). Rab27a: A key to melanosome transport in human melanocytes. *The Journal of Cell Biology*, *152*(4), 843–850.

Bastian, B. C. (2014). The molecular pathology of melanoma: an integrated taxonomy of melanocytic neoplasia. *Annual Review of Pathology*, *9*, 239–271.

Baumann, V., Wiesbeck, M., Breunig, C. T., Braun, J. M., Köferle, A., Ninkovic, J., Götz, M., & Stricker, S. H. (2019). Targeted removal of epigenetic barriers during transcriptional reprogramming. *Nature Communications*, *10*(1), 2119.

Beji, A., Horst, D., Engel, J., Kirchner, T., & Ullrich, A. (2012). Toward the prognostic significance and therapeutic potential of HER3 receptor tyrosine kinase in human colon cancer. *Clinical Cancer Research: An Official Journal of the American Association for Cancer Research*, *18*(4), 956–968.

Bell, R. J. A., Rube, H. T., Kreig, A., Mancini, A., Fouse, S. D., Nagarajan, R. P., Choi, S., Hong, C., He, D., Pekmezci, M., Wiencke, J. K., Wrensch, M. R., Chang, S. M., Walsh, K. M., Myong, S., Song, J. S., & Costello, J. F. (2015). Cancer. The transcription factor GABP selectively binds and activates the mutant TERT promoter in cancer. *Science*, *348*(6238), 1036–1039.

Bell, R. J. A., Rube, H. T., Xavier-Magalhães, A., Costa, B. M., Mancini, A., Song, J. S., &

Costello, J. F. (2016). Understanding TERT Promoter Mutations: A Common Path to Immortality. *Molecular Cancer Research: MCR*, *14*(4), 315–323.

Bennett, D. C. (2003). Human melanocyte senescence and melanoma susceptibility genes. *Oncogene*, *22*(20), 3063–3069.

Bertolotto, C., Lesueur, F., Giuliano, S., Strub, T., de Lichy, M., Bille, K., Dessen, P., d'Hayer, B., Mohamdi, H., Remenieras, A., Maubec, E., de la Fouchardière, A., Molinié, V., Vabres, P., Dalle, S., Poulalhon, N., Martin-Denavit, T., Thomas, L., Andry-Benzaquen, P., … Bressac-de Paillerets, B. (2011). A SUMOylation-defective MITF germline mutation predisposes to melanoma and renal carcinoma. *Nature*, *480*(7375), 94–98.

Bianchi-Smiraglia, A., Bagati, A., Fink, E. E., Moparthy, S., Wawrzyniak, J. A., Marvin, E. K., Battaglia, S., Jowdy, P., Kolesnikova, M., Foley, C. E., Berman, A. E., Kozlova, N. I., Lipchick, B. C., Paul-Rosner, L. M., Bshara, W., Ackroyd, J. J., Shewach, D. S., & Nikiforov, M. A. (2017). Microphthalmia-associated transcription factor suppresses invasion by reducing intracellular GTP pools. *Oncogene*, *36*(1), 84–96.

Bill, A., Schmitz, A., Albertoni, B., Song, J.-N., Heukamp, L. C., Walrafen, D., Thorwirth, F., Verveer, P. J., Zimmer, S., Meffert, L., Schreiber, A., Chatterjee, S., Thomas, R. K., Ullrich, R. T., Lang, T., & Famulok, M. (2010). Cytohesins are cytoplasmic ErbB receptor activators. *Cell*, *143*(2), 201–211.

Birck, A., Ahrenkiel, V., Zeuthen, J., Hou-Jensen, K., & Guldberg, P. (2000). Mutation and allelic loss of the PTEN/MMAC1 gene in primary and metastatic melanoma biopsies. *The Journal of Investigative Dermatology*, *114*(2), 277–280.

Bishop, D. T., Demenais, F., Goldstein, A. M., Bergman, W., Bishop, J. N., Bressac-de Paillerets, B., Chompret, A., Ghiorzo, P., Gruis, N., Hansson, J., Harland, M., Hayward, N., Holland, E. A., Mann, G. J., Mantelli, M., Nancarrow, D., Platz, A., Tucker, M. A., & Melanoma Genetics Consortium. (2002). Geographical variation in the penetrance of CDKN2A mutations for melanoma. *Journal of the National Cancer Institute*, *94*(12), 894–903.

Blainey, P., Krzywinski, M., & Altman, N. (2014). Points of significance: replication. *Nature*

Methods, *11*(9), 879–880.

Blind, R. D. (2014). Disentangling biological signaling networks by dynamic coupling of signaling lipids to modifying enzymes. *Advances in Biological Regulation*, *54*, 25–38.

Bollag, G., Hirth, P., Tsai, J., Zhang, J., Ibrahim, P. N., Cho, H., Spevak, W., Zhang, C., Zhang, Y., Habets, G., Burton, E. A., Wong, B., Tsang, G., West, B. L., Powell, B., Shellooe, R., Marimuthu, A., Nguyen, H., Zhang, K. Y. J., … Nolop, K. (2010). Clinical efficacy of a RAF inhibitor needs broad target blockade in BRAF-mutant melanoma. *Nature*, *467*(7315), 596–599.

Bondurand, N., Pingault, V., Goerich, D. E., Lemort, N., Sock, E., Le Caignec, C., Wegner, M., & Goossens, M. (2000). Interaction among SOX10, PAX3 and MITF, three genes altered in Waardenburg syndrome. *Human Molecular Genetics*, *9*(13), 1907–1917.

Boni, A., Cogdill, A. P., Dang, P., Udayakumar, D., Njauw, C.-N. J., Sloss, C. M., Ferrone, C. R., Flaherty, K. T., Lawrence, D. P., Fisher, D. E., Tsao, H., & Wargo, J. A. (2010). Selective BRAFV600E inhibition enhances T-cell recognition of melanoma without affecting lymphocyte function. *Cancer Research*, *70*(13), 5213–5219.

Boregowda, R. K., Medina, D. J., Markert, E., Bryan, M. A., Chen, W., Chen, S., Rabkin, A., Vido, M. J., Gunderson, S. I., Chekmareva, M., Foran, D. J., Lasfar, A., Goydos, J. S., & Cohen-Solal, K. A. (2016). The transcription factor RUNX2 regulates receptor tyrosine kinase expression in melanoma. *Oncotarget*, *7*(20), 29689–29707.

Boshuizen, J., Koopman, L. A., Krijgsman, O., Shahrabi, A., van den Heuvel, E. G.-, Ligtenberg, M. A., Vredevoogd, D. W., Kemper, K., Kuilman, T., Song, J.-Y., Pencheva, N., Mortensen, J. T., Foppen, M. G., Rozeman, E. A., Blank, C. U., Janmaat, M. L., Satijn, D., Breij, E. C. W., Peeper, D. S., & Parren, P. W. H. I. (2018). Cooperative targeting of melanoma heterogeneity with an AXL antibody-drug conjugate and BRAF/MEK inhibitors. *Nature Medicine*, *24*(2), 203–212.

Brand, T. M., Iida, M., Stein, A. P., Corrigan, K. L., Braverman, C. M., Coan, J. P., Pearson, H. E., Bahrar, H., Fowler, T. L., Bednarz, B. P., Saha, S., Yang, D., Gill, P. S., Lingen, M. W., Saloura, V., Villaflor, V. M., Salgia, R., Kimple, R. J., & Wheeler, D. L. (2015).

AXL Is a Logical Molecular Target in Head and Neck Squamous Cell Carcinoma. *Clinical Cancer Research: An Official Journal of the American Association for Cancer Research*, *21*(11), 2601–2612.

Bray, F., Ferlay, J., Soerjomataram, I., Siegel, R. L., Torre, L. A., & Jemal, A. (2018). Global cancer statistics 2018: GLOBOCAN estimates of incidence and mortality worldwide for 36 cancers in 185 countries. *CA: A Cancer Journal for Clinicians*, *68*(6), 394–424.

Brenner, M., & Hearing, V. J. (2008). The protective role of melanin against UV damage in human skin. *Photochemistry and Photobiology*, *84*(3), 539–549.

Bublil, E. M., & Yarden, Y. (2007). The EGF receptor family: spearheading a merger of signaling and therapeutics. *Current Opinion in Cell Biology*, *19*(2), 124–134.

Burgess, A. W., Cho, H.-S., Eigenbrot, C., Ferguson, K. M., Garrett, T. P. J., Leahy, D. J., Lemmon, M. A., Sliwkowski, M. X., Ward, C. W., & Yokoyama, S. (2003). An Open-and-Shut Case? Recent Insights into the Activation of EGF/ErbB Receptors. *Molecular Cell*, *12*(3), 541–552.

Buscà, R., Berra, E., Gaggioli, C., Khaled, M., Bille, K., Marchetti, B., Thyss, R., Fitsialos, G., Larribère, L., Bertolotto, C., Virolle, T., Barbry, P., Pouysségur, J., Ponzio, G., & Ballotti, R. (2005). Hypoxia-inducible factor 1{alpha} is a new target of microphthalmia-associated transcription factor (MITF) in melanoma cells. *The Journal of Cell Biology*, *170*(1), 49–59.

Cancer Genome Atlas Network. (2015). Genomic Classification of Cutaneous Melanoma. *Cell*, *161*(7), 1681–1696.

Cancer in Norway. (2018). *Cancer Registry of Norway. Cancer in Norway 2018 - Cancer incidence, mortality, survival and prevalence in Norway. Oslo: Cancer Registry of Norway, 2019*. Cancer Registry of Norway. https://www.kreftregisteret.no/globalassets/cancer-in-norway/2018/cin2018.pdf

Cao, J., Wan, L., Hacker, E., Dai, X., Lenna, S., Jimenez-Cervantes, C., Wang, Y., Leslie, N. R., Xu, G. X., Widlund, H. R., Ryu, B., Alani, R. M., Dutton-Regester, K., Goding, C. R., Hayward, N. K., Wei, W., & Cui, R. (2013). MC1R is a potent regulator of PTEN after UV

exposure in melanocytes. *Molecular Cell*, *51*(4), 409–422.

Capparelli, C., Rosenbaum, S., Berger, A. C., & Aplin, A. E. (2015). Fibroblast-derived neuregulin 1 promotes compensatory ErbB3 receptor signaling in mutant BRAF melanoma. *The Journal of Biological Chemistry*, *290*(40), 24267–24277.

Carreira, S., Goodall, J., Denat, L., Rodriguez, M., Nuciforo, P., Hoek, K. S., Testori, A., Larue, L., & Goding, C. R. (2006). Mitf regulation of Dia1 controls melanoma proliferation and invasiveness. *Genes & Development*, *20*(24), 3426–3439.

Cereseto, A., & Giacca, M. (2004). Integration site selection by retroviruses. *AIDS Reviews*, *6*(1), 13–21.

Chapman, P. B., Hauschild, A., Robert, C., Haanen, J. B., Ascierto, P., Larkin, J., Dummer, R., Garbe, C., Testori, A., Maio, M., Hogg, D., Lorigan, P., Lebbe, C., Jouary, T., Schadendorf, D., Ribas, A., O'Day, S. J., Sosman, J. A., Kirkwood, J. M., … BRIM-3 Study Group. (2011). Improved survival with vemurafenib in melanoma with BRAF V600E mutation. *The New England Journal of Medicine*, *364*(26), 2507–2516.

Cheli, Y., Giuliano, S., Botton, T., Rocchi, S., Hofman, V., Hofman, P., Bahadoran, P., Bertolotto, C., & Ballotti, R. (2011). Mitf is the key molecular switch between mouse or human melanoma initiating cells and their differentiated progeny. *Oncogene*, *30*(20), 2307–2318.

Cheli, Y., Giuliano, S., Fenouille, N., Allegra, M., Hofman, V., Hofman, P., Bahadoran, P., Lacour, J.-P., Tartare-Deckert, S., Bertolotto, C., & Ballotti, R. (2012). Hypoxia and MITF control metastatic behaviour in mouse and human melanoma cells. *Oncogene*, *31*(19), 2461–2470.

Ciardiello, F., & Tortora, G. (2001). A novel approach in the treatment of cancer: targeting the epidermal growth factor receptor. *Clinical Cancer Research: An Official Journal of the American Association for Cancer Research*, *7*(10), 2958–2970.

Cichorek, M., Wachulska, M., Stasiewicz, A., & Tymińska, A. (2013). Skin melanocytes: biology and development. *Postepy Dermatologii I Alergologii*, *30*(1), 30–41.

Cirenajwis, H., Lauss, M., Ekedahl, H., Törngren, T., Kvist, A., Saal, L. H., Olsson, H., Staaf,

J., Carneiro, A., Ingvar, C., & Others. (2017). NF1-mutated melanoma tumors harbor distinct clinical and biological characteristics. *Molecular Oncology*, *11*(4), 438–451.

Ciuffreda, L., Falcone, I., Incani, U. C., Del Curatolo, A., Conciatori, F., Matteoni, S., Vari, S., Vaccaro, V., Cognetti, F., & Milella, M. (2014). PTEN expression and function in adult cancer stem cells and prospects for therapeutic targeting. *Advances in Biological Regulation*, *56*, 66–80.

Cohen-Solal, K. A., Kaufman, H. L., & Lasfar, A. (2018). Transcription factors as critical players in melanoma invasiveness, drug resistance, and opportunities for therapeutic drug development. *Pigment Cell & Melanoma Research*, *31*(2), 241–252.

Cortese, K., Giordano, F., Surace, E. M., Venturi, C., Ballabio, A., Tacchetti, C., & Marigo, V. (2005). The ocular albinism type 1 (OA1) gene controls melanosome maturation and size. *Investigative Ophthalmology & Visual Science*, *46*(12), 4358–4364.

Cory, A. H., Owen, T. C., Barltrop, J. A., & Cory, J. G. (1991). Use of an aqueous soluble tetrazolium/formazan assay for cell growth assays in culture. *Cancer Communications*, *3*(7), 207–212.

Curran, K., Raible, D. W., & Lister, J. A. (2009). Foxd3 controls melanophore specification in the zebrafish neural crest by regulation of Mitf. *Developmental Biology*, *332*(2), 408–417.

Curtin, J. A., Stark, M. S., Pinkel, D., Hayward, N. K., & Bastian, B. C. (2006). PI3-kinase subunits are infrequent somatic targets in melanoma. *The Journal of Investigative Dermatology*, *126*(7), 1660–1663.

Dalby, B., Cates, S., Harris, A., Ohki, E. C., Tilkins, M. L., Price, P. J., & Ciccarone, V. C. (2004). Advanced transfection with Lipofectamine 2000 reagent: primary neurons, siRNA, and high-throughput applications. *Methods* , *33*(2), 95–103.

Davies, H., Bignell, G. R., Cox, C., Stephens, P., Edkins, S., Clegg, S., Teague, J., Woffendin, H., Garnett, M. J., Bottomley, W., Davis, N., Dicks, E., Ewing, R., Floyd, Y., Gray, K., Hall, S., Hawes, R., Hughes, J., Kosmidou, V., … Futreal, P. A. (2002). Mutations of the BRAF gene in human cancer. *Nature*, *417*(6892), 949–954.

Davies, M. A., Stemke-Hale, K., Tellez, C., Calderone, T. L., Deng, W., Prieto, V. G., Lazar,

A. J. F., Gershenwald, J. E., & Mills, G. B. (2008). A novel AKT3 mutation in melanoma tumours and cell lines. *British Journal of Cancer*, *99*(8), 1265–1268.

Desnoo, F., & Hayward, N. (2005). Cutaneous melanoma susceptibility and progression genes. In *Cancer Letters* (Vol. 230, Issue 2, pp. 153–186). https://doi.org/10.1016/j.canlet.2004.12.033

Dheda, K., Huggett, J. F., Bustin, S. A., Johnson, M. A., Rook, G., & Zumla, A. (2004). Validation of housekeeping genes for normalizing RNA expression in real-time PCR. *BioTechniques*, *37*(1), 112–114, 116, 118–119.

Dhillon, A. S., Hagan, S., Rath, O., & Kolch, W. (2007). MAP kinase signalling pathways in cancer. *Oncogene*, *26*(22), 3279–3290.

D'Mello, S. A. N., Finlay, G. J., Baguley, B. C., & Askarian-Amiri, M. E. (2016). Signaling Pathways in Melanogenesis. *International Journal of Molecular Sciences*, *17*(7), 1–2.

Domingues, B., Lopes, J. M., Soares, P., & Pópulo, H. (2018). Melanoma treatment in review. *ImmunoTargets and Therapy*, *7*, 35–49.

Dorsky, R. I., Raible, D. W., & Moon, R. T. (2000). Direct regulation of nacre, a zebrafish MITF homolog required for pigment cell formation, by the Wnt pathway. *Genes & Development*, *14*(2), 158–162.

Dropulić, B. (2011). Lentiviral vectors: their molecular design, safety, and use in laboratory and preclinical research. *Human Gene Therapy*, *22*(6), 649–657.

Dufies, M., Jacquel, A., Belhacene, N., Robert, G., Cluzeau, T., Luciano, F., Cassuto, J. P., Raynaud, S., & Auberger, P. (2011). Mechanisms of AXL overexpression and function in Imatinib-resistant chronic myeloid leukemia cells. *Oncotarget*, *2*(11), 874–885.

Du, J., & Fisher, D. E. (2002). Identification of Aim-1 as the underwhite mouse mutant and its transcriptional regulation by MITF. *The Journal of Biological Chemistry*, *277*(1), 402–406.

Du, J., Miller, A. J., Widlund, H. R., Horstmann, M. A., Ramaswamy, S., & Fisher, D. E. (2003). MLANA/MART1 and SILV/PMEL17/GP100 Are Transcriptionally Regulated by MITF in Melanocytes and Melanoma. In *The American Journal of Pathology* (Vol. 163,

Issue 1, pp. 333–343). https://doi.org/10.1016/s0002-9440(10)63657-7

Du, J., Widlund, H. R., Horstmann, M. A., Ramaswamy, S., Ross, K., Huber, W. E., Nishimura, E. K., Golub, T. R., & Fisher, D. E. (2004). Critical role of CDK2 for melanoma growth linked to its melanocyte-specific transcriptional regulation by MITF. *Cancer Cell*, *6*(6), 565–576.

Dummer, R., Ascierto, P. A., Gogas, H. J., Arance, A., Mandala, M., Liszkay, G., Garbe, C., Schadendorf, D., Krajsova, I., Gutzmer, R., Chiarion Sileni, V., Dutriaux, C., de Groot, J. W. B., Yamazaki, N., Loquai, C., Moutouh-de Parseval, L. A., Pickard, M. D., Sandor, V., Robert, C., & Flaherty, K. T. (2018). Overall survival in patients with BRAF-mutant melanoma receiving encorafenib plus binimetinib versus vemurafenib or encorafenib (COLUMBUS): a multicentre, open-label, randomised, phase 3 trial. *The Lancet Oncology*, *19*(10), 1315–1327.

Egeblad, M., Nakasone, E. S., & Werb, Z. (2010). Tumors as organs: complex tissues that interface with the entire organism. *Developmental Cell*, *18*(6), 884–901.

Eissa, N., Kermarrec, L., Hussein, H., Bernstein, C. N., & Ghia, J.-E. (2017). Appropriateness of reference genes for normalizing messenger RNA in mouse 2,4-dinitrobenzene sulfonic acid (DNBS)-induced colitis using quantitative real time PCR. *Scientific Reports*, *7*, 42427.

Elbashir, S. M., Harborth, J., Lendeckel, W., Yalcin, A., Weber, K., & Tuschl, T. (2001). Duplexes of 21-nucleotide RNAs mediate RNA interference in cultured mammalian cells. *Nature*, *411*(6836), 494–498.

Engelman, J. A., Luo, J., & Cantley, L. C. (2006). The evolution of phosphatidylinositol 3-kinases as regulators of growth and metabolism. *Nature Reviews. Genetics*, *7*(8), 606–619.

Ernfors, P. (2010). Cellular origin and developmental mechanisms during the formation of skin melanocytes. *Experimental Cell Research*, *316*(8), 1397–1407.

Falletta, P., Sanchez-Del-Campo, L., Chauhan, J., Effern, M., Kenyon, A., Kershaw, C. J., Siddaway, R., Lisle, R., Freter, R., Daniels, M. J., Lu, X., Tüting, T., Middleton, M., Buffa,

F. M., Willis, A. E., Pavitt, G., Ronai, Z. A., Sauka-Spengler, T., Hölzel, M., & Goding, C. R. (2017). Translation reprogramming is an evolutionarily conserved driver of phenotypic plasticity and therapeutic resistance in melanoma. *Genes & Development*, *31*(1), 18–33.

Fang, D., Tsuji, Y., & Setaluri, V. (2002). Selective down-regulation of tyrosinase family gene TYRP1 by inhibition of the activity of melanocyte transcription factor, MITF. *Nucleic Acids Research*, *30*(14), 3096–3106.

Fattore, L., Marra, E., Pisanu, M. E., Noto, A., de Vitis, C., Belleudi, F., Aurisicchio, L., Mancini, R., Torrisi, M. R., Ascierto, P. A., & Ciliberto, G. (2013). Activation of an early feedback survival loop involving phospho-ErbB3 is a general response of melanoma cells to RAF/MEK inhibition and is abrogated by anti-ErbB3 antibodies. *Journal of Translational Medicine*, *11*, 180.

Fedorenko, I. V., Gibney, G. T., & Smalley, K. S. M. (2013). NRAS mutant melanoma: biological behavior and future strategies for therapeutic management. *Oncogene*, *32*(25), 3009–3018.

Ferguson, J., Smith, M., Zudaire, I., Wellbrock, C., & Arozarena, I. (2017). Glucose availability controls ATF4-mediated MITF suppression to drive melanoma cell growth. *Oncotarget*, *8*(20), 32946–32959.

Fitzpatrick, T. B., & Breathnach, A. S. (1963). The epidermal melanin unit system. *Dermatologische Wochenschrift*, *147*, 481–489.

Forbes, S. A., Beare, D., Gunasekaran, P., Leung, K., Bindal, N., Boutselakis, H., Ding, M., Bamford, S., Cole, C., Ward, S., & Others. (2015). Tisham De, Jon W. Teague, Michael R. Stratton, Ultan McDermott, and Peter J. Campbell. COSMIC: exploring the world's knowledge of somatic mutations in human cancer. *Nucleic Acids Research*, *43*, D805–D811.

Frederick, D. T., Piris, A., Cogdill, A. P., Cooper, Z. A., Lezcano, C., Ferrone, C. R., Mitra, D., Boni, A., Newton, L. P., Liu, C., Peng, W., Sullivan, R. J., Lawrence, D. P., Hodi, F. S., Overwijk, W. W., Lizée, G., Murphy, G. F., Hwu, P., Flaherty, K. T., … Wargo, J. A. (2013). BRAF inhibition is associated with enhanced melanoma antigen expression and

a more favorable tumor microenvironment in patients with metastatic melanoma. *Clinical Cancer Research: An Official Journal of the American Association for Cancer Research*, *19*(5), 1225–1231.

Fuller, S. J., Sivarajah, K., & Sugden, P. H. (2008). ErbB receptors, their ligands, and the consequences of their activation and inhibition in the myocardium. *Journal of Molecular and Cellular Cardiology*, *44*(5), 831–854.

Garraway, L. A., Widlund, H. R., Rubin, M. A., Getz, G., Berger, A. J., Ramaswamy, S., Beroukhim, R., Milner, D. A., Granter, S. R., Du, J., Lee, C., Wagner, S. N., Li, C., Golub, T. R., Rimm, D. L., Meyerson, M. L., Fisher, D. E., & Sellers, W. R. (2005). Integrative genomic analyses identify MITF as a lineage survival oncogene amplified in malignant melanoma. *Nature*, *436*(7047), 117–122.

Gay, C. M., Balaji, K., & Byers, L. A. (2017). Giving AXL the axe: targeting AXL in human malignancy. *British Journal of Cancer*, *116*(4), 415–423.

Girotti, M. R., Pedersen, M., Sanchez-Laorden, B., Viros, A., Turajlic, S., Niculescu-Duvaz, D., Zambon, A., Sinclair, J., Hayes, A., Gore, M., Lorigan, P., Springer, C., Larkin, J., Jorgensen, C., & Marais, R. (2013). Inhibiting EGF receptor or SRC family kinase signaling overcomes BRAF inhibitor resistance in melanoma. *Cancer Discovery*, *3*(2), 158–167.

Gjerdrum, C., Tiron, C., Høiby, T., Stefansson, I., Haugen, H., Sandal, T., Collett, K., Li, S., McCormack, E., Gjertsen, B. T., Micklem, D. R., Akslen, L. A., Glackin, C., & Lorens, J. B. (2010). Axl is an essential epithelial-to-mesenchymal transition-induced regulator of breast cancer metastasis and patient survival. *Proceedings of the National Academy of Sciences of the United States of America*, *107*(3), 1124–1129.

Goding, C. R., & Arnheiter, H. (2019). MITF-the first 25 years. *Genes & Development*, *33*(15-16), 983–1007.

Goel, V. K., Lazar, A. J. F., Warneke, C. L., Redston, M. S., & Haluska, F. G. (2006). Examination of mutations in BRAF, NRAS, and PTEN in primary cutaneous melanoma. *The Journal of Investigative Dermatology*, *126*(1), 154–160.

Goldstein, A. M., & Tucker, M. A. (2001). Genetic epidemiology of cutaneous melanoma: a global perspective. *Archives of Dermatology*, *137*(11), 1493–1496.

Goodall, J., Carreira, S., Denat, L., Kobi, D., Davidson, I., Nuciforo, P., Sturm, R. A., Larue, L., & Goding, C. R. (2008). Brn-2 represses microphthalmia-associated transcription factor expression and marks a distinct subpopulation of microphthalmia-associated transcription factor-negative melanoma cells. *Cancer Research*, *68*(19), 7788–7794.

Goodall, J., Wellbrock, C., Dexter, T. J., Roberts, K., Marais, R., & Goding, C. R. (2004). The Brn-2 transcription factor links activated BRAF to melanoma proliferation. *Molecular and Cellular Biology*, *24*(7), 2923–2931.

Gopal, Y. N. V., Deng, W., Woodman, S. E., Komurov, K., Ram, P., Smith, P. D., & Davies, M. A. (2010). Basal and treatment-induced activation of AKT mediates resistance to cell death by AZD6244 (ARRY-142886) in Braf-mutant human cutaneous melanoma cells. *Cancer Research*, *70*(21), 8736–8747.

Goyette, M.-A., Duhamel, S., Aubert, L., Pelletier, A., Savage, P., Thibault, M.-P., Johnson, R. M., Carmeliet, P., Basik, M., Gaboury, L., Muller, W. J., Park, M., Roux, P. P., Gratton, J.-P., & Côté, J.-F. (2018). The Receptor Tyrosine Kinase AXL Is Required at Multiple Steps of the Metastatic Cascade during HER2-Positive Breast Cancer Progression. *Cell Reports*, *23*(5), 1476–1490.

Graham, D. K., DeRyckere, D., Davies, K. D., & Earp, H. S. (2014). The TAM family: phosphatidylserine sensing receptor tyrosine kinases gone awry in cancer. *Nature Reviews. Cancer*, *14*(12), 769–785.

Gray-Schopfer, V. C., Cheong, S. C., Chong, H., Chow, J., Moss, T., Abdel-Malek, Z. A., Marais, R., Wynford-Thomas, D., & Bennett, D. C. (2006). Cellular senescence in naevi and immortalisation in melanoma: a role for p16? *British Journal of Cancer*, *95*(4), 496–505.

Greger, J. G., Eastman, S. D., Zhang, V., Bleam, M. R., Hughes, A. M., Smitheman, K. N., Dickerson, S. H., Laquerre, S. G., Liu, L., & Gilmer, T. M. (2012). Combinations of BRAF, MEK, and PI3K/mTOR inhibitors overcome acquired resistance to the BRAF

inhibitor GSK2118436 dabrafenib, mediated by NRAS or MEK mutations. *Molecular Cancer Therapeutics*, *11*(4), 909–920.

Guo, Z., Li, Y., Zhang, D., & Ma, J. (2017). Axl inhibition induces the antitumor immune response which can be further potentiated by PD-1 blockade in the mouse cancer models. *Oncotarget*, *8*(52), 89761–89774.

Guy, G. P., Jr, Thomas, C. C., Thompson, T., Watson, M., Massetti, G. M., Richardson, L. C., & Centers for Disease Control and Prevention (CDC). (2015). Vital signs: melanoma incidence and mortality trends and projections - United States, 1982-2030. *MMWR. Morbidity and Mortality Weekly Report*, *64*(21), 591–596.

Haass, N. K., Smalley, K. S. M., Li, L., & Herlyn, M. (2005). Adhesion, migration and communication in melanocytes and melanoma. *Pigment Cell Research / Sponsored by the European Society for Pigment Cell Research and the International Pigment Cell Society*, *18*(3), 150–159.

Haferkamp, S., Tran, S. L., Becker, T. M., Scurr, L. L., Kefford, R. F., & Rizos, H. (2009). The relative contributions of the p53 and pRb pathways in oncogene-induced melanocyte senescence. *Aging*, *1*(6), 542–556.

Halaban, R., Zhang, W., Bacchiocchi, A., Cheng, E., Parisi, F., Ariyan, S., Krauthammer, M., McCusker, J. P., Kluger, Y., & Sznol, M. (2010). PLX4032, a selective BRAFV600E kinase inhibitor, activates the ERK pathway and enhances cell migration and proliferation of BRAFWT melanoma cells. *Pigment Cell & Melanoma Research*, *23*(2), 190–200.

Hall-Jackson, C. A., Eyers, P. A., Cohen, P., Goedert, M., Boyle, F. T., Hewitt, N., Plant, H., & Hedge, P. (1999). Paradoxical activation of Raf by a novel Raf inhibitor. *Chemistry & Biology*, *6*(8), 559–568.

Hanahan, D., & Weinberg, R. A. (2000). The hallmarks of cancer. *Cell*, *100*(1), 57–70.

Hanahan, D., & Weinberg, R. A. (2011). Hallmarks of cancer: the next generation. *Cell*, *144*(5), 646–674.

Hartman, M. L., & Czyz, M. (2015). MITF in melanoma: mechanisms behind its expression

and activity. *Cellular and Molecular Life Sciences: CMLS*, *72*(7), 1249–1260.

Haslam, A., & Prasad, V. (2019). Estimation of the Percentage of US Patients With Cancer Who Are Eligible for and Respond to Checkpoint Inhibitor Immunotherapy Drugs. *JAMA Network Open*, *2*(5), e192535.

Hayashi, M., Inokuchi, M., Takagi, Y., Yamada, H., Kojima, K., Kumagai, J., Kawano, T., & Sugihara, K. (2008). High expression of HER3 is associated with a decreased survival in gastric cancer. *Clinical Cancer Research: An Official Journal of the American Association for Cancer Research*, *14*(23), 7843–7849.

Hemesath, T. J., Steingrímsson, E., McGill, G., Hansen, M. J., Vaught, J., Hodgkinson, C. A., Arnheiter, H., Copeland, N. G., Jenkins, N. A., & Fisher, D. E. (1994). microphthalmia, a critical factor in melanocyte development, defines a discrete transcription factor family. *Genes & Development*, *8*(22), 2770–2780.

He, M., Huang, H., Wang, M., Chen, A., Ning, X., Yu, K., Li, Q., Li, W., Ma, L., Chen, Z., Wang, X., & Sun, Q. (2015). Fluorescence-Activated Cell Sorting Analysis of Heterotypic Cell-in-Cell Structures. *Scientific Reports*, *5*, 9588.

He, S., Li, C. G., Slobbe, L., Glover, A., Marshall, E., Baguley, B. C., & Eccles, M. R. (2011). PAX3 knockdown in metastatic melanoma cell lines does not reduce MITF expression. *Melanoma Research*, *21*(1), 24–34.

Hodis, E., Watson, I. R., Kryukov, G. V., Arold, S. T., Imielinski, M., Theurillat, J.-P., Nickerson, E., Auclair, D., Li, L., Place, C., Dicara, D., Ramos, A. H., Lawrence, M. S., Cibulskis, K., Sivachenko, A., Voet, D., Saksena, G., Stransky, N., Onofrio, R. C., … Chin, L. (2012). A landscape of driver mutations in melanoma. *Cell*, *150*(2), 251–263.

Hoek, K. S., Eichhoff, O. M., Schlegel, N. C., Döbbeling, U., Kobert, N., Schaerer, L., Hemmi, S., & Dummer, R. (2008). In vivo switching of human melanoma cells between proliferative and invasive states. *Cancer Research*, *68*(3), 650–656.

Hoek, K. S., Schlegel, N. C., Brafford, P., Sucker, A., Ugurel, S., Kumar, R., Weber, B. L., Nathanson, K. L., Phillips, D. J., Herlyn, M., Schadendorf, D., & Dummer, R. (2006). Metastatic potential of melanomas defined by specific gene expression profiles with no

BRAF signature. *Pigment Cell Research / Sponsored by the European Society for Pigment Cell Research and the International Pigment Cell Society*, *19*(4), 290–302.

Hoek, K. S., Schlegel, N. C., & Eichhoff, O. M. (2008). Novel MITF targets identified using a two-step DNA microarray strategy. *Pigment Cell & Melanoma Research*. https://onlinelibrary.wiley.com/doi/abs/10.1111/j.1755-148X.2008.00505.x

Hoek, K. S., Schlegel, N. C., Eichhoff, O. M., Widmer, D. S., Praetorius, C., Einarsson, S. O., Valgeirsdottir, S., Bergsteinsdottir, K., Schepsky, A., Dummer, R., & Steingrimsson, E. (2008). Novel MITF targets identified using a two-step DNA microarray strategy. *Pigment Cell & Melanoma Research*, *21*(6), 665–676.

Hojjat-Farsangi, M. (2015). Novel and emerging targeted-based cancer therapy agents and methods. *Tumour Biology: The Journal of the International Society for Oncodevelopmental Biology and Medicine*, *36*(2), 543–556.

Horn, S., Figl, A., Rachakonda, P. S., Fischer, C., Sucker, A., Gast, A., Kadel, S., Moll, I., Nagore, E., Hemminki, K., Schadendorf, D., & Kumar, R. (2013). TERT promoter mutations in familial and sporadic melanoma. *Science*, *339*(6122), 959–961.

Hsieh, M.-S., Yang, P.-W., Wong, L.-F., & Lee, J.-M. (2016). The AXL receptor tyrosine kinase is associated with adverse prognosis and distant metastasis in esophageal squamous cell carcinoma. *Oncotarget*, *7*(24), 36956–36970.

Huang, F. W., Hodis, E., Xu, M. J., Kryukov, G. V., Chin, L., & Garraway, L. A. (2013). Highly recurrent TERT promoter mutations in human melanoma. *Science*, *339*(6122), 957–959.

Huang, K. T., Chen, Y. H., & Walker, A. M. (2004). Inaccuracies in MTS assays: major distorting effects of medium, serum albumin, and fatty acids. *BioTechniques*, *37*(3), 406, 408, 410–412.

Hubbard, S. R., & Miller, W. T. (2007). Receptor tyrosine kinases: mechanisms of activation and signaling. *Current Opinion in Cell Biology*, *19*(2), 117–123.

Huber, W. E., Price, E. R., Widlund, H. R., Du, J., Davis, I. J., Wegner, M., & Fisher, D. E. (2003). A tissue-restricted cAMP transcriptional response: SOX10 modulates alpha-melanocyte-stimulating hormone-triggered expression of microphthalmia-associated

transcription factor in melanocytes. *The Journal of Biological Chemistry*, *278*(46), 45224–45230.

Hu-Lieskovan, S., Mok, S., Moreno, B. H., Tsoi, J., Robert, L., Goedert, L., Pinheiro, E. M., Koya, R. C., Graeber, T. G., Comin-Anduix, B., & Ribas, A. (2015). Improved antitumor activity of immunotherapy with BRAF and MEK inhibitors in BRAF V600E melanoma. In *Science Translational Medicine* (Vol. 7, Issue 279, pp. 279ra41–ra279ra41). https://doi.org/10.1126/scitranslmed.aaa4691

Hussussian, C. J., Struewing, J. P., Goldstein, A. M., Higgins, P. A., Ally, D. S., Sheahan, M. D., Clark, W. H., Jr, Tucker, M. A., & Dracopoli, N. C. (1994). Germline p16 mutations in familial melanoma. *Nature Genetics*, *8*(1), 15–21.

Hynes, N. E., & Lane, H. A. (2005). ERBB receptors and cancer: the complexity of targeted inhibitors. *Nature Reviews. Cancer*, *5*(5), 341–354.

Ioannidis, J. P. A., Munafò, M. R., Fusar-Poli, P., Nosek, B. A., & David, S. P. (2014). Publication and other reporting biases in cognitive sciences: detection, prevalence, and prevention. *Trends in Cognitive Sciences*, *18*(5), 235–241.

Ishikawa, F., Yasukawa, M., Lyons, B., Yoshida, S., Miyamoto, T., Yoshimoto, G., Watanabe, T., Akashi, K., Shultz, L. D., & Harada, M. (2005). Development of functional human blood and immune systems in NOD/SCID/IL2 receptor γ chainnull mice. *Blood*, *106*(5), 1565–1573.

Iwafuchi-Doi, M., & Zaret, K. S. (2014). Pioneer transcription factors in cell reprogramming. *Genes & Development*, *28*(24), 2679–2692.

Jackson, A. L., Bartz, S. R., Schelter, J., Kobayashi, S. V., Burchard, J., Mao, M., Li, B., Cavet, G., & Linsley, P. S. (2003). Expression profiling reveals off-target gene regulation by RNAi. *Nature Biotechnology*, *21*(6), 635–637.

Ji, Z., Erin Chen, Y., Kumar, R., Taylor, M., Jenny Njauw, C.-N., Miao, B., Frederick, D. T., Wargo, J. A., Flaherty, K. T., Jönsson, G., & Tsao, H. (2015). MITF Modulates Therapeutic Resistance through EGFR Signaling. *The Journal of Investigative Dermatology*, *135*(7), 1863–1872.

Johannessen, C. M., Boehm, J. S., Kim, S. Y., Thomas, S. R., Wardwell, L., Johnson, L. A., Emery, C. M., Stransky, N., Cogdill, A. P., Barretina, J., Caponigro, G., Hieronymus, H., Murray, R. R., Salehi-Ashtiani, K., Hill, D. E., Vidal, M., Zhao, J. J., Yang, X., Alkan, O., … Garraway, L. A. (2010). COT drives resistance to RAF inhibition through MAP kinase pathway reactivation. *Nature*, *468*(7326), 968–972.

John, L. K., Loewenstein, G., & Prelec, D. (2012). Measuring the prevalence of questionable research practices with incentives for truth telling. *Psychological Science*, *23*(5), 524–532.

Kakadia, S., Yarlagadda, N., Awad, R., Kundranda, M., Niu, J., Naraev, B., Mina, L., Dragovich, T., Gimbel, M., & Mahmoud, F. (2018). Mechanisms of resistance to BRAF and MEK inhibitors and clinical update of US Food and Drug Administration-approved targeted therapy in advanced melanoma. *OncoTargets and Therapy*, *11*, 7095–7107.

Kamb, A., Shattuck-Eidens, D., Eeles, R., Liu, Q., Gruis, N. A., Ding, W., Hussey, C., Tran, T., Miki, Y., & Weaver-Feldhaus, J. (1994). Analysis of the p16 gene (CDKN2) as a candidate for the chromosome 9p melanoma susceptibility locus. *Nature Genetics*, *8*(1), 23–26.

Kawakami, A., & Fisher, D. E. (2017). The master role of microphthalmia-associated transcription factor in melanocyte and melanoma biology. *Laboratory Investigation; a Journal of Technical Methods and Pathology*, *97*(6), 649–656.

Kemper, K., de Goeje, P. L., Peeper, D. S., & van Amerongen, R. (2014). Phenotype switching: tumor cell plasticity as a resistance mechanism and target for therapy. *Cancer Research*, *74*(21), 5937–5941.

Kemper, K., Krijgsman, O., Kong, X., Cornelissen-Steijger, P., Shahrabi, A., Weeber, F., & Peeper, D. S. (2016). *BRAF (V600E) kinase domain duplication identified in therapy-refractory melanoma patient-derived xenografts. Cell Rep 16 (1): 263--277*.

Kim, I. S., Heilmann, S., Kansler, E. R., Zhang, Y., Zimmer, M., Ratnakumar, K., Bowman, R. L., Simon-Vermot, T., Fennell, M., Garippa, R., Lu, L., Lee, W., Hollmann, T., Xavier, J. B., & White, R. M. (2017). Microenvironment-derived factors driving metastatic plasticity

in melanoma. *Nature Communications*, *8*, 14343.

Kim, K. B., Flaherty, K. T., Chapman, P. B., Sosman, J. A., Ribas, A., McArthur, G. A., Amaravadi, R. K., Lee, R. J., Nolop, K. B., & Puzanov, I. (2011). Pattern and outcome of disease progression in phase I study of vemurafenib in patients with metastatic melanoma (MM). *Journal of Clinical Orthodontics: JCO*, *29*(15_suppl), 8519–8519.

Kodaz, H., Kostek, O., Hacioglu, M. B., Erdogan, B., Kodaz, C. E., Hacibekiroglu, I., Turkmen, E., Uzunoglu, S., & Cicin, I. (2017). Frequency of RAS Mutations (KRAS, NRAS, HRAS) in Human Solid Cancer. *Breast Cancer* , *7*(12), 5.

Kong, X., Kuilman, T., Shahrabi, A., Boshuizen, J., Kemper, K., Song, J.-Y., Niessen, H. W. M., Rozeman, E. A., Geukes Foppen, M. H., Blank, C. U., & Peeper, D. S. (2017). Cancer drug addiction is relayed by an ERK2-dependent phenotype switch. *Nature*, *550*(7675), 270–274.

Konieczkowski, D. J., Johannessen, C. M., Abudayyeh, O., Kim, J. W., Cooper, Z. A., Piris, A., Frederick, D. T., Barzily-Rokni, M., Straussman, R., Haq, R., Fisher, D. E., Mesirov, J. P., Hahn, W. C., Flaherty, K. T., Wargo, J. A., Tamayo, P., & Garraway, L. A. (2014). A melanoma cell state distinction influences sensitivity to MAPK pathway inhibitors. *Cancer Discovery*, *4*(7), 816–827.

Kos, R., Reedy, M. V., Johnson, R. L., & Erickson, C. A. (2001). The winged-helix transcription factor FoxD3 is important for establishing the neural crest lineage and repressing melanogenesis in avian embryos. *Development* , *128*(8), 1467–1479.

Koumakpayi, I. H., Diallo, J.-S., Le Page, C., Lessard, L., Gleave, M., Bégin, L. R., Mes-Masson, A.-M., & Saad, F. (2006). Expression and nuclear localization of ErbB3 in prostate cancer. *Clinical Cancer Research: An Official Journal of the American Association for Cancer Research*, *12*(9), 2730–2737.

Kozar, I., Margue, C., Rothengatter, S., Haan, C., & Kreis, S. (2019). Many ways to resistance: How melanoma cells evade targeted therapies. *Biochimica et Biophysica Acta, Reviews on Cancer*, *1871*(2), 313–322.

Kraus, M. H., Issing, W., Miki, T., Popescu, N. C., & Aaronson, S. A. (1989). Isolation and

characterization of ERBB3, a third member of the ERBB/epidermal growth factor receptor family: evidence for overexpression in a subset of human mammary tumors. In *Proceedings of the National Academy of Sciences* (Vol. 86, Issue 23, pp. 9193–9197). https://doi.org/10.1073/pnas.86.23.9193

Krauthammer, M., Kong, Y., Bacchiocchi, A., Evans, P., Pornputtapong, N., Wu, C., McCusker, J. P., Ma, S., Cheng, E., Straub, R., Serin, M., Bosenberg, M., Ariyan, S., Narayan, D., Sznol, M., Kluger, H. M., Mane, S., Schlessinger, J., Lifton, R. P., & Halaban, R. (2015). Exome sequencing identifies recurrent mutations in NF1 and RASopathy genes in sun-exposed melanomas. *Nature Genetics*, *47*(9), 996–1002.

Lai, C., & Lemke, G. (1991). An extended family of protein-tyrosine kinase genes differentially expressed in the vertebrate nervous system. *Neuron*, *6*(5), 691–704.

Lang, D., Lu, M. M., Huang, L., Engleka, K. A., Zhang, M., Chu, E. Y., Lipner, S., Skoultchi, A., Millar, S. E., & Epstein, J. A. (2005). Pax3 functions at a nodal point in melanocyte stem cell differentiation. *Nature*, *433*(7028), 884–887.

Larkin, J., Chiarion-Sileni, V., Gonzalez, R., Grob, J.-J., Rutkowski, P., Lao, C. D., Cowey, C. L., Schadendorf, D., Wagstaff, J., Dummer, R., Ferrucci, P. F., Smylie, M., Hogg, D., Hill, A., Márquez-Rodas, I., Haanen, J., Guidoboni, M., Maio, M., Schöffski, P., … Wolchok, J. D. (2019). Five-Year Survival with Combined Nivolumab and Ipilimumab in Advanced Melanoma. *The New England Journal of Medicine*, *381*(16), 1535–1546.

Larkin, J., & Fisher. (2012). Vemurafenib: a new treatment for BRAF-V600 mutated advanced melanoma. In *Cancer Management and Research* (p. 243). https://doi.org/10.2147/cmar.s25284

Lassam, N. J., From, L., & Kahn, H. J. (1993). Overexpression of p53 is a late event in the development of malignant melanoma. *Cancer Research*, *53*(10 Suppl), 2235–2238.

Laurent, P.-A., Severin, S., Gratacap, M.-P., & Payrastre, B. (2014). Class I PI 3-kinases signaling in platelet activation and thrombosis: PDK1/Akt/GSK3 axis and impact of PTEN and SHIP1. *Advances in Biological Regulation*, *54*, 162–174.

Lazebnik, Y. (2010). What are the hallmarks of cancer? *Nature Reviews. Cancer*, *10*(4), 232.

Ledent, V., Paquet, O., & Vervoort, M. (2002). Phylogenetic analysis of the human basic helix-loop-helix proteins. *Genome Biology*, *3*(6), RESEARCH0030.

Lemke, G. (2013). Biology of the TAM receptors. *Cold Spring Harbor Perspectives in Biology*, *5*(11), a009076.

Lemmon, M. A., & Schlessinger, J. (2010). Cell signaling by receptor tyrosine kinases. *Cell*, *141*(7), 1117–1134.

Levy, C., Khaled, M., & Fisher, D. E. (2006). MITF: master regulator of melanocyte development and melanoma oncogene. In *Trends in Molecular Medicine* (Vol. 12, Issue 9, pp. 406–414). https://doi.org/10.1016/j.molmed.2006.07.008

Li, F. Z., Dhillon, A. S., Anderson, R. L., McArthur, G., & Ferrao, P. T. (2015). Phenotype switching in melanoma: implications for progression and therapy. *Frontiers in Oncology*, *5*, 31.

Li, J., Simpson, L., Takahashi, M., Miliaresis, C., Myers, M. P., Tonks, N., & Parsons, R. (1998). The PTEN/MMAC1 tumor suppressor induces cell death that is rescued by the AKT/protein kinase B oncogene. *Cancer Research*, *58*(24), 5667–5672.

Lin, J. Y., & Fisher, D. E. (2007). Melanocyte biology and skin pigmentation. *Nature*, *445*(7130), 843–850.

Lipson, E. J., & Drake, C. G. (2011). Ipilimumab: an anti-CTLA-4 antibody for metastatic melanoma. *Clinical Cancer Research: An Official Journal of the American Association for Cancer Research*, *17*(22), 6958–6962.

Lipton, A., Goodman, L., Leitzel, K., Cook, J., Sperinde, J., Haddad, M., Köstler, W. J., Huang, W., Weidler, J. M., Ali, S., Newton, A., Fuchs, E.-M., Paquet, A., Singer, C. F., Horvat, R., Jin, X., Banerjee, J., Mukherjee, A., Tan, Y., … Bates, M. (2013). HER3, p95HER2, and HER2 protein expression levels define multiple subtypes of HER2-positive metastatic breast cancer. *Breast Cancer Research and Treatment*, *141*(1), 43–53.

Lito, P., Rosen, N., & Solit, D. B. (2013). Tumor adaptation and resistance to RAF inhibitors. *Nature Medicine*, *19*(11), 1401–1409.

Liu, C., Peng, W., Xu, C., Lou, Y., Zhang, M., Wargo, J. A., Chen, J. Q., Li, H. S., Watowich, S. S., Yang, Y., Tompers Frederick, D., Cooper, Z. A., Mbofung, R. M., Whittington, M., Flaherty, K. T., Woodman, S. E., Davies, M. A., Radvanyi, L. G., Overwijk, W. W., … Hwu, P. (2013). BRAF inhibition increases tumor infiltration by T cells and enhances the antitumor activity of adoptive immunotherapy in mice. *Clinical Cancer Research: An Official Journal of the American Association for Cancer Research*, *19*(2), 393–403.

Liu, F., Fu, Y., & Meyskens, F. L., Jr. (2009). MiTF regulates cellular response to reactive oxygen species through transcriptional regulation of APE-1/Ref-1. *The Journal of Investigative Dermatology*, *129*(2), 422–431.

Liu, J., Fukunaga-Kalabis, M., Li, L., & Herlyn, M. (2014). Developmental pathways activated in melanocytes and melanoma. *Archives of Biochemistry and Biophysics*, *563*, 13–21.

Liu, L., Greger, J., Shi, H., Liu, Y., Greshock, J., Annan, R., Halsey, W., Sathe, G. M., Martin, A.-M., & Gilmer, T. M. (2009). Novel mechanism of lapatinib resistance in HER2-positive breast tumor cells: activation of AXL. *Cancer Research*, *69*(17), 6871–6878.

Li, Y., Jia, L., Ren, D., Liu, C., Gong, Y., Wang, N., Zhang, X., & Zhao, Y. (2014). Axl mediates tumor invasion and chemosensitivity through PI3K/Akt signaling pathway and is transcriptionally regulated by slug in breast carcinoma. *IUBMB Life*, *66*(7), 507–518.

Loercher, A. E., Tank, E. M. H., Delston, R. B., & Harbour, J. W. (2005). MITF links differentiation with cell cycle arrest in melanocytes by transcriptional activation of INK4A. *The Journal of Cell Biology*, *168*(1), 35–40.

Lopez-Gines, C., Gil-Benso, R., Ferrer-Luna, R., Benito, R., Serna, E., Gonzalez-Darder, J., Quilis, V., Monleon, D., Celda, B., & Cerdá-Nicolas, M. (2010). New pattern of EGFR amplification in glioblastoma and the relationship of gene copy number with gene expression profile. *Modern Pathology: An Official Journal of the United States and Canadian Academy of Pathology, Inc*, *23*(6), 856–865.

Lowings, P., Yavuzer, U., & Goding, C. R. (1992). Positive and negative elements regulate a melanocyte-specific promoter. *Molecular and Cellular Biology*, *12*(8), 3653–3662.

Low, K. C., & Tergaonkar, V. (2013). Telomerase: central regulator of all of the hallmarks of

cancer. *Trends in Biochemical Sciences*, *38*(9), 426–434.

Macleod, K., Mullen, P., Sewell, J., Rabiasz, G., Lawrie, S., Miller, E., Smyth, J. F., & Langdon, S. P. (2005). Altered ErbB receptor signaling and gene expression in cisplatin-resistant ovarian cancer. *Cancer Research*, *65*(15), 6789–6800.

Maehama, T., & Dixon, J. E. (1998). The tumor suppressor, PTEN/MMAC1, dephosphorylates the lipid second messenger, phosphatidylinositol 3,4,5-trisphosphate. *The Journal of Biological Chemistry*, *273*(22), 13375–13378.

Mangas, C., Potrony, M., Mainetti, C., Bianchi, E., Carrozza Merlani, P., Mancarella Eberhardt, A., Maspoli-Postizzi, E., Marazza, G., Marcollo-Pini, A., Pelloni, F., Sessa, C., Simona, B., Puig-Butillé, J. A., Badenas, C., & Puig, S. (2016). Genetic susceptibility to cutaneous melanoma in southern Switzerland: role of CDKN2A, MC1R and MITF. *The British Journal of Dermatology*, *175*(5), 1030–1037.

Manzano, J. L., Layos, L., Bugés, C., de Los Llanos Gil, M., Vila, L., Martínez-Balibrea, E., & Martínez-Cardús, A. (2016). Resistant mechanisms to BRAF inhibitors in melanoma. *Annals of Translational Medicine*, *4*(12), 237.

Marconcini, R., Spagnolo, F., Stucci, L. S., Ribero, S., Marra, E., Rosa, F. D., Picasso, V., Di Guardo, L., Cimminiello, C., Cavalieri, S., Orgiano, L., Tanda, E., Spano, L., Falcone, A., Queirolo, P., & Italian Melanoma Intergroup (IMI). (2018). Current status and perspectives in immunotherapy for metastatic melanoma. *Oncotarget*, *9*(15), 12452–12470.

Maubec, E., Chaudru, V., Mohamdi, H., Grange, F., Patard, J.-J., Dalle, S., Crickx, B., Paillerets, B. B., Demenais, F., & Avril, M.-F. (2010). Characteristics of the coexistence of melanoma and renal cell carcinoma. *Cancer*, *116*(24), 5716–5724.

McGill, G. G., Haq, R., Nishimura, E. K., & Fisher, D. E. (2006). c-Met expression is regulated by Mitf in the melanocyte lineage. *The Journal of Biological Chemistry*, *281*(15), 10365–10373.

McGill, G. G., Horstmann, M., Widlund, H. R., Du, J., Motyckova, G., Nishimura, E. K., Lin, Y.-L., Ramaswamy, S., Avery, W., Ding, H.-F., Jordan, S. A., Jackson, I. J., Korsmeyer,

S. J., Golub, T. R., & Fisher, D. E. (2002). Bcl2 regulation by the melanocyte master regulator Mitf modulates lineage survival and melanoma cell viability. *Cell*, *109*(6), 707–718.

McNutt, M. (2014). Reproducibility. *Science*, *343*(6168), 229.

Mehnert, J. M., & Kluger, H. M. (2012). Driver mutations in melanoma: lessons learned from bench-to-bedside studies. *Current Oncology Reports*, *14*(5), 449–457.

Miller, M. A., Oudin, M. J., Sullivan, R. J., Wang, S. J., Meyer, A. S., Im, H., Frederick, D. T., Tadros, J., Griffith, L. G., Lee, H., Weissleder, R., Flaherty, K. T., Gertler, F. B., & Lauffenburger, D. A. (2016). Reduced Proteolytic Shedding of Receptor Tyrosine Kinases Is a Post-Translational Mechanism of Kinase Inhibitor Resistance. *Cancer Discovery*, *6*(4), 382–399.

Mishra, R., Patel, H., Alanazi, S., Yuan, L., & Garrett, J. T. (2018). HER3 signaling and targeted therapy in cancer. In *Oncology Reviews* (Vol. 12, Issue 1). https://doi.org/10.4081/oncol.2018.355

Mollica, J. P., Oakhill, J. S., Lamb, G. D., & Murphy, R. M. (2009). Are genuine changes in protein expression being overlooked? Reassessing Western blotting. *Analytical Biochemistry*, *386*(2), 270–275.

Müller, J., Krijgsman, O., Tsoi, J., Robert, L., Hugo, W., Song, C., Kong, X., Possik, P. A., Cornelissen-Steijger, P. D. M., Geukes Foppen, M. H., Kemper, K., Goding, C. R., McDermott, U., Blank, C., Haanen, J., Graeber, T. G., Ribas, A., Lo, R. S., & Peeper, D. S. (2014). Low MITF/AXL ratio predicts early resistance to multiple targeted drugs in melanoma. *Nature Communications*, *5*, 5712.

Murphy, R. M., & Lamb, G. D. (2013). Important considerations for protein analyses using antibody based techniques: down-sizing Western blotting up-sizes outcomes. *The Journal of Physiology*, *591*(23), 5823–5831.

Myers, M. P., Pass, I., Batty, I. H., Van der Kaay, J., Stolarov, J. P., Hemmings, B. A., Wigler, M. H., Downes, C. P., & Tonks, N. K. (1998). The lipid phosphatase activity of PTEN is critical for its tumor supressor function. *Proceedings of the National Academy of*

Sciences of the United States of America, *95*(23), 13513–13518.

Nazarian, R., Shi, H., Wang, Q., Kong, X., Koya, R. C., Lee, H., Chen, Z., Lee, M.-K., Attar, N., Sazegar, H., Chodon, T., Nelson, S. F., McArthur, G., Sosman, J. A., Ribas, A., & Lo, R. S. (2010). Melanomas acquire resistance to B-RAF(V600E) inhibition by RTK or N-RAS upregulation. *Nature*, *468*(7326), 973–977.

Nelson, D. L., & Cox, M. M. (2004). *Lehninger Principles of Biochemistry Lecture Notebook*. W. H. Freeman.

Nielsen, T. O., Borre, M., Nexo, E., & Sorensen, B. S. (2015). Co-expression of HER3 and MUC1 is associated with a favourable prognosis in patients with bladder cancer. *BJU International*, *115*(1), 163–165.

Nosek, B. A., Alter, G., Banks, G. C., Borsboom, D., Bowman, S. D., Breckler, S. J., Buck, S., Chambers, C. D., Chin, G., Christensen, G., Contestabile, M., Dafoe, A., Eich, E., Freese, J., Glennerster, R., Goroff, D., Green, D. P., Hesse, B., Humphreys, M., … Yarkoni, T. (2015). SCIENTIFIC STANDARDS. Promoting an open research culture. *Science*, *348*(6242), 1422–1425.

Nowell, P. C. (1976). The clonal evolution of tumor cell populations. *Science*, *194*(4260), 23–28.

Olayioye, M. A., Neve, R. M., Lane, H. A., & Hynes, N. E. (2000). The ErbB signaling network: receptor heterodimerization in development and cancer. *The EMBO Journal*, *19*(13), 3159–3167.

Padua, R. A., Barrass, N., & Currie, G. A. (1984). A novel transforming gene in a human malignant melanoma cell line. *Nature*, *311*(5987), 671–673.

Park, P. J. (2009). ChIP-seq: advantages and challenges of a maturing technology. *Nature Reviews. Genetics*, *10*(10), 669–680.

Patton, E. E., Widlund, H. R., Kutok, J. L., Kopani, K. R., Amatruda, J. F., Murphey, R. D., Berghmans, S., Mayhall, E. A., Traver, D., Fletcher, C. D. M., Aster, J. C., Granter, S. R., Look, A. T., Lee, C., Fisher, D. E., & Zon, L. I. (2005). BRAF mutations are sufficient to promote nevi formation and cooperate with p53 in the genesis of melanoma. *Current*

Biology: CB, *15*(3), 249–254.

Phung, B., Sun, J., Schepsky, A., Steingrimsson, E., & Rönnstrand, L. (2011). C-KIT signaling depends on microphthalmia-associated transcription factor for effects on cell proliferation. *PloS One*, *6*(8), e24064.

Pogenberg, V., Ogmundsdóttir, M. H., Bergsteinsdóttir, K., Schepsky, A., Phung, B., Deineko, V., Milewski, M., Steingrímsson, E., & Wilmanns, M. (2012). Restricted leucine zipper dimerization and specificity of DNA recognition of the melanocyte master regulator MITF. *Genes & Development*, *26*(23), 2647–2658.

Potrony, M., Badenas, C., Aguilera, P., Puig-Butille, J. A., Carrera, C., Malvehy, J., & Puig, S. (2015). Update in genetic susceptibility in melanoma. *Annals of Translational Medicine*, *3*(15), 210.

Potrony, M., Puig-Butille, J. A., Aguilera, P., Badenas, C., Tell-Marti, G., Carrera, C., Javier Del Pozo, L., Conejo-Mir, J., Malvehy, J., & Puig, S. (2016). Prevalence of MITF p.E318K in Patients With Melanoma Independent of the Presence of CDKN2A Causative Mutations. *JAMA Dermatology* , *152*(4), 405–412.

Potterf, S. B., Virador, V., Wakamatsu, K., Furumura, M., Santis, C., Ito, S., & Hearing, V. J. (1999). Cysteine transport in melanosomes from murine melanocytes. *Pigment Cell Research / Sponsored by the European Society for Pigment Cell Research and the International Pigment Cell Society*, *12*(1), 4–12.

Poulikakos, P. I., Persaud, Y., Janakiraman, M., Kong, X., Ng, C., Moriceau, G., Shi, H., Atefi, M., Titz, B., Gabay, M. T., Salton, M., Dahlman, K. B., Tadi, M., Wargo, J. A., Flaherty, K. T., Kelley, M. C., Misteli, T., Chapman, P. B., Sosman, J. A., … Solit, D. B. (2011). RAF inhibitor resistance is mediated by dimerization of aberrantly spliced BRAF(V600E). *Nature*, *480*(7377), 387–390.

Poynter, J. N., Elder, J. T., Fullen, D. R., Nair, R. P., Soengas, M. S., Johnson, T. M., Redman, B., Thomas, N. E., & Gruber, S. B. (2006). BRAF and NRAS mutations in melanoma and melanocytic nevi. *Melanoma Research*, *16*(4), 267–273.

Prasetyanti, P. R., Capone, E., Barcaroli, D., D'Agostino, D., Volpe, S., Benfante, A., van

Hooff, S., Iacobelli, V., Rossi, C., Iacobelli, S., Medema, J. P., De Laurenzi, V., & Sala, G. (2015). ErbB-3 activation by NRG-1β sustains growth and promotes vemurafenib resistance in BRAF-V600E colon cancer stem cells (CSCs). *Oncotarget*, *6*(19), 16902–16911.

Prickett, T. D., Agrawal, N. S., Wei, X., Yates, K. E., Lin, J. C., Wunderlich, J. R., Cronin, J. C., Cruz, P., Rosenberg, S. A., & Samuels, Y. (2009). Analysis of the tyrosine kinome in melanoma reveals recurrent mutations in ERBB4. *Nature Genetics*, *41*(10), 1127–1132.

Qian, G., Jiang, N., Wang, D., Newman, S., Kim, S., Chen, Z., Garcia, G., MacBeath, G., Shin, D. M., Khuri, F. R., Chen, Z. G., & Saba, N. F. (2015). Heregulin and HER3 are prognostic biomarkers in oropharyngeal squamous cell carcinoma. In *Cancer* (Vol. 121, Issue 20, pp. 3600–3611). https://doi.org/10.1002/cncr.29549

Rajeevan, M. S., Vernon, S. D., Taysavang, N., & Unger, E. R. (2001). Validation of array-based gene expression profiles by real-time (kinetic) RT-PCR. *The Journal of Molecular Diagnostics: JMD*, *3*(1), 26–31.

Rambow, F., Rogiers, A., Marin-Bejar, O., Aibar, S., Femel, J., Dewaele, M., Karras, P., Brown, D., Chang, Y. H., Debiec-Rychter, M., Adriaens, C., Radaelli, E., Wolter, P., Bechter, O., Dummer, R., Levesque, M., Piris, A., Frederick, D. T., Boland, G., … Marine, J.-C. (2018). Toward Minimal Residual Disease-Directed Therapy in Melanoma. *Cell*, *174*(4), 843–855.e19.

Rayess, H., Wang, M. B., & Srivatsan, E. S. (2012). Cellular senescence and tumor suppressor gene p16. *International Journal of Cancer. Journal International Du Cancer*, *130*(8), 1715–1725.

Reifenberger, J., Wolter, M., Boström, J., Büschges, R., Schulte, K. W., Megahed, M., Ruzicka, T., & Reifenberger, G. (2000). Allelic losses on chromosome arm 10q and mutation of the PTEN (MMAC1) tumour suppressor gene in primary and metastatic malignant melanomas. *Virchows Archiv: An International Journal of Pathology*, *436*(5), 487–493.

Reschke, M., Mihic-Probst, D., van der Horst, E. H., Knyazev, P., Wild, P. J., Hutterer, M.,

Meyer, S., Dummer, R., Moch, H., & Ullrich, A. (2008). HER3 is a determinant for poor prognosis in melanoma. *Clinical Cancer Research: An Official Journal of the American Association for Cancer Research*, *14*(16), 5188–5197.

Ribas, A., Hodi, F. S., Callahan, M., Konto, C., & Wolchok, J. (2013). Hepatotoxicity with combination of vemurafenib and ipilimumab. *The New England Journal of Medicine*, *368*(14), 1365–1366.

Ribas, A., Lawrence, D., Atkinson, V., Agarwal, S., Miller, W. H., Jr, Carlino, M. S., Fisher, R., Long, G. V., Hodi, F. S., Tsoi, J., Grasso, C. S., Mookerjee, B., Zhao, Q., Ghori, R., Moreno, B. H., Ibrahim, N., & Hamid, O. (2019). Combined BRAF and MEK inhibition with PD-1 blockade immunotherapy in BRAF-mutant melanoma. *Nature Medicine*, *25*(6), 936–940.

Riethmacher, D., Sonnenberg-Riethmacher, E., Brinkmann, V., Yamaai, T., Lewin, G. R., & Birchmeier, C. (1997). Severe neuropathies in mice with targeted mutations in the ErbB3 receptor. *Nature*, *389*(6652), 725–730.

Rodallec, A., Sicard, G., Fanciullino, R., Benzekry, S., Lacarelle, B., Milano, G., & Ciccolini, J. (2018). Turning cold tumors into hot tumors: harnessing the potential of tumor immunity using nanoparticles. *Expert Opinion on Drug Metabolism & Toxicology*, *14*(11), 1139–1147.

Roskoski, R., Jr. (2014). The ErbB/HER family of protein-tyrosine kinases and cancer. *Pharmacological Research: The Official Journal of the Italian Pharmacological Society*, *79*, 34–74.

Rothlin, C. V., Carrera-Silva, E. A., Bosurgi, L., & Ghosh, S. (2015). TAM receptor signaling in immune homeostasis. *Annual Review of Immunology*, *33*, 355–391.

Russell, W. M. S., & Burch, R. L. (1959). *The Principles of Humane Experimental Technique*. Methuen.

Saiz-Baggetto, S., Méndez, E., Quilis, I., Igual, J. C., & Bañó, M. C. (2017). Chimeric proteins tagged with specific 3xHA cassettes may present instability and functional problems. *PloS One*, *12*(8), e0183067.

Sánchez-Martín, M., Rodríguez-García, A., Pérez-Losada, J., Sagrera, A., Read, A. P., & Sánchez-García, I. (2002). SLUG (SNAI2) deletions in patients with Waardenburg disease. *Human Molecular Genetics*, *11*(25), 3231–3236.

Sansal, I., & Sellers, W. R. (2004). The biology and clinical relevance of the PTEN tumor suppressor pathway. *Journal of Clinical Oncology: Official Journal of the American Society of Clinical Oncology*, *22*(14), 2954–2963.

Sapkota, B., Hill, C. E., & Pollack, B. P. (2013). Vemurafenib enhances MHC induction in BRAFV600E homozygous melanoma cells. *Oncoimmunology*, *2*(1), e22890.

Sarkisian, S., & Davar, D. (2018). MEK inhibitors for the treatment of NRAS mutant melanoma. *Drug Design, Development and Therapy*, *12*, 2553–2565.

Schmidt, D., Wilson, M. D., Spyrou, C., Brown, G. D., Hadfield, J., & Odom, D. T. (2009). ChIP-seq: using high-throughput sequencing to discover protein-DNA interactions. *Methods* , *48*(3), 240–248.

Schmittgen, T. D., Zakrajsek, B. A., Mills, A. G., Gorn, V., Singer, M. J., & Reed, M. W. (2000). Quantitative Reverse Transcription–Polymerase Chain Reaction to Study mRNA Decay: Comparison of Endpoint and Real-Time Methods. *Analytical Biochemistry*, *285*(2), 194–204.

Sensi, M., Catani, M., Castellano, G., Nicolini, G., Alciato, F., Tragni, G., De Santis, G., Bersani, I., Avanzi, G., Tomassetti, A., Canevari, S., & Anichini, A. (2011). Human cutaneous melanomas lacking MITF and melanocyte differentiation antigens express a functional Axl receptor kinase. *The Journal of Investigative Dermatology*, *131*(12), 2448–2457.

Shain, A. H., & Bastian, B. C. (2016). From melanocytes to melanomas. *Nature Reviews. Cancer*, *16*(6), 345–358.

Shain, A. H., Yeh, I., Kovalyshyn, I., Sriharan, A., Talevich, E., Gagnon, A., Dummer, R., North, J., Pincus, L., Ruben, B., Rickaby, W., D'Arrigo, C., Robson, A., & Bastian, B. C. (2015). The Genetic Evolution of Melanoma from Precursor Lesions. *The New England Journal of Medicine*, *373*(20), 1926–1936.

Shampay, J., & Blackburn, E. H. (1988). Generation of telomere-length heterogeneity in Saccharomyces cerevisiae. *Proceedings of the National Academy of Sciences of the United States of America*, *85*(2), 534–538.

Sharma, S. V., Haber, D. A., & Settleman, J. (2010). Cell line-based platforms to evaluate the therapeutic efficacy of candidate anticancer agents. *Nature Reviews. Cancer*, *10*(4), 241–253.

Shekar, S. N., Duffy, D. L., Youl, P., Baxter, A. J., Kvaskoff, M., Whiteman, D. C., Green, A. C., Hughes, M. C., Hayward, N. K., Coates, M., & Martin, N. G. (2009). A population-based study of Australian twins with melanoma suggests a strong genetic contribution to liability. *The Journal of Investigative Dermatology*, *129*(9), 2211–2219.

Shi, H., Hong, A., Kong, X., Koya, R. C., Song, C., Moriceau, G., Hugo, W., Yu, C. C., Ng, C., Chodon, T., Scolyer, R. A., Kefford, R. F., Ribas, A., Long, G. V., & Lo, R. S. (2014). A novel AKT1 mutant amplifies an adaptive melanoma response to BRAF inhibition. *Cancer Discovery*, *4*(1), 69–79.

Shi, H., Moriceau, G., Kong, X., Lee, M.-K., Lee, H., Koya, R. C., Ng, C., Chodon, T., Scolyer, R. A., Dahlman, K. B., Sosman, J. A., Kefford, R. F., Long, G. V., Nelson, S. F., Ribas, A., & Lo, R. S. (2012). Melanoma whole-exome sequencing identifies V600EB-RAF amplification-mediated acquired B-RAF inhibitor resistance. *Nature Communications*, *3*, 724.

Shultz, L. D., Lyons, B. L., Burzenski, L. M., & Gott, B. (2005). Human lymphoid and myeloid cell development in NOD/LtSz-scid IL2Rγnull mice engrafted with mobilized human hemopoietic stem cells. *The Journal of*. https://www.jimmunol.org/content/174/10/6477.short

Siegel, R. L., Miller, K. D., & Jemal, A. (2018). Cancer statistics, 2018. *CA: A Cancer Journal for Clinicians*, *68*(1), 7–30.

Siegfried, J. M., Lin, Y., Diergaarde, B., Lin, H.-M., Dacic, S., Pennathur, A., Weissfeld, J. L., Romkes, M., Nukui, T., & Stabile, L. P. (2015). Expression of PAM50 Genes in Lung Cancer: Evidence that Interactions between Hormone Receptors and HER2/HER3

Contribute to Poor Outcome. *Neoplasia* , *17*(11), 817–825.

Simon, J. D., Peles, D., Wakamatsu, K., & Ito, S. (2009). Current challenges in understanding melanogenesis: bridging chemistry, biological control, morphology, and function. *Pigment Cell & Melanoma Research*, *22*(5), 563–579.

Singh, A. B., & Harris, R. C. (2005). Autocrine, paracrine and juxtacrine signaling by EGFR ligands. *Cellular Signalling*, *17*(10), 1183–1193.

Smalley, K. S. M., Haass, N. K., Brafford, P. A., Lioni, M., Flaherty, K. T., & Herlyn, M. (2006). Multiple signaling pathways must be targeted to overcome drug resistance in cell lines derived from melanoma metastases. *Molecular Cancer Therapeutics*, *5*(5), 1136–1144.

Smith, M. P., Brunton, H., Rowling, E. J., Ferguson, J., Arozarena, I., Miskolczi, Z., Lee, J. L., Girotti, M. R., Marais, R., Levesque, M. P., Dummer, R., Frederick, D. T., Flaherty, K. T., Cooper, Z. A., Wargo, J. A., & Wellbrock, C. (2016). Inhibiting Drivers of Non-mutational Drug Tolerance Is a Salvage Strategy for Targeted Melanoma Therapy. *Cancer Cell*, *29*(3), 270–284.

Smith, M. P., Rana, S., Ferguson, J., Rowling, E. J., Flaherty, K. T., Wargo, J. A., Marais, R., & Wellbrock, C. (2019). A PAX3/BRN2 rheostat controls the dynamics of BRAF mediated MITF regulation in MITF high /AXL low melanoma. In *Pigment Cell & Melanoma Research* (Vol. 32, Issue 2, pp. 280–291). https://doi.org/10.1111/pcmr.12741

Sondka, Z., Bamford, S., Cole, C. G., Ward, S. A., Dunham, I., & Forbes, S. A. (2018). The COSMIC Cancer Gene Census: describing genetic dysfunction across all human cancers. *Nature Reviews. Cancer*, *18*(11), 696–705.

Song, M. S., Salmena, L., & Pandolfi, P. P. (2012). The functions and regulation of the PTEN tumour suppressor. *Nature Reviews. Molecular Cell Biology*, *13*(5), 283–296.

Soo, J. K., Mackenzie Ross, A. D., Kallenberg, D. M., Milagre, C., Heung Chong, W., Chow, J., Hill, L., Hoare, S., Collinson, R. S., Hossain, M., Keith, W. N., Marais, R., & Bennett, D. C. (2011). Malignancy without immortality? Cellular immortalization as a possible late

event in melanoma progression. *Pigment Cell & Melanoma Research*, *24*(3), 490–503.

Stransky, N., Cerami, E., Schalm, S., Kim, J. L., & Lengauer, C. (2014). The landscape of kinase fusions in cancer. *Nature Communications*, *5*, 4846.

Straussman, R., Morikawa, T., Shee, K., Barzily-Rokni, M., Qian, Z. R., Du, J., Davis, A., Mongare, M. M., Gould, J., Frederick, D. T., Cooper, Z. A., Chapman, P. B., Solit, D. B., Ribas, A., Lo, R. S., Flaherty, K. T., Ogino, S., Wargo, J. A., & Golub, T. R. (2012). Tumour micro-environment elicits innate resistance to RAF inhibitors through HGF secretion. *Nature*, *487*(7408), 500–504.

Stretch, J. R., Gatter, K. C., Ralfkiaer, E., Lane, D. P., & Harris, A. L. (1991). Expression of mutant p53 in melanoma. *Cancer Research*, *51*(21), 5976–5979.

Strub, T., Giuliano, S., Ye, T., Bonet, C., Keime, C., Kobi, D., Le Gras, S., Cormont, M., Ballotti, R., Bertolotto, C., & Davidson, I. (2011). Essential role of microphthalmia transcription factor for DNA replication, mitosis and genomic stability in melanoma. *Oncogene*, *30*(20), 2319–2332.

Sturm, R. A. (2002). Skin colour and skin cancer - MC1R, the genetic link. *Melanoma Research*, *12*(5), 405–416.

Sturm, R. A., Duffy, D. L., Box, N. F., Chen, W., Smit, D. J., Brown, D. L., Stow, J. L., Leonard, J. H., & Martin, N. G. (2003). The role of melanocortin-1 receptor polymorphism in skin cancer risk phenotypes. *Pigment Cell Research / Sponsored by the European Society for Pigment Cell Research and the International Pigment Cell Society*, *16*(3), 266–272.

Sviderskaya, E. V., Gray-Schopfer, V. C., Hill, S. P., Smit, N. P., Evans-Whipp, T. J., Bond, J., Hill, L., Bataille, V., Peters, G., Kipling, D., & Others. (2003). p16/cyclin-dependent kinase inhibitor 2A deficiency in human melanocyte senescence, apoptosis, and immortalization: possible implications for melanoma progression. *Journal of the National Cancer Institute*, *95*(10), 723–732.

Tachibana, M. (1999). Sound needs sound melanocytes to be heard. *Pigment Cell Research / Sponsored by the European Society for Pigment Cell Research and the International*

Pigment Cell Society, *12*(6), 344–354.

Tagliabue, E., Gandini, S., Bellocco, R., Maisonneuve, P., Newton-Bishop, J., Polsky, D., Lazovich, D., Kanetsky, P. A., Ghiorzo, P., Gruis, N. A., Landi, M. T., Menin, C., Fargnoli, M. C., García-Borrón, J. C., Han, J., Little, J., Sera, F., & Raimondi, S. (2018). MC1R variants as melanoma risk factors independent of at-risk phenotypic characteristics: a pooled analysis from the M-SKIP project. *Cancer Management and Research*, *10*, 1143–1154.

Takeda, K., Yasumoto, K., Takada, R., Takada, S., Watanabe, K., Udono, T., Saito, H., Takahashi, K., & Shibahara, S. (2000). Induction of melanocyte-specific microphthalmia-associated transcription factor by Wnt-3a. *The Journal of Biological Chemistry*, *275*(19), 14013–14016.

Tanner, B., Hasenclever, D., Stern, K., Schormann, W., Bezler, M., Hermes, M., Brulport, M., Bauer, A., Schiffer, I. B., Gebhard, S., Schmidt, M., Steiner, E., Sehouli, J., Edelmann, J., Läuter, J., Lessig, R., Krishnamurthi, K., Ullrich, A., & Hengstler, J. G. (2006). ErbB-3 predicts survival in ovarian cancer. *Journal of Clinical Oncology: Official Journal of the American Society of Clinical Oncology*, *24*(26), 4317–4323.

Thiery, J. P. (2003). Epithelial–mesenchymal transitions in development and pathologies. *Current Opinion in Cell Biology*, *15*(6), 740–746.

Thomas, A. J., & Erickson, C. A. (2009). FOXD3 regulates the lineage switch between neural crest-derived glial cells and pigment cells by repressing MITF through a non-canonical mechanism. *Development* , *136*(11), 1849–1858.

Thomson, J. A., Murphy, K., Baker, E., Sutherland, G. R., Parsons, P. G., Sturm, R. A., & Thomson, F. (1995). The brn-2 gene regulates the melanocytic phenotype and tumorigenic potential of human melanoma cells. *Oncogene*, *11*(4), 691–700.

Thomson, S., Petti, F., Sujka-Kwok, I., Epstein, D., & Haley, J. D. (2008). Kinase switching in mesenchymal-like non-small cell lung cancer lines contributes to EGFR inhibitor resistance through pathway redundancy. *Clinical & Experimental Metastasis*, *25*(8), 843–854.

Thurber, A. E., Douglas, G., Sturm, E. C., Zabierowski, S. E., Smit, D. J., Ramakrishnan, S. N., Hacker, E., Leonard, J. H., Herlyn, M., & Sturm, R. A. (2011). Inverse expression states of the BRN2 and MITF transcription factors in melanoma spheres and tumour xenografts regulate the NOTCH pathway. *Oncogene*, *30*(27), 3036–3048.

Tirosh, I., Izar, B., Prakadan, S. M., Wadsworth, M. H., 2nd, Treacy, D., Trombetta, J. J., Rotem, A., Rodman, C., Lian, C., Murphy, G., Fallahi-Sichani, M., Dutton-Regester, K., Lin, J.-R., Cohen, O., Shah, P., Lu, D., Genshaft, A. S., Hughes, T. K., Ziegler, C. G. K., … Garraway, L. A. (2016). Dissecting the multicellular ecosystem of metastatic melanoma by single-cell RNA-seq. *Science*, *352*(6282), 189–196.

Varna, M., Bertheau, P., & Legrès, L. G. (2014). Tumor microenvironment in human tumor xenografted mouse models. *J Anal Oncol*, *3*, 159–166.

Vella, L. J., Pasam, A., Dimopoulos, N., Andrews, M., Knights, A., Puaux, A.-L., Louahed, J., Chen, W., Woods, K., & Cebon, J. S. (2014). MEK inhibition, alone or in combination with BRAF inhibition, affects multiple functions of isolated normal human lymphocytes and dendritic cells. *Cancer Immunology Research*, *2*(4), 351–360.

Verfaillie, A., Imrichova, H., Atak, Z. K., Dewaele, M., Rambow, F., Hulselmans, G., Christiaens, V., Svetlichnyy, D., Luciani, F., Van den Mooter, L., Claerhout, S., Fiers, M., Journe, F., Ghanem, G.-E., Herrmann, C., Halder, G., Marine, J.-C., & Aerts, S. (2015). Decoding the regulatory landscape of melanoma reveals TEADS as regulators of the invasive cell state. *Nature Communications*, *6*, 6683.

Villanueva, J., Vultur, A., Lee, J. T., Somasundaram, R., Fukunaga-Kalabis, M., Cipolla, A. K., Wubbenhorst, B., Xu, X., Gimotty, P. A., Kee, D., Santiago-Walker, A. E., Letrero, R., D'Andrea, K., Pushparajan, A., Hayden, J. E., Brown, K. D., Laquerre, S., McArthur, G. A., Sosman, J. A., … Herlyn, M. (2010). Acquired resistance to BRAF inhibitors mediated by a RAF kinase switch in melanoma can be overcome by cotargeting MEK and IGF-1R/PI3K. *Cancer Cell*, *18*(6), 683–695.

Vink, A. A., & Roza, L. (2001). Biological consequences of cyclobutane pyrimidine dimers. *Journal of Photochemistry and Photobiology. B, Biology*, *65*(2-3), 101–104.

Vouri, M., Croucher, D. R., Kennedy, S. P., An, Q., Pilkington, G. J., & Hafizi, S. (2016). Axl-EGFR receptor tyrosine kinase hetero-interaction provides EGFR with access to pro-invasive signalling in cancer cells. *Oncogenesis*, *5*(10), e266.

Vucic, D., Stennicke, H. R., Pisabarro, M. T., Salvesen, G. S., & Dixit, V. M. (2000). ML-IAP, a novel inhibitor of apoptosis that is preferentially expressed in human melanomas. *Current Biology: CB*, *10*(21), 1359–1366.

Wagle, N., Emery, C., Berger, M. F., Davis, M. J., Sawyer, A., Pochanard, P., Kehoe, S. M., Johannessen, C. M., Macconaill, L. E., Hahn, W. C., Meyerson, M., & Garraway, L. A. (2011). Dissecting therapeutic resistance to RAF inhibition in melanoma by tumor genomic profiling. *Journal of Clinical Oncology: Official Journal of the American Society of Clinical Oncology*, *29*(22), 3085–3096.

Wakamatsu, K., Takasaki, A., Kågedal, B., Kageshita, T., & Ito, S. (2006). Determination of eumelanin in human urine. *Pigment Cell Research / Sponsored by the European Society for Pigment Cell Research and the International Pigment Cell Society*, *19*(2), 163–169.

Walsh, J. H., Karnes, W. E., Cuttitta, F., & Walker, A. (1991). Autocrine growth factors and solid tumor malignancy. *The Western Journal of Medicine*, *155*(2), 152–163.

Wang, J. X., Fukunaga-Kalabis, M., & Herlyn, M. (2016). Crosstalk in skin: melanocytes, keratinocytes, stem cells, and melanoma. *Journal of Cell Communication and Signaling*, *10*(3), 191–196.

Wang, Z., Longo, P. A., Tarrant, M. K., Kim, K., Head, S., Leahy, D. J., & Cole, P. A. (2011). Mechanistic insights into the activation of oncogenic forms of EGF receptor. *Nature Structural & Molecular Biology*, *18*(12), 1388–1393.

Watanabe, A., Takeda, K., Ploplis, B., & Tachibana, M. (1998). Epistatic relationship between Waardenburg syndrome genes MITF and PAX3. *Nature Genetics*, *18*(3), 283–286.

Webster, D. E., Barajas, B., Bussat, R. T., Yan, K. J., Neela, P. H., Flockhart, R. J., Kovalski, J., Zehnder, A., & Khavari, P. A. (2014). Enhancer-targeted genome editing selectively blocks innate resistance to oncokinase inhibition. *Genome Research*, *24*(5), 751–760.

Weinstock, M. A., & Sober, A. J. (1987). The risk of progression of lentigo maligna to lentigo maligna melanoma. *The British Journal of Dermatology*, *116*(3), 303–310.

Weiss, W. A., Taylor, S. S., & Shokat, K. M. (2007). Recognizing and exploiting differences between RNAi and small-molecule inhibitors. *Nature Chemical Biology*, *3*(12), 739–744.

Wellbrock, C., & Marais, R. (2005). Elevated expression of MITF counteracts B-RAF-stimulated melanocyte and melanoma cell proliferation. *The Journal of Cell Biology*, *170*(5), 703–708.

Wellbrock, C., Rana, S., Paterson, H., Pickersgill, H., Brummelkamp, T., & Marais, R. (2008). Oncogenic BRAF Regulates Melanoma Proliferation through the Lineage Specific Factor MITF. In *PLoS ONE* (Vol. 3, Issue 7, p. e2734). https://doi.org/10.1371/journal.pone.0002734

Wendt, J., Rauscher, S., Burgstaller-Muehlbacher, S., Fae, I., Fischer, G., Pehamberger, H., & Okamoto, I. (2016). Human Determinants and the Role of Melanocortin-1 Receptor Variants in Melanoma Risk Independent of UV Radiation Exposure. *JAMA Dermatology* , *152*(7), 776–782.

Wenger, S. L., Senft, J. R., Sargent, L. M., Bamezai, R., Bairwa, N., & Grant, S. G. (2004). Comparison of established cell lines at different passages by karyotype and comparative genomic hybridization. *Bioscience Reports*, *24*(6), 631–639.

Whittaker, S. R., Theurillat, J.-P., Van Allen, E., Wagle, N., Hsiao, J., Cowley, G. S., Schadendorf, D., Root, D. E., & Garraway, L. A. (2013). A genome-scale RNA interference screen implicates NF1 loss in resistance to RAF inhibition. *Cancer Discovery*, *3*(3), 350–362.

Widlund, H. R., Horstmann, M. A., Price, E. R., Cui, J., Lessnick, S. L., Wu, M., He, X., & Fisher, D. E. (2002). Beta-catenin-induced melanoma growth requires the downstream target Microphthalmia-associated transcription factor. *The Journal of Cell Biology*, *158*(6), 1079–1087.

Wiedemann, G. M., Aithal, C., Kraechan, A., Heise, C., Cadilha, B. L., Zhang, J., Duewell, P., Ballotti, R., Endres, S., Bertolotto, C., & Kobold, S. (2019). Microphthalmia-Associated

Transcription Factor (MITF) Regulates Immune Cell Migration into Melanoma. *Translational Oncology*, *12*(2), 350–360.

Wilmott, J. S., Long, G. V., Howle, J. R., Haydu, L. E., Sharma, R. N., Thompson, J. F., Kefford, R. F., Hersey, P., & Scolyer, R. A. (2012). Selective BRAF inhibitors induce marked T-cell infiltration into human metastatic melanoma. *Clinical Cancer Research: An Official Journal of the American Association for Cancer Research*, *18*(5), 1386–1394.

Woodman, S. E., & Davies, M. A. (2010). Targeting KIT in melanoma: a paradigm of molecular medicine and targeted therapeutics. *Biochemical Pharmacology*, *80*(5), 568–574.

Workman, P., Aboagye, E. O., Balkwill, F., Balmain, A., Bruder, G., Chaplin, D. J., Double, J. A., Everitt, J., Farningham, D. A. H., Glennie, M. J., Kelland, L. R., Robinson, V., Stratford, I. J., Tozer, G. M., Watson, S., Wedge, S. R., Eccles, S. A., & An ad hoc committee of the National Cancer Research Institute. (2010). Guidelines for the welfare and use of animals in cancer research. *British Journal of Cancer*, *102*(11), 1555–1577.

Wróbel, S., Przybyło, M., & Stępień, E. (2019). The Clinical Trial Landscape for Melanoma Therapies. *Journal of Clinical Medicine Research*, *8*(3). https://doi.org/10.3390/jcm8030368

Yajima, I., Kumasaka, M. Y., Thang, N. D., Goto, Y., Takeda, K., Iida, M., Ohgami, N., Tamura, H., Yamanoshita, O., Kawamoto, Y., Furukawa, K., & Kato, M. (2011). Molecular Network Associated with MITF in Skin Melanoma Development and Progression. *Journal of Skin Cancer*, *2011*, 730170.

Yasumoto, K., Yokoyama, K., Shibata, K., Tomita, Y., & Shibahara, S. (1995). Microphthalmia-associated transcription factor as a regulator for melanocyte-specific transcription of the human tyrosinase gene. *Molecular and Cellular Biology*, *15*(3), 1833.

Yokoyama, S., Woods, S. L., Boyle, G. M., Aoude, L. G., MacGregor, S., Zismann, V., Gartside, M., Cust, A. E., Haq, R., Harland, M., Taylor, J. C., Duffy, D. L., Holohan, K., Dutton-Regester, K., Palmer, J. M., Bonazzi, V., Stark, M. S., Symmons, J., Law, M. H., … Brown, K. M. (2011). A novel recurrent mutation in MITF predisposes to familial and

sporadic melanoma. *Nature*, *480*(7375), 99–103.

Zhang, G., Kong, X., Wang, M., Zhao, H., Han, S., Hu, R., Huang, J., & Cui, W. (2018). AXL is a marker for epithelial-mesenchymal transition in esophageal squamous cell carcinoma. *Oncology Letters*, *15*(2), 1900–1906.

Zhang, Z., Lee, J. C., Lin, L., Olivas, V., Au, V., LaFramboise, T., Abdel-Rahman, M., Wang, X., Levine, A. D., Rho, J. K., Choi, Y. J., Choi, C.-M., Kim, S.-W., Jang, S. J., Park, Y. S., Kim, W. S., Lee, D. H., Lee, J.-S., Miller, V. A., … Bivona, T. G. (2012). Activation of the AXL kinase causes resistance to EGFR-targeted therapy in lung cancer. *Nature Genetics*, *44*(8), 852–860.

Zhou, L., Liu, X.-D., Sun, M., Zhang, X., German, P., Bai, S., Ding, Z., Tannir, N., Wood, C. G., Matin, S. F., Karam, J. A., Tamboli, P., Sircar, K., Rao, P., Rankin, E. B., Laird, D. A., Hoang, A. G., Walker, C. L., Giaccia, A. J., & Jonasch, E. (2016). Targeting MET and AXL overcomes resistance to sunitinib therapy in renal cell carcinoma. *Oncogene*, *35*(21), 2687–2697.

Zuo, L., Weger, J., Yang, Q., Goldstein, A. M., Tucker, M. A., Walker, G. J., Hayward, N., & Dracopoli, N. C. (1996). Germline mutations in the p16INK4a binding domain of CDK4 in familial melanoma. *Nature Genetics*, *12*(1), 97–99.

Zuo, Q., Liu, J., Huang, L., Qin, Y., Hawley, T., Seo, C., Merlino, G., & Yu, Y. (2018). AXL/AKT axis mediated-resistance to BRAF inhibitor depends on PTEN status in melanoma. *Oncogene*, *37*(24), 3275–3289.

I

MITF depletion elevates expression levels of ERBB3 receptor and its cognate ligand NRG1-beta in melanoma

Tine N. Alver[1], Timothy J. Lavelle[1], Ane S. Longva[1], Geir F. Øy[1], Eivind Hovig[1,2,3], Sigurd L. Bøe[1]

[1]Department of Tumor Biology, Institute for Cancer Research, Oslo University Hospital, Oslo, Norway

[2]Institute for Cancer Genetics and Informatics, The Norwegian Radium Hospital, Oslo University Hospital, Oslo, Norway

[3]Department of Informatics, University of Oslo, Oslo, Norway

Correspondence to: *Tine N. Alver,* ***email:*** *tinalv@rr-research.no*

Keywords: *MITF, ERBB3, NRG1-beta, PI3K signaling, melanoma*

Received: *March 11, 2016* ***Accepted:*** *June 27, 2016* ***Published:*** *July 06, 2016*

ABSTRACT

The phosphatidylinositol-4,5-bisphosphate 3-kinase (PI3K) pathway is frequently hyper-activated upon vemurafenib treatment of melanoma. We have here investigated the relationship between SRY-box 10 (SOX10), forkhead box 3 (FOXD3) and microphthalmia-associated transcription factor (MITF) in the regulation of the receptor tyrosine-protein kinase ERBB3, and its cognate ligand neuregulin 1-beta (NRG1-beta). We found that both NRG1-beta and ERBB3 mRNA levels were elevated as a consequence of MITF depletion, induced by either vemurafenib or MITF small interfering RNA (siRNA) treatment. Elevation of ERBB3 receptor expression after MITF depletion caused increased activation of the PI3K pathway in the presence of NRG1-beta ligand. Together, our results suggest that MITF may play a role in the development of acquired drug resistance through hyper-activation of the PI3K pathway.

INTRODUCTION

Malignant melanoma is an aggressive cancer form with limited treatment options and poor survival for patients with advanced disease. The small-molecular inhibitor vemurafenib, that specifically inhibits the BRAFV600 mutated protein function, has shown remarkable response when used in patients [1–3]. Unfortunately, virtually all responders acquire resistance over time [4]. Several resistance mechanisms have been characterized [5–11], including receptor tyrosine kinase (RTK) up-regulation or activation leading to sustained cell survival and proliferation [12, 13]. Two recent reports have suggested that microphthalmia-associated transcription factor (MITF) loss is involved in the development of vemurafenib resistance through up-regulation or activation of RTKs such as AXL and EGFR [12, 13].

The EGFR family members of RTKs consist of four family members; receptor tyrosine-protein kinase ERBB1 to 4 (ERBB1/EGFR, ERBB2/HER2, ERBB3/HER3, ERBB4/HER4, respectively). These receptors are important regulators of normal growth and cell differentiation. Their dysregulation in the form of amplification, overexpression or mutation is associated with tumor development and poor clinical prognosis in most human cancers [14]. Previous studies have suggested that increase in both EGFR and ERBB3 expression and phosphorylation can be induced after mitogen-activating protein kinase (MAPK) inhibitor treatment [12, 15–20], and that targeting EGFR and ERBB3 can prevent and extend the establishment of MAPK inhibitor-induced resistance in melanoma [12, 15, 17]. Transcription factors such as FOXO1, FOXO3A, FOXD3, and SOX10 have been reported to activate ERBB3 expression [15, 21–23]. Interestingly, SOX10 has been found to activate MITF expression [24], while MITF is reported to repress FOXD3 expression and *vice versa* [25, 26].

Preliminary gene expression arrays suggested to us that ERBB3 expression was elevated after MITF depletion in the SKMEL28 cell line. Based on these data, we have here investigated the relationship between SOX10, FOXD3 and MITF in the regulation of the receptor tyrosine-protein kinase ERBB3, and its cognate ligand NRG1-beta. We found that depletion of MITF protein resulted in elevation of ERBB3 and NRG1-beta levels. The novel mechanism described here may

have implications for the development of acquired drug resistance in melanoma.

RESULTS

Basal expression levels of SOX10, MITF, FOXD3 and ERBB3 in a melanoma cell line panel

We compared basal mRNA expression levels of SOX10, MITF, FOXD3, and ERBB3 in immortalized melanocytes, and in a panel of melanomas spanning various genetic backgrounds (see Figure 1A-1D and Supplementary Table S1). Out of the 18 cell lines analyzed for mRNA expression, we selected 9 cell lines for further protein expression analysis, representing various alterations in the MAPK pathway (NRAS, BRAF, NF1) and variable MITF expression levels (Figure 1E). We found that mRNA and protein expression levels correlated well for all cell lines tested. FOXD3 and SOX10 have been reported to be activators of ERBB3 transcription [15, 21], which is in agreement with what we observed, as depletion of FOXD3 and SOX10 levels resulted in reduced ERBB3 expression. To our knowledge, no reports exist concerning MITF regulation of ERBB3. Our results show that MITF protein expression has an inverse association with ERBB3 protein expression in the MITF-expressing cell lines, particular in the immortalized melanocyte cell line Hermes 4C, WM983B and WM115 (Figure 1E).

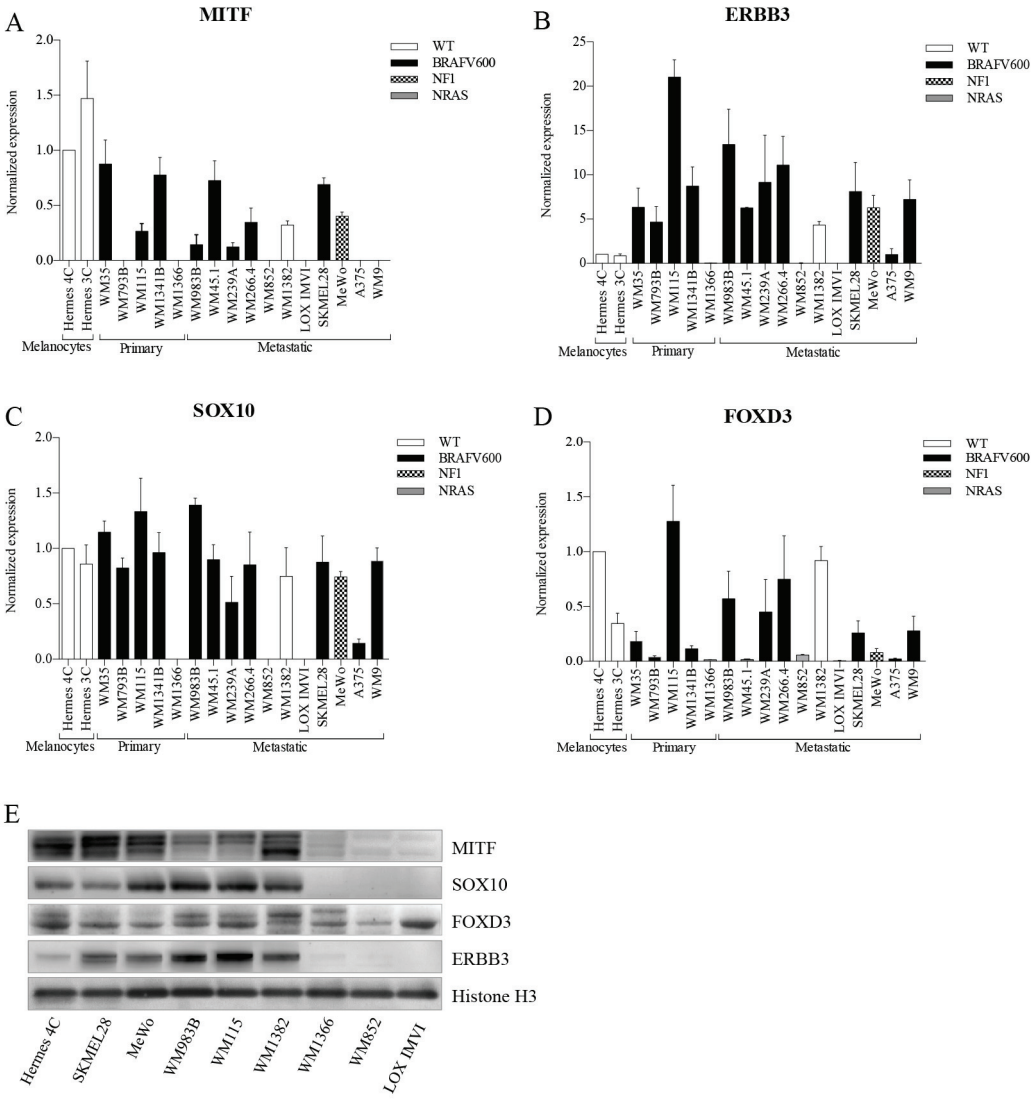

Figure 1: Basal expression levels of MITF, ERBB3, SOX10 and FOXD3 in various melanoma cell lines. A-D. qRT-PCR was used to evaluate mRNA levels of MITF **(A)**, ERBB3 **(B)**, SOX10 **(C)**, and FOXD3 **(D)** in melanoma cell lines by normalizing against immortalized cultured melanocytes (Hermes 4C). Bars represent mean ± SD of three separate experiments **(E).** Representative western blots of MITF, SOX10, FOXD3 and ERBB3 protein levels shown in 9 different cell lines representing various disease stage and genetic background. Histone H3 was used as loading control.

Depletion of MITF elevates ERBB3 expression at the transcriptional level

To further explore the relationship between MITF and ERBB3, we depleted MITF and ERBB3 levels by the use of siRNA molecules in five MITF-expressing cell lines differing in MAPK pathway backgrounds (see Supplementary Table S1). Elevation of the ERBB3 mRNA and protein levels were detected 72h post siMITF treatment for all five cell lines tested (Figure 2A-2E). Transfection of the same cell lines with siERBB3 resulted in reduction of MITF protein levels in Hermes 4C and MeWo, while no changes were observed in WM1382, WM983B and SKMEL28. To ensure that the elevated ERBB3 levels after siMITF treatment was not caused by an off-target effect, we also tested two other siMITF sequences and an additional negative siRNA control. All the three individual siMITF molecules resulted in elevation of ERBB3, compared to untreated control and negative siRNA controls (Supplementary Figure S1). In addition to siMITF treatment, we also overexpressed the melanocyte-specific variant 4 (NM_000248) MITF protein by MITF mRNA delivery, resulting in reduction of ERBB3 mRNA levels after 24h in A375 and MeWo (See Supplementary Figure S2).

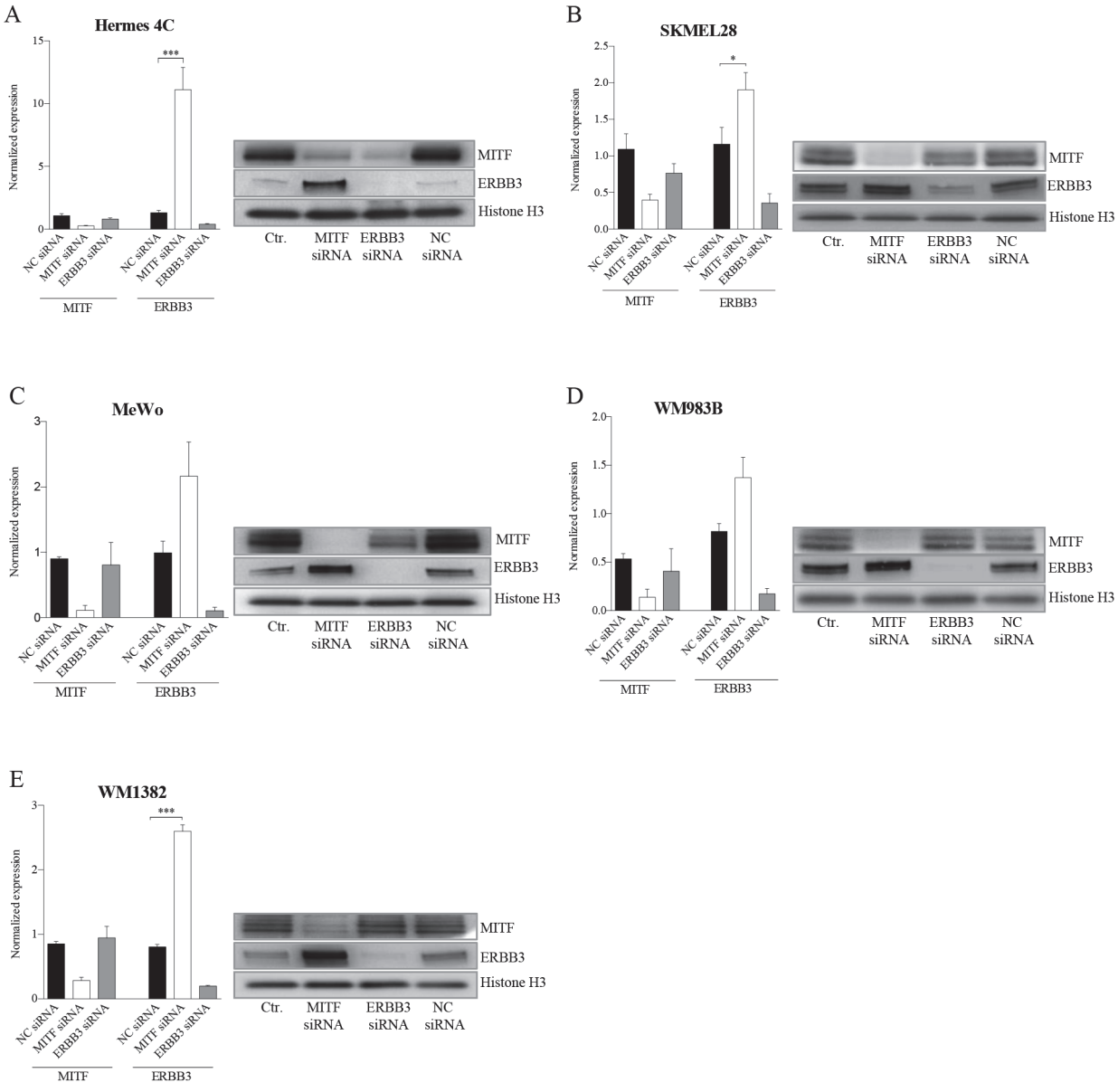

Figure 2: MITF suppresses ERBB3 expression at the transcriptional level in various cell lines after siRNA transfections. Assessment of mRNA and protein levels of MITF and ERBB3 in a panel of cell lines 72h after siRNA-induced reduction of MITF and ERBB3. **A.** Hermes 4C (immortalized melanocytes). **B.** SKMEL28 (BRAFV600E) **C.** MeWo (NF1) **D.** WM983B (BRAFV600E) **E.** WM1382 (wild-type for BRAF and NRAS). Graphs represent qRT-PCR expression data from three separate experiments normalized to untreated control cells and plotted as mean ± SD. * =$p < 0.05$, *** =$p < 0.005$ (*t*-test). A representative western blot of the corresponding treatments is shown to the right, with Histone H3 as loading control.

Elevation of the ERBB3 receptor expression levels increases pAKT levels

To address whether depletion of MITF protein activates the PI3K pathway through NRG1-beta/ERBB3 signaling in both mutant and wild-type BRAF melanoma cell lines, we co-transfected WM983B and MeWo with MITF and ERBB3 siRNA molecules in combination with NRG1-beta treatment (Figure 3A–3B), or without NRG1-beta treatment (See Supplementary Figure S3A-S3B). After 72h of siMITF treatment, we observed an induction of both phospho-ERBB3-T1289 (pERBB3) and total ERBB3 expression, together with an increase in pAKT (S473) in both cell lines tested. In contrast to siMITF transfection alone, co-transfection of the WM983B and MeWo cell lines with siMITF and siERBB3 resulted in loss of pERBB3 (T1289), total ERBB3 and pAKT (S473). In MeWo, a complete depletion of pAKT (S473) levels was observed after co-transfection, while only the hyper-activated levels of pAKT (S473) were depleted in the WM983B cell line. To address the observed increase in pERBB3 (T1289) levels after siMITF treatment observed in non-NRG1-beta treated WM983B samples (See Supplementary Figure S3A), we measured the NRG1-beta mRNA levels. We found an increase in NRG1-beta mRNA expression levels in WM983B (Figure 3C). No measureable levels of NRG1-beta mRNA were detected in MeWo by qPCR analysis. Since we did not detect any NRG1-beta in the BRAF wild-type cell line MeWo, we investigated two other BRAF wild-type cell lines, the metastatic melanoma cell line WM1382 (Figure 3D) and the immortalized melanocyte cell line Hermes 4C (Figure 3E). Also these cell lines showed elevation of NRG1-beta mRNA levels after MITF depletion. When overexpressing MITF protein by mRNA

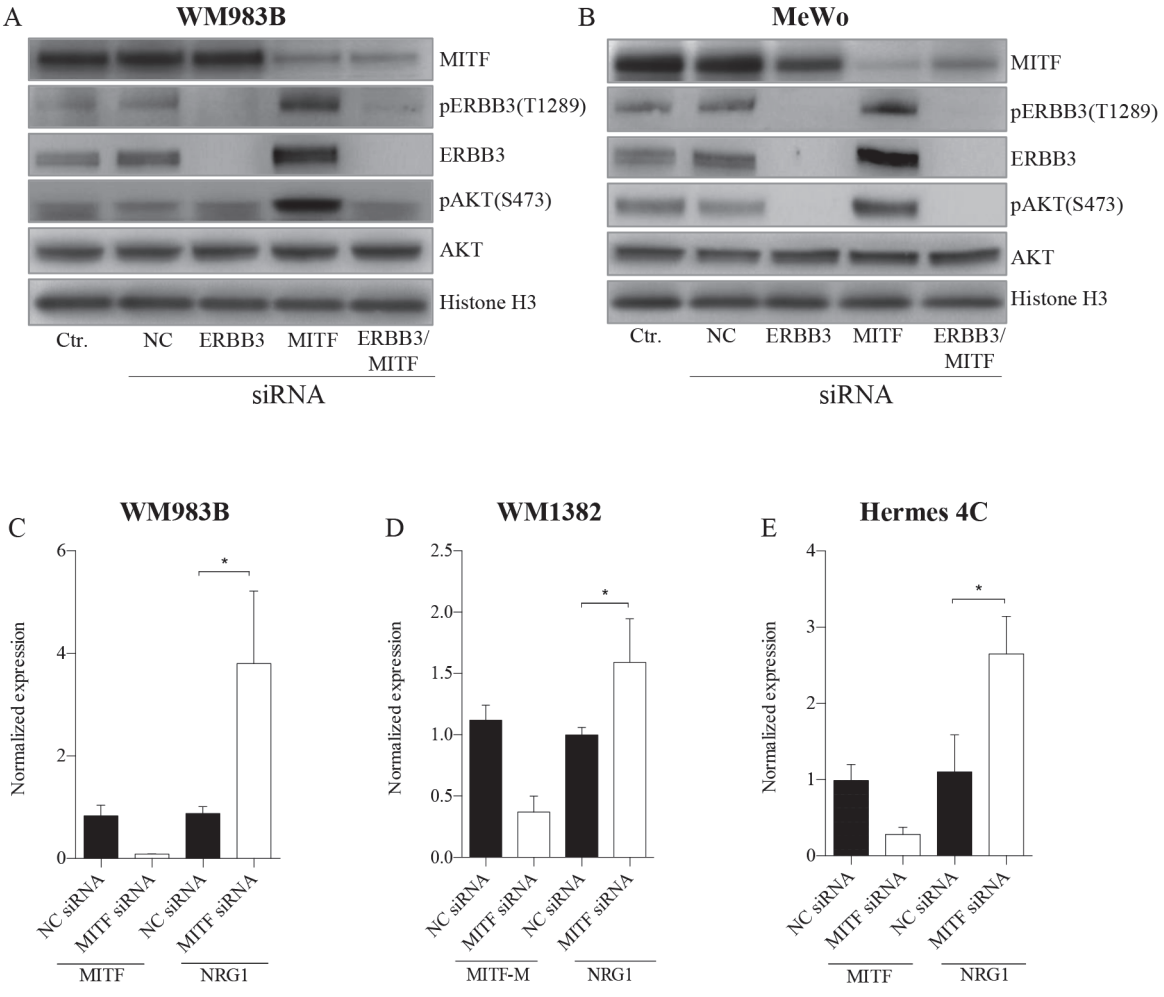

Figure 3: MITF suppress the PI3K-pathway through NRG1-beta/ERBB3 signaling. A-B. Representative western blots show the effect of MITF siRNA treatment on NRG1-beta/ERBB3 signaling pathway members, leading to p-AKT (S473) activation in WM983B **(A)** and MeWo **(B)**. Cell lines were transfected with MITF and ERBB3 siRNA alone and in combination for 72h, and treated either with or without (see Supplementary Figure S3A-S3B) 10ng/ml NRG1-beta ligand 15min prior to harvesting. All experiments were performed in triplicate. Histone H3 was used as loading control. **C-D.** qRT-PCR data show mRNA elevation of NRG1-beta ligand after MITF depletion in WM983B **(C)**, WM1382 **(D)** and Hermes 4C **(E).** Graphs represent qRT-PCR expression data from three separate experiments normalized to untreated control cells and plotted as mean ± SD. * =$p < 0.05$ (*t*-test).

transfection in A375 harboring low MITF levels, we observed a minor reduction of NRG1-beta mRNA levels after 24h (See Supplementary Figure S2A).

MITF regulates ERBB3 in a FOXD3 dependent and independent manner

To investigate the role of SOX10, MITF, and FOXD3 and the reported effects due to BRAF status in ERBB3 regulation, we depleted the three former genes individually and in combination for MITF/FOXD3 by the use of siRNA in three melanoma cell lines: WM983B, MeWo and WM115. MeWo represent BRAF wild type, while WM983B and WM115 harbor mutant BRAF. Additionally, the WM115 cell line was utilized in a previous study by Abel et al. [15], were the authors reported that FOXD3 is an activator of ERBB3 expression only in V600 cell lines. Our results show that siSOX10 treatment reduces the MITF, FOXD3 and ERBB3 protein levels in all cell lines (Figure 4A–4C). In contrast, siMITF treatment resulted in an increase in both ERBB3 and FOXD3 protein levels (Figure 4A–4C). When transfecting the cell lines with siFOXD3 alone, no differences in ERBB3 protein levels were detected in MeWo compared to a negative siRNA control. However, we observed a minor reduction of ERBB3 protein levels in WM983B and WM115. To explore whether MITF depletion results in elevation of ERBB3 through FOXD3, we performed an siRNA co-transfection of MITF and FOXD3 in all three cell lines, demonstrating an increase in ERBB3 protein levels compared to negative siRNA control in WM983B and MeWo, while no change was detected in WM115.

MITF binding sites in ERBB3, NRG1-beta and FOXD3

To address whether MITF protein binds DNA in the proximity of ERBB3, NRG1-beta, and FOXD3, we performed a 3xHA-tagged MITF ChIP-seq analysis in the Hermes 4C cell line. Results showed a strong MITF binding signal in the putative regulatory region, approximately 18kb upstream of the transcription start

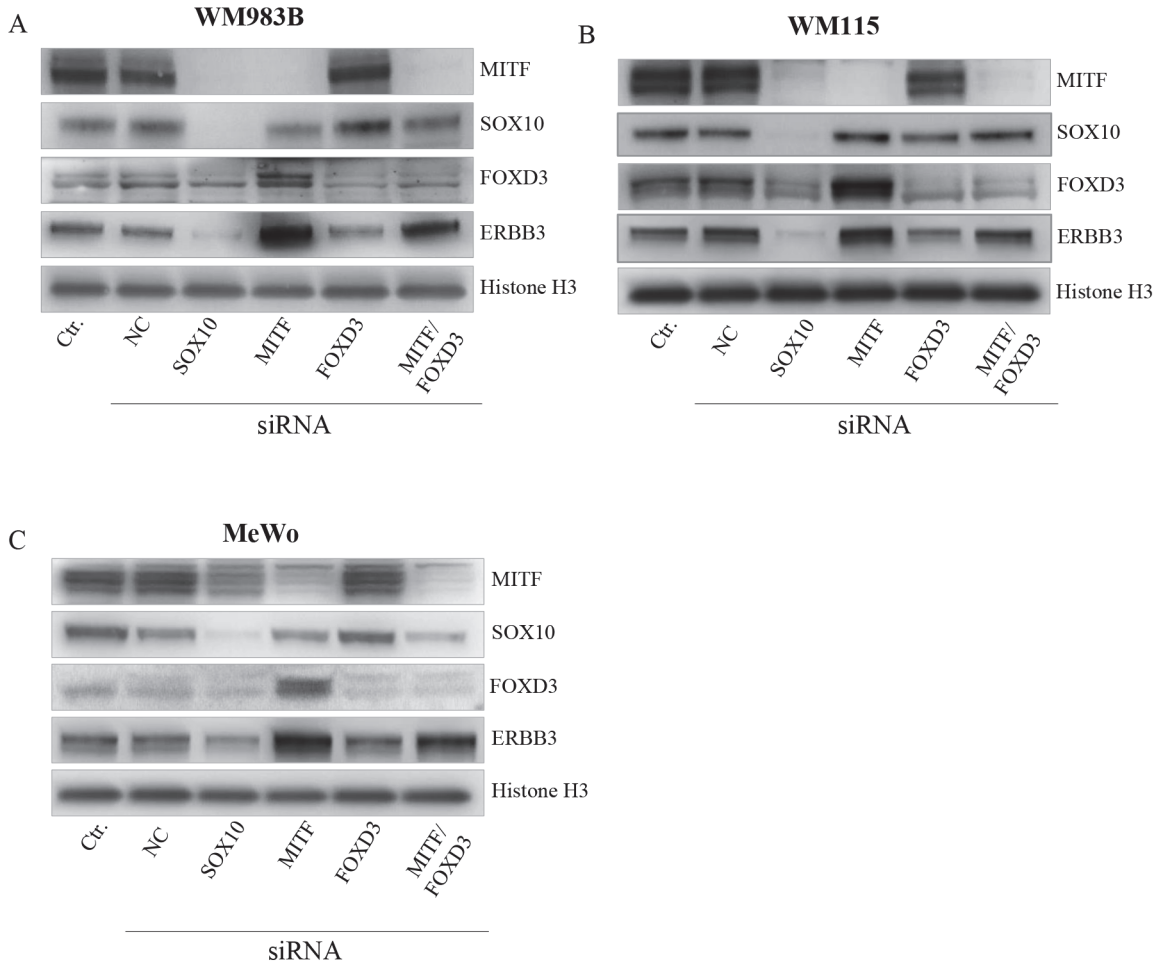

Figure 4: MITF suppress ERBB3 expression, both through and without FOXD3. Representative western blot showing the effect of SOX10, MITF and FOXD3 siRNA treatment upon ERBB3 expression after 72h in WM983B **(A).** WM115 **(B).** and MeWo **(C).** siRNA treatment was performed in triplicate. Histone H3 was used as loading control.

site, and two minor binding signals in the promoter region of ERBB3 (Figure 5A). In the putative regulatory region, we detected both an E-box (CACATG) and a SOX10 binding motif (AACAAT), while no E-boxes were found in the promoter region. In the NRG1-beta gene, we detected a strong MITF binding signal in the regulatory region within the first intron. This MITF binding signal contained two E-box motifs and was located approximately 30kb downstream of the transcription start site. Furthermore, we detected a minor MITF binding signal in the proximal promoter region of NRG1-beta, without any E-box motifs (Figure 5B). When investigating the FOXD3 gene, we found a MITF binding signal containing an E-box motif in the promoter region (Figure 5C).

Correlation between SOX10 and ERBB3 in patient samples

To investigate the relationship between SOX10, MITF, FOXD3, ERBB3 and NRG1 in patient samples, we utilized The Cancer Genome Atlas (TCGA, SKCM), which contains a set of 474 melanoma patient samples. A strong correlation (R = 0.74, P = <0.0001)

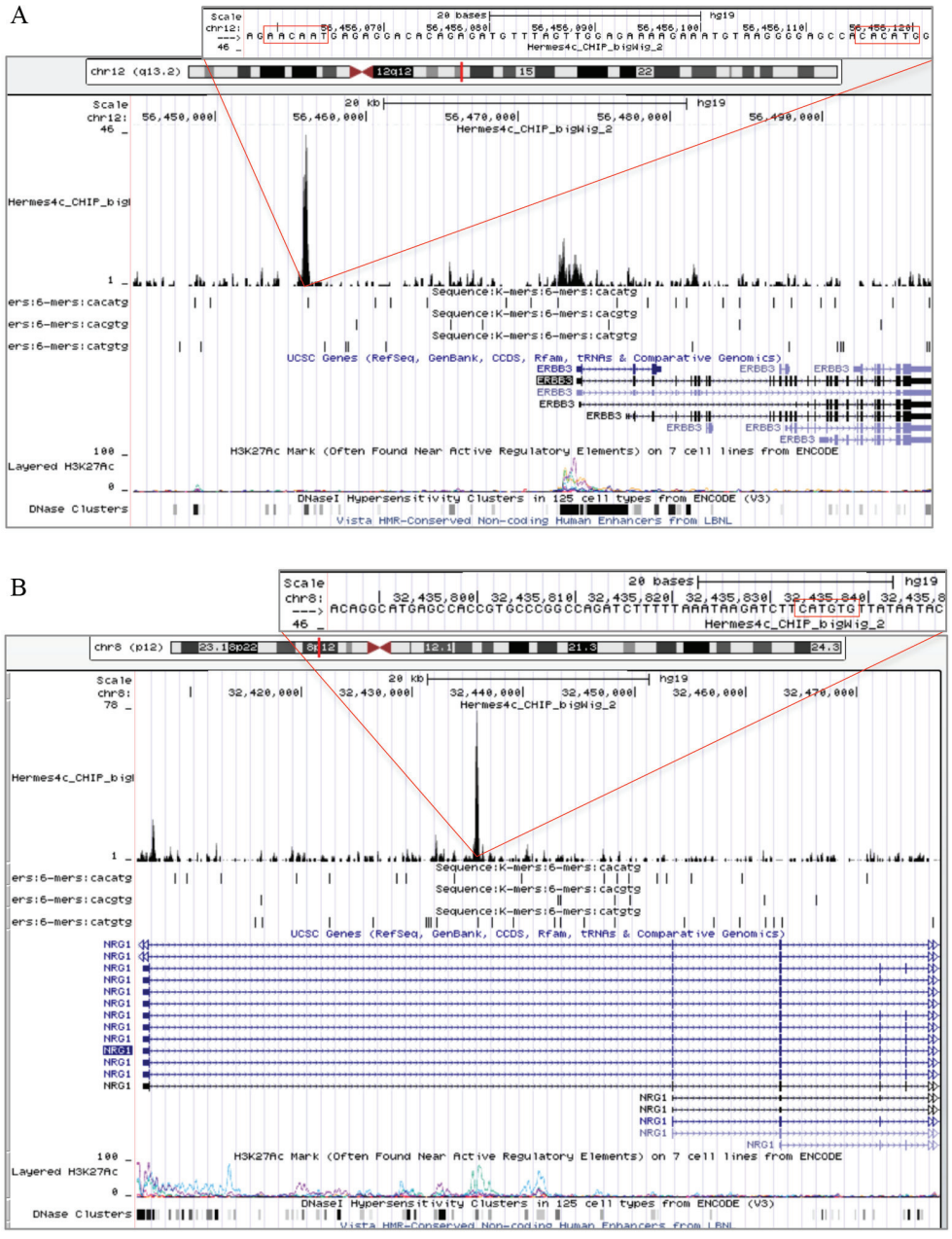

Figure 5: MITF binding sites in ERBB3, NRG1-beta and FOXD3. Snapshots from the University of California Santa Cruz (UCSC) genome browser of the ERBB3 **(A).** NRG1-beta **(B).** and FOXD3 (*Continued*)

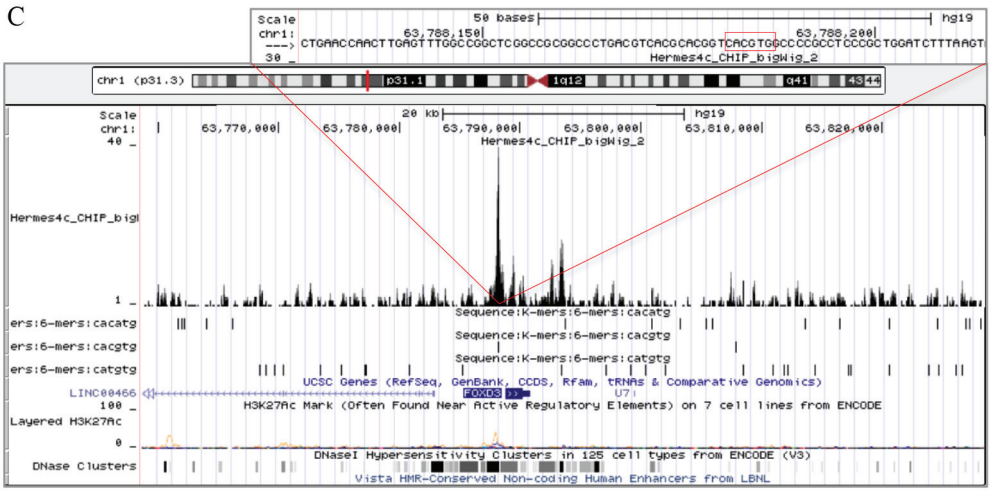

Figure 5: (*Continued*) MITF binding sites in ERBB3, NRG1-beta and FOXD3. (C). genes in Hermes 4c cells expressing 5′ HA-tagged MITF in the hg19 assembly. The figure includes tracks for MITF ChIP-seq, RefSeq Genes, three E-box motifs (CACATG, CACGTG and CATGTG), and ENCODE regulation (H3K27Ac/DNase clusters). The scale in the MITF ChIP-seq tracks indicates the intensity of MITF enrichment. (A): MITF ChIP-seq results shows that a MITF enriched site was found in the regulatory region of ERBB3, approximately 18kb upstream of the transcription start site of the gene. The MITF enriched site was co-localized with an E-box (CACATG) and the DNA binding motif of SOX10 (AACAAT). Enrichment of MITF was also detected in the promoter region of the ERBB3 gene. (B): A MITF enriched site together with an E-box (CATGTG) motif was found in the first intron of the NRG1-beta gene. (C): MITF enrichment together with an E-box (CACGTG) motif was found in the promoter region of FOXD3.

was found between SOX10 and ERBB3 (Figure 6). Correlations were also detected between FOXD3 and ERBB3 (R = 0.55, P = <0.0001), SOX10 and FOXD3 (R = 0.56, P = <0.0001), and SOX10 and MITF (R = 0.49, P = <0.0001). Among the genes investigated, MITF and NRG1 showed weakest correlation with ERBB3, with R = 0.43 and R = 0.18, respectively. Interestingly, we observed an inverse correlation between MITF and NRG1 (R = -0.4, P = <0.0001) in the TCGA data. TYR, in addition to two genes assumed uncorrelated to MITF, RPLPO and ACTB, were included as controls.

Vemurafenib treatment results in loss of MITF and elevation of FOXD3 and ERBB3

As vemurafenib has been reported to induce loss of MITF, we measured the protein expression levels of MITF, SOX10, FOXD3 and ERBB3 after inhibitor treatment in the WM983B and SKMEL28 cell lines (Figure 7). An extensive decrease in MITF protein levels after two weeks of vemurafenib treatment was observed in both cell lines, while a minor reduction in SOX10 levels could be detected. In contrast, we measured elevated ERBB3 and FOXD3 protein levels in the same samples.

DISCUSSION

In this study, we have demonstrated that the ERBB3 receptor and its cognate ligand NRG1-beta are elevated after MITF depletion in various melanoma cell lines. Our data is supported by previous studies showing that both ERBB3 expression and phosphorylation can be elevated after MAPK inhibitor treatment [15–20]. Hyper-activation of the PI3K/AKT pathway due to increased NRG1-beta/ERBB3 pathway signaling has previously been reported to be responsible for acquired drug resistance in BRAFV600 melanomas [15, 17]. However, also low MITF/AXL and MITF/EGFR ratios have been suggested to be involved in early resistance to vemurafenib in a subset of melanomas [12, 13]. Together, these reports suggest that MITF loss after vemurafenib treatment, followed by PI3K/AKT elevation, is a key element to overcome drug treatment and in acquiring drug resistance against MAPK inhibitors. Both gain and loss of MITF after vemurafenib has been reported [13]. The molecular mechanism behind these alterations in MITF levels is presently not known. In the SKMEL28 and WM983B cell lines, we observed that SOX10, an activator of MITF transcription, was reduced after vemurafenib treatment. However, as also both gain and loss of SOX10 protein after vemurafenib-induced MITF loss have been reported in the literature [13], the role of SOX10 in vemurafenib-induced MITF loss remains unclear.

SOX10 and FOXD3 have been reported to activate ERBB3 expression [15, 21], in addition to also activating and repressing MITF expression, respectively [24, 25, 27]. In this context, we investigated their role in ERBB3 regulation. When depleting FOXD3 in the two BRAFV600 cell lines WM983B and WM115, we

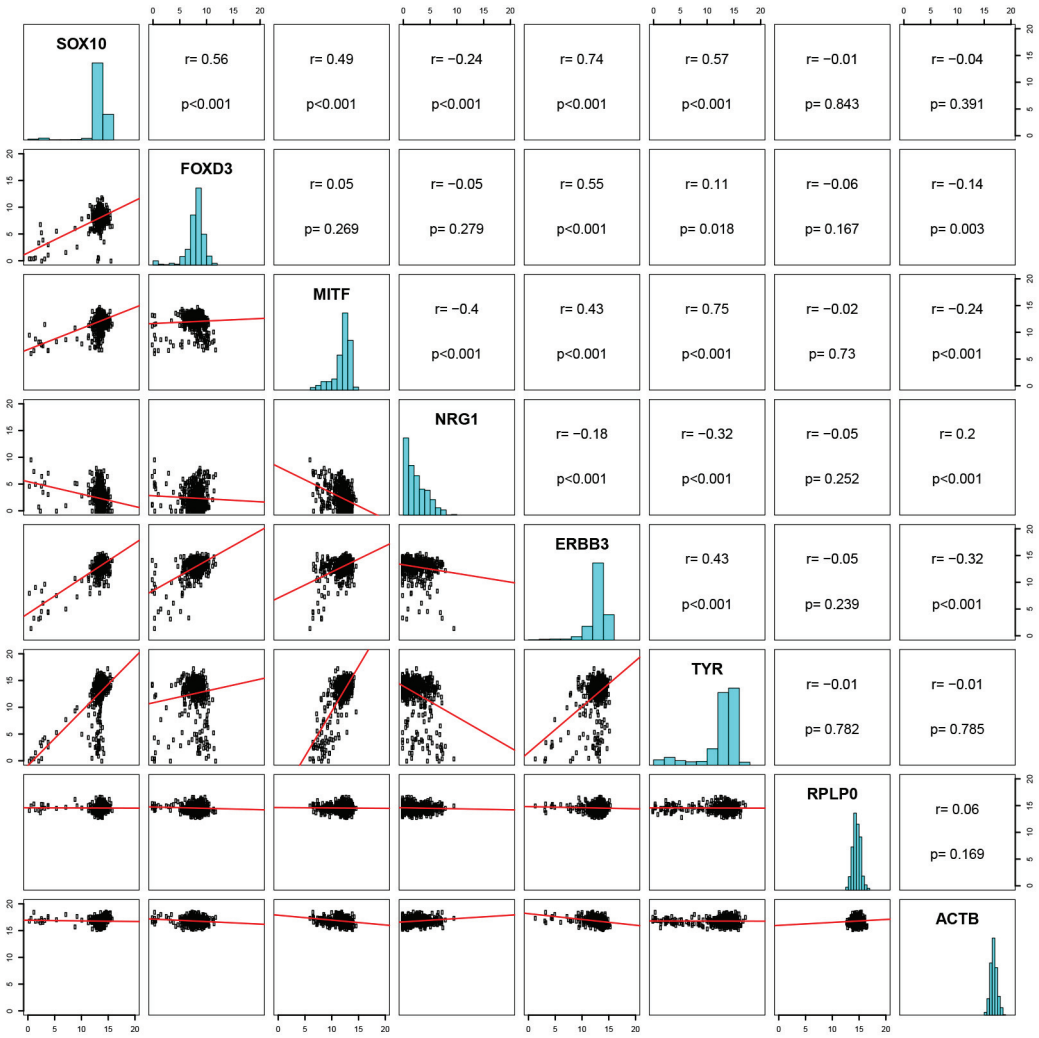

Figure 6: Correlation between SOX10 and ERBB3 in patient samples. A pairwise correlation plot of the cutaneous skin cancer (n=473) exon expression cases of TCGA (data set available at https://tcga-data.nci.nih.gov/docs/publications/skcm_2015/). IlluminaHiSeq-defined RNAseq is shown for the genes SOX10, FOXD3, MITF, NRG1, ERBB3 and TYR are shown, in addition to two genes uncorrelated, RPLP0 and ACTB. Both axes display log2 expression values.

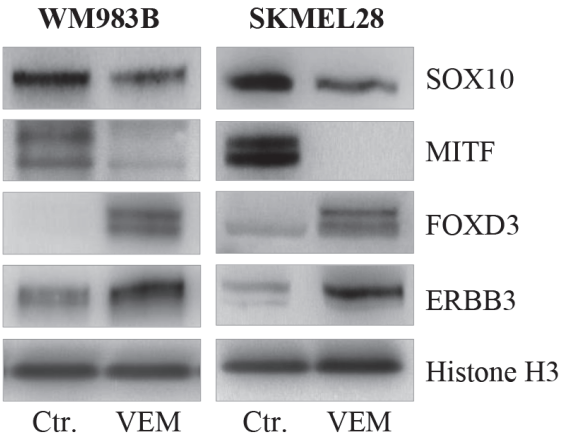

Figure 7: Vemurafenib treatment results in loss of MITF and gain of FOXD3 and ERBB3. Representative western blots showing MITF loss and subsequent gain of ERBB3 and FOXD3 protein after 2 weeks of vemurafenib treatment (0.5μM) in the WM983B and SKMEL28 cell lines. Vemurafenib-cultured cells were performed in triplicate. Histone H3 was used as loading control.

detected a minor reduction of ERBB3 protein, which is in agreement with what Abel *et al*. [15] measured in the WM115 cell line. In the MeWo cell line, FOXD3 depletion alone did not affect ERBB3 protein expression. This is supported by Abel and Aplin [28], who showed that FOXD3 does not regulate ERBB3 expression in BRAF wild-type melanoma cells, nor in melanocytes. Furthermore, our siRNA depletion results demonstrated that SOX10 and MITF have opposite roles in the regulation of FOXD3 and ERBB3 expression. The observed FOXD3 elevation after MITF depletion is in agreement with He *et al*. [26] and implies that MITF can repress ERBB3 expression indirectly by suppressing FOXD3 in V600 cell lines. However, our data also demonstrate that MITF protein can bind directly to the regulatory region of ERBB3, as well as NRG1-beta and FOXD3. Together with our siRNA experiments, these latter results suggest that MITF can repress ERBB3 both with and without FOXD3 involvement, depending on the BRAF mutational status, as shown in this study. In the regulatory region of ERBB3, we detected a SOX10 binding site 40 bp downstream of the MITF-binding E-box, suggesting SOX10/MITF co-localization. Co-localization of MITF and SOX10 in the form of MITF-associated regulatory elements (MARE), where MITF alone, or with SOX10, binds between two BRG1-bound nucleosomes, has previously been described [29]. However, the precise mechanism(s) by which MITF represses ERBB3, FOXD3 and NRG1-beta expression remains the subject of ongoing investigation. An inverse relationship between MITF and ERBB3 protein expression levels was observed in our cell panel, and this was particularly evident in the immortalized melanocyte cell line Hermes 4C, and in the melanoma cell lines WM983B and WM115. Simultaneously, our results show that high MITF protein levels, in Hermes 4C, are not able to completely abolish ERBB3 transcription, implying the existence of a threshold with respect to MITF-induced repression of ERBB3 expression. This is also supported by the moderate suppression of ERBB3 expression detected when overexpressing MITF protein in MeWo and A375. We also observed an inverse correlation between MITF and NRG1-beta in the 474 patient samples from TCGA. In contrast, no inverse correlation was observed between MITF and ERBB3 in the TCGA samples. The reason for the lack of inverse correlation between MITF and ERBB3 in patient samples is not known, but could result from the fact that MITF suppression of ERBB3 seems to be only partial, and to depend on SOX10 expression. SOX10-dependent MITF repression of ERBB3 is supported by the observation that cell lines without both SOX10 and MITF (WM1366, WM852, LOXIMVI) lack ERBB3.

In summary, we have in this study shown that MITF depletion results in elevated expression levels of both the ERBB3 receptor and its cognate ligand NRG1-beta, which may have potential implications for acquired drug resistance in melanoma.

MATERIALS AND METHODS

Cell lines and culture conditions

The SKMEL28, MeWo, and A375 cell lines were obtained from the American Type Culture Collection (ATCC; Rockville, MD, USA), WM35, WM115, WM1341B, WM1366, WM983B, WM45.1, WM239A, WM266.4, WM852, WM1382, WM9, WM793B from the Wistar Institute, and LOXIMVI established in-house. For genetic background information, see Supplementary Table S1. The immortalized melanocyte cell line Hermes 3C and 4C were purchased from Wellcome Trust Functional Genomics Cell Bank [30]. Hermes 3C and 4C were cultured and maintained in 254 medium (Gibco, Invitrogen, Oslo, Norway) supplemented with 10% fetal calf serum (FCS) (PAA, New Bedford, MA, USA), 200nM phorbol-12-myristate-13-acetate (TPA; Sigma-Aldrich), 200pM (Hermes 3C) and 2pM (Hermes 4C) cholera toxin (Sigma-Aldrich), 10ng/ml human stem cell factor (hSCF; Thermo Fisher) and 10nM endothilin (EDN1; Millipore, Oslo, Norway) with the exception of where noted in the text. All melanoma cell lines were cultured and maintained in RPMI 1640 medium (Bio Whittaker, Verviers, Belgium), supplemented with 10% fetal calf serum (FCS) (PAA, New Bedford, MA, USA) and 2mM GlutaMAX (Gibco, Invitrogen, Oslo, Norway) with the exception of where noted in the text. The cells were maintained at 37°C in a humidified atmosphere containing 5% CO_2 and were routinely tested for *Mycoplasma* infections (VenorGeM, Minerva Biolabs, Berlin, Germany), and the cell line identities were also verified by short tandem repeat (STR) analysis.

Transfection and RNA interference

Cells were seeded in 6-well plates and grown to 60% confluence before being transfected and incubated for 72h with siRNA directed against MITF-M and SOX10 (Eurogentec, Seraing, Belgium), ERBB3 (Life Technologies) and FOXD3 (Dharmacon). The reason for choosing 72h incubation time was to ensure optimal reduction of our targets at the protein level. The cells were transfected with a final concentration of 25pmol siRNA, using Lipofectamine RNAiMAX (Invitrogen) as described in the manufacturers protocol. Sequences for siRNA can be found in the Supplementary Methods. All siRNA transfections were performed in triplicate.

Western immunoblotting

Preparations of whole cell lysates were performed by addition of lysis buffer (150mM NaCl, 50mM Tris-HCl pH 7.5, 0.1% Nondient P-40, 1x Complete tablets mini

EASYpack and 1x PhosSTOP from Roche), to frozen, dry cell pellets. The samples were left on ice for 30min with intermittent vortexing, followed by sonication and centrifugation to remove cell debris. Protein quantification was done using a standard Bradford protein assay (Bio-Rad Laboratories, Inc., CA). Protein lysates (30µg) were separated on 4-12% NuPAGE® Novex Bis-Tris Midi-Gels (Invitrogen, Carlsbad, CA) and then transferred to a membrane using an iBlot Dry Blotting system (Invitrogen, Carlsbad, CA) according to the manufacturers instruction. The membranes were subsequently blocked in TBS/T (137mM NaCl, 20mM Tris-HCl pH 7.5 and 0.1% tween20) containing 5% BSA (Sigma-Aldrich, Steinheim, Germany) for 1h, and then incubated with primary antibodies over night at 4°C with gentle agitation. Residual primary antibodies were removed by washing 3 × 10min in TBS/T. The membranes were thereafter incubated for 1h at RT with horse radish peroxidase conjugated (HRP) secondary antibody. The membranes were then washed 3 × 10min with TBS/T. The protein bands were visualized in the G-Box iChemi Chemiluminescence Image Capture (Syngene, England) using the SuperSignal chemiluminescence detection system (Pierce).

Antibodies and inhibitors

The following antibodies were purchased from Cell Signaling Technology (Danvers, MA, USA); MITF (1:1000; #12590), Her3/ERBB3 XP (1:1000; #12708), Phospho-Her3/ERBB3-Tyrosine-1289 (1:1000; #4791), FOXD3 (1:1000; #2019), SOX10 (1:1000; #14374), Akt (1:2000; #9272), Phospho-Akt-Serine-473 XP (1:2000; #4060), and Histone H3 (1:3000; #4499) was used as loading control. Secondary antibody against rabbit (1:5000; P0448) was purchased from Dako (Agilent Technologies, Glostrup, Denmark). The small molecular inhibitor vemurafenib (Plexxikon 4032) was obtained from Selleck Chemicals (Houston, TX, USA). The NRG1-beta ligand was purchased from ImmunoTools GmbH (Friesoythe, Germany). The NRG1-beta ligand was used to enhance the pERBB3 (T1289) signal, as our Phospho-Her3/ERBB3-Tyrosine-1289 antibody did not detect pERBB3 (T1289) levels without NRG1-beta addition (see also Supplementary Figure S3A-S3B). The reason for choosing 15min of incubation time and a NRG1-beta ligand concentration of 10ng/ml was due to a previous study where they showed efficient activation of the ERBB3 receptor in the WM115 cell line under these conditions [18].

Quantitative reverse transcriptase PCR

Total cellular RNA was isolated with the GenElute Mammalian Total RNA Miniprep Kit (Sigma-Aldrich, Steinheim, Germany) and the qScript™ cDNA Synthesis Kit (Quanta Biosciences, Gaithersburg, USA) was used for reverse transcription. Both kits were used according to the manufacturers manuals. RNA concentration was measured using NANODROP 2000 (Thermo Scientific). Real-time detection was obtained by use of SYBR Green. For each PCR, 100ng cDNA, 30µl PerfeCTa™ SYBR® Green SuperMix for iQ (Quanta Biosciences, Gaithersburg, USA), 300nM of each primer and nuclease-free water was added to a final volume of 60µl. The final volume of 60µl was then split into two parallels of 25µl and added to the PCR plate. Primers against MITF-M, ERBB3, SOX10, FOXD3 and NRG1-beta were ordered from Integrated DNA technologies (IDT). Real-time reactions were run on a CFX Connect Real-Time PCR Detection System (Bio-Rad) with the following amplification protocol: 3 min initial denaturation at 95°C, 40 cycles of 15s denaturation at 95°C and 35s annealing/extension at 60°C, one hold at 95°C for 10 s followed by a hold for 30s at 60°C. Finally, a melt curve analysis was performed, starting at 60°C, increasing with 0.5°C steps (8s) until reaching a final temperature of 95°C. The quality of the RNA samples was verified by amplification of two housekeeping genes, the TATA-binding protein (TBP) and the human acidic ribosomal phosphoprotein PO (RPLPO). These housekeeping genes were chosen as they were unchanged by the different treatment modalities in this study (data not shown). Bio-Rad, CFX manager 3.1, was used for the quantitative calculations. The program performs calculations based on the $\Delta\Delta C_T$ method [31], which allows comparison of cycle threshold values obtained using different sets of primers on the same set of samples.

Chromatin immuno-precipitation sequencing (ChIPseq) protocol

Hermes 4C was transduced by lentiparticles carrying pLX3xHAvar4mCherry. Stable cell lines expressing the 3xHA tagged MITFvar4 were subsequently sorted based on the presence of mCherry and used further (sorted by Flow Cytometry Core Facility, OUS, Norway). Chromatin immuno-precipitation sequencing (ChIPseq) experiments were performed twice as described by Dahl JA and Collas P [32] with modifications. Briefly, chromatin from native Hermes 4C and Hermes 4C cells (mycoplasma unverified) stably transfected with a lentiviral vector expressing 3xHA-tagged MITF were fixed with 1% formaldehyde for 8min to cross-link DNA and proteins. Cross-linking was stopped with 125mM glycine for 5min. Cells were rinsed twice in phosphate buffered saline (PBS), harvested using trypsination and sedimented. Cells were resuspended in ice-cold lysis buffer (1% SDS, 10mM EDTA, 50mM Tris–HCl, pH 8.0) containing protease and phosphatase inhibitors. Cells were sonicated at 4°C using a Covaris S2 instrument to yield chromatin fragments of 300–500 bp. Chromatin was cleared by centrifugation, concentration determined by A260, and chromatin was diluted in RIPA buffer (0.1% SDS, 0.1% Na-deoxycholate, 1% Triton X-100, 1mM

EDTA, 0.5mM EGTA, 140mM NaCl, 10mM Tris–HCl, pH 8.0) to 2 A260 units. Each immunoprecipitation was performed in 250µl RIPA buffer with 1µg antibody overnight at 4°C. The antibody: anti-HA-tag (12CA5, Roche) was used. Antibody-bound chromatin was precipitated using Dynabeads protein G (Invitrogen) and washed 3 times in RIPA buffer, once in TE buffer (10mM Tris–HCl, pH 8.0, 10mM EDTA) and eluted in 1% SDS with 100mM NaHCO3. Eluted chromatin was incubated at 65°C with proteinase K (Sigma-Aldrich; 50µg/ml) over night, and DNA was purified by phenol-chloroform-isoamylalcohol extraction (25:24:1) and once with chloroform/isoamylalcohol (24:1) followed by ethanol precipitation. DNA was dissolved in H2O and used for high-throughput sequencing using an Illumina Hiseq 2500 sequencer. The sequencing reads were aligned to hg19 using Bowtie v.1.0.0, after which MACS v 1.4.2 was used to call peaks. To get a common set of peaks for the two samples, the two. bed files containing the peaks were put together and sorted before using BEDTools v2.7.1 to merge them. IntersectBed was then used to get the number of reads falling into each peak for all samples. The counts were read into R, where two sets of normalized counts were computed, one using size normalization and one using quantile normalization from the package preprocessCore. Logfold2 change was computed for the two CHIPed samples. CHIP vs INPUT counts were plotted for Hermes4c and histograms were made of the log fold change values.

Construction of pLX3xHAvar4mCh

The construction of pLX 3xHAvar4mCh was performed by two sequential clonings. The human MITF variant 4 cDNA was prepared by PCR amplification of the cDNA clone MGC:75121 (IMAGE:6066096) (Invitrogen) using the BglII containing MITF forward primer:5′-AA AAAAAGATCTACCATGCTGGAAATGCTAG-3′ and the EcoRI containing reverse primer: 5′-AAAAAGA TTTCATCTCGCTAACAAGTGTGC. Subsequent to restriction digestion by BglII and EcoRI the insert was gel purified. The mouse equivalent of the human MITF var4 cDNA was removed from pCMV3xHAvar4 plasmid by BglII/ EcoRI endonuclease digestion [33]. The insert and vector were then ligated overnight at 14°C, transformed into chemically competent DH5α and selected candidates were screened by PCR for the presence of the insert. The successful construct pCMV3xHAvar4 was digested with NheI/XbaI and the 5′ 3xHA tagged MITF variant 4 fusion insert was isolated by gel purification. The insert was then ligated into gene cleaned (Genomed) SpeI linearized pLVX IRES mCh (Clontech) producing the Lenti-expression vector pLX3xHAvar4mCherry and transformed into chemically competent STBL3 (Invitrogen). pLX3xHAvar4mCherry was subsequently sequenced to confirm the correctness of the insertion.

Production of lentiviral particles

Lentiparticles were produced in Lenti-X 293T (Clontech) using the designated lenti-expression vector and the second generation packaging system utilizing pCMV-dR8.2 dvpr and pCMV-VSV-G as previously described [34] with the following modification: The transfection reagent Fugene (Promega) was replaced by Turbofect (Thermo Fisher Scientific) and applied as recommended by the manufacturer.

Statistical analysis

P values were calculated using a student t-test. Values $p < 0.05$ were considered statistically significant.

ACKNOWLEDGMENTS

We thank the Flow Core Facility OUS, Norway for sorting our cells and Thomas Strub and Stein Sæbøe-Larssen for providing us with the pCMV3xHAvar4 plasmid and mRNA molecules, respectively. We also gratefully acknowledge Vegard Nygaard, Bioinformatics Core Facility, OUS, Norway for TCGA analysis.

CONFLICTS OF INTEREST

The authors declare that they have no competing interests.

GRANT SUPPORT

We gratefully acknowledge the funding by Helse Sør-Øst (project number 2014044), and the support of The Norwegian Cancer Society (project number 71220 - PR-2006-0433).

REFERENCES

1. Bollag G, Hirth P, Tsai J, Zhang J, Ibrahim PN, Cho H, Spevak W, Zhang C, Zhang Y, Habets G, Burton EA, Wong B, Tsang G, West BL, Powell B, Shellooe R, et al. Clinical efficacy of a RAF inhibitor needs broad target blockade in BRAF-mutant melanoma. Nature. 2010; 467:596-599.
2. Chapman PB, Hauschild A, Robert C, Haanen JB, Ascierto P, Larkin J, Dummer R, Garbe C, Testori A, Maio M, Hogg D, Lorigan P, Lebbe C, Jouary T, Schadendorf D, Ribas A, et al. Improved survival with vemurafenib in melanoma with BRAF V600E mutation. N Engl J Med. 2011; 364:2507-2516.
3. Tsai J, Lee JT, Wang W, Zhang J, Cho H, Mamo S, Bremer R, Gillette S, Kong J, Haass NK, Sproesser K, Li L, Smalley KS, Fong D, Zhu YL, Marimuthu A, et al. Discovery of a selective inhibitor of oncogenic B-Raf kinase with potent antimelanoma activity. Proc Natl Acad Sci U S A. 2008; 105:3041-3046.

4. Wagle N, Emery C, Berger MF, Davis MJ, Sawyer A, Pochanard P, Kehoe SM, Johannessen CM, Macconaill LE, Hahn WC, Meyerson M and Garraway LA. Dissecting therapeutic resistance to RAF inhibition in melanoma by tumor genomic profiling. J Clin Oncol. 2011; 29:3085-3096.
5. Nazarian R, Shi H, Wang Q, Kong X, Koya RC, Lee H, Chen Z, Lee MK, Attar N, Sazegar H, Chodon T, Nelson SF, McArthur G, Sosman JA, Ribas A and Lo RS. Melanomas acquire resistance to B-RAF(V600E) inhibition by RTK or N-RAS upregulation. Nature. 2010; 468:973-977.
6. Emery CM, Vijayendran KG, Zipser MC, Sawyer AM, Niu L, Kim JJ, Hatton C, Chopra R, Oberholzer PA, Karpova MB, MacConaill LE, Zhang J, Gray NS, Sellers WR, Dummer R and Garraway LA. MEK1 mutations confer resistance to MEK and B-RAF inhibition. Proc Natl Acad Sci U S A. 2009; 106:20411-20416.
7. Poulikakos PI, Persaud Y, Janakiraman M, Kong X, Ng C, Moriceau G, Shi H, Atefi M, Titz B, Gabay MT, Salton M, Dahlman KB, Tadi M, Wargo JA, Flaherty KT, Kelley MC, et al. RAF inhibitor resistance is mediated by dimerization of aberrantly spliced BRAF(V600E). Nature. 2011; 480:387-390.
8. Johannessen CM, Johnson LA, Piccioni F, Townes A, Frederick DT, Donahue MK, Narayan R, Flaherty KT, Wargo JA, Root DE and Garraway LA. A melanocyte lineage program confers resistance to MAP kinase pathway inhibition. Nature. 2013; 504:138-142.
9. Straussman R, Morikawa T, Shee K, Barzily-Rokni M, Qian ZR, Du J, Davis A, Mongare MM, Gould J, Frederick DT, Cooper ZA, Chapman PB, Solit DB, Ribas A, Lo RS, Flaherty KT, et al. Tumour micro-environment elicits innate resistance to RAF inhibitors through HGF secretion. Nature. 2012; 487:500-504.
10. Shi H, Hugo W, Kong X, Hong A, Koya RC, Moriceau G, Chodon T, Guo R, Johnson DB, Dahlman KB, Kelley MC, Kefford RF, Chmielowski B, Glaspy JA, Sosman JA, van Baren N, et al. Acquired resistance and clonal evolution in melanoma during BRAF inhibitor therapy. Cancer Discov. 2014; 4:80-93.
11. Shi H, Kong X, Ribas A and Lo RS. Combinatorial treatments that overcome PDGFRbeta-driven resistance of melanoma cells to V600EB-RAF inhibition. Cancer Res. 2011; 71:5067-5074.
12. Ji Z, Erin Chen Y, Kumar R, Taylor M, Jenny Njauw CN, Miao B, Frederick DT, Wargo JA, Flaherty KT, Jonsson G and Tsao H. MITF Modulates Therapeutic Resistance through EGFR Signaling. J Invest Dermatol. 2015; 135:1863-1872.
13. Muller J, Krijgsman O, Tsoi J, Robert L, Hugo W, Song C, Kong X, Possik PA, Cornelissen-Steijger PD, Foppen MH, Kemper K, Goding CR, McDermott U, Blank C, Haanen J, Graeber TG, et al. Low MITF/AXL ratio predicts early resistance to multiple targeted drugs in melanoma. Nat Commun. 2014; 5:5712.
14. Ma J, Lyu H, Huang J and Liu B. Targeting of erbB3 receptor to overcome resistance in cancer treatment. Mol Cancer. 2014; 13:105.
15. Abel EV, Basile KJ, Kugel CH, 3rd, Witkiewicz AK, Le K, Amaravadi RK, Karakousis GC, Xu X, Xu W, Schuchter LM, Lee JB, Ertel A, Fortina P and Aplin AE. Melanoma adapts to RAF/MEK inhibitors through FOXD3-mediated upregulation of ERBB3. J Clin Invest. 2013; 123:2155-2168.
16. Fattore L, Marra E, Pisanu ME, Noto A, de Vitis C, Belleudi F, Aurisicchio L, Mancini R, Torrisi MR, Ascierto PA and Ciliberto G. Activation of an early feedback survival loop involving phospho-ErbB3 is a general response of melanoma cells to RAF/MEK inhibition and is abrogated by anti-ErbB3 antibodies. J Transl Med. 2013; 11:180.
17. Fattore L, Malpicci D, Marra E, Belleudi F, Noto A, De Vitis C, Pisanu ME, Coluccia P, Camerlingo R, Roscilli G, Ribas A, Di Napoli A, Torrisi MR, Aurisicchio L, Ascierto PA, Mancini R, et al. Combination of antibodies directed against different ErbB3 surface epitopes prevents the establishment of resistance to BRAF/MEK inhibitors in melanoma. Oncotarget. 2015; 6:24823-24841.
18. Kugel CH, 3rd, Hartsough EJ, Davies MA, Setiady YY and Aplin AE. Function-blocking ERBB3 antibody inhibits the adaptive response to RAF inhibitor. Cancer Res. 2014; 74:4122-4132.
19. Lito P, Pratilas CA, Joseph EW, Tadi M, Halilovic E, Zubrowski M, Huang A, Wong WL, Callahan MK, Merghoub T, Wolchok JD, de Stanchina E, Chandarlapaty S, Poulikakos PI, Fagin JA and Rosen N. Relief of profound feedback inhibition of mitogenic signaling by RAF inhibitors attenuates their activity in BRAFV600E melanomas. Cancer Cell. 2012; 22:668-682.
20. Montero-Conde C, Ruiz-Llorente S, Dominguez JM, Knauf JA, Viale A, Sherman EJ, Ryder M, Ghossein RA, Rosen N and Fagin JA. Relief of feedback inhibition of HER3 transcription by RAF and MEK inhibitors attenuates their antitumor effects in BRAF-mutant thyroid carcinomas. Cancer Discov. 2013; 3:520-533.
21. Prasad MK, Reed X, Gorkin DU, Cronin JC, McAdow AR, Chain K, Hodonsky CJ, Jones EA, Svaren J, Antonellis A, Johnson SL, Loftus SK, Pavan WJ and McCallion AS. SOX10 directly modulates ERBB3 transcription via an intronic neural crest enhancer. BMC Dev Biol. 2011; 11:40.
22. Garrett JT, Olivares MG, Rinehart C, Granja-Ingram ND, Sanchez V, Chakrabarty A, Dave B, Cook RS, Pao W, McKinely E, Manning HC, Chang J and Arteaga CL. Transcriptional and posttranslational up-regulation of HER3 (ErbB3) compensates for inhibition of the HER2 tyrosine kinase. Proc Natl Acad Sci U S A. 2011; 108:5021-5026.
23. Chakrabarty A, Sanchez V, Kuba MG, Rinehart C and Arteaga CL. Feedback upregulation of HER3 (ErbB3) expression and activity attenuates antitumor effect of PI3K inhibitors. Proc Natl Acad Sci U S A. 2012; 109:2718-2723.

24. Bondurand N, Pingault V, Goerich DE, Lemort N, Sock E, Le Caignec C, Wegner M and Goossens M. Interaction among SOX10, PAX3 and MITF, three genes altered in Waardenburg syndrome. Hum Mol Genet. 2000; 9:1907-1917.

25. Thomas AJ and Erickson CA. FOXD3 regulates the lineage switch between neural crest-derived glial cells and pigment cells by repressing MITF through a non-canonical mechanism. Development. 2009; 136:1849-1858.

26. He S, Li CG, Slobbe L, Glover A, Marshall E, Baguley BC and Eccles MR. PAX3 knockdown in metastatic melanoma cell lines does not reduce MITF expression. Melanoma Res. 2011; 21:24-34.

27. Murisier F, Guichard S and Beermann F. The tyrosinase enhancer is activated by Sox10 and Mitf in mouse melanocytes. Pigment Cell Res. 2007; 20:173-184.

28. Abel EV and Aplin AE. FOXD3 is a mutant B-RAF-regulated inhibitor of G(1)-S progression in melanoma cells. Cancer Res. 2010; 70:2891-2900.

29. Laurette P, Strub T, Koludrovic D, Keime C, Le Gras S, Seberg H, Van Otterloo E, Imrichova H, Siddaway R, Aerts S, Cornell RA, Mengus G and Davidson I. Transcription factor MITF and remodeller BRG1 define chromatin organisation at regulatory elements in melanoma cells. Elife. 2015; 4.

30. Gray-Schopfer VC, Cheong SC, Chong H, Chow J, Moss T, Abdel-Malek ZA, Marais R, Wynford-Thomas D and Bennett DC. Cellular senescence in naevi and immortalisation in melanoma: a role for p16? Br J Cancer. 2006; 95:496-505.

31. Vandesompele J, De Preter K, Pattyn F, Poppe B, Van Roy N, De Paepe A and Speleman F. Accurate normalization of real-time quantitative RT-PCR data by geometric averaging of multiple internal control genes. Genome Biol. 2002; 3:RESEARCH0034 0031-0011.

32. Dahl JA and Collas P. A rapid micro chromatin immunoprecipitation assay (microChIP). Nat Protoc. 2008; 3:1032-1045.

33. Strub T, Giuliano S, Ye T, Bonet C, Keime C, Kobi D, Le Gras S, Cormont M, Ballotti R, Bertolotto C and Davidson I. Essential role of microphthalmia transcription factor for DNA replication, mitosis and genomic stability in melanoma. Oncogene. 2011; 30:2319-2332.

34. Stewart SA, Dykxhoorn DM, Palliser D, Mizuno H, Yu EY, An DS, Sabatini DM, Chen IS, Hahn WC, Sharp PA, Weinberg RA and Novina CD. Lentivirus-delivered stable gene silencing by RNAi in primary cells. RNA. 2003; 9:493-501.

35. Saeboe-Larssen S, Fossberg E and Gaudernack G. mRNA-based electrotransfection of human dendritic cells and induction of cytotoxic T lymphocyte responses against the telomerase catalytic subunit (hTERT). J Immunol Methods. 2002; 259:191-203.

MITF depletion elevates expression levels of ERBB3 receptor and its cognate ligand NRG1-beta in melanoma

SUPPLEMENTARY METHODS

RNA interference

MITF-M3 siRNA molecule sequence: Sense (5′- GCA-GUA-CCU-UUC-UAC-CAC-U -3′) anti sense (5′- AGU-GGU-AGA-AAG-GUA-CUG-C- 3′)

MITF-M1 siRNA molecule sequence: Sense (5′- GGU-GAA-UCG-GAU-CAU-CAA-G -3′) anti sense (5′- CUU-GAU-GAU-CCG-AUU-CAC-C- 3′)

MITF-M2 siRNA molecule sequence: Sense (5′- AGC-AGU-ACC-UUU-CUA-CCA-C -3′) anti sense (5′- GUG-GUA-GAA-AGG-UAC-UGC-U- 3′)

ERBB3 siRNA molecule sequence: Sense (5′- UCG-UCA-UGU-UGA-ACU-AUA-A- 3′) anti sense (5′- UUA-UAG-UUC-AAC-AUG-ACG-A -3′)

SOX10 siRNA molecule sequence: Sense (5′- GGU-CAA-GAA-GGA-ACA-GCA-G -3′) anti sense (5′- CUG-CUG-UUC-CUU-CUU-GAC-C -3′)

FOXD3 siRNA molecule sequence: M-009152-03-0010, siGenome Human FOXD3 (27022) siRNA-SMARTpool.

Quantitative reverse transcriptase PCR primers

Primers against MITF-M forward (5′-CAT-TGT-TAT-GCT-GGA-AAT-GCT-AGA-3′) and reverse (5′-GC-TAA-AGT-GGT-AGA-AAG-GTA-CTG-C-3′), MITF forward (5′-TTT-TCC-CAC-AGA-GTC-TGA -AGC-3′) and reverse (5′-TGT-TAA-ATC-TTC-TTC-TTC-GTT-CAA-TC-3′), ERBB3 forward (5′-CTG-ATC-ACC-GGC-CTC-AAT-3′) and reverse (5′-GGA-AGA-CAT-TGA-GCT-TCT-CTG-G-3′), SOX10 forward (5′-GAC-CAG-TAC-CCG-CAC-CTG-3′) and reverse (5′-CGC-TTG-TCA-CTT-TCG-TTC-AG-3′), FOXD3 forward (5′-GAA-GCC-GCC-TTA-CTC-GTA-CA-3′) and reverse (5′-CGC-TCA-GGG-TCA-GCT-TCT-T-3′), NRG1 forward (5′-CCC-ATG-AAA-GTC-CAA-AAC-CA-3′) and reverse (5′-CCG-GTT-ATG-GTC-AGC-ACT-CT-3′) TATA-binding protein (TBP) with forward primer 5′-GCC-CGA-AAC-GCC-GAA-TAT-3′ and reverse primer (5′-CGT-GGC-TCT-CTT-ATC-CTC-ATG-A-3′) and the human acidic ribosomal phosphoprotein PO (RPLPO) with forward primer (5′-CGC-TGC-TGA-ACA-TGC-TCA-AC-3′) and reverse primer (5′-TCG-AAC-ACC-TGC-TGG-ATG-AC-3′)

Production of mRNA molecules

3′3xHA-tagged MITFvar4 or 3′3xHA-tagged MITFdnR215del (dominant negative) mRNA molecules were produced as described previously [35].

mRNA transfection

Cells were seeded in 6-well plates and grown to 60% confluence before being transfected and incubated for 24h with Lipofectamine 2000 (Invitrogen) combined with 3′3xHA-tagged MITFvar4 or 3′3xHA-tagged MITFdnR215del (dominant negative) mRNA molecules according to the manufactures instructions.

SUPPLEMENTARY FIGURES AND TABLE

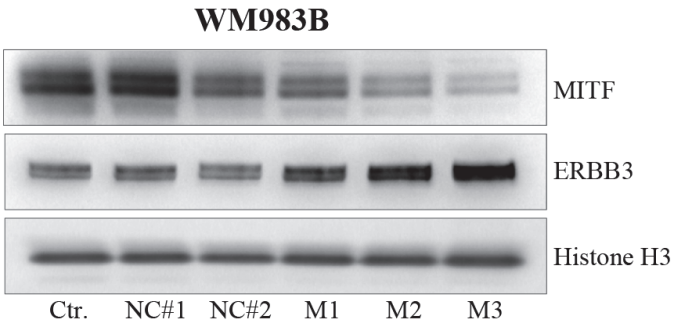

Supplementary Figure S1: Western blots showing the effect of negative siRNA controls and MITF siRNAs on MITF and ERBB3 in the WM983B cell line. Representative western blots showing negative siRNA control and MITF siRNAs effect on MITF and ERBB3 in WM983B after 72h. Two different negative siRNA control sequences (NC#1 and NC#2) and three different siRNA sequences against MITF were used (M1-M3). siRNA-induced depletion of MITF was performed in triplicate. Histone H3 was used as loading control.

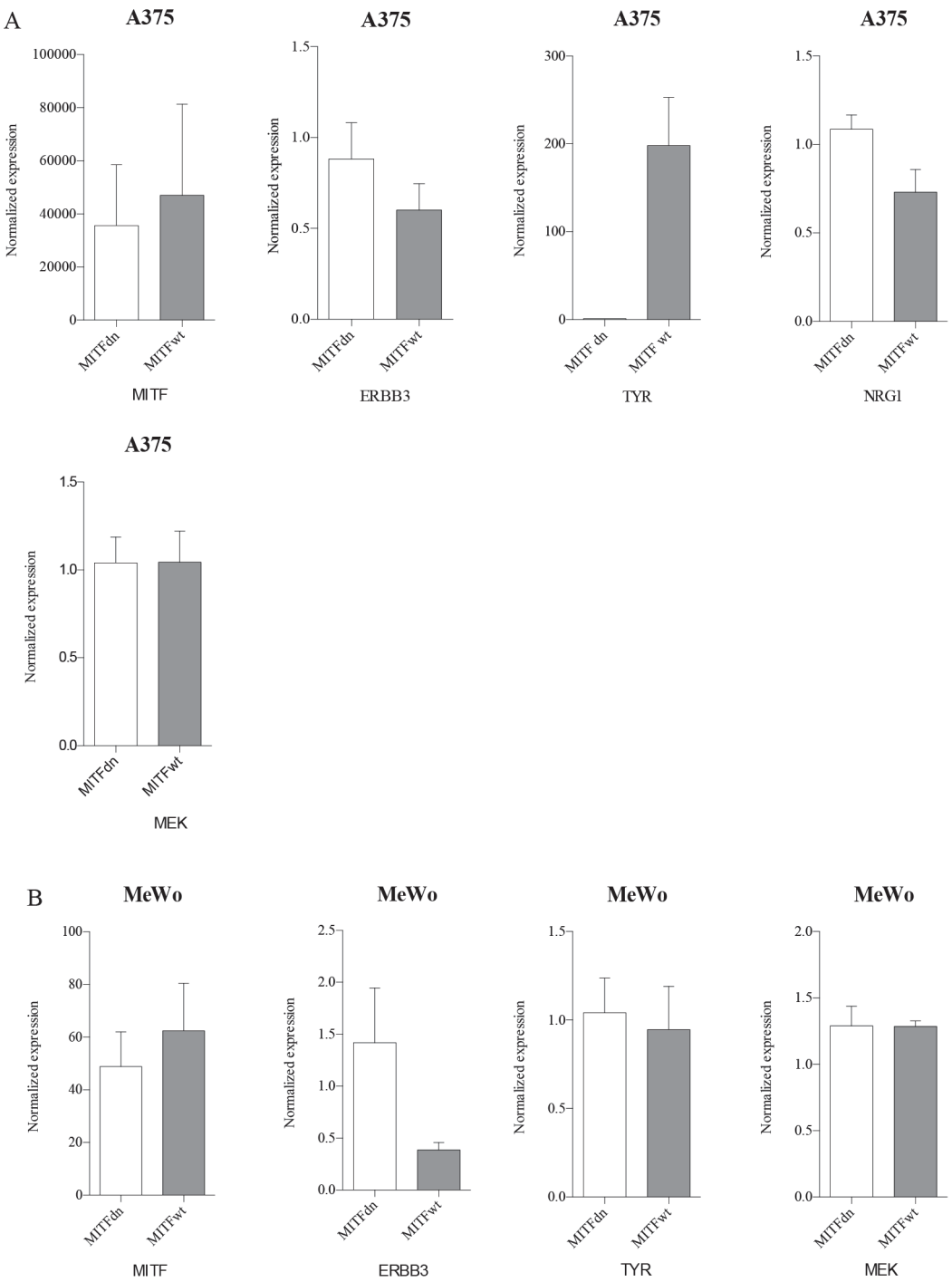

Supplementary Figure S2: MITF overexpression leads to reduction of ERBB3 mRNA levels in A375 and MeWo. HA-tagged MITF wild type (3xHA-tagged MITFvar4) and its nonfunctional control HA-tagged MITF dominant negative (3xHA-tagged MITFdnR215del) was overexpressed in A375 **A.** and MeWo cells **B.** by mRNA transfection. The expression of MITF, ERBB3, TYR and MEK were assessed by qRT-PCR 24hr post mRNA transfection in A375 (A) and MeWo (B) cells. In addition the expression of NRG1-beta was also assessed in A375. Bars represent mean ± SD of three separate experiments.

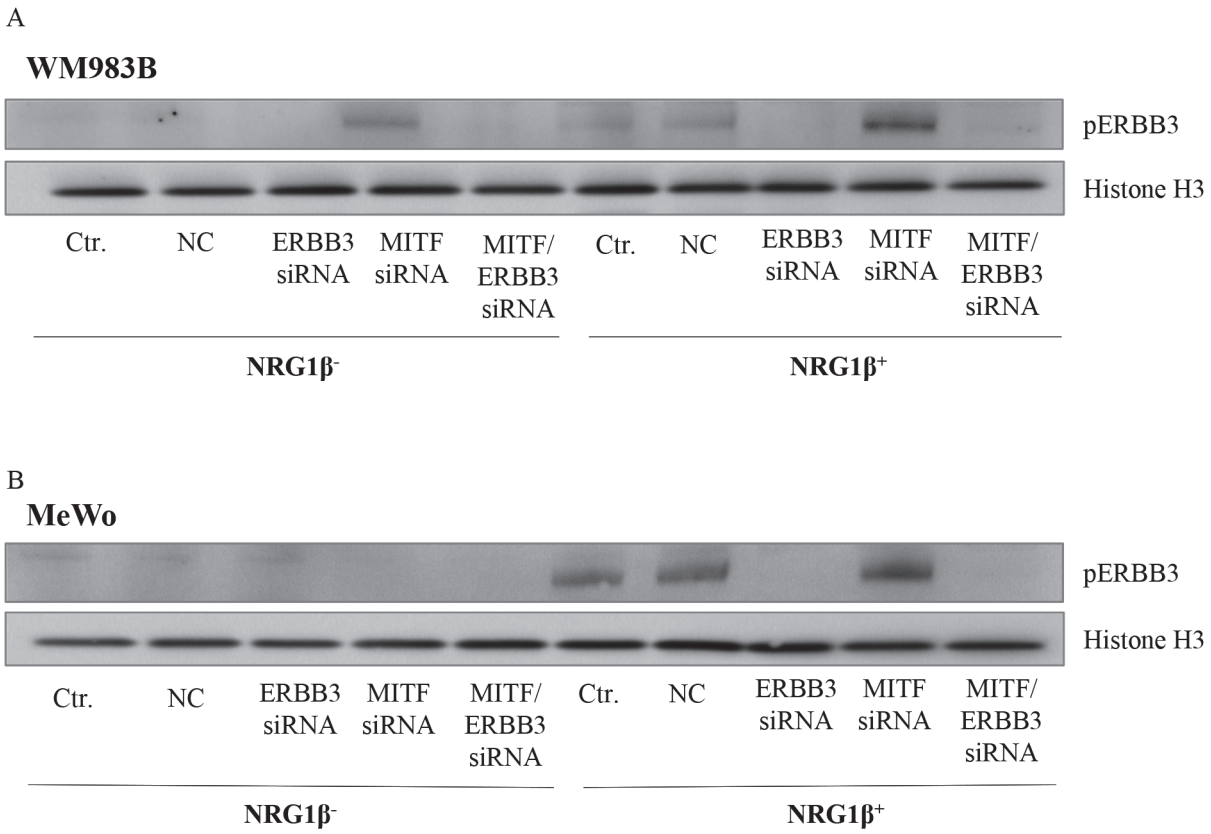

Supplementary Figure S3: The effect of NRG1-beta ligand upon pERBB3 levels. Representative western blots showing pERBB3 levels after various siRNA treatments against ERBB3, MITF, and the ERBB3/MITF combination, either without NRG1-beta ligand or with 10ng/ml NRG1-beta ligand for 15min prior to harvesting.

Supplementary Table S1: Characterization of the cell panel used in the study

Cell line	Stage	BRAF	H/N-RAS	NF1	MITF	ERBB3	SOX10	FOXD3
Hermes 4C	**Melanocyte**	WT	WT	WT	3	1	3	3
Hermes 3c	**Melanocyte**	WT	WT	WT	3	1	3	2
WM35	**Primary**	V600E het	WT	WT	3	2	3	1
WM793B	**Primary**	V600E het	WT	WT	0	2	3	1
WM115	**Primary**	V600E het	WT	WT	2	3	3	3
WM1341B	**Primary**	V600E het	WT	WT	3	2	3	1
WM1366	**Primary**	WT	61L	WT	0	0	0	1
WM983B	**Metastatic**	V600E het	WT	WT	2	3	3	3
WM45.1	**Metastatic**	V600E het	WT	WT	3	2	3	1
WM239	**Metastatic**	V600E het	WT	WT	2	2	2	3
WM266.4	**Metastatic**	V600E het	WT	WT	2	2	3	3
WM852	**Metastatic**	WT	61R	WT	0	0	0	1
WM1382	**Metastatic**	WT	WT	WT	2	2	3	3
LOXIMVI	**Metastatic**	V600D het	WT	WT	0	0	0	0
SKMEL28	**Metastatic**	V600E hom	WT	WT	3	2	3	2
MeWo	**Metastatic**	WT	WT	Q1336	2	2	3	1
A375	**Metastatic**	V600E hom	WT	WT	1	1	1	1
WM9	**Metastatic**	V600E het	WT	WT	0	2	3	2

The table shows cell lines used in the study and their respective disease stage, mutational status (BRAF, RAS, NF1) and relative amount of SOX10/MITF/FOXD3 and ERBB3 mRNA expression levels (3>2>1>0). Strongest inverse association between MITF and ERBB3 expression are marked with black boxes, while medium is marked with grey boxes

II

Dysregulation of MITF in the context of defective MC1R and RB1/p16/CDK4 leads to melanocyte transformation

Tine Norman Alver*[1], Timothy John Lavelle*[1], Karen-Marie Heintz[1], Patrik Wernhoff[1], Vegard Nygaard[1], Sigve Nakken[1,2], Geir Frode Øy[1], Sigurd Leinæs Bøe[3,#], Alfonso Urbanucci[1,#], Eivind Hovig[1,4,#]

1 Department of Tumor Biology, Institute for Cancer Research, Oslo University Hospital, Oslo, Norway.

2 Centre for Cancer Cell Reprogramming, Institute of Clinical Medicine, Faculty of Medicine, University of Oslo, Oslo, Norway.

3 Department of Medical Biochemistry, Oslo University Hospital, Radiumhospitalet, Oslo, Norway

4 Department of Informatics, University of Oslo, Oslo, Norway

* These authors contributed equally to this work

# These authors contributed equally to this work

Correspondence should be addressed to:

Dr Alfonso Urbanucci, PhD

Department of Tumor Biology

Institute for Cancer Research

Oslo University Hospital,

Postbox 4950 Nydalen, 0424 Oslo Norway

alfonsourbanucci@gmail.com

Prof. Eivind Hovig

Department of Tumor Biology

Institute for Cancer Research

Oslo University Hospital,

Postbox 4950 Nydalen, 0424 Oslo Norway

ehovig@ifi.uio.no

Dr Sigurd Leinæs Bøe, PhD

Department of Medical Biochemistry

Oslo University Hospital,

Radiumhospitalet, Nydalen, Box 4953, 0424 Oslo, Norway

sigurdbo@ous-hf.no

Key words: Melanoma, Melanocyte transformation, MITF, MC1R, AXL inhibitor, familial melanoma

Running title: MITF-M and MC1R are oncogenic switches for melanoma

Word count: 5643

Abstract

The MC1R/cAMP/MITF pathway is a key determinant for growth, differentiation, and survival of melanocytes and melanoma. Here we use two melanocyte lines to show that forced expression of HA-tagged MITF-M through lentiviral transduction represents an oncogenic insult leading to consistent cell transformation in the MC1R compound mutant and immortalized melanocyte cell line Hermes 4C, but not in the MC1R wild type cell line Hermes 3C. Transformed HA-tagged MITF-M transduced Hermes 4C form colonies in soft agar, grow tumors in mice, display increased MITF chromatin binding, and transcriptional reprogramming. Consistent with an invasive melanoma phenotype, gene expression analyses show increased transcription of epithelial-mesenchymal transition genes and repression of key melanocyte-specific genes in the transformed cells. Mechanistically, forced expression of MITF-M drives the upregulation of AXL, with concomitant downregulation of PTEN, which leads to increased activation of the MAPK and PI3K pathways. Interestingly, treatment with AXL inhibitors reduces growth of the transformed cells by reverting AKT activation. Notably, immortalization of the Hermes melanocytes recapitulates the most common features of heritable melanoma, by an introduced aberration in the RB1/p16/CDK4 pathway and an hTERT alteration. An analysis of the TCGA melanoma cohort revealed high prevalence of MC1R loss of function, which points to the clinical relevance of this melanogenesis model.

In conclusion, here we show that in the context of inactivation of MC1R, and independent of sun exposure, MITF-M dysregulation can lead to melanoma development. The model presented provides a basis for further study of critical changes in the melanocyte transformation process.

Introduction

Cutaneous melanoma (CM) arises from melanocytes, and is the most aggressive form of skin cancer (1). Only 1% of all skin cancers are melanomas, but they are responsible for more than 75% of all skin cancer-related deaths (1). Surgery and chemoprevention have been persistent treatment options, until the more recent additions of BRAF and MEK inhibitors, followed by emerging immunotherapy options. However, no effective cure is yet available for highly metastatic melanoma (2).

The cyclin-dependent kinase inhibitor 2A (*CDKN2A*) gene was identified as the first melanoma susceptibility gene more than 20 years ago, and continues to be the main high-risk gene for familial melanoma (3). CDKN2A encodes two transcripts with alternative transcriptional start sites, *i.e.* p16INK4a and p14ARF (4). The p16-retinoblastoma (Rb) pathway controls cell-cycle G1-phase exit, while the p14ARF-p53 pathway promotes cell cycle arrest and apoptosis. In addition to being mutated in familial melanoma, p16INK4a forms a functional protein complex with CDK4, and cyclin D1, leading to phosphorylation of the RB1 protein, with subsequent impact on the G1-S control of the cell cycle. This signaling is altered in 90-100% of melanomas (5, 6) through alterations in these proteins, and germline *CDKN2A* mutations have been found in up to 20-40% of the melanoma-prone families worldwide.

In case-control studies, the melanocortin-1 receptor (*MC1R*) has been found to be a low-risk melanoma susceptibility gene (7, 8), and *MC1R* variants have been shown to increase the melanoma frequency in families possessing *CDKN2A* mutations (9). Recently, it has been proposed that a malignant transformation of melanocytes expressing CDKN2A mutation and MC1R loss-of-function allele(s) requires acquisition

of somatic mutations, facilitated by the MC1R genotype or aberrant microenvironment due to CDKN2A (10). The *MC1R* gene locus is highly polymorphic in populations of European ancestry, and more than 200 coding region variants have been identified to date, with a combined prevalence of any *MC1R* variant being present in ~60% of healthy controls. Among these variants are the red hair color (RHC) variants associated with red hair, light skin, poor tanning ability, and heavy freckling (11). Carriers of any MC1R variant have been shown to have a 66% higher risk of developing melanomas compared to wild-type subjects (12). The relative melanoma impact of RHC- or non-RHC variants is still being debated, as population-specific allele frequencies exist, and with differing disease consequences (12-14). Individuals of European ancestry have a higher incidence rate for CM than non-Europeans, which is attributed to their fair skin type. The degree of UV-protection in the skin is defined by the amount and type of pigment mediated from the melanocortin-1 receptor (MC1R). UVB exposure triggers the PTEN protein interaction with wild-type, but not RHC-associated, MC1R variants, protecting PTEN from degradation, and leads to AKT inactivation (15). Functionally, the MC1R pathway normally leads to pigmentation of melanocytes through increased cytosolic cAMP, which activates the Microphthalmia-associated Transcription Factor (MITF). Therefore, RHC variant carriers exhibit reduced cAMP production, resulting in reduced eumelanin production with consequently decreased photoprotection (16). Solar ultraviolet (UV) radiation exposure is deemed a common risk factor for the initiation of CM, through induction of cyclobutane pyrimidine dimers (CPDs) and pyrimidine (6-4) pyrimidone photoproducts (6-4PP) in DNA, leading to somatic mutations impacting cellular function (17). However, evidence exists that melanoma also occurs in non-sun

exposed skin (18-20), and this argues for additional factors contributing to the development of melanoma.

In recent years, significant progress has been made in the understanding of the genetic basis of both sporadic and familial melanoma. New melanoma susceptibility pathways have emerged (21), and a gain-of-function mutation detected in the microphthalmia-associated transcription factor isoform 4, or MITF-M (hereby referred to as MITF), p.E318K, has been associated with both familiar and sporadic melanoma susceptibility (22). Carriers of this variant are associated with high nevi counts and a 3 to 4-fold increased risk for melanoma incidence. The MC1R/cAMP/MITF pathway is implicated in growth, differentiation and survival of melanocytes, as well as in malignant melanoma (23, 24). MITF is essential for melanocyte development, function and survival. However, MITF has also been shown to possess oncogenic potential in immortalized melanocytes having BRAFV600E activating mutation (25). Besides MITF, it has currently also become evident that several high penetrance genes involved in telomere lengthening (*TERT*) or telomere maintenance play a role in familial melanoma predisposition (26), as well as other genes, such as *BAP1*, *POT1*, *ACD*, and *TERF2IP* (27).

Here we report the use of the immortalized melanocyte cell lines Hermes 3C and 4C to establish a model for studying the mechanisms underlying the non-UV related mechanisms of melanoma initiation and progression in the context of familial melanoma. The Hermes 4C line recapitulates essential features of the most frequent familial high melanoma risk factors in being RHC, as a compound heterozygote MC1R, R160W/D294N, which results in inactivation of the MC1R protein, combined with

having a loss of CDKN2A function and being TERT-expressing. Hermes 3C is WT for MC1R, but otherwise carries the same alterations as Hermes 4C. Here we show that forced expression of human influenza hemagglutinin (HA)-tagged MITF leads to oncogenic transformation of Hermes 4C but not Hermes 3C. The transformation of Hermes 4C is characterized by an epithelial-mesenchymal transition (EMT)-like phenotype, reduced PTEN expression, and hyperactivation of pAKT via the receptor tyrosine kinase (RTK) AXL. The transformed cells acquire an invasive-like cell state with a transcriptional profile resembling those of established melanoma cell lines models and patient biopsies, which, importantly, respond to AXL inhibitors.

Results

MITF dysregulation induces transformation in an MC1R-mutated genetic background

Gray-Schopfer *et al.* developed immortalized melanocyte cell lines for both wild type and RHC MC1R alleles (R160W/D294N), called the Hermes 3 series and the Hermes 4 series, respectively (28). We selected the cell lines immortalized via ectopic expression of hTERT and inactivation of the RB1/p16/CDK4 complex through transduction of HPV16-E7. The lines Hermes 3C, and Hermes 4C, have been shown to display diploid chromosomes, melanocytic growth requirements and normal morphologies, thus broadly retaining the *in vitro* culture features of normal melanocytes.

In order to investigate the role of MITF on the enhanced risk of developing melanoma in varying RHC background, HA-tagged MITF was introduced in both the wild type MC1R Hermes 3C and in the compound mutant MC1R R160W/D294 Hermes 4C melanocytes. The resulting cells are hereafter referred as 3C-HA-MITF and 4C-HA-MITF, respectively. To confirm successful transduction, we measured exogenous and endogenous MITF levels by both western blotting and RT-PCR (Fig. 1A and B). Surprisingly, we found that endogenous MITF was downregulated to undetectable levels examining both RNA and protein in 4C-HA-MITF, and to a lesser degree in 3C-HA-MITF, when compared to their respective control transduced lines, hereafter referred as 3C and 4C (see methods). We also found that SOX10, a transcriptional activator of MITF transcription and a major cofactor of MITF in the pigmentation process was concomitantly suppressed in 4C-HA-MITF (Fig. 1A and B).

Both SOX10 and MITF are important factors of melanocyte biology, including mediating pigmentation of melanocytes (29). On harvesting the cells, we observed a loss of pigmentation in the transduced HA-MITF cells, which was more marked in 4C-HA-MITF pellets (Fig. 1C), compared to 3C-HA-MITF. To investigate the cause of the pigment loss, we examined whether the inserted HA-tagged MITF protein was functionally active. We were able to detect activation of the tyrosinase promoter (an acknowledged MITF target) in 3C-HA-MITF, but not in 4C-HA-MITF (Supplementary Fig. 1A), by RT-PCR. We also verified the functionality of the HA-MITF protein by transducing an established osteosarcoma cell line, U2OS, known to be available for MITF-induced tyrosinase activation (30). Transduction of U2OS cells with HA-MITF did indeed induce expression of tyrosinase transcripts, while transduction of the empty control (IRES) did not (Supplementary Fig. 1B and C).

Importantly, after lentiviral transduction of HA-tagged MITF, we also observed a transformed morphology in 4C-HA-MITF, which we did not observe in 3C-HA-MITF cells (Fig. 1D), in terms of loss of dendricity, flattening and more spread morphology, and greater clustering of cell distribution. To validate that Hermes 4C cells were indeed transformed after HA-MITF transduction, we subjected the Hermes lines and derivatives to a growth factor independence assay. Only 4C-HA-MITF cells were able to form colonies under these conditions (Fig. 1E). Similarly, only these cells displayed anchorage-independence in a growth assay on soft agarose (Fig. 1F). Growth and cell proliferation assays confirmed that HA-MITF transduction enhanced proliferation and viability of 4C, but not 3C, in the presence and absence of cholera toxin (Supplementary Fig. 1D-H). The transformation was reproduced four out of four times at similar frequencies (data not shown).

In order to examine the possibility that the transformation could be due to other mutations possibly incurred through the experimental procedures, we assayed for BRAF mutations and performed whole exome sequencing in both HA-MITF transduced cells and non-transduced parental cell lines. We could not identify any alterations in the transduced cell lines, when compared to their respective controls. A list of identified somatic variants, and status of *CDK4*, *CDKN2A*, *MITF* and *MC1R*, in all cell lines is reported in Supplementary Table 1. Next, to verify the tumorigenic potential, we xenografted Hermes 4C (parental), 4C (control transduced), and the derivative 4C-HA-MITF cells into NOD scid gamma (NSG) mice. All the mice injected with 4C-HA-MITF cells developed tumors (n=10; Fig. 1G), while mice injected with the other cells did not. The tumors were passaged to new mice to investigate whether it could be considered a stable line that would continue to grow. We indeed found that palpable tumors re-formed in shorter time spans after passaging than in the initial engraftment (Fig. 1H-I). We then investigated and confirmed the levels of HA-MITF in the tumor xenografts by Western blotting and RT-PCR to ensure that the tumors were the result of outgrowth of 4C-HA-MITF transformed cells (Supplementary Fig. 1I-M). Taken together, these data suggest that forced expression of HA-MITF in the context of RHC MC1R, appears to be an oncogenic insult inducing melanomagenesis.

Dysregulation of MITF alters the melanocytic transcriptional program

In order to identify direct targets of MITF, we performed RNA-seq of the parental Hermes 3C and Hermes 4C cells following MITF knock down (KD) using siRNA against MITF. Analysis of significantly ($p<0.05$ and $|\log2 \text{ fold change}| > 1$) differentially expressed genes (DEGs) returned a highly co-expressed (>50%) set of 235 putative

direct gene targets of MITF in the Hermes 3C line, and a set of 543 in the Hermes 4C line (Fig. 2A and Supplementary Table 2), of which 129 were overlapping, indicating that dysregulation of MITF transcriptionally affects the Hermes 4C more than the Hermes 3C cells. Of the 235 genes affected in Hermes 3C, 91 genes were downregulated, and melanosome and pigmentation regulation were the most significantly enriched functional associations of these genes (Fig 2A and Supplementary Fig. 2A). The 144 upregulated genes upon MITF KD in Hermes 3C were ontology-enriched for terms associated to both response to interferon signaling, to angiogenesis, and development of neural and other adult tissue (Fig 2A and Supplementary Fig. 2B). Similar ontologies were also enriched within the 270 genes upregulated upon KD of MITF in Hermes 4C cells (Fig. 2A and Supplementary Fig. 2C). In Hermes 4C cells, MITF downregulation induced downregulation of 273 genes with functions related to metabolic processes implicated in pigmentation, but also to protein modifications such as O-linked glycosylation and phosphorylation (Fig. 2A and Supplementary Fig. 2D). Other genes encoding proteins within the PI3K-AKT pathway and the canonical MYC pathway were also downregulated by MITF KD in the Hermes 4C cells. Interestingly, the PI3K-AKT pathway, which is commonly activated in many cancers, including melanoma (31), seems to be under MITF regulation in Hermes 4C with the MC1R inactive variant background. Moreover, in Hermes 4C, MITF in seems to selectively maintain the expression of genes deputed to epithelial differentiation, proliferation and migration (Fig. 2A and Supplementary Fig. 2E).

Overall, these data suggest that MITF directs the expression of different target genes in the MC1R variant-bearing cell line Hermes 4C, compared to the MC1R WT cell line Hermes 3C.

We then compared array-based gene expression data of 3C-HA-MITF and the transformed 4C-HA-MITF to their control-transduced counterparts 3C and 4C (Supplementary Table 3). In agreement with our results on MITF KD in parental Hermes cells, 4C cells were most affected by the transduction of HA-MITF (Fig. 2B). About four times more genes were significantly differentially expressed in 4C-HA-MITF than in 3C-HA-MITF, compared to their control-transduced counterparts. The genes scored as downregulated in 4C-HA-MITF cells were associated to melanosome formation and pigmentation, reflecting a progressive loss of cell identity and differentiation (Fig. 2B) and indicating a loss of MITF canonical function in these cells. Upregulated genes in 4C-HA-MITF mostly reflected an increased metabolic activity and responses to external signaling, such as response to cytokines and cell adhesion. GSEA retrieved gene sets such as that downregulated in the NCI60 panel in association with p53 mutation (P53_DN.V1_DN [192] ($p= 6.05\ e^{-37}$), and the gene set up-regulated in fibroblasts after KD of RB1 (CHICAS_RB1_TARGETS_CONFLUENT [567] ($p=1.89\ e^{-51}$)), respectively, suggesting a possible implication of p53 function, and pRB in the process of transformation of 4C-HA-MITF. Interestingly, we could not observe a marked ($\log10\ (p) < -5.0 = p<0.00001$) enrichment of biological processes among downregulated genes in 3C-HA-MITF vs 3C-control, while upregulated genes showed enrichment for unfolded protein response and ER stress-related genes (Fig. 2B), suggesting that 3C cells may use these pathways to avoid transformation (32).

Next, to restrict the search for important MITF target genes mediating 4C-HA-MITF transformation, we focused on genes exclusively upregulated in 4C-HA-MITF versus 4C that were not upregulated in 4C versus 3C, nor in 3C-HA-MITF versus 3C (Fig. 2C). We shortlisted 205 highly upregulated genes in 4C-HA-MITF (Supplementary Table 3). Interestingly, some of the 205 genes were among the top-listed MITF siRNA-treated

direct target genes, including *GREM1*, *SPOCK1*, *TGFBI*, *AXL*, *EGFR* and *IL6* (Fig. 2C).

GSEA of the 205 genes revealed a marked enrichment (17.5%; p=3.57 e^{-46}) of genes encoding proteins implicated in epithelial to mesenchymal transition (EMT; Fig. 2D and Supplementary Table 3). Among them e.g. *GREM1*, *SPOCK1*, *TGFBI*, *AXL*, and *IL6* have all been associated with EMT (33-37). Therefore, we took an unbiased approach to define whether the EMT was the process that led to the transformation of 4C-HA-MITF.

First, we used a set of 200 genes defining EMT from GSEA (gene set: HALLMARK_EPITHELIAL_MESENCHYMAL_TRANSITION [200]) for cluster analysis of the control 3C and 4C cell lines and their transduced derivatives (Supplementary Fig. 2F). 4C-HA-MITF clustered separately from the other cell lines. A core set of 35 genes (out of the 200 genes contained in the Hallmark EMT GSEA signature) was consistently upregulated exclusively in these 4C-HA-MITF cells (Fig. 2E), suggesting that EMT is a result of the HA-MITF transduction leading to 4C transformation. In order to examine whether tumor samples could be clustered with this EMT-related gene signature, we reanalyzed the melanoma TCGA data. This analysis recapitulated previous findings from Verfaillie et al. (38), displaying a distinct separation of invasive and proliferative tumor phenotypes characterized by EMT, based on expression profile (38). One of the major determinants of the invasive subgroup was indeed the mesenchymal signature. According to the definition of the invasive phenotype by Verfaille (38), the 4C-HA-MITF is a cell line resembling an invasive tumor (Supplementary Fig. 2G).

Taken together these data suggest that HA- MITF in the context of MC1R inactivation induces upregulation of direct MITF targets of EMT-related genes, in this way inducing oncogenic transformation with subsequent acquisition of invasive properties.

MITF binding to the chromatin in melanocytes carrying MC1R-inactivating variants is increased compared to wild-type MC1R carrying melanocytic cells

Given the transformation of 4C cells when transduced with HA-MITF, we hypothesized that differential binding to chromatin might be a factor in the transformation process. To this end, we performed a chromatin immunoprecipitation followed by sequencing analysis (ChIP-seq). The reason for utilizing an HA-tag in our construct was that high-quality antibodies specific for the MITF-M protein isoform are still lacking. We therefore utilized the HA-tag to ensure antibody-specificity to the MITF-M isoform.

We performed two biological ChIP-seq experiments in each cell line, and identified 42075 high confidence (common to both experiments) MITF-M binding sites (MITFBSs) in 3C-HA-MITF cells, and almost twice as many (80215 high confidence sites) in 4C-HA-MITF cells. The MITFBSs overlapped to a significant extent between the two cell lines, as approximately 70% of the MITFBSs in 3C-HA-MITF were also found in 4C-HA-MITF (Fig. 3A), and therefore we defined them as consensus MITFBSs, as opposed to the union of all MITFBSs found in the two cell lines, which we called compendium MITFBs.

To evaluate the quality of the MITFBSs observed in the Hermes cell lines, we compared our MITF-M ChIP-seq data with data from previously published data (39) (Fig. 3A). Common MITFBSs found in both Hermes cell lines overlapped 40-60 % with

these datasets. We further noted that less than 30% of the MITF bindings sites found in the three melanoma cell lines COLO829 (40), MM031, and MM011 (38), for which public data on MITF Chip-seq were available, overlapped. Around 50% of the MITFBSs have been reported to locate in a 10Kb segment around the transcription start sites (TSSs) in the melanoma cell line 501Mel (41), while more distant MITF bound enhancers, such as one -67Kb away from the MET gene, have also been shown to be clinically relevant (40). In line with previously published results on melanoma cell lines and melanocytes (38, 40, 42), we found that MITFBSs present in both Hermes cell lines were more frequent in promoter-proximal regions (+- 1Kb from TSSs), as well as in intronic and intergenic regions (Fig. 3B). 70% of the genes modulated by transduction of HA-MITF in Hermes cells had at least one MITFBs within 25kb upstream and downstream of the gene (Supplementary Table 2). The binding of HA-MITF was nevertheless enhanced in 4C-HA-MITF cells, with multiple MITFBSs in proximity of several of these genes (e.g. *AXL, IL6, TGFBI*, and *EGFR*,) compared to HA-MITF binding in 3C-HA-MITF (Supplementary Fig 3A-D). Based on this, we proceeded to validate the expression changes for *AXL*, *IL6*, *TGFBI*, *SPOCK1*, and *GREM1* in the Hermes cell lines, via RT-PCR (Fig 3C). We further found that HA-MITF was bound to the promoter regions of both the *MITF* and *SOX10* genes in both cell lines (Supplementary Fig. 3E-F), and we verified MITF binding by use of ChIP-qPCR (Supplementary Fig. 3G). The data suggest that these loci are under complex regulation by MITF in both cell lines, and support the recent findings that both *MITF* and *SOX10* are transcriptionally regulated by MITF-M (43). An enrichment analysis of binding of MITF of the ChIP-seq reads around the MITF consensus motifs indicated enhanced binding of MITF in 4C (Fig. 3D) and compendium (Supplementary Fig. 3H) MITFBSs in Hermes cells.

MITF binding is associated with open chromatin

Next, to examine whether MITFBSs could be associated with chromatin structure as mapped in a melanoma setting, we compiled high-confidence maps (see Methods) of open genomic regions enriched for H3K27Ac and H3K27me3 marks, indicating active or repressed chromatin, respectively, from twelve melanoma cell lines taken from published studies (38), and performed the same enrichment analysis of MITF ChIP-seq reads in 3C- and 4C-HA-MITF cells. We found that MITF chromatin binding in 4C-HA-MITF is enhanced preferentially in open regions associated with active transcription, as marked with H3K27Ac (Fig. 3E and Supplementary Fig. 3I-J), and as opposed to regions marked with the repressive mark H3K27me3 (Supplementary Fig. 3K). We also compiled high-confidence MITFBSs maps from the three melanoma cell lines COLO829, MM011, and MM031, having constitutively active expression of BRAFV600E (38, 40). Enrichment analysis of MITF ChIP-seq reads on these mapped sites revealed an increased frequency of MITF binding in 4C-HA-MITF cells (Fig. 3F and Supplementary Fig. 3L).

A motif-enrichment analysis was undertaken for both 3C and 4C -HA-MITF cells consensus MITFBSs (Supplementary Fig. 3M-N). The main 3C-HA-MITF-binding patterns related to the E-box-binding patterns (44), while the 4C-HA-binding patterns related to AP-1 transcription factors, including FRA1 (FOSL1), FOSL2, and JUN-AP1. In a *de novo* motif discovery analysis looking for motifs of length between 6bp and 18bp, we again found that in 3C-HA-MITF cells, the E-box motifs were the top enriched motifs (Fig. 3G). In 4C-HA-MITF, other binding motifs were more prominent, notably factors previously reported to be involved in phenotype switching to an invasive

phenotype having low MITF expression, such as FRA1 (FOSL1), TEAD, NFKB1 (Fig. 3H) (38, 45). Taken together, these results indicate that transformed melanocytes with MC1R-loss of function variants display an enhanced MITF-binding to the chromatin compared to MC1R WT-carrying melanocytic cells. However, these results do not delineate the sequence of events controlling the observed transformation.

MITF-dependent dysregulation of AXL contributes to altered proliferation of 4C-HA-MITF cells

We sought to examine how MITF dysregulation could impact the increased proliferative potential of the 4C-HA-MITF cells. AXL was one of the top upregulated genes in 4C-HA-MITF cells (Fig. 2C and Fig. 3C). Previous studies have implicated the activation of the AKT pathway by AXL in melanoma (46). We first confirmed selective AXL upregulation in the transformed 4C-HA-MITF cells at the protein level (Fig. 4A). AXL was also upregulated in 4C-HA-MITF xenografts at the mRNA level (Fig. 4B) and protein level (Supplementary Fig. 1I). We hypothesized that AXL upregulation would result in AKT activation also in our melanoma transformation model. By Western-blot analysis, we confirmed that under cholera toxin-starved conditions, 4C cells, and to a greater extent 4C-HA-MITF cells, displayed higher basal levels of pERK and pAKT, compared to the 3C and 3C-HA-MITF cell lines (Fig. 4C)), which could be seen also in the xenografted 4C-HA-MITF (Supplementary Fig. 1I). The expression data also revealed that PTEN, a known suppressor of the PI3K/AKT pathway, showed lower expression in 4C-HA-MITF compared to 4C (Supplementary Table 2). Accordingly, we found that PTEN was significantly downregulated in 4C-HA-MITF compared to 4C at the protein (Fig. 4C) and mRNA level (Fig. 4D), while this was not the case in 3C-HA-MITF versus 3C cells. To examine whether PTEN downregulation could directly

increase pAKT, we depleted PTEN by siRNA transfection in the 4C cell lines. As expected, 4C and 4C-HA-MITF responded with an increase in pAKT phosphorylation upon PTEN depletion, demonstrating a repressive effect of PTEN upon PI3K signaling (Fig. 4E).

Next, we targeted AXL by an AXL siRNA and an AXL inhibitor (R428) to assess whether this could counter the increased proliferation observed in 4C-HA-MITF cells. Depletion of AXL by the siRNA and inhibitor abolished the phosphorylation of AKT, while only the siRNA reduced the AXL level (Fig. 4F). Surprisingly, the inhibitor seemed to increase the expression of AXL. AXL inhibition alone led to the greatest reduction of cell proliferation and viability (Fig. 4G-H). To explore whether the decrease in cell proliferation and viability was due to pAKT reduction itself or other possible effects of the AXL inhibitor, we used an AKT inhibitor (MK-2206) and a MEK inhibitor (Trametinib) (Fig. 4I and 4G, respectively), which proved highly effective in inhibiting AKT-induced growth and survival of 4C-HA-MITF cells (Fig. 4G-H). We found that inhibiting the MAPK pathway using Trametinib was less effective than targeting the PI3K-AKT pathway using the AKT inhibitor MK-2206. Together, these findings suggest that 4C-HA-MITF transformation is highly dependent on transcriptional upregulation of AXL by HA-MITF, and that this leads to activation of the PI3K-AKT pathway.

MC1R inactivation is a feature of melanoma

MITF is amplified in around 20% of melanoma tumors, and this is thought to contribute to tumor progression (47). It is also known that the variants of MC1R that inactivate or reduce the function of the receptor have been linked to an increased risk of developing melanoma, especially under sun exposure (11). We therefore examined The Cancer Genome Atlas (TCGA), containing a panel of 470 melanoma cases, for expression status of MITF (Supplementary Fig. 4A), and 10-15% of the tumors had relatively high expression of MITF (Z-score > 1). We found no correlation between MITF and MC1R expression status. However, more than 60% of the samples presented with inactivating variants of MC1R (Fig. 4J), and this percentage was similar in highly expressing MITF tumors. Regardless of the lack of correlation between MITF expression and MC1R status, MC1R inactivation appears to be a crucial feature of the majority of malignant melanomas. The frequency of occurrence of point mutations in the *MC1R* gene was in the range of 39% in this dataset, with samples having an MC1R variant with one mutation, while 28% had variants of MC1R with two to four mutations (Fig. 4J and Supplementary Table 4). The most frequent mutations in the MC1R gene reflected variants associated prevalently with risk of melanoma, photoaging, and with phenotypes such as red hair and light skin (RHC phenotype) (Fig. 4K). This frequent MC1R inactivation as a feature of melanoma is compatible with MITF-M dysregulation in the context of defective MC1R with subsequent resultant melanomagenesis.

Discussion

The mechanisms behind oncogenesis in melanoma are currently not well understood, as the availability of relevant experimental models is limited. We present here a melanomagenesis model based upon melanocyte cells that recapitulate features of heritable melanoma to study the association between MC1R and oncogenesis. In our model, we find that the lineage-specific master regulator of melanocyte development and survival, MITF, acts as an oncogene when transduced in the form of HA-MITF in an hTERT/RB1/CDK4/p16/MC1R RHC background. Transformation of melanocytes was first described by Garraway and colleagues as an event that required dual transduction of BRAFV600E and HA-MITF in an hTERT/p53DD/CDK4(R24C) background (47). Later, it has been suggested that BRAFV600E-transduction alone is sufficient for transformation of hTERT/p53DD/CDK4(R24C) human melanocytes depleted for MC1R, in that MC1R WT protects PTEN protein against degradation after UVB-exposure (15). Loss of this function in the form of MC1R RHC, followed by degradation of PTEN, is associated with enhanced PI3K/AKT pathway signaling (15). Epigenetic, mutational and deletion events are believed to account for PTEN dysregulation in as many as 40-50% of sporadic melanomas (48). Interestingly, the PI3K/AKT pathway has been found to disrupt BRAFV600E-induced senescence (15) , which further emphasizes an oncogenic role of this signaling pathway within melanoma initiation and development.

In the model presented here, HA-MITF transduction alone is sufficient to induce transformation of 4C cells. The transformed melanocytes (MC1R RHC) display increased MITF-binding to the chromatin compared to MC1R WT-carrying melanocytic cells. Moreover, MITF-binding reflects aberrant chromatin structure observed in

melanoma (38). Interestingly, the binding distribution of MITF coincides with DNA motifs of TFs involved in melanoma development such as SOX10, MITF, AP-1, TEAD and others. In agreement with Verfaillie et al. and others (38, 49), we also observe a concomitant transcriptional reprogramming with subsequent acquisition of invasive properties after the loss of endogenous transcription factors SOX10/MITF and gain of FOS/FOSL (members of AP-1). The role of HA-MITF behind the transformation process needs further clarification. However, in agreement with previous reports (50), our study suggests a negative feedback loop controlling transcriptionally the expression of both SOX10 and MITF. The transition from a proliferative towards an invasive phenotype was further characterized by upregulation of relevant EMT genes such as AXL. We identified PTEN downregulation and up-regulation of AXL receptor and its cognate ligand GAS6, all modulators of the PI3K/AKT signaling pathway (51). Consistently, we find activation of AKT, and ERK, to a lesser extent. Moreover, growth and proliferation of the transformed cells is effectively disrupted by the use of AKT or AXL inhibitors, supporting the hypothesis that PI3K/AKT signaling pathway is the main driver of proliferation.

In conclusion, we propose a model of melanomagenesis based upon the innate oncogenic properties of MC1R RHC, representing enhanced risk for PI3K/AKT pathway activation and oncogenic transformation in families possessing CDKN2A loss of function. Our study opens the path for further investigations on the potential oncogenic role of MITF-M as a molecular switch in MC1R RHC backgrounds.

Methods

Cell lines and culture conditions

The immortalized melanocyte cell lines Hermes 3C and 4C were purchased from Wellcome Trust Functional Genomics Cell Bank. All Hermes lines and their derivatives were cultured as described previously (39) with the following modifications: RPMI was replaced by M254 medium (Cascade Biologics) and cells were incubated in 5% CO_2. Sk-Mel-28 was purchased from ATCC and grown in RPMI (Sigma Aldrich) with 8% FBS (PAA), 5% CO_2, at 37°C. U2OS cells were obtained from ATCC and grown in RPMI (Sigma Aldrich) with 8% FBS (PAA), 5% CO2, at 37°C. Further details about clonings, constructs, and lentiviral production, culture conditions, growth factor and anchorage independence assays, as well as siRNA experiments, isolation of RNA, and establishment of tumor xenografts are provided in Supplementary methods.

Generation of Amino terminal 3xHA tagged MITF Hermes melanocytes

Hermes 3C and Hermes 4C melanocytes were subjected to lenti-particle transduction of pLX 3xHAvar4mCh (vector expressing 3xHA tagged MITF-M (variant 4)) or control vector pLVX IRES mCh at a MOI of < 1. After 5 passages the cells were sorted for the expression of bicistronic mCherry and allowed to expand further. Stable cell lines were subsequently re-sorted based on the presence of mCherry and used further. Cell sorting was performed by flow cytometry at the Oslo University Hospital Core Facility. This process resulted in four cells lines which we called 3C and 4C, for control vector transduced cells, and 3C-HA-MITF and 4C-HA-MITF, for cells transduced with the vector expressing 3xHA tagged MITF-M.

Western Blot analysis

Western Blot analysis was performed as previously described (39). The following antibodies were purchased from Cell Signaling Technology (Danvers, MA, USA); MITF (1:1000; #12590), SOX10 (1:1000; #14374, Phospho-Akt-Serine-473 XP (1:2000; #4060), Phospho-ERK –Thr202/Tyr204) XP (1:3000; #4370), PTEN XP (1:1000; #9188) and Histone H3 (1:3000; #4499) was used as loading control.), anti-HA-tag (12CA5) was purchased from Roche. Secondary antibody against rabbit (1:5000; P0448) was purchased from Dako (Agilent Technologies, Glostrup, Denmark).

Establishment of xenografts

Animal experiments were approved and performed as stated by the Norwegian Animal Authority (Permit number 12080), and conducted according to the regulations of the Federation of European Laboratory Animal Science. NSG mice were anesthetized with 3% Sevoflurane (Baxter) and subcutaneously injected on both flanks with 5 million of Hermes 4c (parental), Hermes 4c transduced with pLVXIRESmCh (vector control transduced 4C cells) and Hermes 4c cells transduced with pLX3xHAvar4mCh vector (4C-HA-MITF) in 200µl RPMI1640. Tumor volume and body weight was registered once a week. More details are provided in the Supplementary Methods.

Chromatin immunoprecipitation

3C-HA-MITF and 4C-HA-MITF were used for the Chromatin immuno-precipitation with sequencing (ChIP-seq) experiments in two replicates, essentially as described in (39) using anti-HA-tag (12CA5) for immuno-precipitation of HA-tagged MITF.

Quantitative reverse transcriptase and ChIP -PCR

Quantitative real time and ChIP PCR were performed as previously described (39). Primers used for ChIP-PCR (proximal to *MITF*, *SOX10*, *TGFBI*, *AXL*, *IL6*, *EGFR*, *PRM1* genes) and primers used for Real-time (*MITF-M*, *SOX10*, *TBP*, *RPLP0*, *AXL*, *SPOCK1*, *GREM1* and *IRES*) were purchased from Integrated DNA technologies (IDT). Primers for *PTEN*, *TGFBI* and *IL6* were purchased from Bio-RAD Laboratories, Inc., CA. All sequences are given in Supplementary Table 5.

ChIP, RNA, and exome sequencing, expression microarray hybridization, and analyses

ChIP-seq analysis was performed as previously described (52) with minor modifications described in Supplementary methods. Reads distribution was performed with bwtool (53) with average of both replicates, motif analysis with *de novo* discovery settings looking at motifs from 6 bp to 18bp and peaks annotations on genomic features with HOMER package (54).

High-confidence maps of genomic regions enriched for H3K27Ac (36357 sites), H3K27me3 (49821 sites), and open chromatin (11065 sites) were compiled with Bedtools (55) intersecting ChIP-seq data for H3K27Ac, H3K27me3 and Formaldehyde assisted isolation of regulatory elements (FAIRE)-seq datasets of 12 melanoma cell lines (MM001, MM011, MM031, MM034, MM047, MM057, MM074, MM087, MM099,

MM117, MM118, and SKMEL5). A separate map was generated intersecting consensus H3K27Ac sites with consensus open chromatin sites (5170 sites). Two maps of high-confidence MITFBSs in primary transformed and melanoma cell lines were retrieved by intersecting MITFBSs in transformed melanocytes with enforced expression of BRAFV600E and melanoma cell lines COLO827 (treated with DMSO condition only) from Webster et al (40). This MITFBS had 4023 sites. A second high-confidence MITFBSs map (234 sites) was build intersecting MITFBSs retrieved in the melanoma cell lines MM011 and MM031 from Verfaillie et al (38).

RNA-seq data on MITF knockdown in 3C and 4C cells were analyzed using STAR (v 20201) with default parameters for alignment to hg19. Resulting bam files were then fed into cuffdiff (v 2.2.1) using all conditions to build base for transcript analysis.

Gene ontology and pathway analysis was performed using, geneMania (56) and metascape (57), and GSEA (58). Mutation analysis from exome sequencing and microarray analyses are described in Supplementary methods.

All data is deposited in GEO under the accession number GSE142018.

Statistical analysis of melanoma cohorts

TCGA-SKCM cohort (59) transcripts per million (TPM) expression data was downloaded from cBioportal (http://www.cbioportal.org). Heatmaps and clustering of Z-scores were performed on log2(TPM+1) transformation in aheatmap (NMF package, version 0.21.0) (60) in R version R 3.5.0.

RNA-seq for SKCM-TCGA, BAM files (n=472) were obtained from the GDC (https://portal.gdc.cancer.gov) using manifest download verification (59).

The MC1R mutations were analyzed by extracting sequences for MC1R gene region from BAM files using samtools view and mpileup options (version 1.9) (61). Pooled

VCF (variant calling format) files were constructed in BCF tools (version 1.8-41) by normalizing, filtering, and merge options. Annotation of the MC1R variants was done in ANNOVAR (62), using humandb hg38 (Ensembl) (63), by filtering against known mutations in databases: refGene, exac03, avsnp147, dbnsfp30a, cosmic81, ALL.sites.2015_08. Annotated MC1R variants were summarized using vcf2table (64) and added as phenotypic information to heatmaps.

Acknowledgments

The plasmid p3xHAMITF was a kind gift from Dr. Thomas Strub. pCMV-dR8.2 dvpr and pCMV-VSV-G were kind gifts from Dr. Lina Prasmickaite. AU is funded by the Norwegian Cancer Society (Grant number #198016-2018). We are grateful for the sequencing services provided by the Genomics Core Facility, South East Health Region/Oslo University Hospital.

Conflict of interest

The authors declare no conflict of interest

Supplementary information

Supplementary information is available at Oncogene's website

Figure Legends

Figure 1 HA-MITF-M leads to transformation of immortalized MC1R mutant 4C melanocytes.

(A) Western blot analysis of endogenous (endo) and ectopically transduced (exo) MITF-M through 3x HA Tag (HA-Tag) expression vector in 3C-HA-MITF and 4C-HA-MITF and control (Ctr) transduced lines (3C pLVX IRES mCherry and 4C pLVX IRES mCherry cells). Protein levels of SOX10 are also indicated. Histone H3 was used as loading control. The image is representative of n=3 experiments.

(B) qRT-PCR analysis showing (endogenous) MITF-M and SOX10 levels in 3C-HA-MITF and 4C-HA-MITF compared to 3C and 4C control cells.

(C) Visual inspection of pelleted 4C-HA-MITF and 3C-HA-MITF compared to 3C and 4C control cells' pellets.

(D) Phase contrast and fluorescent micrographs of 3C, 4C, 3C-HA-MITF and 4C-HA-MITF cells documenting the transformed morphology of 4C-HA-MITF and MITF/mCherry bicistronic expression.

(E) Representative images of the growth factors independence assay for the indicated cells growing in growth factor deprived media for 21 days. NT: Non-transduced parental cells. Ctr: Control. 3C-HA-MITF and 4C-HA-MITF cells.

(F) Representative images of the anchorage independent assay for 4C, 4C-HA-MITF and SK-Mel-28 cells growing in agarose. The SK-Mel-28 melanoma cells are used as positive control.

(G) 4C-HA-MITF -derived tumor volume measurements in NSG mice. Each line represents a different xenograft and legends represent time of measurement.

(H) Tumor volume measurements in NSG mice injected with newly established xenografts from 4C-HA-MITF cells at a second passage.

(I) Representative images of NSG mice bearing 4C-HA-MITF xenograft tumors.

Figure 2 HA-MITF directs specific transcription leading to melanocyte transformation.

(A) Differentially expressed genes (up and down regulated) upon knockdown of MITF-M in parental Hermes 3C and Hermes 4C cells.

(B) Differentially expressed genes upon HA-MITF transduction in 3C-HA-MITF and 4C-HA-MITF cells compared to control transduced 3C and 4C cells. The boxes also show top enriched biological processes ($p<0.00001$) according to gene ontology analysis

(C) Identification of MITF-M target genes important for Hermes 4C transformation based on overlap of genes that were down and up regulated upon MITF-M knockdown in parental Hermes 4C cells (all genes are listed in the speech bubbles along with the Log 2 fold change in 4C-HA-MITF vs 4C control) with genes that were exclusively upregulated in 4C-HA-MITF vs 4C control (n=205; see also Supplementary Table 2; top 10 upregulated genes are listed in the related speech bubble).

(D) Gene set enrichment analysis for genes exclusively upregulated in 4C-HA-MITF cells compared to 4C control cells transduced with control vector, not concomitantly upregulated in 3C-HA-MITF vs 3C control nor 4C control vs 3C control (n=205; see also Supplementary Table 2). Clustering analysis of Hermes cells and derivatives transduced with HA-MITF (**E**) and 371 TCGA melanoma (**F**) according to the expression of 35 genes exclusively upregulated in 4C-HA-MITF 200 genes included in the epithelial to mesenchymal transition (EMT) hallmark signature.

Figure 3 HA-MITF-M enhances the chromatin binding and reprograms transcription.

(A) MITF binding sites (MITFBSs) number in Hermes 3C-HA-MITF and Hermes 4C-HA-MITF and overlap with the indicated datasets. MITFBSs in COLO829 and Melanocytes data are from Webster et al (40), MITFBSs in Melanoma cell lines MM011 and MM031 are from Verfaillie et al (38).

(B) Genomic regions annotation of MITF binding sites (MITFBSs) from this study and publicly available datasets as indicated.

(C) Expression analysis of the indicated MITF target genes via qRT-PCR in Hermes cell derivatives

(D) Distribution analysis of MITF ChIP-seq reads in 3C-HA-MITF and 4C-HA-MITF cells around consensus MITF binding sites (MITFBSs) in Hermes cells.

(E) Distribution analysis of MITF ChIP-seq reads in 3C-HA-MITF and 4C-HA-MITF cells around high confidence open chromatin marked with H3K27Ac in 12 melanoma cell lines from Verfaillie et al (38) (see Methods).

(F) Distribution analysis of MITF ChIP-seq reads in 3C-HA-MITF and 4C-HA-MITF cells around high-confidence MITFBSs retrieved from the melanoma cell line COLO829 and transformed Melanocyte through forced expression of BRAFV600E from Webster et al (40) (see Methods).

(G) *De novo* motif discovery analysis using 42075 MITFBSs' DNA sequences retrieved from 3C-HA-MITF cells.

(H) *De novo* motif discovery analysis using 80215 MITFBSs' DNA sequences retrieved from 4C-HA-MITF cells.

Figure 4 AXL and PI3/AKT pathway mediates HA-MITF transformation through PTEN downregulation

(A) Western Blot analysis of AXL in 3C-HA-MITF and 4C-HA-MITF compared to parental cell lines. Histone H3 was used as loading control. Representative blot from three different experiments.

(B) RT-PCR of AXL levels in 4C-HA-MITF, and in 4C-HA-MITF cells xenografted in mice normalized to 4C levels (n=3).

(C) Western Blot analysis of pAKT, PTEN and pERK after cholera toxin starvation in 3C-HA-MITF and 4C-HA-MITF normalized to 3C and 4C levels. Histone H3 was used as loading control. Representative blot from three different experiments.

(D) qRT-PCR analyses of PTEN levels in 3C-HA-MITF, and in 4C-HA-MITF cells normalized to control 3C and 4C cells (n=3).

(E) Western Blot analysis of the indicated proteins levels after PTEN depletion in the parental 4C cell line and transduced 4C-HA-MITF compared to scrambled siRNA and non-treated control (NT). Histone H3 was used as loading control. Representative blot from three different experiments.

(F) Western blot analysis of AXL, pAKT and pERK in 4C-HA-MITF treated with AXL inhibitor R428 (2μM) and siAXL compared to non-transduced (NT), scrambled siRNA and DMSO control. Histone H3 was used as loading control. Representative blot from three different experiments.

(G) Growth curves measured using IncuCyte of 4C-HA-MITF cells untreated (NT), or control treated with DMSO (DMSO), or MK-2206 (9μM), Trametinib (1.5 nM), R428 (2μM), a combination of Trametinib (1,5nM) with MK2206 (9μM), and a combination of Trametinib (1,5nM) and R428 (2μM) (n=3).

(H) Cell viability measurements using MTS of 4C-HA-MITF after 90 hours treatment with the indicated inhibitor treatments (n=3).

(I) Western blot analysis of testing the efficacy of the MK-2206 inhibitor in 4C control.

(J) Frequency of MC1R co-occurring mutations in the TCGA melanoma cohort (n=471), and in 73 melanoma cases from the same cohort that displayed high expression of MITF (cut off = Z-score >=1)

(K) Frequency of the indicated MC1R mutations in the TCGA melanoma cohort (n=471) and in the 73 cases with high expression of MITF. Their associated phenotypes according to (65-67) are indicated (N/A is not applicable or not known) as well as whether the variant is highly (double arrow), or mildly (single arrow) impairing MC1R function. * indicates the MC1R variants co-occurring in Hermes 4C cell lines; ** indicates the synonymous mutation of the MC1R that does not alter the amino acid sequence of MC1R.

References

1. Siegel RL, Miller KD, Jemal A. Cancer Statistics, 2017. CA Cancer J Clin. 2017;67(1):7-30.

2. Schadendorf D, van Akkooi ACJ, Berking C, Griewank KG, Gutzmer R, Hauschild A, et al. Melanoma. Lancet. 2018;392(10151):971-84.

3. Soura E, Eliades PJ, Shannon K, Stratigos AJ, Tsao H. Hereditary melanoma: Update on syndromes and management: Genetics of familial atypical multiple mole melanoma syndrome. J Am Acad Dermatol. 2016;74(3):395-407; quiz 8-10.

4. Stone S, Jiang P, Dayananth P, Tavtigian SV, Katcher H, Parry D, et al. Complex structure and regulation of the P16 (MTS1) locus. Cancer Res. 1995;55(14):2988-94.

5. Cancer Genome Atlas N. Genomic Classification of Cutaneous Melanoma. Cell. 2015;161(7):1681-96.

6. Bartkova J, Lukas J, Guldberg P, Alsner J, Kirkin AF, Zeuthen J, et al. The p16-cyclin D/Cdk4-pRb pathway as a functional unit frequently altered in melanoma pathogenesis. Cancer Res. 1996;56(23):5475-83.

7. Box NF, Duffy DL, Chen W, Stark M, Martin NG, Sturm RA, et al. MC1R genotype modifies risk of melanoma in families segregating CDKN2A mutations. Am J Hum Genet. 2001;69(4):765-73.

8. Horn S, Figl A, Rachakonda PS, Fischer C, Sucker A, Gast A, et al. TERT promoter mutations in familial and sporadic melanoma. Science. 2013;339(6122):959-61.

9. Fargnoli MC, Gandini S, Peris K, Maisonneuve P, Raimondi S. MC1R variants increase melanoma risk in families with CDKN2A mutations: a meta-analysis. Eur J Cancer. 2010;46(8):1413-20.

10. Hernando B, Swope VB, Guard S, Starner RJ, Choi K, Anwar A, et al. In vitro behavior and UV response of melanocytes derived from carriers of CDKN2A mutations and MC1R variants. Pigment Cell Melanoma Res. 2019;32(2):259-68.

11. Tagliabue E, Gandini S, Bellocco R, Maisonneuve P, Newton-Bishop J, Polsky D, et al. MC1R variants as melanoma risk factors independent of at-risk phenotypic characteristics: a pooled analysis from the M-SKIP project. Cancer Manag Res. 2018;10:1143-54.

12. Pasquali E, Garcia-Borron JC, Fargnoli MC, Gandini S, Maisonneuve P, Bagnardi V, et al. MC1R variants increased the risk of sporadic cutaneous melanoma in darker-pigmented Caucasians: a pooled-analysis from the M-SKIP project. Int J Cancer. 2015;136(3):618-31.

13. Scherer D, Nagore E, Bermejo JL, Figl A, Botella-Estrada R, Thirumaran RK, et al. Melanocortin receptor 1 variants and melanoma risk: a study of 2 European populations. Int J Cancer. 2009;125(8):1868-75.

14. Harding RM, Healy E, Ray AJ, Ellis NS, Flanagan N, Todd C, et al. Evidence for variable selective pressures at MC1R. Am J Hum Genet. 2000;66(4):1351-61.

15. Cao J, Wan L, Hacker E, Dai X, Lenna S, Jimenez-Cervantes C, et al. MC1R is a potent regulator of PTEN after UV exposure in melanocytes. Mol Cell. 2013;51(4):409-22.

16. Valverde P, Healy E, Jackson I, Rees JL, Thody AJ. Variants of the melanocyte-stimulating hormone receptor gene are associated with red hair and fair skin in humans. Nat Genet. 1995;11(3):328-30.

17. Premi S, Wallisch S, Mano CM, Weiner AB, Bacchiocchi A, Wakamatsu K, et al. Photochemistry. Chemiexcitation of melanin derivatives induces DNA photoproducts long after UV exposure. Science. 2015;347(6224):842-7.

18. Curtin JA, Fridlyand J, Kageshita T, Patel HN, Busam KJ, Kutzner H, et al. Distinct sets of genetic alterations in melanoma. N Engl J Med. 2005;353(20):2135-47.

19. Elwood JM, Jopson J. Melanoma and sun exposure: an overview of published studies. Int J Cancer. 1997;73(2):198-203.

20. Rhodes AR, Weinstock MA, Fitzpatrick TB, Mihm MC, Jr., Sober AJ. Risk factors for cutaneous melanoma. A practical method of recognizing predisposed individuals. JAMA. 1987;258(21):3146-54.

21. Read J, Wadt KA, Hayward NK. Melanoma genetics. J Med Genet. 2016;53(1):1-14.

22. Potjer TP, Bollen S, Grimbergen A, van Doorn R, Gruis NA, van Asperen CJ, et al. Multigene panel sequencing of established and candidate melanoma susceptibility genes in a large cohort of Dutch non-CDKN2A/CDK4 melanoma families. Int J Cancer. 2019;144(10):2453-64.

23. Wolf Horrell EM, Jarrett SG, Carter KM, D'Orazio JA. Divergence of cAMP signalling pathways mediating augmented nucleotide excision repair and pigment induction in melanocytes. Exp Dermatol. 2017;26(7):577-84.

24. Herraiz C, Garcia-Borron JC, Jimenez-Cervantes C, Olivares C. MC1R signaling. Intracellular partners and pathophysiological implications. Biochim Biophys Acta Mol Basis Dis. 2017;1863(10 Pt A):2448-61.

25. Wellbrock C, Arozarena I. Microphthalmia-associated transcription factor in melanoma development and MAP-kinase pathway targeted therapy. Pigment Cell Melanoma Res. 2015;28(4):390-406.

26. Rachakonda S, Kong H, Srinivas N, Garcia-Casado Z, Requena C, Fallah M, et al. Telomere length, telomerase reverse transcriptase promoter mutations, and melanoma risk. Genes Chromosomes Cancer. 2018;57(11):564-72.

27. Rossi M, Pellegrini C, Cardelli L, Ciciarelli V, Di Nardo L, Fargnoli MC. Familial Melanoma: Diagnostic and Management Implications. Dermatol Pract Concept. 2019;9(1):10-6.

28. Gray-Schopfer VC, Cheong SC, Chong H, Chow J, Moss T, Abdel-Malek ZA, et al. Cellular senescence in naevi and immortalisation in melanoma: a role for p16? Br J Cancer. 2006;95(4):496-505.

29. Tudrej KB, Czepielewska E, Kozlowska-Wojciechowska M. SOX10-MITF pathway activity in melanoma cells. Arch Med Sci. 2017;13(6):1493-503.

30. Vachtenheim J, Novotna H, Ghanem G. Transcriptional repression of the microphthalmia gene in melanoma cells correlates with the unresponsiveness of target genes to ectopic microphthalmia-associated transcription factor. J Invest Dermatol. 2001;117(6):1505-11.

31. Janku F, Yap TA, Meric-Bernstam F. Targeting the PI3K pathway in cancer: are we making headway? Nat Rev Clin Oncol. 2018;15(5):273-91.

32. Corazzari M, Gagliardi M, Fimia GM, Piacentini M. Endoplasmic Reticulum Stress, Unfolded Protein Response, and Cancer Cell Fate. Front Oncol. 2017;7:78.

33. Song X, Han P, Liu J, Wang Y, Li D, He J, et al. Up-regulation of SPOCK1 induces epithelial-mesenchymal transition and promotes migration and invasion in esophageal squamous cell carcinoma. J Mol Histol. 2015;46(4-5):347-56.

34. Liu Y, Li Y, Hou R, Shu Z. Knockdown GREM1 suppresses cell growth, angiogenesis, and epithelial-mesenchymal transition in colon cancer. J Cell Biochem. 2019;120(4):5583-96.

35. Chen WY, Tsai YC, Yeh HL, Suau F, Jiang KC, Shao AN, et al. Loss of SPDEF and gain of TGFBI activity after androgen deprivation therapy promote EMT and bone metastasis of prostate cancer. Sci Signal. 2017;10(492).

36. Antony J, Huang RY. AXL-Driven EMT State as a Targetable Conduit in Cancer. Cancer Res. 2017;77(14):3725-32.

37. Sullivan NJ, Sasser AK, Axel AE, Vesuna F, Raman V, Ramirez N, et al. Interleukin-6 induces an epithelial-mesenchymal transition phenotype in human breast cancer cells. Oncogene. 2009;28(33):2940-7.

38. Verfaillie A, Imrichova H, Atak ZK, Dewaele M, Rambow F, Hulselmans G, et al. Decoding the regulatory landscape of melanoma reveals TEADS as regulators of the invasive cell state. Nat Commun. 2015;6:6683.

39. Alver TN, Lavelle TJ, Longva AS, Oy GF, Hovig E, Boe SL. MITF depletion elevates expression levels of ERBB3 receptor and its cognate ligand NRG1-beta in melanoma. Oncotarget. 2016;7(34):55128-40.

40. Webster DE, Barajas B, Bussat RT, Yan KJ, Neela PH, Flockhart RJ, et al. Enhancer-targeted genome editing selectively blocks innate resistance to oncokinase inhibition. Genome Res. 2014;24(5):751-60.

41. Strub T, Giuliano S, Ye T, Bonet C, Keime C, Kobi D, et al. Essential role of microphthalmia transcription factor for DNA replication, mitosis and genomic stability in melanoma. Oncogene. 2011;30(20):2319-32.

42. Davis CA, Hitz BC, Sloan CA, Chan ET, Davidson JM, Gabdank I, et al. The Encyclopedia of DNA elements (ENCODE): data portal update. Nucleic Acids Res. 2018;46(D1):D794-D801.

43. Seberg HE, Van Otterloo E, Cornell RA. Beyond MITF: Multiple transcription factors directly regulate the cellular phenotype in melanocytes and melanoma. Pigment Cell Melanoma Res. 2017;30(5):454-66.

44. Khan A, Fornes O, Stigliani A, Gheorghe M, Castro-Mondragon JA, van der Lee R, et al. JASPAR 2018: update of the open-access database of transcription factor binding profiles and its web framework. Nucleic Acids Res. 2018;46(D1):D260-D6.

45. Arozarena I, Wellbrock C. Phenotype plasticity as enabler of melanoma progression and therapy resistance. Nat Rev Cancer. 2019;19(7):377-91.

46. Zuo Q, Liu J, Huang L, Qin Y, Hawley T, Seo C, et al. AXL/AKT axis mediated-resistance to BRAF inhibitor depends on PTEN status in melanoma. Oncogene. 2018;37(24):3275-89.

47. Garraway LA, Widlund HR, Rubin MA, Getz G, Berger AJ, Ramaswamy S, et al. Integrative genomic analyses identify MITF as a lineage survival oncogene amplified in malignant melanoma. Nature. 2005;436(7047):117-22.

48. Zhou XP, Gimm O, Hampel H, Niemann T, Walker MJ, Eng C. Epigenetic PTEN silencing in malignant melanomas without PTEN mutation. Am J Pathol. 2000;157(4):1123-8.

49. Muller J, Krijgsman O, Tsoi J, Robert L, Hugo W, Song C, et al. Low MITF/AXL ratio predicts early resistance to multiple targeted drugs in melanoma. Nat Commun. 2014;5:5712.

50. Hoek KS, Schlegel NC, Eichhoff OM, Widmer DS, Praetorius C, Einarsson SO, et al. Novel MITF targets identified using a two-step DNA microarray strategy. Pigment Cell Melanoma Res. 2008;21(6):665-76.

51. Zhu C, Wei Y, Wei X. AXL receptor tyrosine kinase as a promising anti-cancer approach: functions, molecular mechanisms and clinical applications. Mol Cancer. 2019;18(1):153.

52. Urbanucci A, Barfeld SJ, Kytola V, Itkonen HM, Coleman IM, Vodak D, et al. Androgen Receptor Deregulation Drives Bromodomain-Mediated Chromatin Alterations in Prostate Cancer. Cell Rep. 2017;19(10):2045-59.

53. Pohl A, Beato M. bwtool: a tool for bigWig files. Bioinformatics. 2014;30(11):1618-9.

54. Heinz S, Benner C, Spann N, Bertolino E, Lin YC, Laslo P, et al. Simple combinations of lineage-determining transcription factors prime cis-regulatory elements required for macrophage and B cell identities. Mol Cell. 2010;38(4):576-89.

55. Quinlan AR, Hall IM. BEDTools: a flexible suite of utilities for comparing genomic features. Bioinformatics. 2010;26(6):841-2.

56. Warde-Farley D, Donaldson SL, Comes O, Zuberi K, Badrawi R, Chao P, et al. The GeneMANIA prediction server: biological network integration for gene prioritization and predicting gene function. Nucleic Acids Res. 2010;38(Web Server issue):W214-20.

57. Zhou Y, Zhou B, Pache L, Chang M, Khodabakhshi AH, Tanaseichuk O, et al. Metascape provides a biologist-oriented resource for the analysis of systems-level datasets. Nat Commun. 2019;10(1):1523.

58. Subramanian A, Tamayo P, Mootha VK, Mukherjee S, Ebert BL, Gillette MA, et al. Gene set enrichment analysis: a knowledge-based approach for interpreting genome-wide expression profiles. Proc Natl Acad Sci U S A. 2005;102(43):15545-50.

59. Grossman RL, Heath AP, Ferretti V, Varmus HE, Lowy DR, Kibbe WA, et al. Toward a Shared Vision for Cancer Genomic Data. N Engl J Med. 2016;375(12):1109-12.

60. Gaujoux R, Seoighe C. A flexible R package for nonnegative matrix factorization. BMC Bioinformatics. 2010;11:367.

61. Li H, Handsaker B, Wysoker A, Fennell T, Ruan J, Homer N, et al. The Sequence Alignment/Map format and SAMtools. Bioinformatics. 2009;25(16):2078-9.

62. Wang K, Li M, Hakonarson H. ANNOVAR: functional annotation of genetic variants from high-throughput sequencing data. Nucleic Acids Res. 2010;38(16):e164.

63. Hunt SE, McLaren W, Gil L, Thormann A, Schuilenburg H, Sheppard D, et al. Ensembl variation resources. Database (Oxford). 2018;2018.

64. Lindenbaum P, Karakachoff M, Redon R. Vcf2Table: a VCF prettifier 2018 [

65. Elfakir A, Ezzedine K, Latreille J, Ambroisine L, Jdid R, Galan P, et al. Functional MC1R-gene variants are associated with increased risk for severe photoaging of facial skin. J Invest Dermatol. 2010;130(4):1107-15.

66. Raimondi S, Sera F, Gandini S, Iodice S, Caini S, Maisonneuve P, et al. MC1R variants, melanoma and red hair color phenotype: a meta-analysis. Int J Cancer. 2008;122(12):2753-60.

67. Saleha S, Khan TA, Zafar S. MC1R gene variants involvement in human OCA phenotype. Open Life Science. 2016;11(1):142-50.

SUPPLEMENTARY INFORMATION

Supplementary methods

Construction of pLX3xHAvar4mCh vector expressing 3xHA tagged MITF-M

The construction of pLX 3xHAvar4mCh was performed by two sequential clonings. The human MITF variant 4 cDNA was prepared by PCR amplification of the cDNA clone MGC:75121 (IMAGE:6066096) (Invitrogen) using the BglII containing MITF forward primer:5′-AA AAAAAGATCTACCATGCTGGAAATGCTAG-3′ and the EcoRI containing reverse primer: 5′-AAAAAGATTTCATCTCGCTAACAAGTGTGC. Subsequent to restriction digestion by BglII/EcoRI (NEB), the MITF variant 4 cDNA containing insert was gel purified using the JetStar Gel extraction Kit (Genomed). The murine MITF variant 4 cDNA was removed from pCMV3xHAvar4 plasmid by BglII/ EcoRI endonuclease digestion (NEB) (Strub et al., 2011) and the vector backbone containing the 5´3xHA tag was isolated by gel extraction as described above. The insert and vector were then ligated overnight at 14°C using T4 DNA ligase (NEB), transformed into chemically competent DH5α (Invitrogen) and selected candidates were screened by PCR for the presence of the insert. The successful construct pCMV3xHAvar4 was digested with NheI/XbaI (NEB) and the 5′ 3xHA tagged MITF variant 4 fusion insert was isolated by gel purification. The insert was then ligated into gene cleaned (Genomed) SpeI linearized pLVX IRES mCh (Clontech) producing the Lenti-expression vector pLX3xHAvar4mCherry and transformed into chemically competent STBL3 (Invitrogen). pLX3xHAvar4mCherry was subsequently sequenced (Eurofins) utilizing the commercially available pCMV_F(21mer) MWG-Biotech AG and

IPCR IRES 1R primers to confirm the correctness of the PCR derived human MITF variant 4 cDNA insert.

Production of lentiviral particles

Lentiparticles were produced in Lenti-X 293T (Clontech) using the designated lenti-expression vector and the second-generation packaging system utilizing pCMV-dR8.2 dvpr and pCMV-VSV-G as previously described (Stewart et al., 2003) with the following modification: The transfection reagent Fugene (Promega) was replaced by Turbofect (Thermo Fisher Scientific) and applied as recommended by the manufacturer

Growth factor independence assay

Cells were seeded out in Nunc 6-well plates (Corning) at a density of 2.5 x104 cells per well in RPMI-1640 Medium (Sigma-Aldrich) supplemented with 0.5% FBS (PAA) and incubated at 37°C and 5% CO2 for 21 days. Medium was replaced every 4-5 days until the completion of the assay. At completion, cells were washed twice with ice-cold PBS before a 10 min. fixation by the addition of ice-cold methanol. Staining was achieved by the addition of 0.5% crystal violet solution at room temperature for 10 min, followed by washing in ddH2O until only cell-retained dye remained. Plates were then dried overnight and photographs were captured on a Nikon D5200 using a 28mm lens.

Anchorage independence assays

2.5x104 cells were inoculated in 1 ml 0.4% agarose RPMI supplemented with 8% FBS and plated in triplicate on 0.6% agarose RPMI supplemented with 8% FBS and penicillin/streptomycin for 28 days at 37°C and 5% CO2. Cells were fed every 4-5 days.

Cells were grown for 21 days in 0.3% LGT agarose RPMI 10% FBS supplemented with antibiotics. Hermes4C and the metastatic melanoma cell line SKmel28 was used as negative and positive control, respectively.

Cells were plated at a density of 2.5 x104 cells per well in 0.3% LGT agarose RPMI supplemented with 10% FBS and antibiotics. Plates were then incubated at 37°C and 5% CO2 21 days with the addition of fresh medium every 4 to 5 days. Upon completion, 400µl NTB (1mg/ml) was added and the plates were incubated overnight under culture condition as described. Photographs were captured on a Nikon D5200 using a 28mm lens.

Growth curve

Approximately 800 cells were seeded in 96-well plates and growth was followed with the IncuCyte system (Essen Bioscience). When indicated, cells were starved of cholera toxin for 3 days after which media containing the appropriate concentration of cholera toxin was replaced.

Establishment of xenografts

Animal experiments were approved and performed as stated by the Norwegian Animal Authority (Permit number 12080), and conducted according to the regulations of the Federation of European Laboratory Animal Science (FELASA). NOD scid gamma (NSG) mice (NOD.Cg-Prkdcscid Il2rgtm1Wjl/SzJ) were locally bread and housed according to the guidelines at the Section of Comparative Medicine, the Norwegian Radiumhospital. Briefly, the mice were housed in open cages with free accesses to food and water. The environmental parameters in the animal rooms were as follows; 12 hours light/dark cycle, constant temperature of 21+/- 2C, a relative humidity of 30-

70% and approximately ten air changes every hour. For establishment of xenografts, NSG mice were anesthetized with 3% Sevoflurane (Baxter) and subcutaneously injected on both flanks with 5 million of Hermes 4c (parental), Hermes 4c transduced with pLVXIRESmCh (vector control transduced 4C cells) and Hermes 4c cells transduced with pLX3xHAvar4mCh vector (4C-HA-MITF) in 200µl RPMI1640. Tumor volume and body weight was registered once a week. The diameter of the tumors was measured using a caliper, and tumor volume was calculated as follows: V=w2×L×0.5 (were w and L are the shortest and longest tumor diameter respectively). The mice were sacrificed when tumor volume reached approximately 800-1000mm^3, and tumor pieces (2x2mm) were passaged on to new animals.

Cell culture Imaging

2.5 x104 cells per well were plated in 6-well plates for micrographic documentation of Hermes 3C, Hermes 4C and their pLX HA-MITF mCherry and pLVX IRES mCherry derivatives. The micrographs were captured using the 10X objective for phase contrast (white light) and Texas Red filtered (UV) fluorescent imaging on a Zeiss S200 fluorescent confocal microscope using Axiovision software.

siRNA experiments

5x10^4 cells per well were plated in 6-well plates seeded in 6-well plates and grown to 60% confluence before being transfected using siRNA directed against MITF-M (Eurogentec, Seraing, Belgium). The cells were incubated for 72h to ensure optimal target reduction at the protein level. The cells were transfected with a final concentration of 25pmol siRNA, using Lipofectamine RNAiMAX (Invitrogen) as

described in the manufacturer's protocol. Sequences for siRNA are described in supplementary methods. All transfections were performed in triplicate.

Isolation of RNA

Total RNA was isolated using the GenElute Mammalian Total RNA Miniprep Kit (Sigma-Aldrich, Steinheim, Germany). Reverse transcription was performed using the qScript™ cDNA Synthesis Kit (Quanta Biosciences, Gaithersburg, USA). Both kits were used according to the manufacturer's manuals. RNA concentrations were measured using the NANODROP 2000 (Thermo Scientific).

ChIP and RNA Sequencing, expression microarray hybridization, and analyses

ChIP-seq analysis was performed as previously described (1) with minor modifications. Briefly, reads were aligned to hg19 using Bowtie v.1.0.0 allowing a maximum of 2 mismatches and suppressing multiple reads alignments if found. Peak calling was performed using MACS (v macs14 1.4.2 (2)) with default parameters and using option "-g 2.63e9" for effective genome size. Reads distribution with bwtool (3) with average of both replicates, motif analysis with d*e novo* discovery settings looking at motifs from 6 bp to 18bp and peaks annotations on genomic features with HOMER package (4).

High confidence maps of genomic regions enriched for H3K27Ac (36357 sites), H3K27me3 (49821 sites), and open chromatin (11065 sites) were compiled with Bedtools (5) intersecting ChIP-seq data for H3K27Ac, H3K27me3 and Formaldehyde assisted isolation of regulatory elements (FAIRE)-seq datasets of 12 melanoma cell lines (MM001, MM011, MM031, MM034, MM047, MM057, MM074, MM087, MM099, MM117, MM118, and SKMEL5). A separate map was generated intersecting consensus H3K27Ac sites with consensus open chromatin sites (5170 sites). Two

maps of high confidence MITF binding sites (MITFBSs) in primary transformed and melanoma cell lines were retrieved by intersecting MITF-BS in transformed melanocytes with enforced expression of BRAFV600E and melanoma cell lines COLO827 (treated with DMSO condition only) from Webster et al (6). This MITF-BS had 4023 sites. A second high confidence MITF-BS map (234 sites) was build intersecting MITF-BS retrieved in the melanoma cell lines MM011 and MM031 from Verfaillie et al (7).

RNA-seq data on MITF knockdown in 3c and 4c cells were analyzed using STAR (v 20201) with default parameters for alignment to hg19. Resulting bam files were then fed into cuffdiff (v 2.2.1) using all conditions to build base for transcript analysis.

RNA for microaaray expression analysis was hybridized to Illumina platform array according to the manufacturer instruction at the local core facilty. The raw signal was then quantile normalized and log 2-trransformed. A gene was considered to be differentially expressed within a given sample if the following condition was matched: |log2 fold change| > 1.5.

Gene ontology and pathway analysis was performed using, geneMania (8) and metascape (9), and GSEA (10).

All the data is deposited in GEO under the accession number GSE142018.

Mutation analysis of Hermes 3C and 4C lines derivatives

Genomic DNA from Hermes cells derivatives was extracted with a Maxwell 16 DNA purification kit (Promega, Madison, WI, U.S.A.). Library preparation was carried out using SureSelectXT Human All Exon V5 (Agilent, California, USA) per manufacturer's instructions at the Oslo University Hospital Genomics Core Facility, and whole exome capture and paired-end sequencing was performed using the Illumina HiSeq 2500

platform at an average sequencing depth of 224X. A bioinformatics workflow following GATK best-practices was applied to preprocess the raw sequencing reads, as previously described (11). Single nucleotide variants and short insertions/deletions were identified with SuperFreq and MuTect2 (12, 13). Variants with a sequencing depth lower than 20 were considered low-confident and discarded. We furthermore used the Personal Cancer Genome Reporter (PCGR v8.0) for functional variant annotation (14). We applied several filtering procedures available in PCGR to exclude the bulk of known germline variation in the callsets. Specifically, from the initial raw call-set pr. cell line, we excluded: (1) All variants that overlapped germline variants called by the 1000 Genomes Project phase 3 (minor allele frequency (MAF) > 0.2% in any population), or gnomAD (MAF > 0.2% in any population). The MAF threshold (0.2%) was chosen based on recommendations in a recent study on tumor variant filtration strategies (15). (2) Variants that overlapped any of ~730,000 germline variants detected in an in-house dataset comprising 789 WES samples (blood). (3) Likely heterozygous germline variants, i.e. variants with an allelic fraction between 0.4 and 0.6, and with an existing record in dbSNP or gnomAD. (4) Variants registered in ClinVar with a germline origin. (5) Non-exonic variants (exonic variants retained included coding region variants, i.e. synonymous, missense, stopgain, stoploss, inframe, frameshift, as well as canonical splice site variants (+/- 2bp donor/acceptor)).

Supplementary figures legends

Supplementary Figure 1 HA-MITF-M leads to transformation of immortalized MC1R mutant 4C melanocytes.

(A) qRT-PCR analysis showing TYR levels in 4C-HA-MITF and 3C-HA-MITF compared to parental 3C and 4C cell lines **(B)** and in U2OS cells transduced with the same HA-MITF construct or with the construct only containing the IRES sequence (control construct) compared to parental U2OS. **(C)** qRT-PCR analysis showing IRES construct levels in U2OS cells transduced with HA-MITF-M construct, or control construct, compared to parental U2OS (n=3).

(D) Image-based analysis over time of area confluence for the indicated cell lines grown in cholera toxin starved condition.

(E) Image-based analysis over time of area confluence for the indicated Hermes 3C cell lines derivatives grown in presence of the recommended concentration of cholera toxin (20pM).

(F) Image-based analysis over time of area confluence for the indicated Hermes 4C cell lines derivatives grown in presence of the recommended concentration of cholera toxin (2pM).

(G) Cell proliferation assay (MTS) of Hermes 3C cell lines derivatives grown in presence of the indicated concentrations of cholera toxin for 150 hours.

(H) Cell proliferation assay (MTS) of Hermes 4C cell lines derivatives grown in presence of the indicated concentrations of cholera toxin for 150 hours.

(I) Western blot analysis of endogenous (endo) and ectopically transduced (exo) MITF-M in Hermes 4C parental cells, 4C-HA-MITF, and a representative tumor xenograft. Expression analysis of SOX10, AXL, pAKT and total AKT are also shown. The image

is representative of n=3 experiments. qRT-PCR gene expression analyses of (endogenous) MITF-M **(J)** IRES construct **(K),** SOX10 **(L),** and TYR **(M)** transcripts in 4C, 4C-HA-MITF, and a representative tumor xenograft compared to expression levels in parental 4C cells. Histone H3 was used as loading control. Representative blot from three different experiments.

Supplementary Figure 2 HA-MITF directs specific transcription leading to melanocyte transformation.

Gene Ontology, pathway and function analysis of **(A)** genes downregulated upon MITF-M knockdown in Hermes 3c cells and **(B)** genes upregulated upon MITF-M knockdown in Hermes 3c cells, **(C)** genes upregulated upon MITF-M knockdown in Hermes 4c cells and **(D)** genes downregulated upon MITF-M knockdown in Hermes 4c cells (analysis of GO and pathway analysis with metascape is also shown in the left bottom panel). **(E)** Metascape Gene Ontology (GO), pathway and function analysis of genes upregulated upon MITF-M knockdown in exclusively in Hermes 4c cells but not in Hermes 3c cells. Clustering analysis of Hermes cells derivatives transduced with HA-MITF or control vector according to the expression of 200 genes included in the epithelial to mesenchymal transition (EMT) hallmark signature **(F)** and according to the expression of genes included in the core signature of the invasive melanoma phenotype **(G)** by Verfaille et al. (7).

Supplementary Figure 3 HA-MITF-M enhances the chromatin binding

Representative UCSC genome browser snapshot showing enrichment of MITF-M binding in proximity of *EGFR* **(A)**, *AXL* gene **(B)**, the *IL6* gene **(C)**, the *TGFBI* gene **(D)**, *MITF* **(F)**, and *SOX10* **(G)** genes. The UCSC genome browser bigwig files tracks are

labeled and indicated by the black horizontal arrow on the left side of each panel. Shorter green horizontal arrows point at BED files tracks consensus MITF binding sites (MITFBS) in each cell lines. ChIPqPCR validated MITF binding sites in the indicated cell lines (**G**) are indicated with a red point-down triangle and are reported as % of input. The MITF target gene PRM1 promoter region was used as control. **(H)** Distribution analysis of MITF ChIP-seq reads in 3C-HA-MITF and 4C-HA-MITF cells around the compendium of all MITF binding sites (MITFBSs) in Hermes cells. **(J)** Distribution analysis of MITF ChIP-seq reads in 3C-HA-MITF and 4C-HA-MITF cells around high confidence H3K27Ac marked sites in 12 melanoma cell lines from Verfaillie et al (7) (see Methods). **(K)** Distribution analysis of MITF ChIP-seq reads in 3C-HA-MITF and 4C-HA-MITF cells around high confidence open chromatin in 12 melanoma cell lines from Verfaillie et al (7) (see Methods). **(I)** Distribution analysis of MITF ChIP-seq reads in 3C-HA-MITF and 4C-HA-MITF cells around high confidence H3K27me3 marked sites in 12 melanoma cell lines from Verfaillie et al (7) (see Methods). **(L)** Distribution analysis of MITF ChIP-seq reads in 3C-HA-MITF and 4C-HA-MITF cells around high confidence MITFBSs in the melanoma cell lines MM011 and MM931 from Verfaillie et al (7) (see Methods). Note that all these sites were present in the sites relative to main figure 2E. **(M)** Known DNA motifs enrichment analysis using 41200 MITFBSs' DNA sequences retrieved from 3C-HA-MITF cells. **(N)** Known DNA motifs enrichment analysis using 80070 MITFBSs' DNA sequences retrieved from 4C-HA-MITF cells. **(O)** Representation of Jaspar database similarity clustering analysis of transcription factors

Supplementary Figure 4 MITF-M and MC1R in the TCGA dataset

(**A**) Expression analysis of MC1R and MITF genes in the 471 tumors from the TCGA melanoma cohort.

Supplementary References

1. Urbanucci A, Barfeld SJ, Kytola V, Itkonen HM, Coleman IM, Vodak D, et al. Androgen Receptor Deregulation Drives Bromodomain-Mediated Chromatin Alterations in Prostate Cancer. Cell Rep. 2017;19(10):2045-59.
2. Zhang Y, Liu T, Meyer CA, Eeckhoute J, Johnson DS, Bernstein BE, et al. Model-based analysis of ChIP-Seq (MACS). Genome Biol. 2008;9(9):R137.
3. Pohl A, Beato M. bwtool: a tool for bigWig files. Bioinformatics. 2014;30(11):1618-9.
4. Heinz S, Benner C, Spann N, Bertolino E, Lin YC, Laslo P, et al. Simple combinations of lineage-determining transcription factors prime cis-regulatory elements required for macrophage and B cell identities. Mol Cell. 2010;38(4):576-89.
5. Quinlan AR, Hall IM. BEDTools: a flexible suite of utilities for comparing genomic features. Bioinformatics. 2010;26(6):841-2.
6. Webster DE, Barajas B, Bussat RT, Yan KJ, Neela PH, Flockhart RJ, et al. Enhancer-targeted genome editing selectively blocks innate resistance to oncokinase inhibition. Genome Res. 2014;24(5):751-60.
7. Verfaillie A, Imrichova H, Atak ZK, Dewaele M, Rambow F, Hulselmans G, et al. Decoding the regulatory landscape of melanoma reveals TEADS as regulators of the invasive cell state. Nat Commun. 2015;6:6683.
8. Warde-Farley D, Donaldson SL, Comes O, Zuberi K, Badrawi R, Chao P, et al. The GeneMANIA prediction server: biological network integration for gene prioritization and predicting gene function. Nucleic Acids Res. 2010;38(Web Server issue):W214-20.

9. Zhou Y, Zhou B, Pache L, Chang M, Khodabakhshi AH, Tanaseichuk O, et al. Metascape provides a biologist-oriented resource for the analysis of systems-level datasets. Nat Commun. 2019;10(1):1523.
10. Subramanian A, Tamayo P, Mootha VK, Mukherjee S, Ebert BL, Gillette MA, et al. Gene set enrichment analysis: a knowledge-based approach for interpreting genome-wide expression profiles. Proc Natl Acad Sci U S A. 2005;102(43):15545-50.
11. Birkeland E, Zhang S, Poduval D, Geisler J, Nakken S, Vodak D, et al. Patterns of genomic evolution in advanced melanoma. Nat Commun. 2018;9(1):2665.
12. Cibulskis K, Lawrence MS, Carter SL, Sivachenko A, Jaffe D, Sougnez C, et al. Sensitive detection of somatic point mutations in impure and heterogeneous cancer samples. Nat Biotechnol. 2013;31(3):213-9.
13. Flensburg C, Sargeant T, Oshlack A, Majewski I. SuperFreq: Integrated mutation detection and clonal tracking in cancer. BioRxiv2019.
14. Nakken S, Fournous G, Vodak D, Aasheim LB, Myklebost O, Hovig E. Personal Cancer Genome Reporter: variant interpretation report for precision oncology. Bioinformatics. 2018;34(10):1778-80.
15. Sukhai MA, Misyura M, Thomas M, Garg S, Zhang T, Stickle N, et al. Somatic Tumor Variant Filtration Strategies to Optimize Tumor-Only Molecular Profiling Using Targeted Next-Generation Sequencing Panels. J Mol Diagn. 2019;21(2):261-73.

Supplementary tables

Table 1
http://ous-research.no/hovig/docs/Tine/Supplementary table 1.xlsx

Table 2
http://ous-research.no/hovig/docs/Tine/Supplementary table 2.xlsx

Table 3
http://ous-research.no/hovig/docs/Tine/Supplementary table 3.xlsx

Table 4
http://ous-research.no/hovig/docs/Tine/Supplementary table 4.xlsx

Supplementary Table 5. Primers and Oligos sequences	
Gene name	**Primer sequence for ChIP-qPCR**
SOX10	LEFT (5´-CAG-GAA-AAT-CAG-GCC-GTT-GT-3´)
	RIGHT (5´-AAG-AGG-CCA-GGG-AAG-ACT-TG-3´)
TGFBI	LEFT (5´-AGA-ATC-TGG-TTT-CCC-TCC-GG-3`)
	RIGHT (5´AAG-TAC-CCA-ACC-ACA-CAC-CA-3´)
AXL	LEFT (5´-ATG-GAG-GTG-GTA-GTG-TCA-GC-3`)
	RIGHT (5´-TTC-TGC-AAG-GGA-ACA-CAA-GC-3`)
IL6	LEFT (5´-GCT-GCA-GGA-CAT-GAC-AAC-TC-3`)
	RIGHT (5´-CTA-CAT-TTG-CCG-AAG-AGC-CC-3`)
EGFR	LEFT (5´-TTC-AAA-GCC-GTG-AGT-CAA-CC-3´)
	RIGHT (5´ATG-AGA-GAT-GCA-GAG-CGT-GA-3´)
MITF	LEFT (5´-CGG-GCT-CTG-TTC-TCA-CTT-TC-3´)
	RIGHT (5´-TGA-AAC-TCC-TCC-CCG-ACT-TC-3´)
CONTR-PRM1	LEFT (5'-CCA CGG AGG AGT CAT CTT GT -3')
	RIGHT (5'- GGC CTG CAT CAT GTC CAT AT -3')
	Primer sequences qRT-PCR
MITF-M	FORWARD (5′-CAT-TGT-TAT-GCT-GGA-AAT-GCT-AGA-3′)
	REVERSE (5′-GC-TAA-AGT-GGT-AGA-AAG-GTA-CTG-C-3′)
SOX10	FORWARD (5′-GAC-CAG-TAC-CCG-CAC-CTG-3′)
	REVERSE (5′-CGC-TTG-TCA-CTT-TCG-TTC-AG-3′)
TBP	FORWARD 5′-GCC-CGA-AAC-GCC-GAA-TAT-3′
	REVERSE (5′-CGT-GGC-TCT-CTT-ATC-CTC-ATG-A-3′)
RPLPO	FORWARD (5′-CGC-TGC-TGA-ACA-TGC-TCA-AC-3′)
	REVERSE (5′-TCG-AAC-ACC-TGC-TGG-ATG-AC-3′)
AXL	FORWARD (5`-AAC-CAG-GAC-GAC-TCC-ATC-C-3′)
	REVERSE (5′-AGC-TCT-GAC-CTC-GTG-CAG-AT-3′)
SPOCK1	FORWARD (5'-CAC- GAG-GAT-GCG-AAC-AGA-GT-3')
	REVERSE (5'-GAA-GGG-TCA-AGC-AGG-AGG-TC-3')
GREM1	FORWARD (5'-CGG-AGC-GCA-AAT-ACC-TGA-AG-3')
	REVERSE (5'-GGT-TGA-TGA-TGG-TGC-GAC-TGT-3')
IRES	FORWARD (5´-CTA-ACG-TTA-CTG-GCC-GAA-GC-3´)
	REVERSE (5´-TCA-CAT-TGC-CAA-AAG-ACG-GC-3)
PTEN	Unique Assay ID: qHsaCED0036796
TGFBI	Unique Assay ID: qHsaCED0057289
IL6	IL6 Unique Assay ID: qHsaCED0044677
	RNA interference sequences
MITF	Sense (5´-GCA-GUA-CCU-UUC-UAC-CAC-U-3´)
	anti sense (5´-AGU-GGU-AGA-AAG-GUA-CUG-C-3´)

Figure 1.

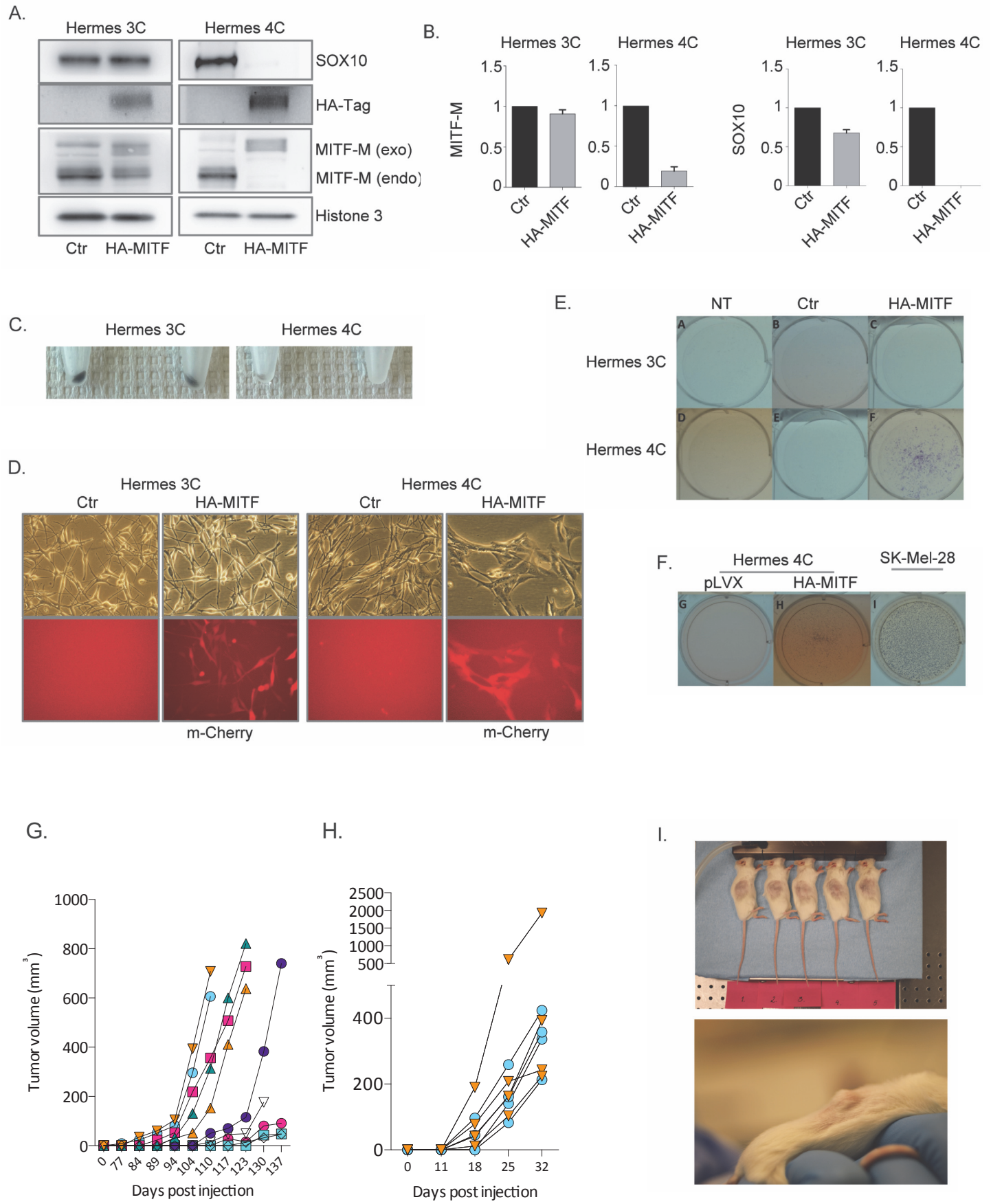
A.
Hermes 3C
Hermes 4C
SOX10
HA-Tag
MITF-M (exo)
MITF-M (endo)
Histone 3
Ctr
HA-MITF
Ctr
HA-MITF
B.
Hermes 3C
Hermes 4C
Hermes 3C
Hermes 4C
MITF-M
SOX10
1.5
1
0.5
0
Ctr
HA-MITF
C.
Hermes 3C
Hermes 4C
D.
Hermes 3C
Hermes 4C
Ctr
HA-MITF
Ctr
HA-MITF
m-Cherry
m-Cherry
E.
NT
Ctr
HA-MITF
Hermes 3C
Hermes 4C
A
B
C
D
E
F
F.
Hermes 4C
SK-Mel-28
pLVX
HA-MITF
G
H
I
G.
Tumor volume (mm3)
1000
800
600
400
200
0
0
77
84
89
94
104
110
117
123
130
137
Days post injection
H.
Tumor volume (mm3)
2500
2000
1500
1000
500
400
200
0
0
11
18
25
32
Days post injection
I.

Figure 2.

A.

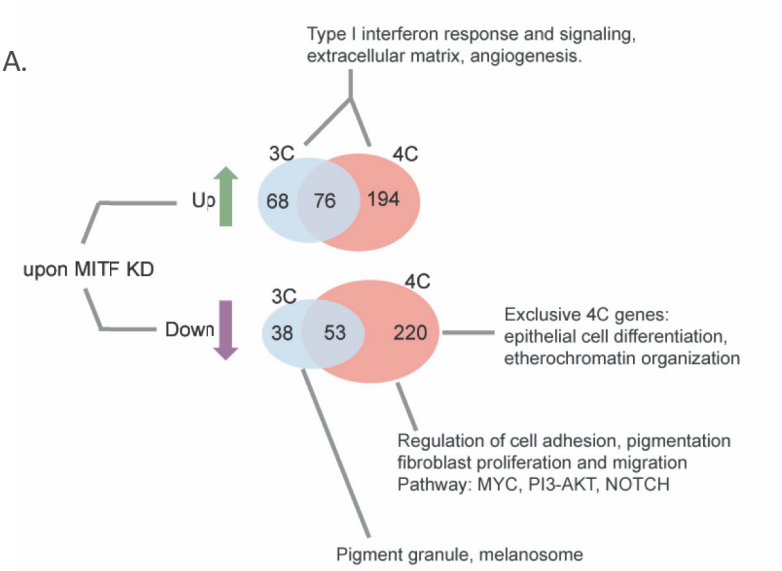
Type I interferon response and signaling,
extracellular matrix, angiogenesis.
3C
4C
Up
68
76
194
upon MITF KD
3C
4C
Down
38
53
220
Exclusive 4C genes:
epithelial cell differentiation,
etherochromatin organization
Regulation of cell adhesion, pigmentation
fibroblast proliferation and migration
Pathway: MYC, PI3-AKT, NOTCH
Pigment granule, melanosome

B.

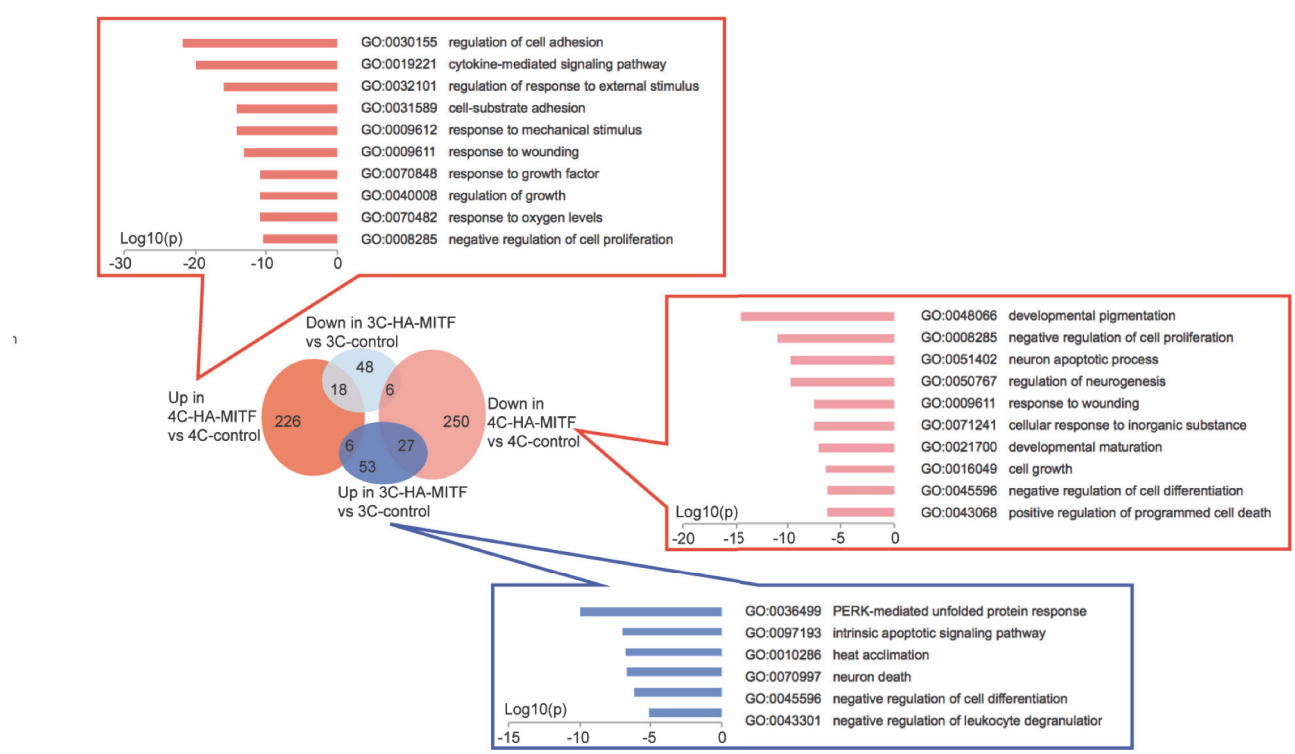
GO:0030155 regulation of cell adhesion
GO:0019221 cytokine-mediated signaling pathway
GO:0032101 regulation of response to external stimulus
GO:0031589 cell-substrate adhesion
GO:0009612 response to mechanical stimulus
GO:0009611 response to wounding
GO:0070848 response to growth factor
GO:0040008 regulation of growth
GO:0070482 response to oxygen levels
GO:0008285 negative regulation of cell proliferation
Log10(p)
-30 -20 -10 0
Down in 3C-HA-MITF
vs 3C-control
48
18
6
Up in
4C-HA-MITF
vs 4C-control
226
250
Down in
4C-HA-MITF
vs 4C-control
6
27
53
Up in 3C-HA-MITF
vs 3C-control
GO:0048066 developmental pigmentation
GO:0008285 negative regulation of cell proliferation
GO:0051402 neuron apoptotic process
GO:0050767 regulation of neurogenesis
GO:0009611 response to wounding
GO:0071241 cellular response to inorganic substance
GO:0021700 developmental maturation
GO:0016049 cell growth
GO:0045596 negative regulation of cell differentiation
GO:0043068 positive regulation of programmed cell death
Log10(p)
-20 -15 -10 -5 0
GO:0036499 PERK-mediated unfolded protein response
GO:0097193 intrinsic apoptotic signaling pathway
GO:0010286 heat acclimation
GO:0070997 neuron death
GO:0045596 negative regulation of cell differentiation
GO:0043301 negative regulation of leukocyte degranulation
Log10(p)
-15 -10 -5 0

C.

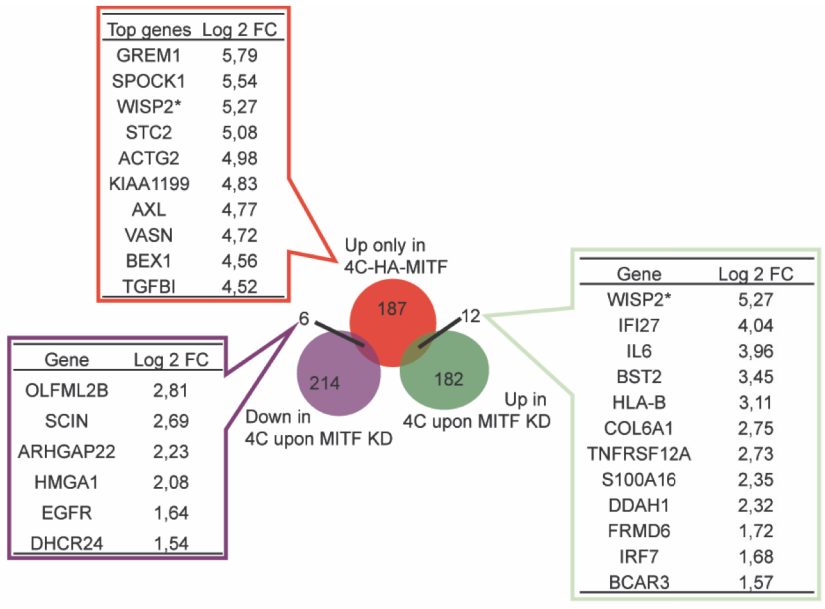
Top genes Log 2 FC
GREM1 5,79
SPOCK1 5,54
WISP2* 5,27
STC2 5,08
ACTG2 4,98
KIAA1199 4,83
AXL 4,77
VASN 4,72
BEX1 4,56
TGFBI 4,52
Up only in
4C-HA-MITF
187
6
12
214
182
Down in
4C upon MITF KD
Up in
4C upon MITF KD
Gene Log 2 FC
OLFML2B 2,81
SCIN 2,69
ARHGAP22 2,23
HMGA1 2,08
EGFR 1,64
DHCR24 1,54
Gene Log 2 FC
WISP2* 5,27
IFI27 4,04
IL6 3,96
BST2 3,45
HLA-B 3,11
COL6A1 2,75
TNFRSF12A 2,73
S100A16 2,35
DDAH1 2,32
FRMD6 1,72
IRF7 1,68
BCAR3 1,57

Figure 2.

D.

Gene Set Name [# Genes (K)]	Description	# Genes in Overlap (k)	p-value	FDR q-value
HALLMARK_EPITHELIAL_MESENCHYMAL_TRANSITION [200]	Genes defining epithelial-mesenchymal transition, as in wound healing, fibrosis and metastasis.	35	$3.57\ e^{-46}$	$6.36\ e^{-42}$
CHICAS_RB1_TARGETS_CONFLUENT [567]	Genes up-regulated in confluent IMR90 cells (fibroblast) after knockdown of RB1 [GeneID=5925] by RNAi.	46	$7.45\ e^{-45}$	$6.63\ e^{-41}$
NUYTTEN_EZH2_TARGETS_UP [1037]	Genes up-regulated in PC3 cells (prostate cancer) after knockdown of EZH2 [GeneID=2146] by RNAi.	53	$2.11\ e^{-41}$	$1.26\ e^{-37}$
SCHUETZ_BREAST_CANCER_DUCTAL_INVASIVE_UP [351]	Genes up-regulated in invasive ductal carcinoma (IDC) relative to ductal carcinoma in situ (DCIS, non-invasive).	36	$9.58\ e^{-39}$	$4.27\ e^{-35}$
WONG_ADULT_TISSUE_STEM_MODULE [721]	The 'adult tissue stem' module: genes coordinately up-regulated in a compendium of adult tissue stem cells.	44	$1,73\ e^{-37}$	$6.15\ e^{-34}$

E.

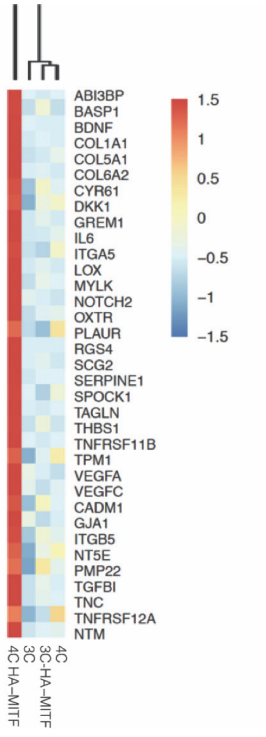

F.

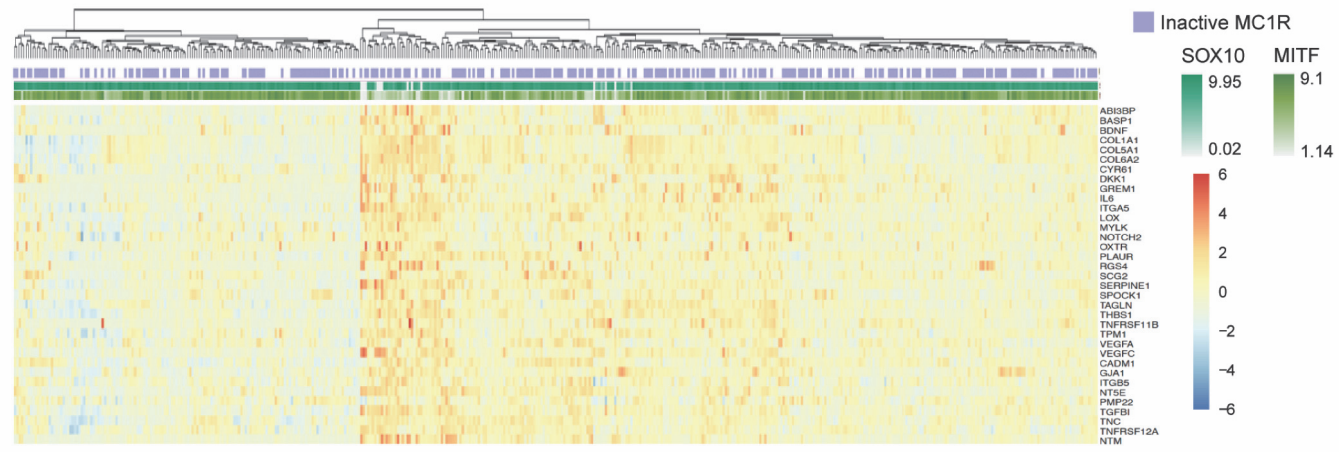

Figure 3.

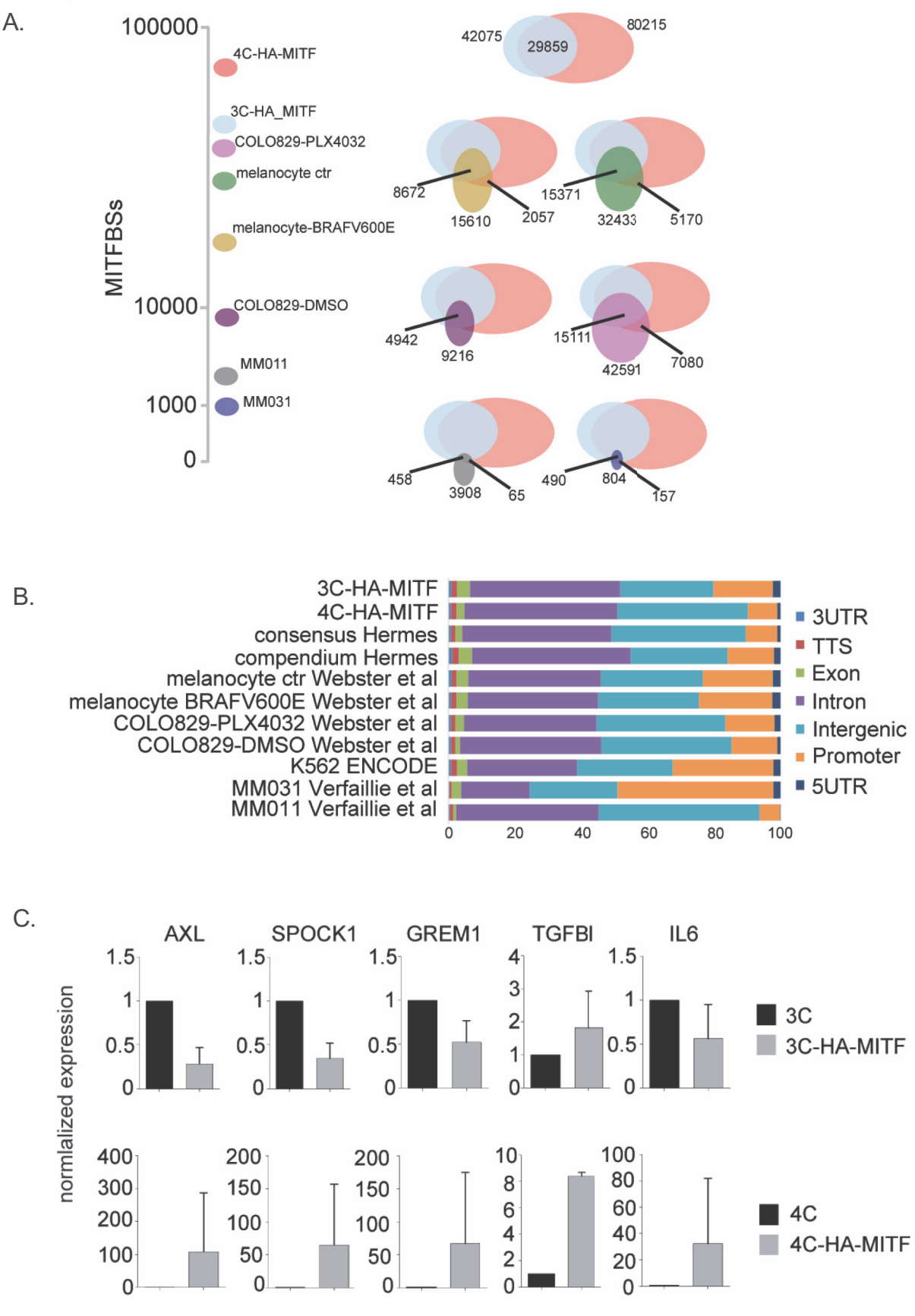
A.
100000
10000
1000
0
MITFBSs
4C-HA-MITF
3C-HA_MITF
COLO829-PLX4032
melanocyte ctr
melanocyte-BRAFV600E
COLO829-DMSO
MM011
MM031
42075
29859
80215
8672
15610
2057
15371
32433
5170
4942
9216
15111
42591
7080
458
3908
65
490
804
157
B.
3C-HA-MITF
4C-HA-MITF
consensus Hermes
compendium Hermes
melanocyte ctr Webster et al
melanocyte BRAFV600E Webster et al
COLO829-PLX4032 Webster et al
COLO829-DMSO Webster et al
K562 ENCODE
MM031 Verfaillie et al
MM011 Verfaillie et al
0
20
40
60
80
100
3UTR
TTS
Exon
Intron
Intergenic
Promoter
5UTR
C.
AXL
SPOCK1
GREM1
TGFBI
IL6
normalized expression
3C
3C-HA-MITF
4C
4C-HA-MITF

Figure 3.

D.

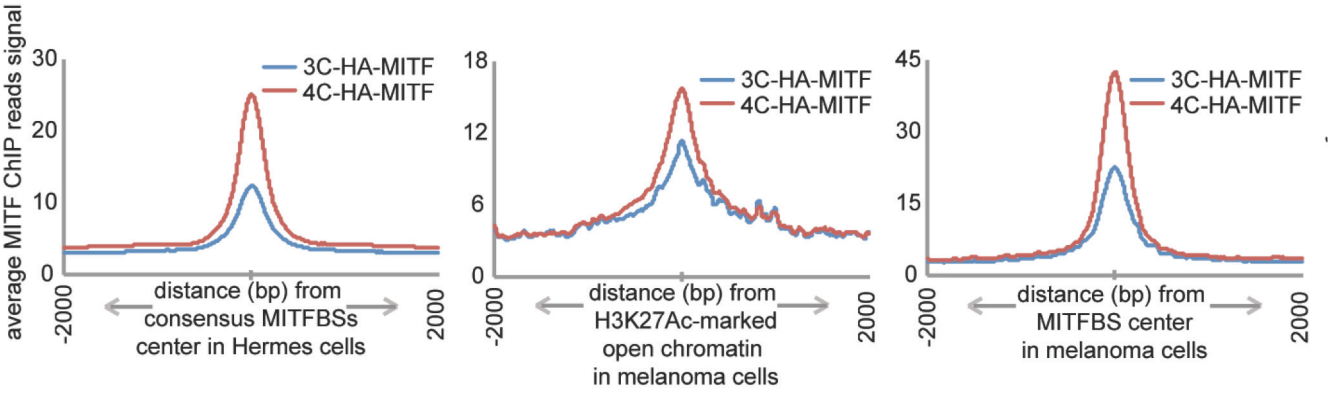
average MITF ChIP reads signal
3C-HA-MITF
4C-HA-MITF
distance (bp) from consensus MITFBSs center in Hermes cells
distance (bp) from H3K27Ac-marked open chromatin in melanoma cells
distance (bp) from MITFBS center in melanoma cells
-2000
2000

E

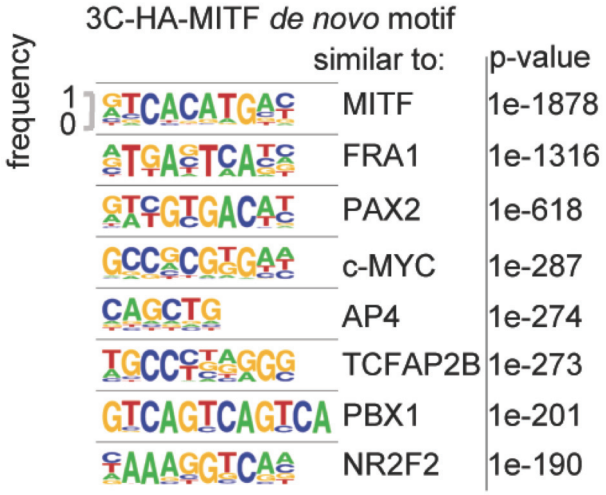
3C-HA-MITF de novo motif
frequency
similar to:
p-value
MITF 1e-1878
FRA1 1e-1316
PAX2 1e-618
c-MYC 1e-287
AP4 1e-274
TCFAP2B 1e-273
PBX1 1e-201
NR2F2 1e-190

F.

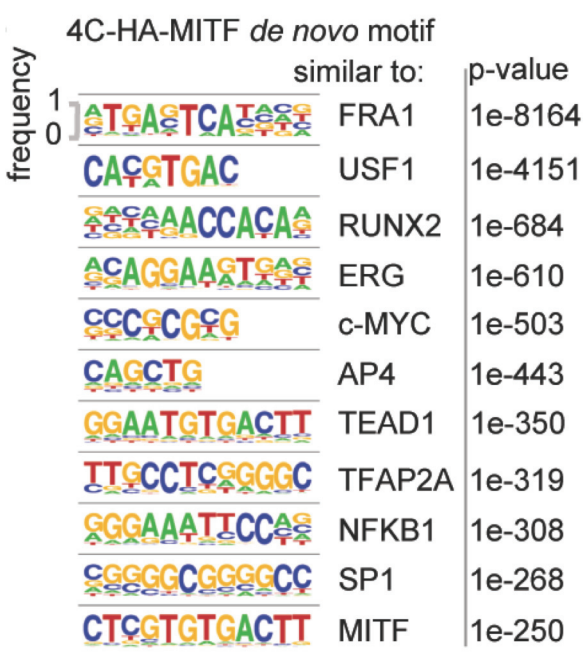
4C-HA-MITF de novo motif
frequency
similar to:
p-value
FRA1 1e-8164
USF1 1e-4151
RUNX2 1e-684
ERG 1e-610
c-MYC 1e-503
AP4 1e-443
TEAD1 1e-350
TFAP2A 1e-319
NFKB1 1e-308
SP1 1e-268
MITF 1e-250

Figure 4.

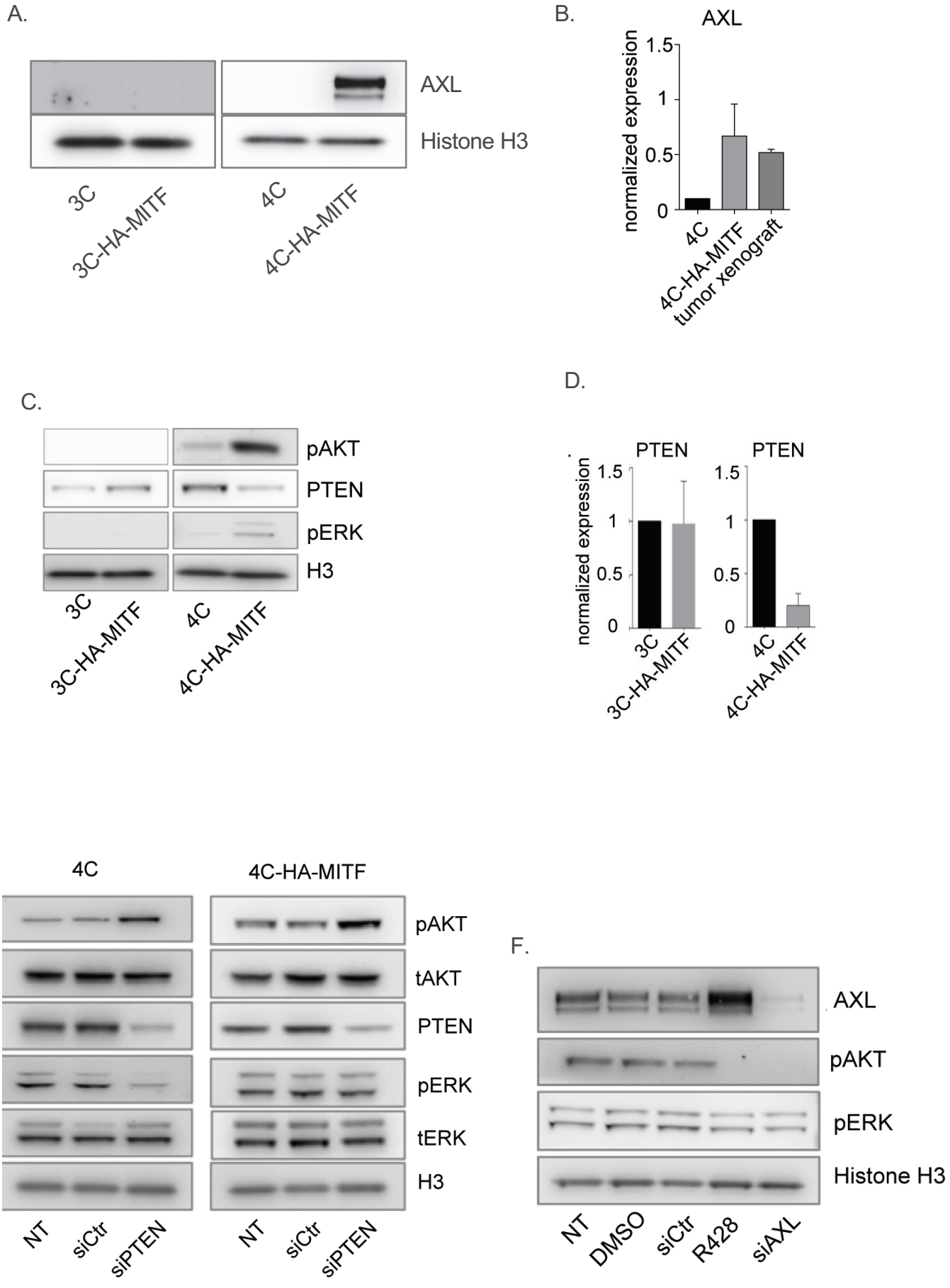
A.
AXL
Histone H3
3C
3C-HA-MITF
4C
4C-HA-MITF
B.
AXL
normalized expression
1.5
1
0.5
0
4C
4C-HA-MITF
tumor xenograft
C.
pAKT
PTEN
pERK
H3
3C
3C-HA-MITF
4C
4C-HA-MITF
D.
PTEN
PTEN
normalized expression
1.5
1
0.5
0
3C
3C-HA-MITF
4C
4C-HA-MITF
E.
4C
4C-HA-MITF
pAKT
tAKT
PTEN
pERK
tERK
H3
NT
siCtr
siPTEN
NT
siCtr
siPTEN
F.
AXL
pAKT
pERK
Histone H3
NT
DMSO
siCtr
R428
siAXL

Figure 4.

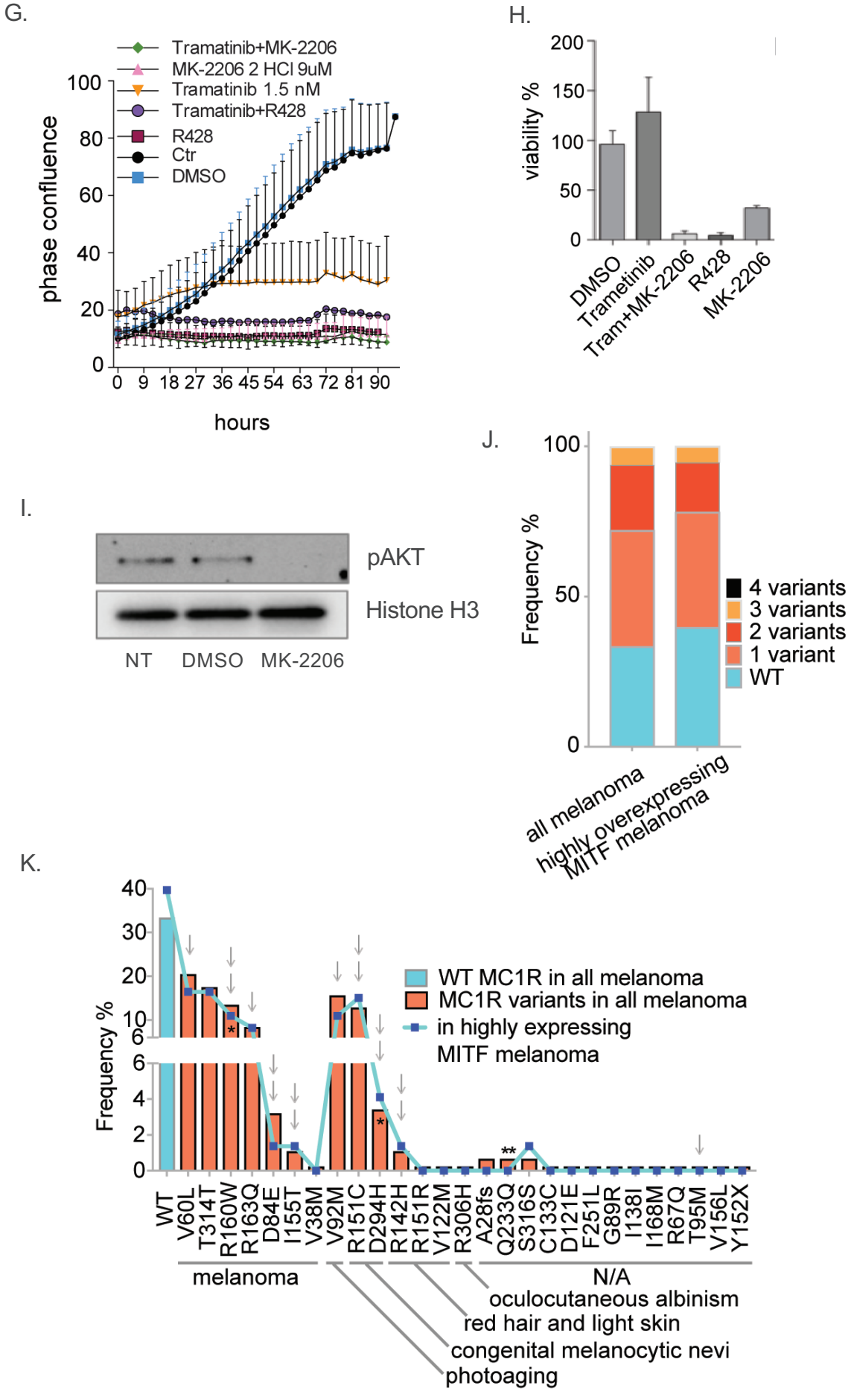
G.
Tramatinib+MK-2206
MK-2206 2 HCl 9uM
Tramatinib 1.5 nM
Tramatinib+R428
R428
Ctr
DMSO
phase confluence
hours
H.
viability %
DMSO
Trametinib
Tram+MK-2206
R428
MK-2206
I.
pAKT
Histone H3
NT
DMSO
MK-2206
J.
Frequency %
4 variants
3 variants
2 variants
1 variant
WT
all melanoma
highly overexpressing MITF melanoma
K.
Frequency %
WT MC1R in all melanoma
MC1R variants in all melanoma
in highly expressing MITF melanoma
WT
V60L
T314T
R160W
R163Q
D84E
I155T
V38M
V92M
R151C
D294H
R142H
R151R
V122M
R306H
A28fs
Q233Q
S316S
C133C
D121E
F251L
G89R
I138I
I168M
R67Q
T95M
V156L
Y152X
melanoma
N/A
oculocutaneous albinism
red hair and light skin
congenital melanocytic nevi
photoaging

Supplementary Figure 1.

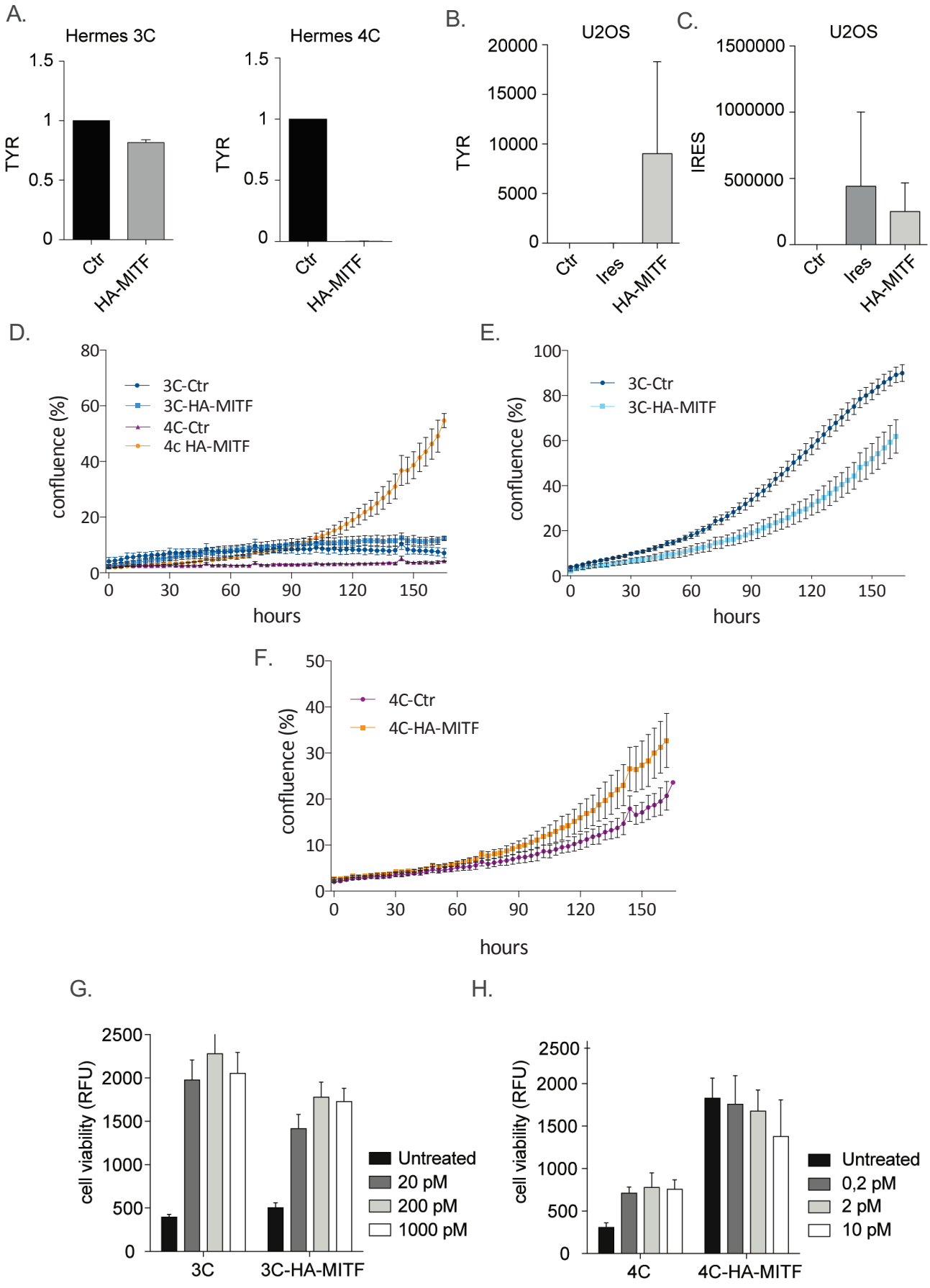

Supplementary Figure 1.

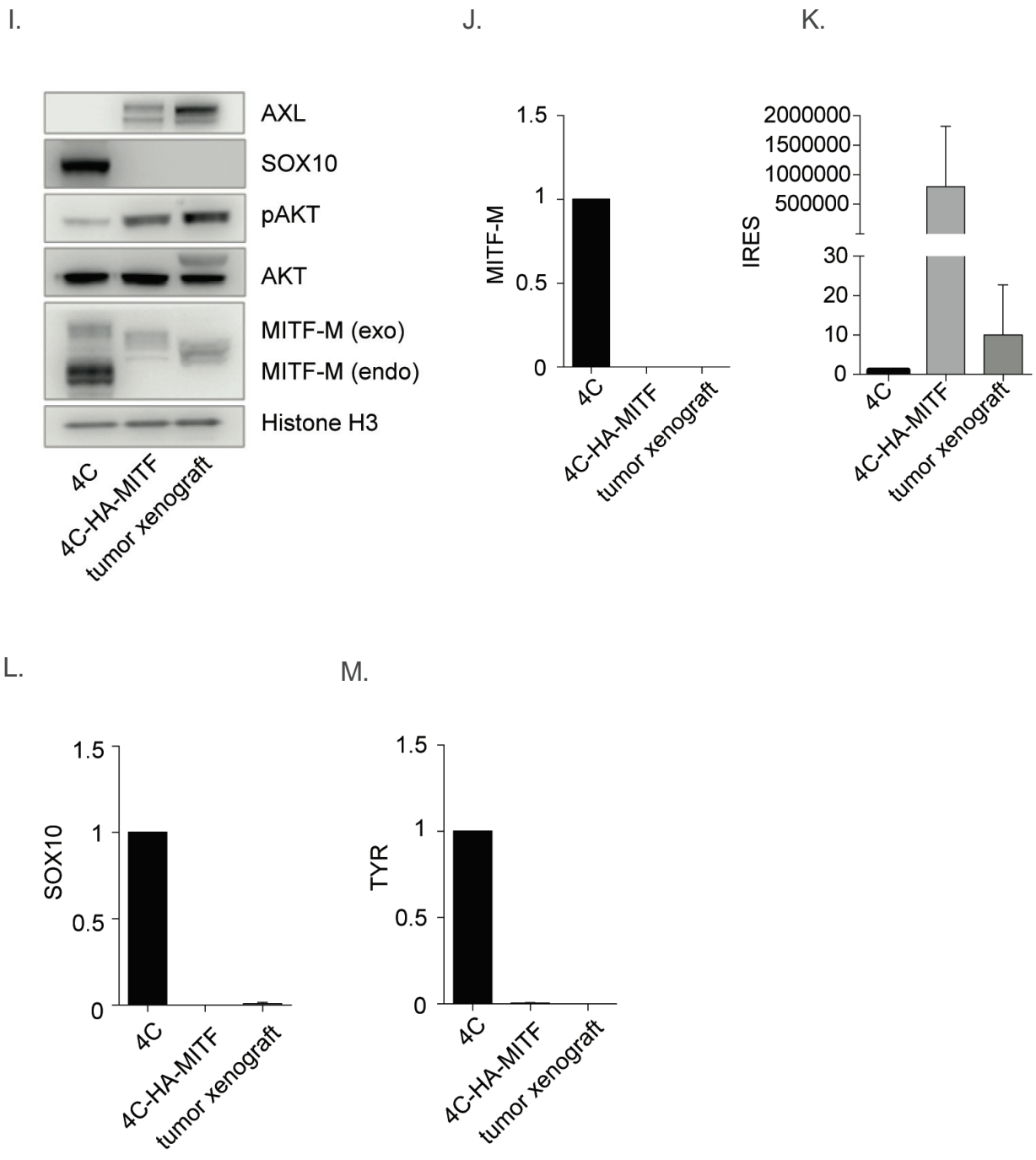

Supplementary Figure 2.

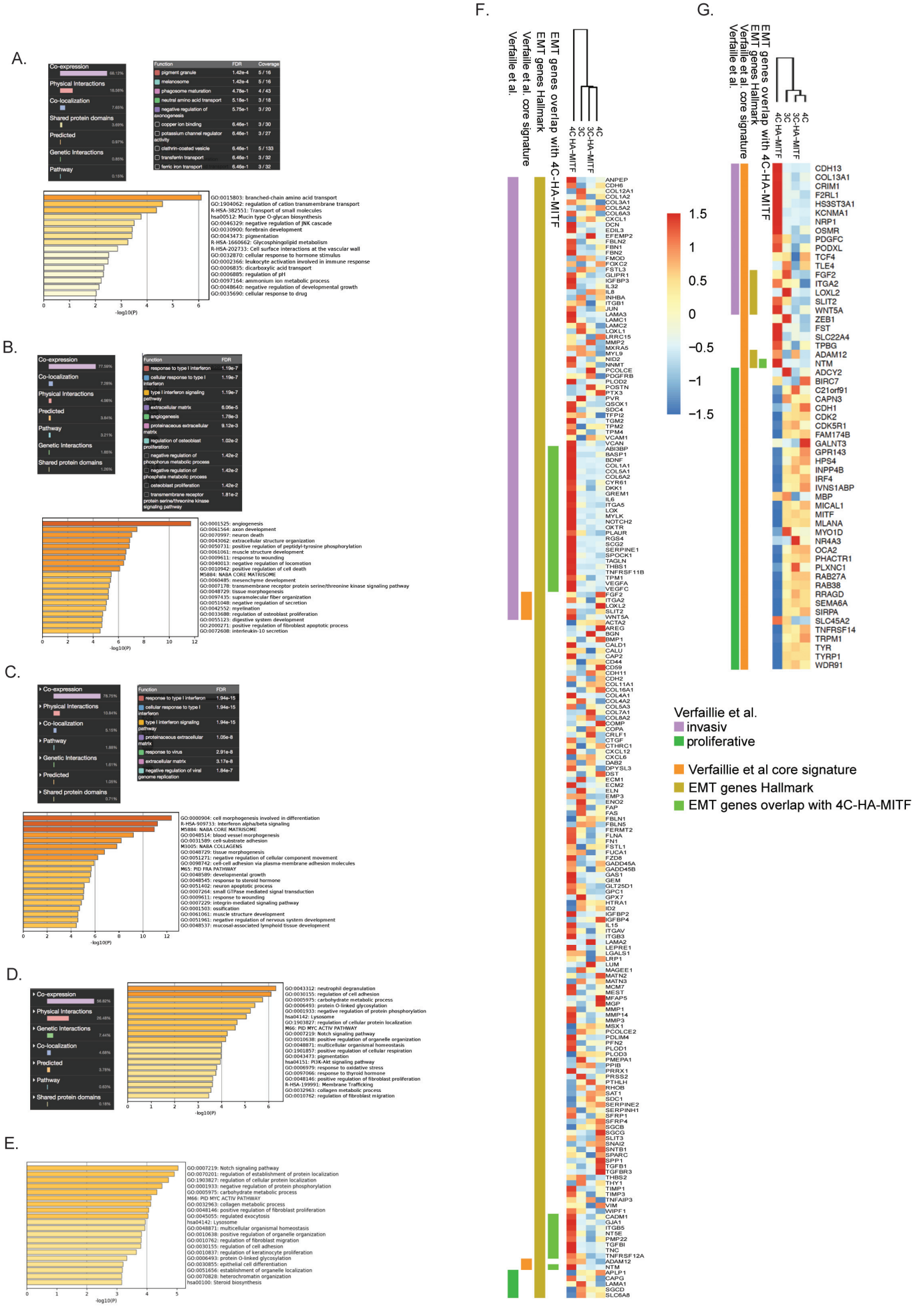

Supplementary Figure 3.

A.

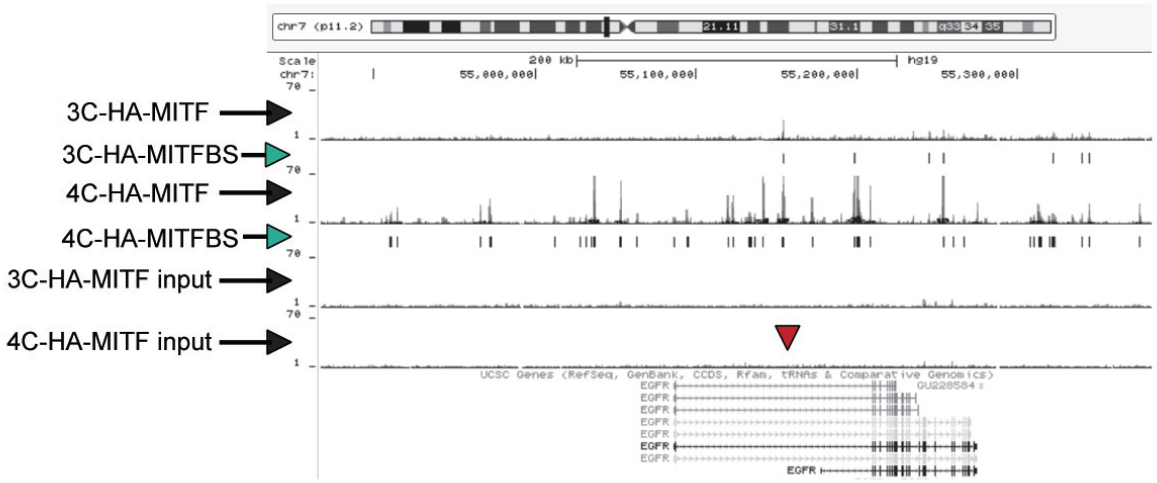

B.

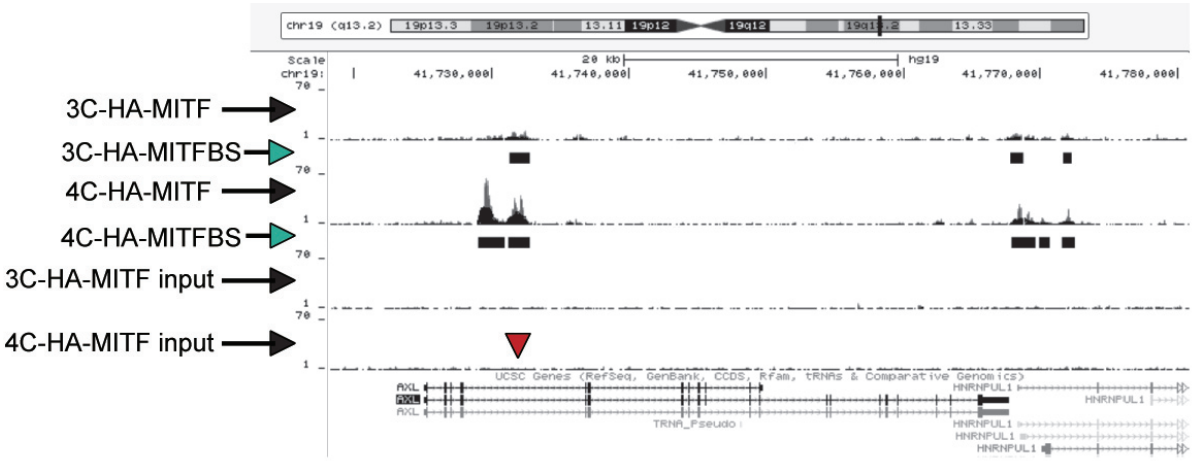

C.

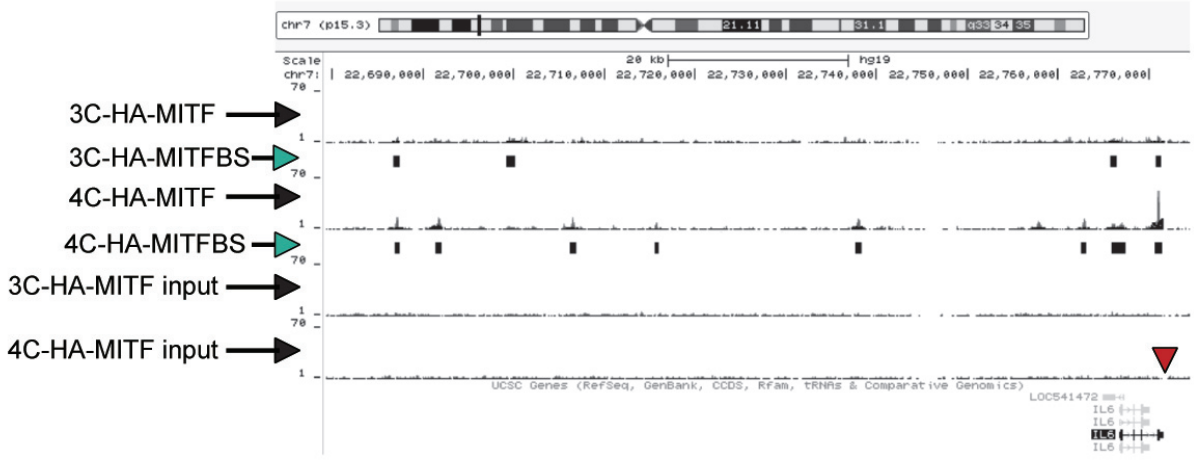

Supplementary Figure 3.

D.

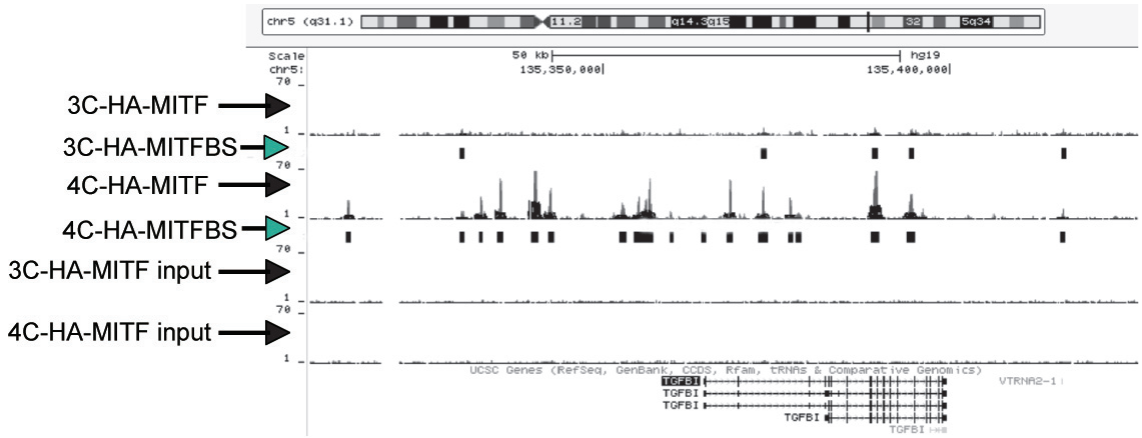

E.

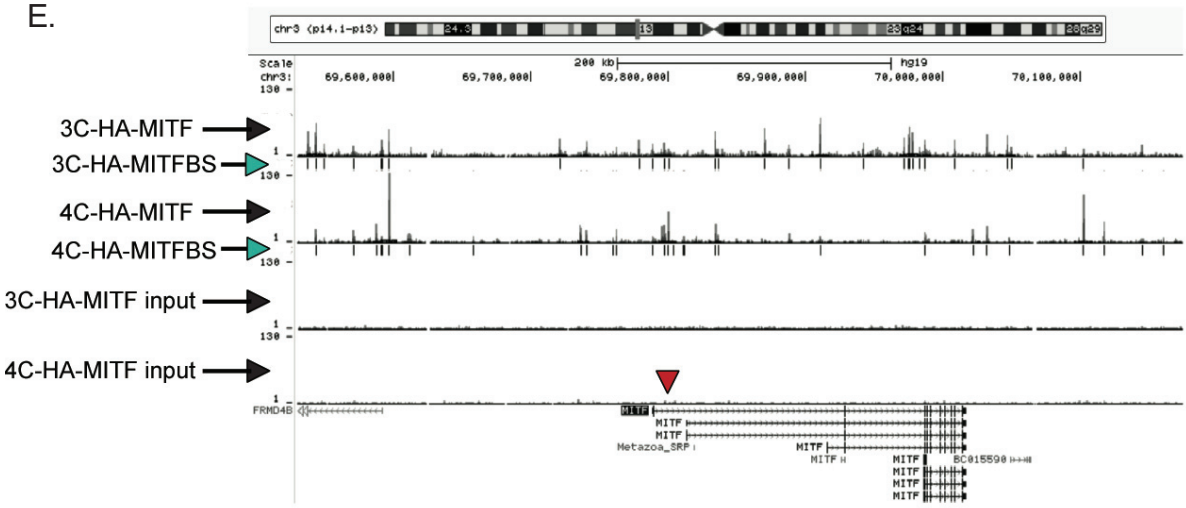

F.

Supplementary Figure 3.

G.

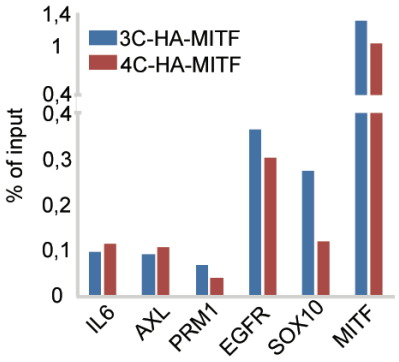

H.

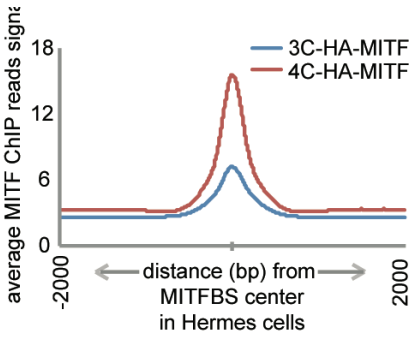

I.

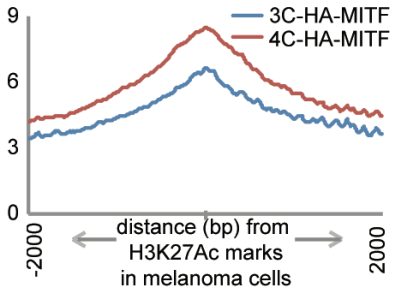

J.

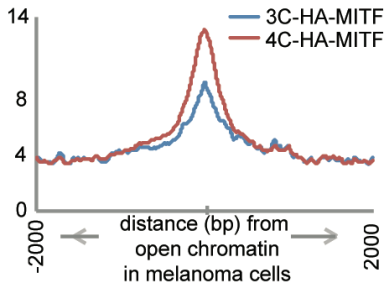

K.

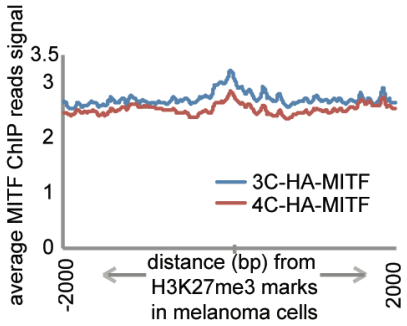

L.

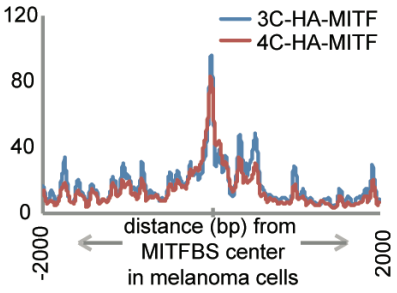

M.

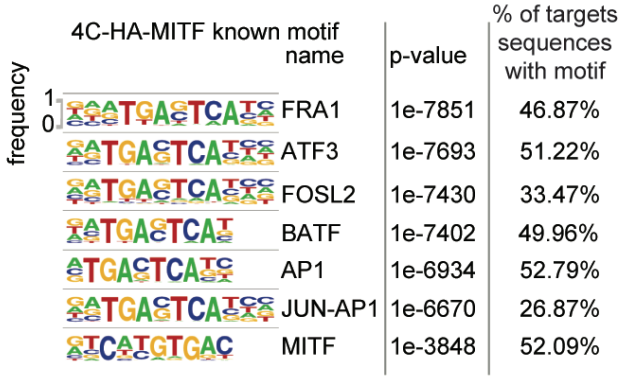

N.

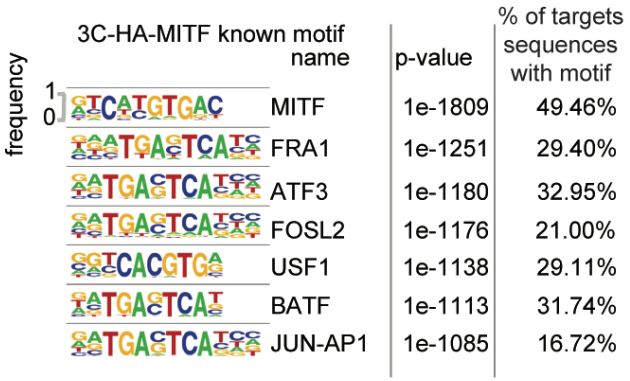

Supplementary Figure 4.

A.